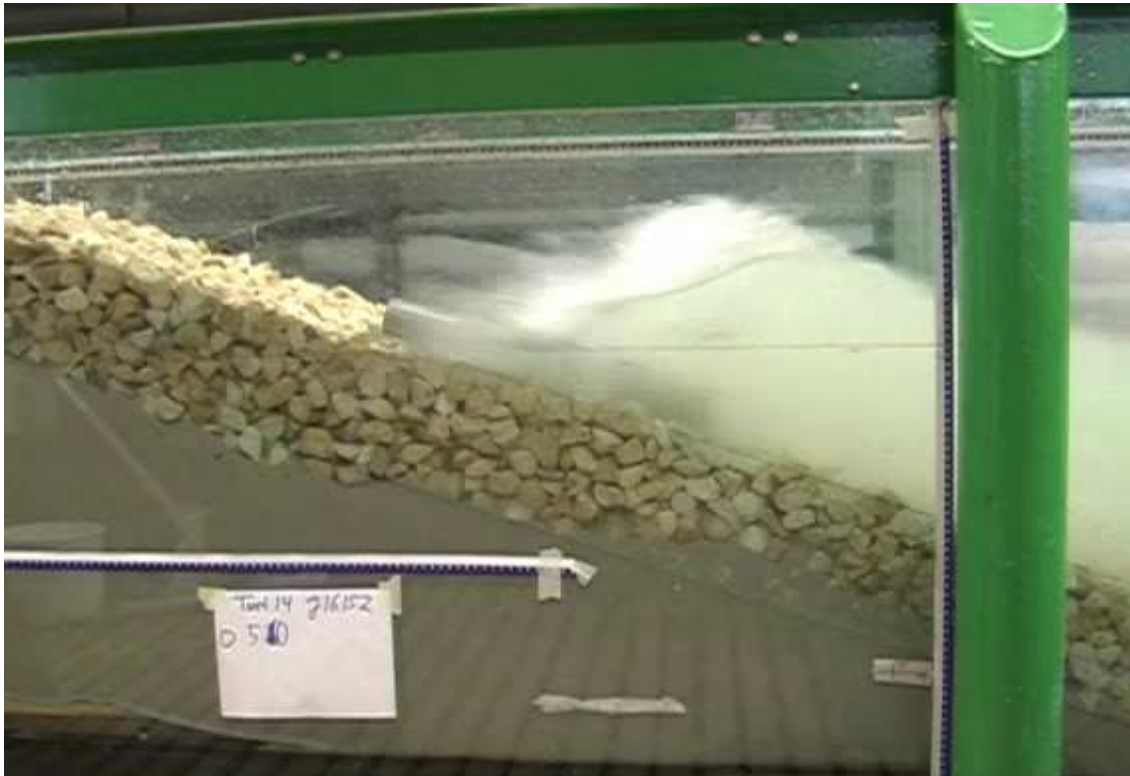


Open filters in breakwaters with a sand core



*Study into the stability of granular geometrically open,
hydraulically sand-open filters in breakwaters with a sand
core*

Msc. Thesis report of W.J.Ockeloen

Open filters in breakwaters with a sand core

**Study into the stability of granular geometrically open,
hydraulically sand-open filters in breakwaters with a sand
core**

Report

Msc. Thesis of W.J.Ockeloen

Graduation committee:

Prof. dr. ir. M.J.F. Stive

Ir. H.J. Verhagen

Dr.ir. W.S.J. Uijttewaal

Ir. G. Smith

***Delft University of Technology
Faculty of Civil Engineering and Geosciences
Section Hydraulic Engineering***

Preface

This report presents the findings of the study into geometrically open, hydraulically sand-open filters to be applied in breakwaters with a sand core. The study was initiated by Van Oord Dredging and Marine Contractors bv, in cooperation with the Hydraulic Engineering section of the faculty of Civil Engineering. Van Oord is one of the largest dredging companies worldwide with a lot of experience in coastal protection works like breakwaters. The company actively participates in this type of research by supervising thesis students together with the University.

Physical model tests have been performed in the long sediment transport flume (wave flume) of the Fluid Mechanics Laboratory of the section of Fluid Mechanics at the faculty of Civil Engineering. The laboratory facilitates research of thesis students, phd-students and others in the field of Fluid Mechanics and Hydraulic Engineering.

A graduation committee has been formed to supervise the study and evaluate the results:

Prof. dr. ir. M.J.F. Stive

Professor of Coastal Engineering at the section of Hydraulic Engineering and Chairman of the committee.

Ir. H.J. Verhagen

Lecturer of Coastal Engineering (bed, bank and shore protection, breakwaters and closure dams) at the section of Hydraulic Engineering and supervisor of the thesis work.

Dr.ir. W.S.J. Uijtewaal

Associate professor of Environmental Fluid Mechanics and responsible for the Fluid Mechanics Laboratory. Supervisor from the Fluid Mechanics section.

Ir. G. Smith

Senior Engineer at Van Oord Engineering Department and supervisor from the participating company.

Wouter Ockeloen

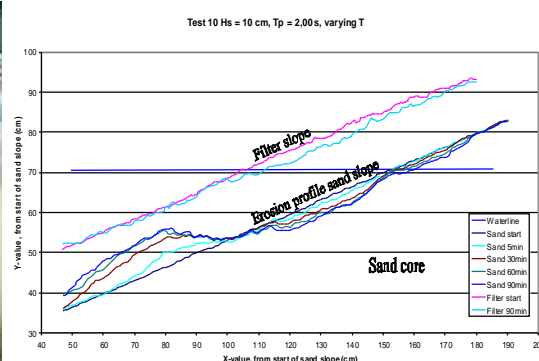
May 2007

wouterockeloen@hotmail.com

Dutch abstract

Open filters in golfbrekers met een zandkern

Afstudeeronderzoek naar een alternatief ontwerp voor golfbrekers van granulair materiaal zoals zand en breuksteen. De golfbreker wordt bij dit ontwerp opgebouwd uit een kern van zand, met direct daarop een laag grote stenen, zonder de tussenliggende filterlagen die gebruikelijk zijn. De enkele laag stenen fungeert als één open filterlaag die de door de golven opgewekte stroming en turbulentie genoeg moet reduceren om de erosie van zand door de filterlaag te beperken tot een acceptabele hoeveelheid. Door een gecontroleerde hoeveelheid erosie toe te staan en de noodzaak van onderhoud te accepteren, kan het alternatief ontwerp over de levensduur van de constructie zeer kostenbesparend zijn.



In samenwerking met Van Oord, een van de wereldmarktleiders op gebied van baggeren en kustwaterbouw, is aan de TU Delft een onderzoek gestart naar de toepasbaarheid van de zeer open filters op een zandkern. Mijn afstudeeronderzoek is het tweede achtereenvolgende in dit grotere onderzoek dat tot doel heeft om een goede theoretische beschrijving van de optredende en maatgevende processen te geven en een praktische ontwerpmethodode te ontwikkelen voor het gebruik van een zeer open filterlaag op zand. In mijn afstudeeronderzoek richt ik mij op de relatie tussen de golfhoogte, -periode en -regelmatigheid en de hoeveelheid erosie die daarbij optreedt.

Modelproeven voor het onderzoek zijn uitgevoerd in de lange sedimenttransport goot van het Vloeistofmechanica laboratorium. Deze goot beschikt over een golfgenerator die de constructie belast met een gewenst golfspectrum. De resultaten zijn geanalyseerd voor relaties tussen belasting en erosie.

Afstudeercommissie:

Prof.dr.ir. M.J.F. Stive
ir. H.J. Verhagen
dr.ir. W.S.J. Uijtewaai
ir. G. Smith

*TU Delft, Faculteit Civiele Techniek
Sectie Waterbouwkunde
i.s.m. Van Oord bv*

Summary

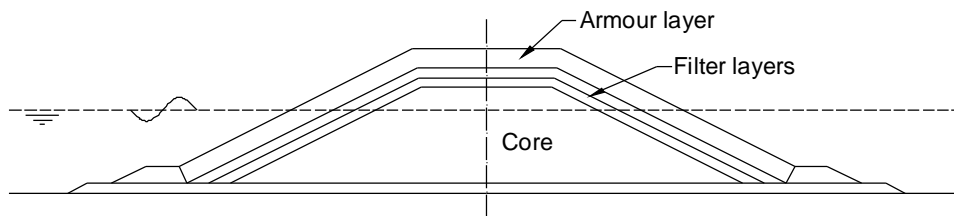
Breakwaters are found all around the world where a structure, beach, harbour entrance or another object on the coast has to be protected against waves. In this study, focus is aimed at rubble mound breakwaters, constructed of granular materials like quarry rock and sand. Recent developments in construction methods and lifetime cost calculations have led to interest in designs with sand cores covered by only one or two layers of relatively large stones (hydraulically sand-open filter), resulting in a breakwater that is unstable when the traditional criteria are applied. Deformation to some degree in a storm and maintenance works after a storm can be accepted if the circumstances allow it and if the savings in construction costs outweigh the extra maintenance costs.

Objective

The objective of this study is to find relations for the influence of variations of the hydraulic loading, slope steepness and grading of filter material on the stability and erosion patterns of core material in a breakwater configuration with a hydraulically sand-open filter on a sand core. The growth pattern of the erosion and the occurrence of an equilibrium situation in this erosion, are the main interests as results of the tests.

Breakwater layout and filters

The core of the breakwater has to fill a large volume and has to be strong enough to support the filter and armour layers. Sometimes the core is made of sand, but usually of quarry-run, a variation of grain sizes that comes from the quarry and needs very little selection.



The purpose of a filter layer is to block the underlying stones from being washed out and to let water flow in and out to prevent excess water pressures inside the pores. For the traditional geometrically closed filters, the open spaces between the grains in a filter layer are smaller than the characteristic grain size of the underlying material and the permeability has to be higher than that of the underlying material. Simple rules for geometrically closed filters can be applied to achieve this. Geometrically open filters, for which the grains of the under layer are now kept in place by the reduction of the loading, are presently used as well. The filter layer has to give enough resistance to the loading to reduce it below the point at which grains of the under layer begin to move. When the grains of the filter layer are even larger, the filter layer is in fact not stable anymore. The loading is reduced, but not well enough to prevent transport of the grains of the under layer; some erosion of material through the filter layer will occur. This type of filter is called hydraulically sand-open and is the subject of this study.

Geometrically open filter processes

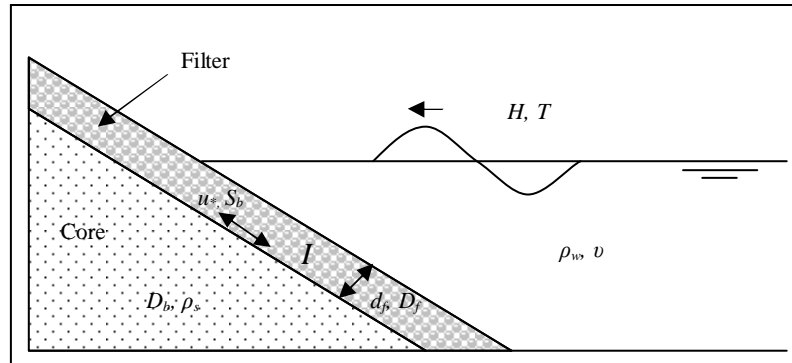
Breaking waves are the dominant loading force for breakwaters. Inside the rubble material, the energy from the waves is reduced. The velocities and turbulence caused by the waves rapidly diminish inside the filter, indicating that a thicker filter gives more reduction. The waves induce a hydraulic gradient which drives the porous flow. For the present study parallel flow through the filter layer was found to be the most important loading mechanism. With parallel flow, the velocity in the filter is much higher than in the core with its higher resistance. The velocity difference at the interface causes a shear stress on the upper grains of the base material, causes grains to move along the interface. Sand is transported parallel to the interface.

Scale effects

The scaling down from a prototype to a model gives significant problems. The different properties of water cannot all be scaled down with the same factor because the effects are not linear. One can keep the Froude number the same in prototype and in model (Froude-scaling) to keep the inertia and gravity forces in the same ratio, but then the Reynolds number changes and viscous forces become too large. Sand cannot be scaled down because the range of grain sizes is limited. Smaller grains become silt or clay and behave differently. Scale effects have been analysed and quantified theoretically and found to be limited to about 5% deviation of porous flow velocities.

Dimensional analysis of the processes

With a dimensional analysis, a process is described by non-dimensional parameters to be able to see influences of different parameters regardless of the scale or the absolute quantity.

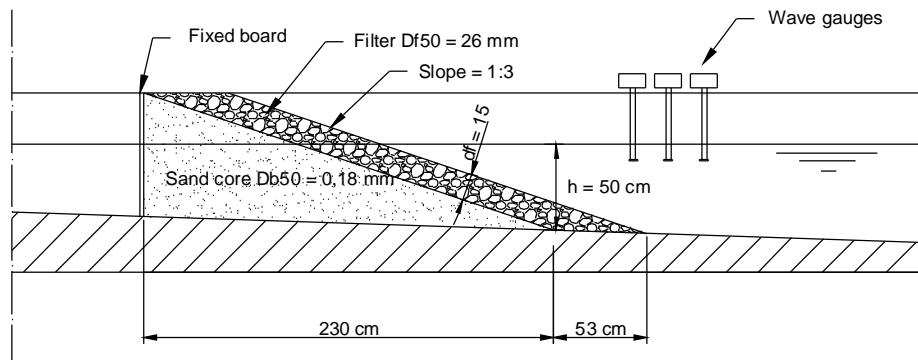


The most useful result is a combination of dimensionless terms describing the erosion area as a function of wave and structure parameters:

$$\frac{A_s}{HgT^2} = F \left\{ I, N, \frac{d_f}{D_f}, \frac{D_b}{D_f}, \frac{\tan \alpha}{\sqrt{\frac{2\pi H}{gT^2}}}, \frac{\rho_s}{\rho_w}, \frac{\sqrt{gHD_f}}{v} \right\} = F \left\{ I, N, m, \frac{D_b}{D_f}, m, \xi, \frac{\rho_s}{\rho_w}, \text{Re} \right\}$$

Test program and setup

Many parameters are involved in the erosion processes inside the breakwater. They have been analysed and a test program has been made in which the relevant adjustable parameters are varied. 17 tests have been performed in which the wave height, period, regularity, steepness, filter grading and slope steepness have been varied. The basic setup of the reference tests is shown in the figure below.



Test results and observations

The results and observations of test 10 are shown because the long period makes clear observations of the erosion process possible. After 5 minutes of wave attack, a thin erosion area and a bit larger accretion are visible already. After 90 minutes, the erosion and accretion area are clearly visible. The erosion grows fast in the beginning of the test, but the growth rate decreases gradually during the test.



After 5 minutes



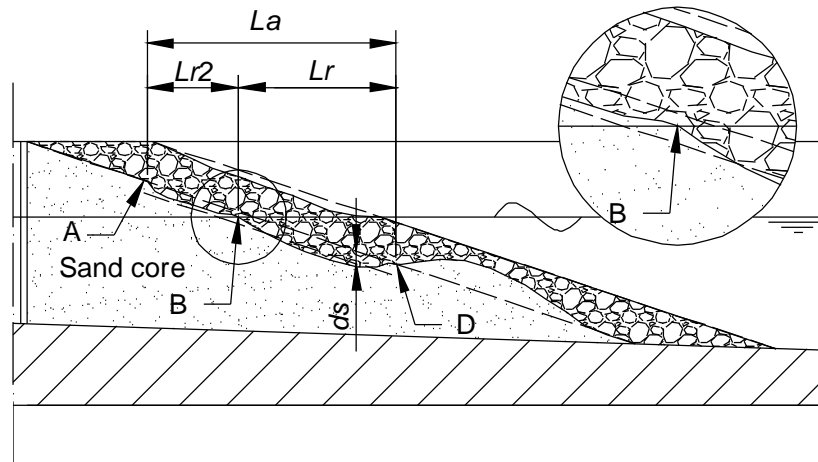
After 90 minutes

Waves are generated by the wave board and travel through the flume towards the breakwater cross section on which they break. On the interface between filter and core, the sand slope, the waves do not break; the internal water level just runs up and down the sand slope. The amplitude of this internal wave is much smaller than that of the external wave that drives it, while the period is the same. Sand is transported over the sand slope through the pores of the filter layer. When the internal wave runs down over the sand slope, bedload sand transport can be observed for smaller waves and suspended-load transport also for larger waves. For waves with smaller heights than about 4 to 5 cm (of the external wave), no transport is visible. When a wave is running up, the cloud of sand tends to move under an upward angle. The duration of this is short, about a quarter of the total wave period or even less. When a wave is running down, the suspended sand moves down with the water flow over the sand slope.

During wave run-up most sand transport is suspended-load transport, induced by the strong acceleration during a short time. During wave rundown both bedload and suspended-load transport occur; the up-building flow first induces bedload transport and when the flow gets stronger suspended-load transport is added. For smaller waves only bedload transport occurs and for very small waves ($H < 5$ cm in the tests) no transport occurs at all.

Analysis of the test results

The erosion area is the area between the original sand slope and the eroded sand slope in the part of the slope where erosion takes place.



During the tests, the erosion area grows. Observations show that the growth-rate decreases during the tests, but without reaching an equilibrium state. The erosion was found to grow as a function of \sqrt{N} (N = number of waves). $A_s \propto \sqrt{N}$, with a constant factor that is different for each test.

Erosion area relations

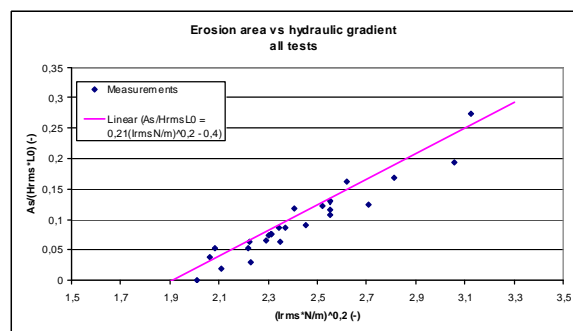
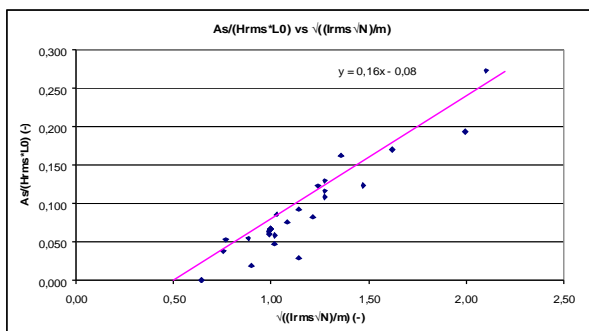
The erosion area seems to be related to the square root of the wave height. Because of this quadratic relation, the root-mean-squared wave height H_{rms} can be more interesting than the H_s , since it is related to square values of the wave heights as well. It was found that $A_s \propto H_{rms}^2$ for $H_{rms} \geq H_{threshold}$, and $\xi = const.$. Like this relation, the other dimensional relations that were investigated show consistency for only a certain part of the tests, with e.g. a constant ξ .

Existing open filter design criteria

In the test results, a threshold value of the loading (i.e. the wave height) has been found below which no erosion occurs. This threshold coincides with the existing design criteria for geometrically open (but hydraulically sand-tight) filters.

Dimensionless parameter relations

Two interesting results were found, of which the first (left figure) is based on the dimensionless relation shown above and the second (right figure) is a further curve-fitting of these parameters to fit the test data as good as possible.



In both relations, the parallel hydraulic gradient plays an important role. This gradient, which was estimated for all tests including those of Uelman, drives the parallel porous flow which is the dominant loading mechanism for the erosion process. In formula form, the found relations are:

$$\text{First: } \frac{A_s}{H_{rms} L_0} = 0,16 \sqrt{I_{rms} \frac{\sqrt{N}}{m}} - 0,08. \text{ Second: } \frac{A_s}{H_{rms} L_0} = 0,21 \left(I_{rms} \frac{N}{m} \right)^{0,2} - 0,4$$

The shortcomings of these relations are that the hydraulic gradient is difficult to calculate from wave and structure parameters and that the influence of the core grain size is not in the relations. Further research is recommended for this.

Conclusions

- Parallel downward porous flow is the dominant loading process rather than turbulence by the breaking waves.
- The parallel downward porous flow is driven by the hydraulic gradient that sets in from the internal setup- or run-up level to the external rundown level.
- The amount of erosion grows with the square-root of the number of waves. An equilibrium state has not been found during the relatively long tests.
- A threshold value for the loading has been found below which no erosion takes place. This threshold coincides with the existing design criteria for geometrically open filters.
- The amount of erosion was found to depend on the wave height and length, the hydraulic gradient, the number of waves and the relative filter layer thickness. The hydraulic gradient is a complex function of wave parameters and structure parameters.
- The erosion area and erosion depth are both related to the square of the root-mean-squared wave height. The regular wave height of tests with regular waves can be compared to this H_{rms} .
- The erosion length is related to the significant wave height.
- The wave period has a large influence on the erosion process.
- Two dimensionless relations have been found (mentioned above) which apply to all tests including Uelman's. The influence of core grain size and a calculation method for the hydraulic gradient still have to be found.

Recommendations for further research

- It is recommended to search for relations for the hydraulic gradient, by getting good estimates of the wave rundown on rubble mound slopes, combined with the wave run-up and to relate it to the gradient.
- It is recommended to perform a scale series test program to get more certainty about the magnitude of scale effects, for instance in the same wave flume.
- It is recommended to perform wave flume tests with varying grain sizes of the sand in the core. This can easily be combined with the recommended scale series tests by extending the program.
- It is recommended to perform physical model tests in the wave flume to study the influence of a berm, low/ submerged crest and water level variations and to perform tests in a wave basin to study the influence of oblique incident waves, the behaviour of the breakwater head and the combination of waves and currents.

Table of contents

<i>PREFACE</i>	V
<i>DUTCH ABSTRACT</i>	VI
<i>SUMMARY</i>	VII
<i>LIST OF FIGURES</i>	XV
<i>LIST OF TABLES</i>	XVII
<i>NOTATION</i>	XVIII
CHAPTER 1 INTRODUCTION	2
1.1 <i>GENERAL INTRODUCTION</i>	2
1.2 <i>BREAKWATERS</i>	4
1.2.1 Granular or rubble mound breakwaters.....	4
1.2.2 Developments in granular breakwater design.....	5
1.3 <i>STRUCTURE OF THE REPORT</i>	6
CHAPTER 2 THEORY GEOMETRICALLY OPEN FILTERS	10
2.1 <i>EXISTING DESIGN CRITERIA AND NEW DEVELOPMENTS</i>	10
2.2 <i>GEOMETRICALLY OPEN FILTER PROCESSES</i>	11
2.2.1 Loading.....	11
2.2.2 Porous flow and hydraulic gradient.....	12
2.2.3 Stability.....	13
2.2.4 Transport of material.....	14
2.2.5 Deformation of the structure.....	14
2.3 <i>SCALING PROBLEMS</i>	15
2.4 <i>RESEARCH DONE BY E.F. UELMAN</i>	17
2.5 <i>MATERIALS AND THEIR INFLUENCE</i>	19
2.5.1 Core material: sand.....	19
2.5.2 Filter material: rock.....	19
2.5.3 Grain size ratios and grading.....	20
2.6 <i>SCHEMATISATION OF PROCESSES</i>	22
2.6.1 The process from loading to erosion.....	22
2.6.2 Physical parts and their processes.....	23
2.7 <i>ESSENTIAL PARAMETERS FOR THE EROSION PROCESS</i>	24
2.7.1 Loading: breaking waves.....	24
2.7.2 Filter layer and filter-core interface.....	24
2.7.3 Core.....	25
2.7.4 Stability, transport and erosion.....	25
2.7.5 Material properties.....	25
2.7.6 Scale effects.....	26
2.7.7 Remarks.....	26
CHAPTER 3 PROBLEM ANALYSIS AND OBJECTIVE	28
3.1 <i>PROBLEM DESCRIPTION; LACKING KNOWLEDGE</i>	28
3.1.1 Loading: breaking waves.....	28
3.1.2 Filter layer and filter-core interface.....	28
3.1.3 Core.....	29
3.1.4 Erosion and equilibrium.....	29
3.1.5 Material properties.....	30
3.1.6 Scale effects.....	31
3.2 <i>CHOICE OF FURTHER RESEARCH DIRECTION</i>	33
3.2.1 Scaling effects for practical application.....	33
3.2.2 Hydraulic loading: influence of variations.....	34
3.2.3 Influence of structure layout.....	35
3.2.4 Choice of research direction: hydraulic variations.....	36
3.3 <i>CHOICE OF GENERAL TEST SETUP</i>	38
3.3.1 Wave flume.....	38
3.3.2 Wave basin.....	39
3.3.3 Wave tunnel.....	39
3.3.4 Prototype on the coast.....	40
3.3.5 Choice of test setup: small scale wave flume.....	41
3.4 <i>OBJECTIVE</i>	42
3.4.1 Problem definition.....	42
3.4.2 Ultimate goal of the research.....	42
3.4.3 Objective of this thesis study.....	43

CHAPTER 4	SCALE EFFECTS	46
4.1	<i>DIMENSIONAL ANALYSIS OF THE PROCESSES</i>	46
4.1.1	Pi-theorem	46
4.1.2	Application of the Pi-theorem	47
4.1.3	Conclusions of the dimensional analysis	54
4.2	<i>COMPARISON AND QUANTIFICATION OF THE SCALE EFFECTS</i>	57
4.2.1	Comparison of the dimensional analysis with literature	57
4.2.2	Scale effects from other studies	60
4.2.3	Scaling requirements for open filters on a sand core	61
4.2.4	Quantification of scale effects for this research	63
CHAPTER 5	TEST PROGRAM FOR HYDRAULIC VARIATIONS	68
5.1	<i>PARAMETER ADJUSTMENTS</i>	68
5.1.1	Loading	68
5.1.2	Material properties	69
5.1.3	Structure layout	70
5.2	<i>EXPECTED RELATIONS AND PARAMETER VARIATION CHOICES</i>	71
5.2.1	Wave height variation	71
5.2.2	Number of waves for equilibrium	71
5.2.3	Wave period variation	72
5.2.4	Irregular waves: Jonswap	72
5.2.5	Swell waves	72
5.2.6	Grading variation	73
5.2.7	Slope steepness variation	73
5.2.8	Tidal water level variation	73
5.3	<i>TEST PROGRAM</i>	75
5.4	<i>MEASURING TECHNIQUES</i>	77
5.4.1	Transport and erosion	77
5.4.2	Loading	78
5.5	<i>TEST SET-UP</i>	79
5.5.1	Setup of the reference test	79
5.5.2	Measurement devices	80
5.5.3	Measurement setup	81
5.5.4	Granular materials	82
5.5.5	Placement of the core and filter	84
CHAPTER 6	TEST RESULTS AND OBSERVATIONS	86
6.1	<i>RESULTS OF TEST 10</i>	86
6.2	<i>OBSERVATIONS</i>	90
6.2.1	Water motion	90
6.2.2	Stability of the filter layer	91
6.2.3	Transport of sand, two mechanisms	91
6.2.4	Observations test 10, $H_s = 10$ cm, $T_p = 2,00$ s	92
6.2.5	Observations test 13, $H_s = 5$ cm, $T_p = 0,85$ s	96
6.2.6	Observations test 14, $H_s = 16$ cm, $T_p = 1,52$ s	96
6.2.7	Observations test 15, $H = 3$ cm, $T = 2,0$ s	97
6.2.8	Observations test 16, $H_s = 10$ cm, $T_p = 1,2$ s, $\tan\alpha = 1:4$	97
6.3	<i>RESULTS OF ALL THE TESTS</i>	98
6.3.1	Test 1 reference test regular waves	99
6.3.2	Test 2 rerun reference test regular waves	100
6.3.3	Test 3 reference test regular waves	101
6.3.4	Test 4 reference test Jonswap waves	102
6.3.5	Test 5 variation of H	103
6.3.6	Test 6 variation of H	104
6.3.7	Test 7 reference test regular waves	105
6.3.8	Test 8 variation of T	106
6.3.9	Test 9 variation of T	107
6.3.10	Test 10 variation of T	108
6.3.11	Test 11 swell waves	109
6.3.12	Test 12 wide grading	110
6.3.13	Test 13 variation of H	111
6.3.14	Test 14 variation of H	112
6.3.15	Test 15 swell waves low	113
6.3.16	Test 16 slope steepness variation	114
6.3.17	Test 17 slope steepness variation	115
6.4	<i>VALIDITY OF THE TESTS</i>	116
6.4.1	Setup of the structure	116
6.4.2	Reproducibility of the tests	117
6.4.3	Measurement errors	118
6.4.4	Laboratory effects	118
6.4.5	Conclusions on the errors	120

CHAPTER 7	ANALYSIS OF THE TEST RESULTS	122
7.1	<i>CALCULATION OF PARAMETERS</i>	122
7.2	<i>SAND BALANCE FOR EROSION AND ACCRETION AREA</i>	125
7.3	<i>COMPARISONS WITH UELMAN'S TESTS</i>	127
7.3.1	Observations	127
7.3.2	Parameter relations	128
7.3.3	Conclusions of the comparisons	129
7.4	<i>RELATIONS BETWEEN LOADING AND EROSION</i>	131
7.4.1	Erosion growth as a function of the number of waves	131
7.4.2	Erosion area relations	133
7.4.3	Erosion length and –depth relations	138
7.5	<i>EXISTING OPEN FILTER DESIGN CRITERIA AND SHIELDS</i>	143
7.5.1	Comparison to open filter design formulae	143
7.5.2	Comparison to the Shields criterion	145
7.5.3	The threshold of motion explained	145
7.6	<i>TURBULENCE-DOMINANCE OR POROUS-FLOW-DOMINANCE</i>	146
7.7	<i>DIMENSIONLESS PARAMETER RELATIONS</i>	147
7.7.1	Relations with ξ	147
7.7.2	Relations from the dimensional analysis	148
7.7.3	Combined relations	151
7.7.4	Found relations and remaining uncertainties after analysis	154
7.8	<i>UP-SCALING TO A POSSIBLE PROTOTYPE</i>	156
7.8.1	Up-scaling with general Froude scaling factors	156
7.8.2	Up-scaling for two layers from core to armour to loading	156
7.8.3	Up-scaling with the Shields criterion	158
7.8.4	Conclusions after up-scaling	159
7.9	<i>EVALUATION OF THE ANALYSIS</i>	160
7.9.1	Evaluation of the expected relations	160
7.9.2	Evaluation of the objective	161
CHAPTER 8	CONCLUSIONS AND RECOMMENDATIONS	164
8.1	<i>CONCLUSIONS</i>	164
8.1.1	Evaluation of the objective	164
8.1.2	Concept of the processes after analysis	165
8.1.3	Conclusions from observations and analysis	165
8.1.4	Relations between loading and erosion	166
8.1.5	Lacking knowledge after analysis	167
8.2	<i>RECOMMENDATIONS FOR FURTHER RESEARCH</i>	168
8.2.1	Relations for the parallel hydraulic gradient	168
8.2.2	Prototype scale validation	168
8.2.3	Influence of the core grain size	169
8.2.4	Influence of structural layout and local circumstances	169
	<i>REFERENCES</i>	171
	<i>APPENDIX I STUDY REPORT EVERT UELMAN</i>	<i>I</i>
	Theory open filter processes	<i>I</i>
	Experiments	<i>III</i>
	Recommendations	<i>V</i>
	Comparison test profile with beach erosion profile	<i>V</i>
	<i>APPENDIX II LITERATURE STUDY</i>	<i>VII</i>
	Porous flow	<i>VII</i>
	Criteria and processes for filter design	<i>VII</i>
	Numerical modelling of filter processes	<i>X</i>
	Scaling problems	<i>XII</i>
	Other articles	<i>XX</i>
	<i>APPENDIX III EROSION GROWTH CURVES</i>	<i>XXIII</i>
	<i>APPENDIX IV WORK PLAN AND TIME SCHEDULE</i>	<i>XXV</i>
	Work plan	<i>XXV</i>
	Time schedule	<i>XXVI</i>
	<i>ACKNOWLEDGEMENTS</i>	<i>XXVII</i>

List of figures

Figure 1-1 Left: Breakwater at Provincetown, USA, painted by Barbara Cohen (from: BC-Print) Right: Storm surge hitting the Los Angeles breakwater (from: LA city Lifeguard Association).....	2
Figure 1-2 Example of test 14 before the tests (left) and after 90 minutes of testing (right).....	3
Figure 1-3 Example of a granular breakwater, photo by Gary Curtis (from: fantompoet.com).....	4
Figure 1-4 Basic layout of a standard granular breakwater.....	4
Figure 2-1 Sketch (left) and plot (right) of the result of one of the performed tests. From Uelman.....	17
Figure 3-1 Small scale wave flume at the Fluid mechanics lab of TU Delft.....	38
Figure 3-2 Schematisation of the wave tunnel at WL Delft Hydraulics (from www.wldelft.nl).....	39
Figure 4-1 Sketch of the breakwater layout with important parameters.....	47
Figure 4-2 Viscous scale effects on rubble-mound stability models (from Hughes 1993).....	63
Figure 5-1 Set-up of the flume tests performed by Uelman (from Uelman 2006).....	68
Figure 5-2 Test setup in the wave flume (dimensions in cm).....	79
Figure 5-3 Setup of the reference test.....	79
Figure 5-4 Setup of the wave flume with measurement devices.....	81
Figure 5-5 Sieve curve of the used sand S80.....	82
Figure 5-6 Sieve curve of the used filter material.....	82
Figure 5-7 Sieve curve of the used filter material.....	83
Figure 5-8 samples of the standard filter grading (left) and wide grading (right).....	83
Figure 5-9 Sand profiling structure.....	84
Figure 6-1 setup of test 10 at the start.....	86
Figure 6-2 run-up (left) and rundown (right) of a large wave in test 10.....	86
Figure 6-3 photo series of test 10.....	87
Figure 6-4 graph of the sand slope and filter slope of test 10.....	88
Figure 6-5 erosion- and accretion area growth of test 10.....	89
Figure 6-6 three stages of a breaking wave in test 14.....	90
Figure 6-7 suspended-load sand transport during wave run-up (left) and rundown (right).....	92
Figure 6-8 sketch of the erosion pattern after test 10 with point definitions.....	93
Figure 6-9 test 1 after 5 minutes (left) and after 90 minutes (right).....	99
Figure 6-10 graph of the sand- and filter slope of test 1.....	99
Figure 6-11 test 2 after 5 minutes (left) and after 120 minutes (right).....	100
Figure 6-12 graph of the sand- and filter slope of test 2.....	100
Figure 6-13 test 3 after 5 minutes (left) and after 180 minutes (right).....	101
Figure 6-14 graph of the sand- and filter slope of test 3.....	101
Figure 6-15 test 4 after 5 minutes (left) and after 180 minutes (right).....	102
Figure 6-16 graph of the sand- and filter slope of test 4.....	102
Figure 6-17 test 5 after 5 minutes (left) and after 600 minutes (right).....	103
Figure 6-18 graph of the sand- and filter slope of test 5.....	103
Figure 6-19 test 6 after 5 minutes (left) and after 90 minutes (right).....	104
Figure 6-20 graph of the sand- and filter slope of test 6.....	104
Figure 6-21 test 7 after 5 minutes (left) and after 90 minutes (right).....	105
Figure 6-22 graph of the sand- and filter slope of test 7.....	105
Figure 6-23 test 8 after 5 minutes (left) and after 90 minutes (right).....	106
Figure 6-24 graph of the sand- and filter slope of test 8.....	106
Figure 6-25 test 9 after 5 minutes (left) and after 90 minutes (right).....	107
Figure 6-26 graph of the sand- and filter slope of test 9.....	107
Figure 6-27 test 10 after 5 minutes (left) and after 90 minutes (right).....	108
Figure 6-28 graph of the sand- and filter slope of test 10.....	108
Figure 6-29 test 11 after 5 minutes (left) and after 90 minutes (right).....	109
Figure 6-30 graph of the sand- and filter slope of test 11.....	109
Figure 6-31 test 12 after 5 minutes (left) and after 120 minutes (right).....	110
Figure 6-32 graph of the sand- and filter slope of test 12.....	110
Figure 6-33 test 13 after 5 minutes (left) and after 420 minutes (right).....	111
Figure 6-34 graph of the sand- and filter slope of test 13.....	111
Figure 6-35 test 14 after 5 minutes (left) and after 90 minutes (right).....	112
Figure 6-36 graph of the sand- and filter slope of test 14.....	112
Figure 6-37 test 15 after 5 minutes (left) and after 240 minutes (right).....	113
Figure 6-38 graph of the sand- and filter slope of test 15.....	113
Figure 6-39 test 16 after 5 minutes (left) and after 180 minutes (right).....	114
Figure 6-40 graph of the sand- and filter slope of test 16.....	114

Figure 6-41 test 17 after 5 minutes (left) and after 90 minutes (right).....	115
Figure 6-42 graph of the sand- and filter slope of test 17.....	115
Figure 6-43 comparison of the erosion after 90 minutes of test 2 and test 3.....	116
Figure 6-44 photo of the space under the mesh wire in test 3.....	117
Figure 6-45 erosion of the sand profile of test 1 to 3 at the start and after 90 minutes.....	117
Figure 6-46 comparison of the sand slope after 180 min from the front- and backside for test 4.....	119
Figure 7-1 example of an extracted graph with trendline at the start.....	122
Figure 7-2 definition sketch of erosion length and –depth.....	123
Figure 7-3 chart of the erosion area versus the wave height for all tests.....	124
Figure 7-4 comparison of tests 1-4 with Uelman’s tests, A_s versus m	129
Figure 7-5 erosion area growth in time during the tests.....	132
Figure 7-6 A_s vs \sqrt{N} of test 4.....	132
Figure 7-7 A_s vs \sqrt{N} of test 10.....	132
Figure 7-8 erosion area versus significant wave height for wave height variation tests.....	133
Figure 7-9 erosion area versus root mean squared wave height.....	134
Figure 7-10 erosion area versus peak period of the wave period variation tests.....	135
Figure 7-11 erosion area versus $T_{m-1,0}$	136
Figure 7-12 erosion area versus $\tan\alpha$ for only the slope steepness variation tests.....	136
Figure 7-13 A_s vs H_{rms} after 2400 waves.....	138
Figure 7-14 A_s vs T_p after 2400 waves.....	138
Figure 7-15 Absolute erosion length vs H_{rms}	139
Figure 7-16 Absolute erosion length vs H_s	139
Figure 7-17 Relative erosion length vs H_s	139
Figure 7-18 Relative erosion length 2 vs H_s	139
Figure 7-19 Erosion depth vs H_{rms}	140
Figure 7-20 Erosion depth vs T_p	140
Figure 7-21 Erosion area versus erosion depth after 90 minutes.....	141
Figure 7-22 L_{r2} vs wave run-up.....	142
Figure 7-23 L_r vs wave rundown.....	142
Figure 7-24 Open filter design criteria by Klein Breteler.....	143
Figure 7-25 Open filter design by De Grauw.....	144
Figure 7-26 Critical Shields parameter as function of Re^*	145
Figure 7-27 erosion area versus ζ	147
Figure 7-28 graph of the relations from the dimensional analysis.....	148
Figure 7-29 d_s/H_{rms} vs $Re = \frac{\sqrt{gHD_f}}{v}$	149
Figure 7-30 d_s/H_{rms} vs D_{f50}/H_{rms}	149
Figure 7-31 $A_s/(H_{rms}*L_0)$ vs I_{max}	150
Figure 7-32 $A_s/(H_{rms}*L_0)$ vs Re	150
Figure 7-33 Relation between erosion area and gradient from the partial results.....	152
Figure 7-34 Dimensionless relation between erosion area and gradient.....	152
Figure 7-35 Alternative dimensionless relation between erosion area and gradient.....	153
Figure 7-36 sketch of the scaled-up prototype.....	157
Figure 8-1 Concept of the breakwater configuration.....	165
Figure 8-2 comparison of tests and equilibrium beach profile.....	VI
Figure 8-3 Time schedule.....	XXVI

List of tables

<i>Table 5-1 grain sizes grading variation.....</i>	<i>73</i>
<i>Table 5-2 Test program</i>	<i>75</i>
<i>Table 6-1 original test program.....</i>	<i>98</i>
<i>Table 6-2 test program as executed with measured wave heights and periods</i>	<i>98</i>
<i>Table 6-3 deviations of erosion and accretion over the width of the flume in mm.....</i>	<i>119</i>
<i>Table 6-4 deviations in cm between the front- and backside of the flume.....</i>	<i>120</i>
<i>Table 7-1 erosion parameters of all tests</i>	<i>123</i>
<i>Table 7-2 comparison of erosion- and accretion area</i>	<i>125</i>
<i>Table 7-3 erosion parameters after 2400 waves for $m = 5,8$.....</i>	<i>128</i>
<i>Table 7-4 important loading parameters for all tests.....</i>	<i>131</i>
<i>Table 7-5 copy of the erosion parameters</i>	<i>131</i>
<i>Table 7-6 wave run-up and rundown parameters.....</i>	<i>141</i>
<i>Table 7-7 Dimensionless parameters of all tests.....</i>	<i>150</i>
<i>Table 7-8 scaling with fixed Froude scaling factors.....</i>	<i>156</i>

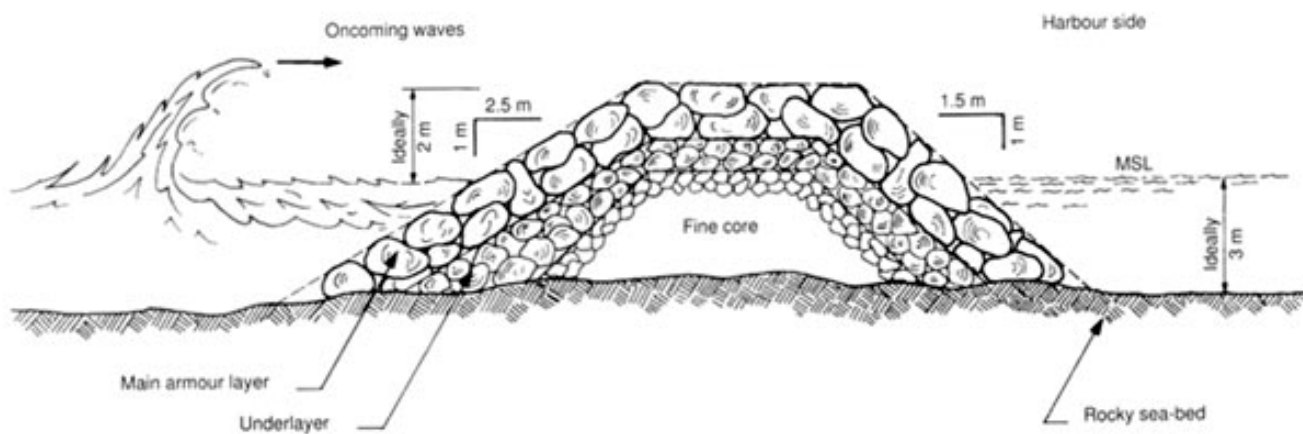
Notation

$a, b, c, \alpha, \beta, \gamma$	-	Dimensional coefficients
A_s	-	Total erosion area
C	-	Concentration
Ca	-	Cauchy number
C_i	-	Empirical constant
D_{bx}	-	Grain size base material (core) of which x % of the mass of the grains has a smaller diameter
d_f	-	Thickness of filter layer
D_{fx}	-	Grain size filter material of which x % of the mass of the grains has a smaller diameter
d_s	-	Erosion depth
E_d	-	Energy dissipated on and within the structure
E_i	-	Incident energy
E_r	-	Reflected energy
E_t	-	Energy transmitted through the breakwater
Eu	-	Euler number
F_D	-	Drag force
F_F	-	Friction force
F_l	-	Lift force
Fr	-	Froude number
F_S	-	Shear force
F_w	-	Gravity force
g	-	Acceleration of gravity
H	-	Wave height
H_m	-	Mean wave height
H_s	-	Significant wave height
H_{rms}	-	Root-mean-squared wave height
I	-	Hydraulic gradient in the filter layer
I_{cr}	-	Critical hydraulic gradient
I_{rms}	-	Equivalent value for the root-mean-squared gradient
K	-	Coefficient to take into account the difference of flow in open channels and in granular filters
L	-	Characteristic length dimension
L_a	-	Absolute erosion length
L_o	-	Deepwater wave length
L_r	-	Relative erosion length
L_{r2}	-	Relative erosion length 2
m	-	Relative filter layer thickness ($= d_f/D_{f50}$)
N	-	Number of waves in a test
n_f	-	Porosity of filter material
n_l	-	Length scale
n_p	-	Pressure scale
n_t	-	Time scale
n_u	-	Velocity scale
n_f	-	Porosity of the filter material
n_x	-	Scale factor of the physical parameter or quantity x
Re	-	Reynolds number
S_b	-	Bedload sand transport

S_s	-	Suspended-load sand transport
St	-	Strouhal number
T	-	Wave period
U	-	Mean velocity of the undisturbed flow
U_{*cr}	-	Critical shear velocity according to Shields
U_f	-	Filter velocity
We	-	Weber number
α	-	Slope angle between the slope and the horizontal
η	-	Dynamic fluid viscosity
ν	-	Kinematic viscosity of water
ρ_s	-	Density of the stone material
ρ_w	-	Density of water
ξ	-	Iribarren parameter or surf similarity parameter
ψ	-	Shields parameter

Chapter 1

Introduction



1.1 General introduction

1.2 Breakwaters

1.3 Structure of the report

Chapter 1 Introduction

Chapter 1 gives a general introduction to this study and report, an introduction to breakwaters with an explanation of rubble mound breakwaters and breakwater design, and a description of the structure of the report.

1.1 General introduction

Breakwaters are found all around the world where a structure, beach, harbour entrance or another object on the coast has to be protected against incoming waves. They take many forms and shapes and are constructed of various materials. In this study, focus is aimed at breakwaters constructed of granular materials like quarry rock and sand. Many examples exist of so called rubble mound breakwaters, constructed mainly of quarry rock. Throughout the years, experience and knowledge of the processes and stability criteria increase, leading to more economic designs.

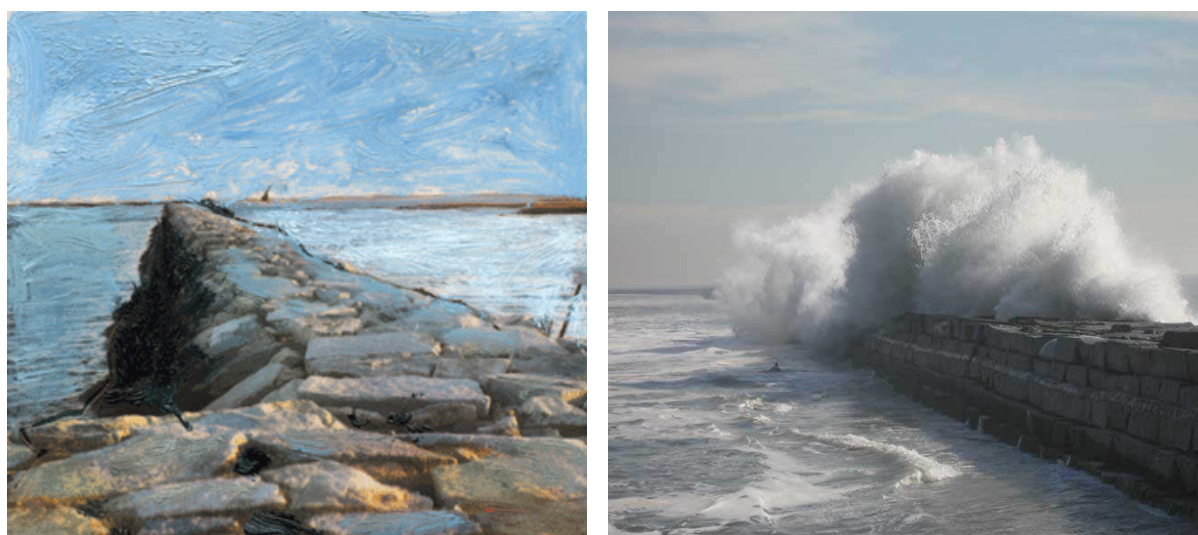


**Figure 1-1 Left: Breakwater at Provincetown, USA, painted by Barbara Cohen (from: BC-Print)
Right: Storm surge hitting the Los Angeles breakwater (from: LA city Lifeguard Association)**

Recent developments in construction methods and lifetime cost calculations have led to designs with for instance a large amount of stones (berm) on the outer slope of breakwaters which are redistributed over the slope by the waves (the so called berm breakwater), and to interest in designs with sand cores covered by only one or two layers of relatively large stones (hydraulically sand-open filter), resulting in a breakwater that is unstable when the traditional criteria are applied. Deformation to some degree in a storm and maintenance works after a storm can be accepted if the circumstances allow it and if the savings in construction costs outweigh the extra maintenance costs.

The interest in breakwaters with a sand core and hydraulically sand-open filter has led to the research into the stability and applicability of these structures, with the eventual goal of having a reliable design tool. A thesis study has been done by E.F.

Uelman¹, who performed physical model tests in a wave flume with regular waves loading the cross section of a breakwater. This breakwater consisted of a sand slope with a steepness of 1:3 and a single layer of stones, with varying grain size and layer thickness in the different tests. The results show erosion of core material during wave attack, but also a tendency of the erosion growth to an equilibrium situation within the duration of the simulated storm, thus showing a potentially valuable design method.

The present thesis study is the next step of the research into the stability of breakwaters with a sand core and hydraulically sand-open filter. The results of the former tests and the available knowledge from adjacent applications form the basis to a new test program in which focus will be at performance of the breakwater design under irregular waves, variation of the wave height and period, variation of slope steepness and filter material grading, and on the magnitude of scale effects that are inevitable for tests on a small scale.



Figure 1-2 Example of test 14 before the tests (left) and after 90 minutes of testing (right)

The objective of this Msc. thesis is to find relations for the influence of variations of the hydraulic loading, slope steepness and grading of filter material on the stability and erosion patterns of core material in a breakwater configuration with a hydraulically sand-open filter on a sand core. This will be done by performing physical model tests in a wave flume. The growth pattern of the erosion and the occurrence of an equilibrium situation in this erosion, are the main interests as results of the tests.

In this report, first the general aspects of breakwaters, filter layers and hydraulically sand-open filters are explained in the introduction, after which chapter 2 gives an overview of relevant existing knowledge, including the results of Uelman (2006), leading to a problem analyses and formulation of the objective in chapter 3. The scale effects and internal processes are further elaborated in chapter 4, after which a test program is put together in chapter 5. The results are presented in chapter 6, followed by their analysis in chapter 7. Chapter 8, finally, summarizes the conclusions and recommendations for further research.

¹ Uelman (2006) [49]

1.2 Breakwaters

The ancient Greeks and Romans already built breakwaters to protect their harbours from the waves of the Mediterranean. Sometimes these were rubble mound breakwaters made from rock found in the vicinity of the harbour, and sometimes even monolithic structures, for instance the concrete breakwaters built by the Romans. From the nineteenth century on, composite structures have been built as well, existing of a foundation berm of rubble material and a monolithic structure on top of the berm. These composite breakwaters showed to be more economic in relatively deep water.² In more shallow water, often rubble mound structures are applied and sometimes monolithic structures are applied when the subsoil is suited for a good foundation. The rubble mound structures are found all around the world.

1.2.1 Granular or rubble mound breakwaters

Granular material is loose, non-cohesive material like quarry rock or sand. Rubble mound breakwaters are made of granular material and therefore also called granular breakwaters. In essence, a granular or rubble mound breakwater exists of a large heap of loose rock, usually with a core of varying grain sizes, on which a number of filter layers with increasing grain sizes are placed, and an outer armour layer with large selected stones that are heavy enough not to be washed away by the waves.



Figure 1-3 Example of a granular breakwater, photo by Gary Curtis (from: fantompoet.com)

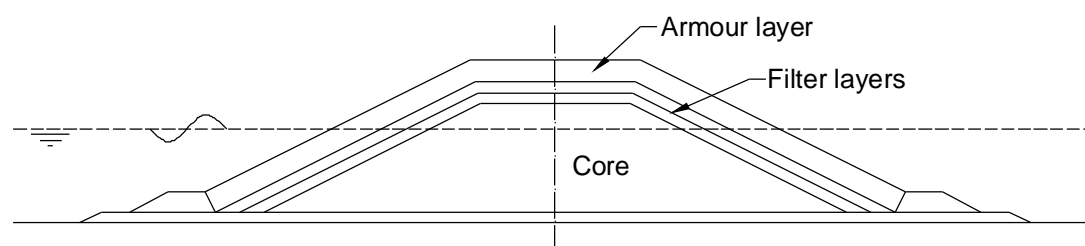


Figure 1-4 Basic layout of a standard granular breakwater

² d' Angremond and van Roode (2001) [4]

Core of the breakwater

The core of the breakwater has to fill a large volume and has to be strong enough to support the filter and armour layers. Additional requirements can for instance be limitations to the amount of transmitted wave energy. Sometimes the core is made of sand, but usually of quarry-run, a variation of grain sizes that comes from the quarry and needs very little selection. Large quantities are needed; therefore relatively inexpensive materials are used.

Geometrically closed filter layers

For the filter layers, selected grains are used with a grading that fits the design. The purpose of a filter layer is to block the underlying stones from being washed out and to let water flow in and out to prevent excess water pressures inside the pores. The open spaces between the grains in a filter layer should therefore be smaller than the characteristic grain size of the underlying material and the permeability should be higher than that of the underlying material. Simple rules for material properties like the Terzaghi³ rules for geometrically closed filters can be applied to achieve this. This type of filter layer is called geometrically closed because the grains of the under layer are physically blocked by the filter layer; the larger grains of the under layer are smaller than the constrictions (open spaces between the grains) of the filter layer.

Geometrically open filter layers

A filter layer, a layer of rock selected on a grading of grain sizes, gives resistance to the porous flow inside, that is driven by the waves or flow loading the structure. The filter layer reduces the loading in this way. If a filter layer has constrictions that are large enough to let the grains of the under layer pass, it is called a geometrically open filter layer. The grains of the under layer are now kept in place by the reduction of the loading; the filter layer has to give enough resistance to the loading to reduce it below the point at which grains of the under layer begin to move and are transported.

Hydraulically sand-open filters

When the grains of the filter layer are even larger (relative to the grains of the under layer) than for geometrically open filters, the filter layer is in fact not stable anymore. The loading is reduced, but not well enough to prevent transport of the grains of the under layer, so it is to be expected that under the design loading, some erosion of material through the filter layer will occur. If this amount of erosion is known beforehand and maintenance is accepted to repair the filter layer after a storm, this type of filter layer can be more economic than the above described types because fewer layers are needed to close the gap between the small grains of the core and the large units of the armour layer. This type of filter is called hydraulically sand-open.

1.2.2 Developments in granular breakwater design

For granular breakwaters, a tendency from geometrically closed structures towards geometrically open structures and possibly initially unstable structures where a certain loss of material is accepted can be observed. For instance the berm breakwater, where a large amount of stones is placed and redistributed into a stable shape by the waves, or a breakwater with a hydraulically sand-open filter on a sand core, where a certain

³ Schiereck (2001) [42]

loss of core material under design conditions is accepted, are either applied or under development. The latter example is the topic of this study.

Increasing knowledge

For geometrically closed filters, the classical way of building filters, simple rules can be applied. The grains are physically blocked by the filter layer above, only the armour units are loaded directly by the loading and have to be designed for the particular loading situation. For geometrically open filters, also the under layers are directly loaded by the external loading as the filter layers only reduce the loading. More knowledge is necessary about the values for threshold of motion of different grain sizes and reduction of the loading by the filter layer to come to a good design. In the nineties of the former century, design relations and diagrams have been constructed for the practical application. For hydraulically sand-open filters, besides the threshold of motion, also the amount of transport and erosion of core material through the filter and the effect of that on the structure as a whole has to be known. Research into this type of filter layers is only very recent and going on.

Accepted maintenance programs

Recent developments in construction methods and labour costs have changed the designs of coastal structures. Labour intensive construction methods have become more expensive where bulk transport and positioning of sand and rock has become relatively less expensive due to larger and more efficient machines like dredgers, stone dumping vessels and other equipment. These developments lead to a situation where maintenance of a structure during its lifetime can be more economic than a very rigid design. The interest for hydraulically sand-open filter structures fit in this development where maintenance is considered in combination with construction costs.

1.3 Structure of the report

This report presents the findings of the thesis project. To give an overview of the contents, the structure is explained per chapter. Extra information, graphs and notes per article from the literature study are shown in the appendices.

Chapter 2 gives an overview of the theory on geometrically open filters as found in the literature study. The important processes and knowledge about similar processes are described.

Chapter 3 analyses the problem of applying hydraulically sand-open filters in a breakwater. The lacking knowledge for this application is studied and the essential parameters are defined. After that, the objective is formulated as a part of a larger research into to the topic of hydraulically sand-open filters.

Chapter 4 describes and analyses the scale effects and the processes that occur inside the filter layer. A dimensional analysis of the process as a whole and of separate parts of the process has been performed and the results are compared with findings in literature for similar processes to come to a quantification of scale effects.

Chapter 5 shows the test program of the model tests with variation of the hydraulic loading. Choices for the parameters of the different tests are made based on the expected influences of those parameters on the erosion process. The test setup, materials and measuring techniques are described as well.

Chapter 6 shows the results of the tests and a detailed description of the observations during the tests. The data obtained from measuring are transformed into graphs and one page with the most important information is shown for each test.

Chapter 7 presents the analysis of the test results. The erosion parameters are calculated and related to the loading parameters. The dimensional analysis from chapter 4 is used to find dimensionless relations between loading and erosion that can be used for design purposes.

Chapter 8 gives the conclusions and recommendations for further research. The conclusions are formed by the main conclusions drawn from the analysis of the tests and by the evaluation of these results to the objective of the study, which allows placement of the results in the larger research into hydraulically sand-open filters. The recommendations give possibilities for different forms of further research to reach the eventual goal of having good descriptions of the erosion processes and making a good design tool.

In the appendices, a study of the report of E.F. Uelman⁴, the first graduate student that studied this subject, is presented, after which a record of the literature study is shown with notes and comments for the studied articles. The work plan is added and extra graphs and plots from the model tests are shown.

⁴ Uelman (2006) [49]

Chapter 2

Theory geometrically open filters



2.1 Existing design criteria and new developments

2.2 Geometrically open filter processes

2.3 Scaling problems

2.4 Research done by E.F. Uelman

2.5 Materials and their influence

2.6 Schematisation of processes

2.7 Essential parameters for the erosion process

Chapter 2 Theory geometrically open filters

This chapter gives a general overview of the theory about geometrically open filters and the processes involved. The theory is obtained from a literature study, of which a more detailed report with references is given in Appendix II.

2.1 Existing design criteria and new developments

Geometrically closed filters

Criteria for geometrically closed filters⁵ often result in uneconomical designs. The resulting multiple thin layers are difficult to construct and a number of gradations are needed. In situations with considerable flow velocities or wave conditions during construction, it can be a problem to construct the first layers of quite fine material. Separation of the graded material and loss of material are hard to prevent.

Geometrically open filters

From around the mid 1980's, new criteria have been developed, for geometrically open, but hydraulically sand-tight filters⁶. The result is a more economic filter design, but more knowledge about the hydraulic conditions is necessary. The research for this topic is aimed at understanding primarily the processes leading to incipient motion, the filter is considered stable when no or a negligible amount of erosion takes place during design circumstances.

Hydraulically sand-open filters

To go one step further towards economically designed filter constructions, the focus is now aimed at geometrically open and also hydraulically sand-open filters⁷, hereby accepting a certain amount of loss of (core) material during design circumstances. This loss can either be supplied by maintenance work, or just be accepted when it poses no threat to the construction at all. For this way of designing filters, however, even more knowledge about the occurring processes is needed.

⁵ De Grauw et al. (1984) [15]

⁶ Klein Breteler et al. (1990) [31]

⁷ Uelman (2006) [49]

2.2 Geometrically open filter processes

The purpose of the filter structure in a breakwater is to protect the core material from being washed out by the pressures and flow forced by the loading. For a breakwater, usually the loading by waves is dominant resulting in cyclic (irregular) pore pressure variations, causing porous flow.

2.2.1 Loading

Breaking waves

Waves are the dominant loading force for breakwaters. At sea, wind-waves are generated with different wave height and period. During storms, waves with a height of 10 m and periods of 10 to 12 s are no exception. Wind-waves are irregular, making them difficult to model; a spectral analysis is usually taken for this purpose. When waves enter too shallow water (or become too steep), they start to break. The type of breaking differs and can be described by the Iribarren parameter⁸:

$\xi = \frac{\tan \alpha}{\sqrt{H/L_0}}$ with $L_0 = \frac{gT^2}{2\pi}$. For values around $\xi = 1,5$, the breaking is called

plunging; the top of the wave forms a separate jet plunging into the trough in front of it. The impact of the jet and the pressure variations caused by this type of breaker are very high and this type of breaker causes the most damage. For typical wind-wave parameters and typical breakwater slopes, this plunging breaker type is very common.

Wave modelling

It is quite difficult to calculate or model waves. Regular, non-breaking waves can be calculated using the linear wave theory, but wind-generated waves loading a breakwater are in fact irregular and breaking. Research into numerical modelling of breaking waves is ongoing, resulting in increasingly good representation of wave loading. The VOF (Volume of Fluid) method⁹, together with some form of the Navier-Stokes equations, gives quite good results.

Load reduction in armour/filter layers

Inside the rubble material, the energy from the waves is reduced. The incoming energy is first divided: $E_i = E_d + E_r + E_t$: incoming energy = absorbed + reflected + transmitted energy. $E_i = \frac{1}{8} \rho g H_i^2$. The velocities and turbulence caused by the waves rapidly diminish inside the filter, indicating that a thicker filter gives more reduction. However, deeper than a distance of about 1,5 D_{f50} inside the filter, no further reduction has been found¹⁰. Thicker filters do work better for erosion prevention, but the cause must be sought in the longer path grains of the core have to travel to get out of the filter, experiencing more resistance.

⁸ Schiereck (2001) [42]

⁹ Van Gent et al. (1994) [13], Troch (1996) [45]

¹⁰ Schiereck et al. (2000) [43]

2.2.2 Porous flow and hydraulic gradient

The pressure fluctuations induced by the waves cause porous flow inside the filter and core. In sand, the flow is laminar and only laminar resistance has to be taken into account. In larger grained material (filter or larger grained core), turbulence and inertial resistance have to be taken into account as well. The (extended) Forchheimer equation¹¹ relates the hydraulic gradient to the pore-velocity:

$$I = a \cdot U + b \cdot U \cdot |U| + c \frac{dU}{dt}$$

Of the terms, the first = laminar, the second = turbulence, the third = inertial resistance. The coefficients a, b and c have their own expressions with empirical coefficients in them. For laminar flow (in sand), only the first term is important, reducing the equation to Darcy's law, with $k = 1/a$.

Hydraulic gradient

The hydraulic gradient is the gradient in hydraulic pressures, and causes the water to flow. The pore-size and with that the resistance of the material depends on the grain-size; sand with a very small grain size has a higher resistance than gravel or rock with larger grain sizes. A higher gradient is then needed to give the same flow rate.

Parallel and perpendicular flow

Two basic flow situations can be separated: parallel and perpendicular flow. With parallel flow, the hydraulic gradient is the same in filter and core, and the velocity in the filter is much higher than in the core with its higher resistance. The difference in velocity also causes a difference in the velocity of the phreatic surface, resulting in a discontinuity between filter and core. This is called the disconnection. With perpendicular flow, continuity demands the same (averaged) flow rate in both filter and core. Therefore a higher gradient in the core than in the filter is needed. Both perpendicular and parallel flow occur under wave loading.

Internal set-up

A phenomenon frequently present in breakwaters is internal set-up¹². The water table inside the breakwater is higher than the still water level outside. Outflow of water mainly happens in the lower part of the slope, the water has to flow through a smaller area than during inflow. This requires a higher pressure gradient, realized by a higher water level inside.

Modelling porous flow

More and more is known about the processes occurring in the rubble material, but the modelling of these processes is still difficult. It is possible to couple a VOF model for breaking waves to a model for porous flow, e.g. using the Navier-Stokes equations with the Forchheimer resistance terms¹³. It is, however, still not possible to solve these equations inside the pores to get the exact flow velocities, due to the complexity of the system and the amount of calculations needed. Therefore, the velocities are averaged over an area larger than a pore, but smaller than the characteristic length scale of the physical problem. It is however still difficult to take the turbulence generation-dissipation properly into account.

¹¹ Van Gent (1995) [14]

¹² De Groot et al. (1988) [17]

¹³ Liu et al. (1999) [33]

2.2.3 Stability

The ratio between the grain sizes of core and filter material is an important parameter for the stability of filters. For open filters the ratio $n_f * D_{f15} / D_{b50}$ is often used. The area of interest for geometrically open filters is¹⁴: $2,5 < (n_f * D_{f15} / D_{b50}) < 6$ à 7. For lower values the filter is geometrically closed; for higher values fluidization occurs and the filter becomes hydraulically sand-open. These higher values are the focus of this study.

Initiation of motion

For parallel flow, the velocity difference at the interface described earlier causes a shear stress on the upper grains of the base material. This shear stress causes grains to move, especially along the interface. For perpendicular flow, a hydraulic gradient above some critical value initiates the transport of core material into and through the filter.

Stabilising mechanisms

Two mechanisms can cause an unstable appearing filter to be stable (perpendicular flow): Grains, set in motion by the wave-induced turbulence and transported through small constrictions, arrive in larger pores with lower water velocities and slow down and stop moving further. The second is arching: small grains form arches over the constrictions preventing wash out. Cyclic loads (waves) destroy arches and have a lower critical gradient than steady loads¹⁵.

Critical hydraulic gradient

The critical hydraulic gradient is the gradient that lies at the initiation of motion and is a function of core- and filter material characteristics, and of the flow type (filter velocity, physical properties of water). De Grauw (1983) related this critical parallel gradient to the critical Shields velocity (empirically):

$$I_{cr} = \left(\frac{0.06}{n_f^3 D_{f15}^{4/3}} + \frac{n_f^{5/3} D_f^{1/3}}{1000 D_{b50}^{5/3}} \right) U_{*cr}^2 .$$

If the pore spaces of the filter are large relative to

the grain size of the core material, the critical shear stress at the interface is assumed to be equal to that at the bottom of an open channel (bed material equals core material). Klein Breteler used the Shields¹⁶ criterion to relate the critical filter velocity to the D50 of the core material. For turbulent flow parallel to the interface at a

horizontal bed this results in: $I_{fer} = \frac{C_7 \psi_b \Delta_b D_{b50}}{\kappa^2 D_{f15}}$.

Modelling problems

With the known theoretical and empirical information, modelling should be possible, but as stated above, the determination of exact gradients and velocities inside the pores is still problematic. Nevertheless, numerical modelling is improving and results are promising.

¹⁴ Schiereck (2001) [42]

¹⁵ De Grauw et al. (1983) [16]

¹⁶ Schiereck (2001) [42]

2.2.4 Transport of material

The transport mechanisms for perpendicular and parallel flow are different and can be described separately, although under wave loading both types occur simultaneously, making the total process rather complicated. To gain understanding about the processes the distinction is made however.

Forces acting on a grain

Flow over a grain results in a drag force, a shear force and a lift force. The submerged weight keeps the grain in place, together with the friction force of friction with other grains. As long as the weight and the friction are large enough to balance the drag, shear and lift forces, the grain stays where it is, but when the flow induced forces become too large, the grain starts to move. The velocity for which there is just a balance is the critical velocity, and the gradient corresponding to it is the critical hydraulic gradient.

Perpendicular transport

The type and magnitude of perpendicular transport depends on the gradient in the core layer¹⁷. For low gradients ($I_{perpendicular} = \text{head difference} / \text{distance} \approx 1-2$), the grains only rotate or shake a bit. For higher gradients ($I_{perpendicular} \approx 2-3$), pores are sporadically suddenly filled with a high density mixture of water and core material. For values of $I_{perpendicular} \approx 3-8$, transport through channels of several constrictions occurs. For gradients higher than approximately $I_{perpendicular} \approx 10$, a thin mixture flows through the filter. The perpendicular transport is always collective, because when a single grain moves from the core, the gradient will decrease and the grain will fall back. This does not happen when the gradient is large enough for collective transport. A sharp boundary between a penetrated and a clean filter is observed.

Parallel transport

Parallel flow results in transport in the same direction, governed by independent movement of grains¹⁸. For low velocities (once or twice the critical velocity), grains move along the interface in a very thin layer of just one grain thickness. For higher velocities the thickness of this layer increases, where the grain velocity is about half the flow velocity.

Modelling transport

For the modelling of the amount of transport, detailed information on the flow velocity field is needed. As this is still difficult for breaking-wave-induced porous flow, the modelling of the transport is also difficult. Research is going on, but no good working model for this is available yet.

2.2.5 Deformation of the structure

When designing breakwaters economically optimal, a certain amount of damage (e.g. loss of core material), can be accepted, when maintenance is expected to cost less than a more rigid design. For this purpose, the amount of material that is transported out of the core and the reaction or deformation of the filter and/ or armour layer to this must be predicted. At this moment, no clear method is available to do this in a reliable way.

¹⁷ Den Adel (1992) [2]

¹⁸ Den Adel (1992) [3]

2.3 Scaling problems

The scaling down from a prototype to a model gives significant problems. The different properties of water cannot all be scaled down with the same factor because the effects are not linear. One can keep the Froude number the same in prototype as in model (Froude-scaling) to keep the inertia and gravity forces in the same ratio, but then the Reynolds number changes. For low Reynolds numbers the viscosity of the water changes the flow type. In coastal engineering, viscous forces easily become too large in the model.

Explanation of the scale effects

First the six main types of scaling are mentioned below¹⁹, after which other scaling aspects related to the topic are treated. In sections 4.1 and 4.2, the specific mechanisms of scaling for a breakwater with an open filter on a sand core are analysed and magnitudes of the scale effects are estimated. Here, the scale effects and scaling laws in general are treated. The main difficulty with the different scaling laws is that they can never all be satisfied simultaneously and therefore compromises are used to get an acceptable result. The scaling laws are based on the assumption that two forces dominate the flow. In these laws, one of the forces is the inertial force, always important, and the other varies, depending on the type of flow.

Scaling laws

$Fr = \frac{U}{\sqrt{gL}}$ Froude scaling: maintaining the same Froude number, $n_{Fr} = 1 \rightarrow n_t = n_u = n_l^{1/2} = n_p^{1/2}$. The Froude number is the square root of the ratio of the inertial force and the gravity force. The Froude scaling law applies when the inertial force is primarily balanced by the gravity force, which is the case for most types of free surface flow and when waves are the dominant forcing mechanism. Froude scaling, however, neglects the effects of viscosity and surface tension. For breaking waves, surface tension effects can be very important, especially when $L < 0,5\text{m}$, or $T < 0,5\text{s}$, and for porous flow, viscous forces can become dominant. For most coastal engineering models, Froude scaling is the most important criterion.

$Re = \frac{UL}{\nu}$ Reynolds scaling: $n_{Re} = 1$. $n_t = n_l^2$; $n_u = n_l^{-1}$; $n_p = n_l^{-2}$. The Reynolds number is the ratio of inertial force and viscous force, and the Reynolds scaling law is important when viscous forces dominate in hydraulic flow. This is the case for flows with relatively low Reynolds numbers, like laminar boundary layer problems or (laminar) flow through for instance sand. For flow through gravel size material, both Froude number and Reynolds number play an important role, leading to the dilemma of which scaling law to follow.

$We = \frac{\rho U^2 L}{\sigma}$ Weber scaling: $n_{We} = 1$. The Weber number is the ratio of inertial force and surface tension force. Surface tension can be a dominant force for flow of very

¹⁹ Hughes (1993) [26] and Tirindelli et al. (2000) [44]

thin films of liquid and for water with entrained air bubbles like in breaking waves. For most coastal engineering problems, the surface tension plays no major role, but for the impact of breaking waves, it might be important because a lot of air can be entrained.

$Ca = \frac{\rho U^2}{E}$ Cauchy scaling: $n_{Ca} = 1$. The Cauchy number is the ratio of inertial force and elastic force. It is related to the Mach number, and is important when compressibility is the dominant factor. Compressibility of water is hardly ever the dominant force for free surface processes, although the compression of air trapped by a breaking wave might be an exception to this.

$Eu = \frac{P}{\rho U^2}$ Euler scaling: $n_{Eu} = 1$. The Euler number is the ratio of pressure force and inertial force and is important when pressure is the dominant force acting on the flow.

$St = \frac{L}{UT}$ Strouhal scaling: $n_{St} = 1$. The Strouhal number is the ratio of temporal and convective inertial forces. It is important in unsteady, oscillating flows.

Gradient scaling

For the scaling of rubble mound breakwater models, Burcharth²⁰ proposes to keep the hydraulic gradient inside the breakwater core the same in model and prototype, because it is believed to be the dominant driving mechanism rather than gravity or viscosity as follows from Froude or Reynolds scaling. The problem with this approach is that the gradient varies in time; therefore a characteristic gradient is used. The deviation of the gradient and velocities from this characteristic remains a problem, as well as the determination of the characteristic gradient in model and prototype situations.

Scaling of sand and rock

Sand is a non-cohesive granular material within a range of particle sizes of about 60 – 2000 μm . Larger particles become gravel, with different behaviour, especially hydraulically. Flow in sand is laminar and in gravel partly turbulent. Smaller particles than 60 μm become silt and are cohesive, giving very different behaviour. Rock or stones, as used in the filter layer, do not change much when scaled down, but the smaller the stones get, the smaller the pores get, and then viscous forces become increasingly important. As long as the Reynolds number stays above 10.000, no problems arise, but below this value the differences increase for decreasing Reynolds numbers.

No easy solution

Altogether, scaling of breaking waves, porous flow and sand transport leads to problems for which no easy solution exists. In chapter 4, the scaling problems will be specified to the topic of open filters in breakwaters with a sand core, by means of a dimensional analysis and comparison of the problem with known similar situations and effects from literature.

²⁰ Burcharth et al. (1999)

2.4 Research done by E.F. Uelman

The Msc. thesis of Evert Uelman (2006)²¹ forms a first step of the study into the stability of granular hydraulically sand-open filters in breakwaters with a sand core. After a literature study he performed model tests in a wave flume with regular waves loading a single layer of riprap (filter and armour in one) on a sand slope for different filter grain sizes and filter thicknesses.

Model set up

A process based model test has been chosen (no scaling of a larger model), because of the problems with scaling described earlier. The parameters D_f and d_f are varied in the tests, the rest is set at a representative value. Regular waves have been used, where H and T are taken as typical values for wind waves, $H = 10$ cm, $T = 1,2$ s. The number of waves is chosen typical for a storm of 8 hours with a T of 12 s which results in 2400 waves. D_b is chosen small to get erosion in the tests. Only one layer is used as filter/ armour layer.

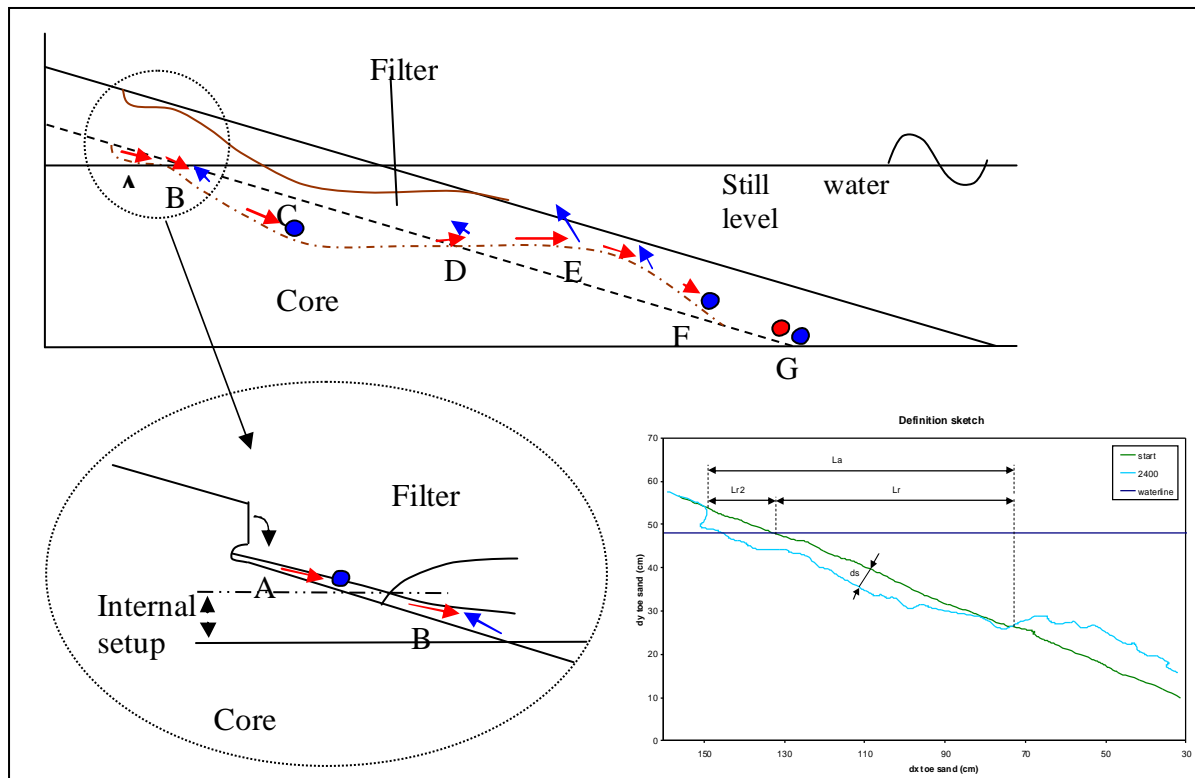


Figure 2-1 Sketch (left) and plot (right) of the result of one of the performed tests. From Uelman

Observations

A profile develops resembling a bar profile on a sandy beach. Both bedload (sheet flow) and suspended-load transport have been observed. The points indicated in the figure are discussed below:

A: erosion, an almost vertical slope develops and is undermined by the up-running wave.

²¹ Uelman (2006) [49]

B: sand is moving up and down by the reduced wave, not in phase with the outside wave.

C: erosion, mainly bedload transport during wave run-down, less transport during wave run-up, but also suspended-load transport.

D: net erosion = zero. Run-down: mainly bedload transport. Run-up: mainly suspended-load transport. D is the bending point of the bar profile.

E: sedimentation, a lot of suspended-load transport.

F: only transport during run-down, first both types, later only bedload transport.

G: no transport.

The internal setup ranges from 0 or 1 to 3 cm for different tests. Between A and B a small wave in the filter layer develops, running up and down the sand slope. Between C and F the outside water layer is much thicker with the up-running wave than with the down-running wave, so more water has to flow through the filter during run-down than during run-up. The result is a higher filter velocity during run-down.

Analysis

The erosion in A is discontinuous, it is hard to tell if it is decreasing in time or not. At B and C the erosion is decreasing in time. At E the sedimentation is decreasing in time. After 2400 waves there is still erosion, but it is decreasing in time. The erosion is considerably less than at the beginning, but equilibrium has not yet been reached. A dependency on $m (=df/Df)$ is clearly visible from the results; a larger m means less erosion. Lr (see figure) increases with increasing filter thickness, probably because point D stays directly under the run-down point of the wave, which shifts further down. Lr increases with increasing Df , because larger stones give less wave reduction. $Lr2$ decreases with increasing m , with increasing df and with decreasing Df . The erosion depth ds (= erosion after 2400 waves / La): a larger Df and a smaller df give a larger ds . Both were to be expected. ds versus m gives a possible linear relation: $d_s \approx 0.058 - 0.4 \times m$. ds decreases with increasing m , so more layers of filter grains reduce the erosion depth.

Remarks

The findings mentioned above are obtained after the study of the test results, for which a number of graphs and plots of combinations of various parameters have been presented. Due to limited available time for the Msc. thesis in general and for the availability of the wave flume in particular, not more tests could be performed.

2.5 Materials and their influence

Materials have properties, of which the grain size and the grading (the distribution of grain sizes) are very important. Other properties like roundness, smoothness, shape and density also have their influence, but for this moment they are not taken into account. The material is assumed to have a normal density of about 2650 kg/m^3 and a shape normal for quarry rock. Besides the properties of the material itself, the thickness of the filter/ armour layer is addressed here, because the combination of grain size and layer thickness is important.

2.5.1 Core material: sand

Sand consists of non-cohesive stone-like particles in the range of $60 \mu\text{m}$ to 2 mm with a typical solid density of 2650 kg/m^3 and an average porosity of $n = 0,35$ to $0,40$.

Grain size core material: D_{b50}

The grain size of the core material (sand in this case) is denoted as D_{b50} , where the b stands for base (= core) and 50 stands for the median grain size: 50% by weight of the grains is smaller than this sieve size.

A larger grain weighs more than a smaller one and is therefore harder to transport by flow. The larger the grains, the stronger the flow has to be to transport them. So, larger core material should give less erosion. The reason that the relatively fine material sand is interesting as core material is that it is available in large amounts on many locations, which saves on quarry operations and sometimes very long hauling distances.

2.5.2 Filter material: rock

The filter/ armour layer is made out of stones (rock). This material comes from quarries, where the rock is blasted from the mountains and crushed in a crusher to get the desired grain sizes and gradings. For smaller stones the D_{50} or D_{n50} (the side of a cube with the same weight as the stone, $D_{n50} \approx 0,84 D_{50}$) are often used, as for larger rock, the mass range is the usual parameter, like e.g. 60-300 kg.

Grain size filter material: D_{f50}

In the tests done by Uelman, a D_{f50} of 18, 33 and 42 mm is used. The results show that the smaller the filter grains are the less erosion of core material occurs. This indicates that the (turbulent) flow inside the filter pores caused by the waves is more reduced when these filter grains and therefore the pores, are smaller. Larger pore holes give room to larger turbulent fluctuations and give less resistance to the total flow. For these reasons one would try to make the filter material relatively small. On the other hand, smaller material is more sensitive to erosion by the waves. Therefore large filter grains are preferred, to prevent the whole filter layer to be washed away by the waves.

Layer thickness: d_f

The thickness of the filter layer is important; the thicker the layer, the less erosion occurs. The filter layer does two things: reduction of the loads and resistance against the transport of core material. One would expect that the turbulent velocities forced by the waves are reduced while going further inside the filter. This does happen, the

velocities rapidly diminish at first, but further than a distance of about $1,5 D_{f50}$ inside the filter, tests show no further reduction²². The reason that a thicker filter layer gives less erosion lays probably in the higher resistance that grains experience during outflow, because the path they have to travel is longer.

Relative layer thickness: m

The relative layer thickness $m = d_f / D_{f50}$ can be seen as the average number of stones on top of each other in the filter layer. This parameter is found to be important and works similar to d_f , a larger m gives less erosion. Uelman (2006) even found a linear relation between the erosion depth and m for $2 < m < 4$. In this range, the influence of m is strong. For traditional, geometrically closed filters, the layers do not have to be larger than about $m = 2$, whereas the very open filters work considerably better for larger values of m .

2.5.3 Grain size ratios and grading

The ratio of the grain sizes of the filter and the core is of great importance for the way the filter functions. Besides that, the grading, i.e. the ratio of internal grain sizes is important as well.

Grain size ratio: D_{f50} / D_{b50}

For small ratios of grain sizes, say D_{f50} / D_{b50} smaller than 5 to 7, the filter is geometrically closed; the core particles are physically restricted to go through the filter. For very high values of D_{f50} / D_{b50} , say higher than 12 to 14, the filter hardly seems to work at all; the core particles are so small compared to the filter stones that they hardly feel resistance to flow through the filter. However, if the filter layer is sufficiently thick and some erosion is accepted, much higher values can still work. Uelman used ratios of D_{f50} / D_{b50} of over 200 where the filter still functions. Slightly different ratios are used often as well: $D_{f15} / D_{b85} < 5$, as stability criterion for geometrically closed filters, or $(n_f^* D_{f15}) / D_{b50}$ as parameter for geometrically open filters. The difference between the different ratios is that other points of the sieve curves are used and therefore other values are found. The result is the same.

Grading

The grading is important for the internal stability of material. If the grading is very wide, e.g. $D_{85} / D_{15} > 2,5$, the difference between the smaller and the larger grains is larger. Usually, layers with large rock have a narrower grading than layers with small stones or sand. The advantage of a wider grading is that the larger particles can prevent the smaller particles from being washed out, giving a larger filter capability. However, if the grading is too wide, the material becomes internally unstable; the smaller grains are easily washed out from between the larger grains. A commonly used criterion for internal stability is the rule by Terzaghi: $D_{f60} / D_{f10} < 10$. Other values for other situations have been proposed by various researchers.

Grading filter material

Especially interesting for this research into open filters on a sand core is the grading of the filter layer. If this grading is relatively wide, the smaller grains will fill the large pores, making the largest constrictions smaller. This way, a filter layer with the same

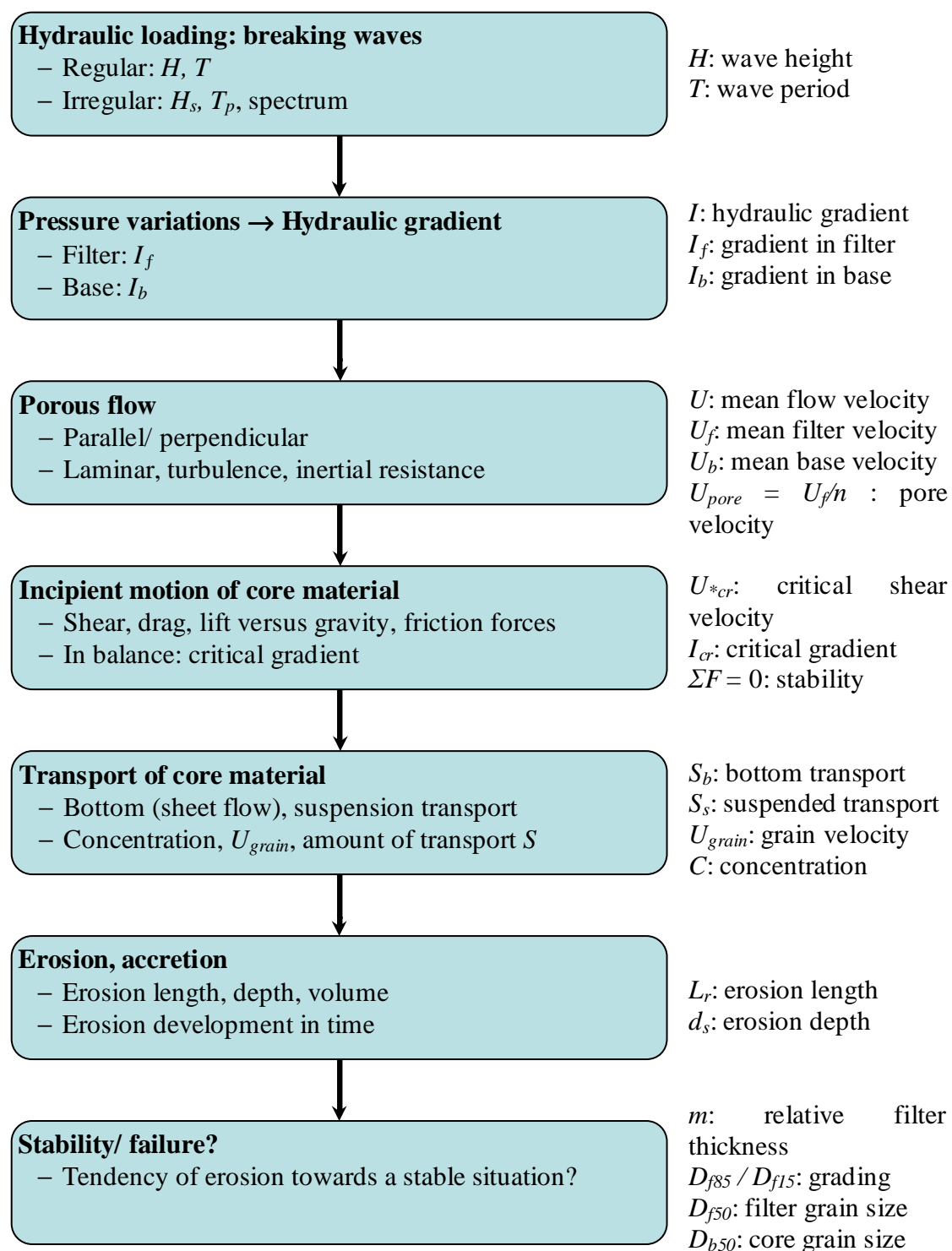
²² Schiereck et al. (2000) [43]

D_{f50} and the same d_f gives less erosion. Wide gradations can be more difficult to place, as separation can occur when the stones are dumped. Equipment for more careful placement is available, like fall-pipe vessels for precise placement on large depths. In the tests by Uelman (2006) no variation in gradation was tested, the used gradations are quite common, and not very wide.

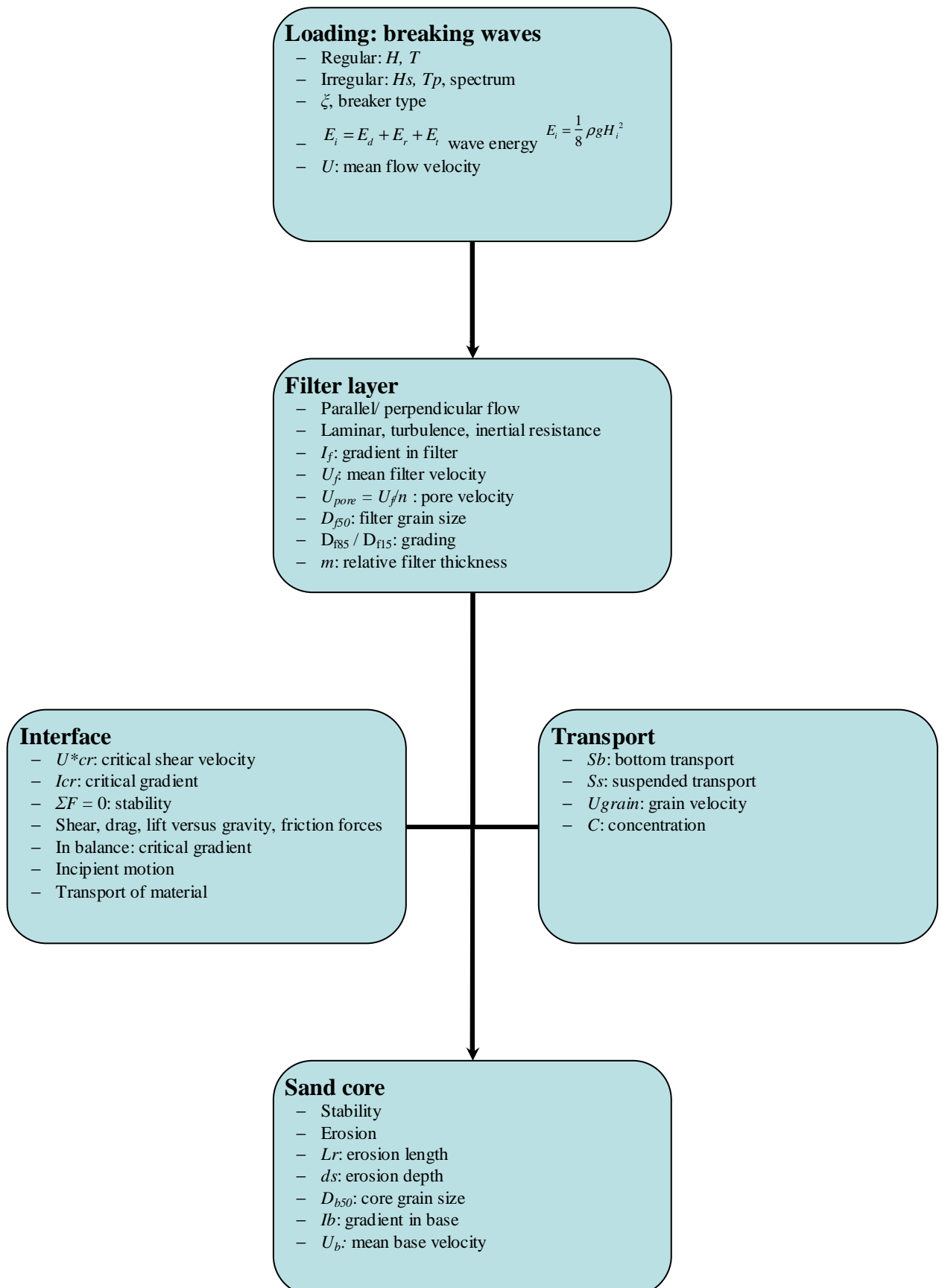
2.6 Schematisation of processes

To get a clear picture of the different processes and parameters involved in the breakwater system, two schemes have been made. Their main purpose is to get a better overview of the processes.

2.6.1 The process from loading to erosion



2.6.2 Physical parts and their processes



2.7 Essential parameters for the erosion process

In the schematisation of the processes of section 2.6 a lot of parameters are listed with these processes. Knowledge of the parameters is essential to understand the processes in the breakwater with hydraulically sand-open filter. Different parameters are associated with different processes in the breakwater. The most important are mentioned here and some remarks are made. A difference is made between adjustable and dependent parameters. Adjustable parameters can be changed by a different test set-up, different test type or different test settings. Dependent parameters depend on these adjustments.

2.7.1 Loading: breaking waves

Adjustable parameters

- H : wave height, determines the amount of energy that is loading the structure. Larger waves give more energy, higher (porous) flow velocities and (expected) more erosion.
- T : wave period, larger periods give more time for porous flow to develop within one period.
- α : slope steepness, influences the type of breaking, milder slopes generally spread the breaking energy dissipation over a longer distance.
- *Regularity of the waves*: irregular waves give a different loading than regular waves.
- *Number of waves*: the duration of the loading is interesting for long-term processes.
- *Structure layout*: e.g. the crest height, berm or no berm can be varied. Expected to have influence on the stability.
- *Water level variations*: a varying water level under influence of a tide will certainly affect the outcome of tests. The level at which the loading works changes with the water level.

Dependent parameters

- ζ : breaker type parameter, depends on the slope and H/L_0 , so on α , H and T .

2.7.2 Filter layer and filter-core interface

Adjustable parameters

- *Parallel/perpendicular flow*: adjustable through the test-type (wave tunnel)
- D_{f50} : filter grain size, larger grains give more core erosion, but more filter layer stability (external)
- D_{f85} / D_{f15} : grading, wider grading gives a larger filter range, but less internal stability.
- m : relative filter thickness, the average number of stone layers, is related to the erosion depth.
- D_{f50} / D_{b50} : ratio of filter/ core material grain size. A larger ratio means a more open filter.

Dependent parameters

- *Laminar, turbulence, inertial resistance*, depends on the model set up and used materials.
- I_f : gradient in filter, depends on the loading.
- U_f : mean filter velocity, depends on the gradient and the resistance, related through the Forchheimer relation.
- $U_{f,pore} = U_f / n$: filter pore velocity

2.7.3 Core*Adjustable parameters*

- D_{b50} : core grain size, larger grains are less easy to transport.

Dependent parameters

- I_b : gradient in base (= core), depends on the filter and core pressures.
- U_b : mean base velocity, depends on the gradient and resistance.

2.7.4 Stability, transport and erosion*Dependent parameters*

- U_{*cr} : critical shear velocity, depends on the core grain size.
- I_{cr} : critical gradient, depends on the critical shear velocity.
- $\Sigma F = 0$: stability, equilibrium of the occurring forces.

- S_b : bottom transport, depends on the porous flow in the filter.
- S_s : suspended transport depends on the porous flow in the filter.
- U_{grain} : grain velocity, is typically about half the flow velocity.
- C : concentration

- L_r : erosion length, the length of slope over which erosion occurs.
- d_s : erosion depth, the depth over which the sand slope erodes.

2.7.5 Material properties*Adjustable parameters*

- D_{b50} : core grain size, larger grains are less easy to transport.
- D_{f50} : filter grain size, larger grains give more core erosion, but more filter layer stability (external)
- D_{f85} / D_{f15} : grading, wider grading gives a larger filter range, but less internal stability.
- m : relative filter thickness, the average number of stone layers, is related to the erosion depth.
- ρ_w : density of the material.

Water properties, adjustable by using another liquid

- ρ_s : density of water.
- ν : kinematic viscosity.

2.7.6 Scale effects

Dependent parameters

- $Fr = \frac{U}{\sqrt{gL}}$ Froude number: used for Froude-scaling
- $Re = \frac{UL}{\nu}$ Reynolds number: for Reynolds-scaling
- $We = \frac{\rho U^2 l}{\sigma}$ Weber number: Weber-scaling.

2.7.7 Remarks

The adjustable parameters can be varied in tests, either by different settings for the wave generator, by the use of different materials, by a different structure layout, or by a different type of test. The dependent parameters cannot be varied directly, but by varying the adjustable parameters, they can be influenced. In general, one tries to put in a desired combination of adjustable parameters, and measure the dependent parameters, to find relations between the input and output.

The parameters that can be adjusted can be summarized as the loading, the material properties, the structure layout and the test setup.

Chapter 3

Problem analysis and objective



3.1 Problem description; lacking knowledge

3.2 Choice of further research direction

3.3 Choice of general test setup

3.4 Objective

Chapter 3 Problem analysis and objective

After the overview of the known theory of geometrically open filter processes, this chapter tries to analyse the lacks of knowledge and what parameters are essential for this particular setup. The objective of the thesis study as a part of a larger research is formulated.

3.1 Problem description; lacking knowledge

As concluded after the literature study and also by Uelman (2006), insufficient knowledge is available to come up with a good design tool for breakwaters with geometrically open, hydraulically sand-open filters on a sand core. In this section, an inventory is made of which knowledge is lacking.

3.1.1 Loading: breaking waves

The process of wave breaking is complex and difficult to model, but more and more is known about it. The wave breaking process will not be studied in this research; only the effects, the velocities and turbulence near the filter layer that cause the gradients and porous flow inside the structure, are important for the internal processes.

Velocities on the outside of the filter

Velocities just outside the filter could be seen as the actual loading of the filter. However, the phreatic surface goes up and down and a large part of the filter surface is exposed with every wave trough, resulting in discontinuous velocity variations.

Wave parameter dependency

The relation between the amount of erosion and parameters like wave height, period, regularity, the number of waves and water level variations (tide), are not known; only the number of waves has been varied in the tests for this topic.

3.1.2 Filter layer and filter-core interface

The loading by the waves results in gradients and porous flow inside the filter layer.

Porous flow

The porous flow is maybe the most important process in the breakwater, causing the sand to move. It is difficult to measure, but the pressure variations might be possible to measure with a device put inside a filter stone or pore. Theoretical knowledge about porous flow induced by breaking waves is still very limited.

Perpendicular flow

Perpendicular flow occurs but is less clear than parallel flow. The combination of perpendicular and parallel flow causes the (stirred up) sediment to move, in which the perpendicular flow, when strong enough, moves the grains out of the filter. The occurring perpendicular velocities in the pores and the distribution between perpendicular and parallel flow are not exactly known.

Parallel flow

In the filter layer, parallel flow is significant; it is clearly observed in the tests done so far and results in drag, shear and lift forces on the grains at the interface. A large part

of the transport is also parallel to the interface. The detailed velocity distribution is not known. When measuring, the measuring device in a constriction affects the flow and with numerical modelling, until now the velocity field is averaged over an area larger than a pore. The exact flow velocities inside the pores are not known.

Interface

The interface between filter and core is the place where the erosion takes place. Here grains can be pushed out by (perpendicular) outflow from the core or they can be set in motion by the drag, shear and lift forces from the (parallel) flow in the filter layer. As mentioned above, the exact flow velocities in the pores and at the interface are not known. If these would be known, a relation between the occurring filter velocities and the critical shear velocity by Shields (threshold of motion), or the amount of transport could be studied.

3.1.3 Core

Especially perpendicular flow inside the core causes erosion. Parallel flow velocities in the core are much lower than in the filter and can be disregarded for the parallel transport which takes place in the filter layer (and interface).

Pressure build-up and outflow

During the run-down of the wave the external water level drops very fast, with the level in the filter following that movement. The level in the core is still high, resulting in a perpendicular gradient, in its turn resulting in perpendicular outflow. When this outflow is strong enough, sand grains are transported. The relation loading → outflow → transport is not known yet.

Transport of core material

The transport of core material leads directly to erosion and deformation of the structure. The amount of transport through the filter is very difficult to measure, because the filter grains are in the way for the usual measuring techniques. Until now, the erosion after a certain number of waves, measured through the side wall of the wave flume, is the only way the amount of transport was estimated in the tests.

3.1.4 Erosion and equilibrium

A certain amount of loss of core material is accepted. In other words, erosion will take place. The question is how much erosion under what circumstances and whether or not an equilibrium situation develops after some time, after some erosion. The tests so far show a bar shaped profile developing in time, and a decreasing erosion rate in time. It looks like a tendency towards a stable equilibrium situation, but there is no evidence of this.

Amount of erosion and measuring

The amount of erosion developing in time is very interesting for the behaviour of the breakwater. Uelman (2006) measured the erosion after every 300 waves by taking a photograph through the glass side wall of the flume and by processing this photo in a software program resulting in x,y coordinates and graphs. The size of the wall effect is not known, it is estimated by visual observation to be not too large. A better estimate of this or another way of measuring the erosion profile would be welcome.

Equilibrium

The development towards an equilibrium situation takes time. In real life, the design conditions occur only during a limited time. The duration of a storm can be e.g. 6 to 12 hours, depending on the climate. So, for the design condition, a limited amount of erosion within the maximum duration seems a good result. Nevertheless, for less severe conditions, some erosion might still occur and these conditions might have longer durations. In order to understand this process, knowledge of an equilibrium situation development is important.

Comparison with dune erosion

Dunes erode during storms. Sand is eroded from the steep dune slope by the high waves that are able to reach the dunes because of the water level set-up (storm surge). The sand is deposited lower, on the gentler slope of the beach. The process looks similar to the process observed by Uelman for the breakwater with sand core. Van der Graaf²³ describes a tendency of this erosion process towards equilibrium although the equilibrium situation is not reached during the storm surge. During the process the overall slope of the cross-shore profile decreases, resulting in erosion decreasing in time. Under normal conditions, erosion is restored towards the normal equilibrium situation. Interesting is the comparing decrease of erosion in time, the tendency towards equilibrium. It is however questionable if the erosion of the breakwater can be partly restored under normal conditions. Certainly, the stones of the filter layer will not be lifted again after settling.

3.1.5 Material properties

The different properties of filter and core material and their influence are described in section 2.5. Effects of some of them have been studied, but still a lot is uncertain.

Grain size

Most is known about the grain size of the filter. It has been varied in the tests. A smaller filter grain size results in less erosion. The grain size of the core has not been varied. This is more difficult to do because it is harder to change all the sand in the flume. Besides, the range of variation is limited when the core material has to be sand. The ratio of filter and core grain sizes, which is believed to be more important, changes with the filter grain size. More variation extends the dataset.

Filter thickness

The effect of different filter thicknesses has been studied. A thicker filter gives less erosion and a larger relative thickness m also gives less erosion, even with a linear relation between m and d_s . As mentioned earlier, the equilibrium in erosion has not been found yet; this can be interesting to investigate related to the filter thickness.

Grading

The grading of the filter material has not been studied. In general, a wider grading has smaller pores and constrictions, which results in a better filter working, until the grading is too wide and becomes internally unstable. The effect of this in relation to this topic is not known.

²³ Van der Graaf (2005) [15]

3.1.6 Scale effects

The tests performed by Uelman (2006) are process based, meaning that they are not a scaled model of a large scale prototype. The problems related to scaling are discussed in section 2.3. In the research so far, scaling problems are not solved; the processes are studied irrespective of the scale. Parameters have been chosen such that important parameters like for instance wave steepness are within the normal range of storm waves.

Large scale tests

It is evident that in full scale models, scale effects are absent. Laboratory effects, differences in results due to different circumstances or boundary effects might still occur, but these are different from scale effects. Full scale model tests for a complete breakwater cross section are difficult to perform, but large scale tests with a length scale factor of for instance 1:5 are possible to perform in a large scale wave flume or tunnel. At these scales most of the scale effects are negligible for most standard breakwater layouts. Three main possibilities are available to conduct large scale tests: a large scale wave flume like the Delta Flume, a wave tunnel or a prototype on the coast.

Large wave flume (Delta Flume)

In the large scale wave flume, large scale models can be loaded with desired waves. This is very valuable for the research, but also very expensive and the facility is not readily available. Results from the large flume can be used to calibrate the dataset from small scale tests, when some of the small scale tests are repeated in the large flume.

Wave tunnel

Testing in a wave tunnel is useful when a certain aspect of the process, like parallel flow through the filter/ core layers, is studied. The complex processes of wave breaking and the wave induced combination of parallel and perpendicular flow cannot all be taken into account, but when one wants to separate especially one type of porous flow (parallel or perpendicular), the tunnel is very valuable. Costs will be less than for a large wave flume.

Prototype on the coast

Somewhere on a coast at a spot exposed to waves one can put a prototype of stones on a sand slope in place, and conduct measurements periodically. When the wave data and deformation are known after a certain period, connections can be made. The drawbacks of this option are that the test takes a lot of time and that the loading cannot be chosen; nature chooses the wave fields attacking the prototype. When a full scale model is applied, the design load will almost certainly not occur during the test. A more vulnerable construction can be applied, i.e. a slightly scaled-down model, to get a relatively more severe loading.

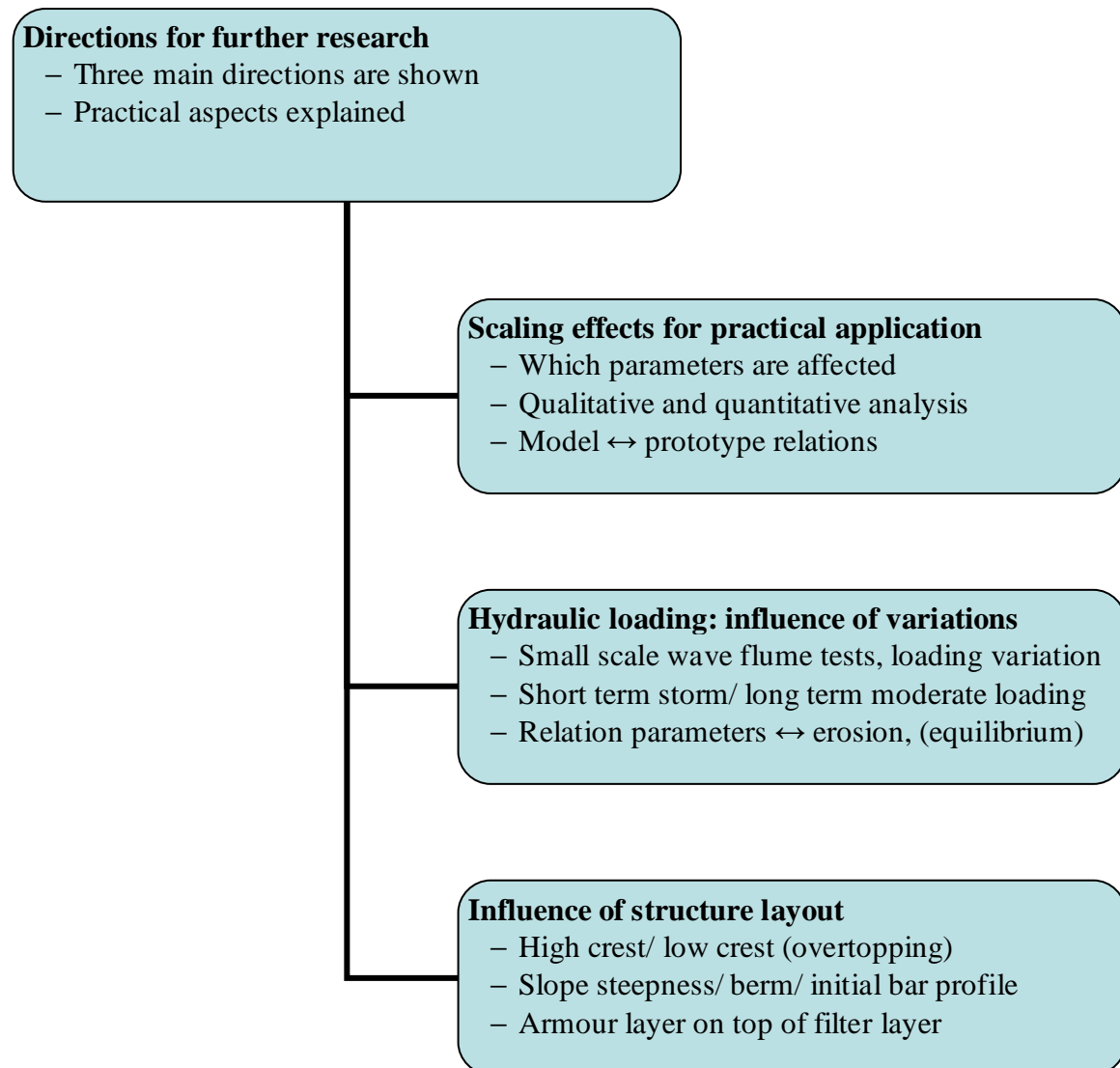
Unknown influence of scale effects

For the performed tests, no comparison with existing large scale situations can be made because data of breakwaters with hydraulically sand-open filters are lacking. Only very recently and with great caution, this type of structure has been applied and prototype measurements are not available yet. Analytical methods of determining scale effects are rather qualitative than quantitative, resulting in a recommended

calibration with large scale tests or prototype data. Until now, the scale effects are unknown.

3.2 Choice of further research direction

This study is only a part of the total research programme into the topic of hydraulically sand-open filters on a sand core, as started by Uelman. The ultimate goal of that total research is to come to a good description of the occurring processes and a practical design tool for such a filter in a breakwater with a sand core. Within this study, only a part of that total research is feasible, because of limitations in time and resources, making choices necessary. In the diagram below the main directions of further research are presented.



Three main directions

Each of the three main directions can form a study in itself, and for all of them a lot of work is necessary in order to understand the topic well enough.

3.2.1 Scaling effects for practical application

Small scale physical model tests are performed for they are more feasible than large scale tests; more test facilities are available and costs for the facility, but also for the

smaller amount and size of the needed materials, are considerably lower. The downscaling of a prototype however, introduces scaling problems, as the properties of e.g. water and sand are not scaled down with the same factor. These and other problems have been explained in general in chapter 2 and will be elaborated on in chapter 4, with a dimensional analysis, where an attempt is made to quantify the scaling effects based on the dimensional analysis and experience from other research.

Scale-series tests

In order to solve the scaling problems, “Scale-series” can be very useful. With this method, a model is applied at different scales, after which the results are extrapolated to the prototype scale. The results should be handled with caution, however, especially when all the tests are applied at a small scale relative to the prototype scale. In this case, small scale effects that are not present at the large scale might affect all the tests, making the extrapolation distorted. The method can however be a very useful tool when carefully executed. A number of tests is needed, where only the scale is changed, the other parameters are to be kept the same, only scaled up or down to the proper scale. This method could be applied in order to predict the behaviour of the breakwater configuration with the hydraulically sand-open filter on a large scale.

3.2.2 Hydraulic loading: influence of variations

The hydraulic loading, the waves and the wave-induced porous flow, is one of the determining aspects in the behaviour of the structure. The breakwater is designed especially to protect a coastline or harbour entrance from this hydraulic loading and therefore needs to be strong enough.

Irregular waves

In the research done so far, only regular waves have been used with the tests in the small scale wave flume. It is expected that irregular waves give a different erosion pattern, or at least a different combination of erosion depth and erosion length. This difference is very important, as in real life situations the waves will always be irregular. Tests can be done, for instance in the same type of wave flume as used for the former tests.

Wave height, period and steepness

In the tests performed so far, the waves were not only regular, their height and period have not been varied either. The influence of wave height, wave period and wave steepness on the erosion process is expected to be very large, making it an important aspect to be studied. The wave steepness is a function of the wave height and length, and because the wave length depends on the period, the steepness is in fact a function of the wave height and period. These three quantities cannot be judged completely separately from each other, so for instance the height can be varied keeping the steepness constant, and the steepness can be varied keeping the either the height or the period constant.

Equilibrium short term design loading

Whether or not an equilibrium situation in the erosion will develop after a certain number of waves is one of the questions still open after Uelmans research. Results show a tendency towards equilibrium, but it is not reached in the tests. Longer tests, with a larger number of waves attacking the structure, can answer this question. It is not absolutely necessary to come to an equilibrium situation for the design conditions,

as the design conditions only occur during heavy storms that last for a number of hours. The erosion during a design storm has to be within acceptable limits, even if this is not the equilibrium situation. It is however interesting for the understanding of the behaviour of the structure to know if equilibrium is reached.

Equilibrium long term moderate loading

For more moderate conditions, the development of equilibrium is very important; these conditions occur over longer time spans. The ‘normal’ conditions are present most of the time and ongoing erosion would certainly lead to failure of the structure. For geometrically closed structures, resistance in normal situations is assured by the requirement that practically no damage is accepted during design conditions, giving also no damage for less severe conditions. For hydraulically sand-open filters however, loss of core material to some degree is accepted. It is therefore necessary to check if the more moderate loading in ‘normal’ circumstances does not give erosion, or at the very least leads to a quick equilibrium profile. It is possible to test a structure in a wave flume under more moderate conditions for this end. Special attention is to be paid to the scaling effects that might have a determining effect on the results.

Relation between loading and erosion pattern

The relation between the hydraulic loading, different types of waves in different combinations, and the erosion pattern and deformation of the structure, are the aim of investigating the influence of variations of the hydraulic loading. Once it is known what type of structure gives what kind of deformation with what erosion depth and length under which kind of hydraulic loading, design tools can be started to be made. Before this is possible, the scaling effects will have to be known and numerical analysis might be used to further study the results, but the relation between hydraulic loading and erosion/ deformation of a certain type of structure is one important step on the way to a design tool.

3.2.3 Influence of structure layout

The layout of the breakwater structure comprises the crest height (above, around or below the water level), the slope steepness of the structure, the application of a berm on the outer slope and the possible application of an initial bar profile, a constructed profile that resembles an equilibrium profile after erosion. All these layout aspects influence the behaviour of the breakwater under hydraulic loading.

Crest height

In the tests performed so far, the crest was higher than the run-up height of the waves, resulting in no overtopping. Other possibilities for breakwaters are low crests, e.g. around the water level, when overtopping waves are accepted, or even submerged breakwaters, when only the higher waves have to be blocked. With these lower crests, the behaviour of the structure as a whole changes, not only the outer slope is attacked by the waves, also the crest and possibly the inner slope are attacked. This means that those parts have to be designed for that specific loading. On the other hand, the loading on the outer slope decreases as part of the energy is absorbed by the crest and the inner slope. For submerged breakwaters, the crest will probably experience the most severe loading. Tests in a wave flume can give insight in these mechanisms and their quantities.

Slope steepness

Until now, tests were performed with a 1:3 slope for this research. A milder slope is expected to spread the energy of the breaking waves over a longer part of the slope, thus leading to a smaller erosion depth and larger erosion length. A steeper slope is expected to have the opposite effect. Besides this spreading effect, also the Iribarren parameter changes, indicating the type of breaking of the waves. Another breaker type leads to another loading situation and therefore another erosion pattern. The combination of these two effects makes the effect of the slope steepness less straightforward than it may look. Wave flume tests could again be used to gain insight in these effects.

Application of a berm

On the outer slope, a berm is sometimes applied in breakwaters. This berm reduces the run-up height of the waves and changes the loading of the structure as a whole. The berm itself will experience heavy loading as it is put directly inside the breaking waves, and for the rest of the structure, the higher part of the slope, the loading is reduced. Often the berm has the level of the (storm) water level. The use of a hydraulically sand-open filter in a breakwater with a berm can be investigated with wave flume tests.

Application of an initial bar profile

After the tests with hydraulically sand-open filters, an erosion profile in the form of a bar has been observed for all the tests. It is possible to construct such a profile beforehand. When this profile is an equilibrium profile for the design conditions, it can result in at least less erosion, or hardly any erosion. It has to be checked however, if this works and if the suggested profile is also stable under different conditions. It is far from certain that such a profile is cost effective. Wave flume tests can demonstrate the technical feasibility.

3.2.4 Choice of research direction: hydraulic variations

Because not all the possibilities mentioned above can be studied, a choice has to be made. For this research, the second direction, influence of variations of hydraulic loading, has been chosen, because it can give more insight in the essential processes and behaviour of the breakwater configuration. As long as these essential processes are not understood, the extensive research into either the scaling effects or the structure layout add only very little to the knowledge of hydraulically sand-open filters in breakwaters.

Choice for influence of hydraulic loading variations

The influence of the hydraulic loading on the erosion of core material and establishment of an equilibrium state in the erosion process is the main focus of this study. The reason this direction has been chosen is that it connects well to the former research and it contributes to the insight in the processes that occur in the breakwater. The dependency of the breakwater configuration on hydraulic loading parameters, and especially the sensitivity to changes in these parameters, is of great importance for the practical applicability of such a structure. It is useful to know more about these dependencies and internal processes, before different structure layouts are tested. When the layout is altered, the behaviour will change, but the principles of sand-open filters on a sand core remain the same and as long as only very little is known about these principles and processes, the variation of the layout will not give such valuable

extra information. The study into scaling effects is still interesting, but again, as long as little is known about the dependency on loading on whatever scale, the exact effects of scaling are less interesting. It is however very important to have an idea about the order of the occurring scale effects for the tests that have been and will be performed. Therefore, a theoretical study into scaling effects for these tests will be done.

Hydraulic loading variation

Physical model tests in a wave flume with different settings for the hydraulic loading are to be performed to study the influence of the loading on the erosion of core material. A test program can be made after an analysis of scaling effects and the dominant processes. Chapter 5 discusses the test program.

Scaling effects, a theoretical study

To study the order of magnitude of the occurring scale effects for the performed tests and for the coming tests for this study, a dimensional analysis will be performed and compared with literature. An attempt will be made to quantify the scale effects, without scale series tests or prototype data. Chapter 4 discusses the scale effects.

Layout variation, only slope steepness and grading

The choice has been made not to focus on the layout of the breakwater, but on the loading. An exception for this is the slope steepness, which is a layout parameter that also affects the loading. The steepness of the slope of the breakwater influences the way of breaking of the waves, and a gentler slope spreads the energy of the breaking waves over a longer distance than a steeper slope. Tests with different slope steepness are of interest to observe this influence. Another parameter that involves the layout of the breakwater is the grading of the filter material. Thus far, quite a narrow grading has been used with little difference in size between the larger and the smaller stones. A wide grading can be very interesting, as the smaller stones can reduce the loading inside the filter effectively and the larger stones can provide more stability against the direct attack of the waves or can allow larger armour stones to be put on the filter layer. A test with a wide grading is of interest.

Main focus and side-interests

In summary, the main focus is the influence of hydraulic loading variations, to be studied by wave flume tests. If enough time is available, variation of the slope steepness and grading of the filter material will be added to these tests. The scale effects will be analysed with a theoretical study only, where a dimensional analysis of the processes in the breakwater and results and analyses from literature will be compared in a quantitative way.

3.3 Choice of general test setup

As discussed in section 3.2, wave flume tests have been chosen as a means to study the influence of varying hydraulic loading on the erosion of core material in the breakwater with sand core. For completeness, the different test possibilities and considerations about advantages and disadvantages of those possibilities are explained here.

3.3.1 Wave flume

In a wave flume the layout of the prototype resembles the real life situation; the actual cross section of a breakwater with certain slope steepness, berm or no berm, crest height, layer structure etcetera can be reproduced. A cross section with a limited width is constructed in the flume, breakwater heads or oblique incident waves (waves that approach the structure under an angle instead of perpendicular) are difficult to simulate in a flume.



Figure 3-1 Small scale wave flume at the Fluid mechanics lab of TU Delft

Small scale wave flume

A small scale wave flume, like the one used by Uelman (2006) is a very practical tool. There are two available in the hydraulics laboratory of Civil Engineering of Delft University of Technology. Costs are lower than for large scale test facilities and the smaller prototypes are easier to construct. Small scale flumes often have glass side walls, through which the processes at the interface between core and filter can be observed very well and through which the internal slope can be measured. The main disadvantage is the necessity of scaling and the problems associated with that.

Large wave flume (Delta Flume)

To overcome part of the scaling problems, a large scale wave flume is a very good option. It can do the same as the small scale flume, but than on a large scale. The disadvantage lies in the high costs and limited availability of the facilities.

3.3.2 Wave basin

In a wave basin, a situation can be created that resembles the real life situation as good as possible with physical model tests, be it on a relatively small scale, typically smaller than in a wave flume. Advantages are the possibility to test a whole structure including breakwater heads and the interaction with objects in the direct vicinity. Another advantage is the possibility to test a breakwater under oblique incident wave loading, which might lead to longshore transport of the sandy core material. Disadvantages are the extra difficulty to conduct measurements inside the breakwater and the small scale at which the tests can be performed. Boundary effects are also introduced, especially by the sides of the basin, where waves are reflected if no special measures are taken.

3.3.3 Wave tunnel

A wave tunnel can be used to separate parallel flow and perpendicular flow by placing a sample horizontally or vertically in the test section. A possible way of using this is to put a layer of filter stones on a layer of sand in the sample box, either horizontally or vertically to get respectively parallel or perpendicular porous flow. The tunnel is best suited for parallel flow. The sample box is located in the middle of the U-shaped tunnel. A piston in one end of the U pushes and pulls the water up and down (the other end has a free surface) to simulate wave action. This method is useful to study e.g. the critical flow velocities or critical gradient in the filter or the core. This can be related to a certain wave height, period, regularity etcetera, but this way of testing gives no direct relation between external loading and deformation. Sediment transport can also be studied, when the tunnel has a sediment trap, like the one at WL | Delft Hydraulics. A large tunnel is available at WL, but needs modifications and preparations before it is operational.

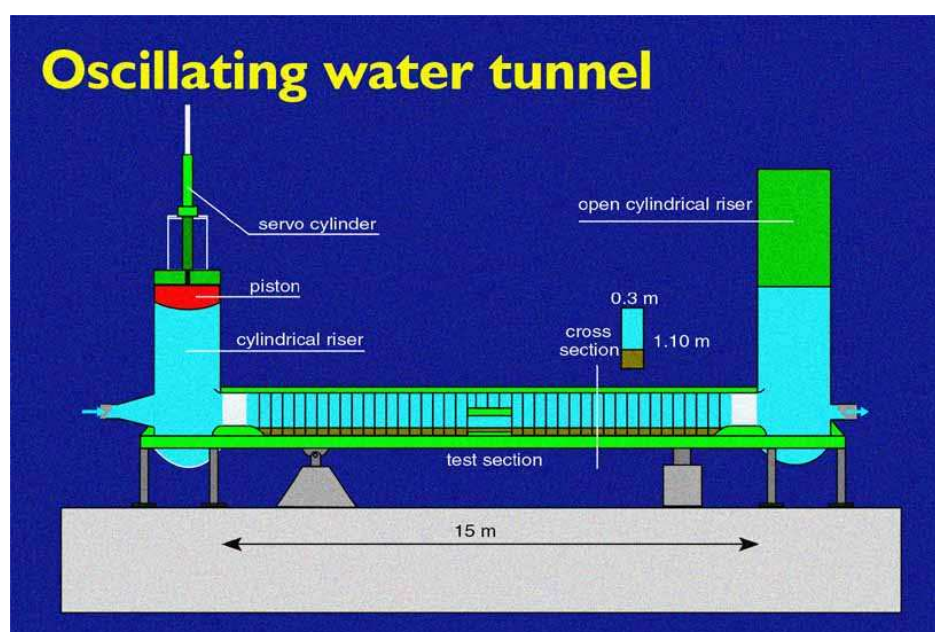


Figure 3-2 Schematisation of the wave tunnel at WL | Delft Hydraulics (from www.wldelft.nl)

Wave tunnel, breaking waves

It is difficult to simulate wave breaking in the tunnel. During the wave run-up, most of the water flows over the slope on the outside, and during run-down, most of the water flows through the filter layer, causing high porous velocities and initiating transport of core material through the filter layer. In the wave tunnel, the water flow is similar in both directions, creating a similar flow type in both directions. It is possible to add a constant flow through the test section and to give the waves some irregularity (exact possibilities are not known), which combination might give similar results for the porous flow.

Wave tunnel, barred profile

Another problem is the creation of the barred profile. The wave action in the tunnel is constant in space over the whole horizontal section, where the waves on a slope give a more severe loading around the water level area than deeper, below the water level. In the slope, the barred profile develops; erosion takes place where the wave loading is more severe and the material is deposited lower on the slope where the loading is less severe. This bar is expected to influence the erosion process, as locally a milder slope of core material develops inside the filter layer, being less sensitive to erosion. It seems problematic to create this effect in the wave tunnel, where the loading is constant over the horizontal section.

Wave tunnel, stability criteria

The wave tunnel is certainly suitable for the determination of the initiation of transport of sand through a filter layer under porous flow, and probably also for the start of the erosion process when the amount of transported material is important. These research options are possible provided that the loading difficulty is satisfyingly solved. But as the deformation will be different from that in a wave flume, stabilisation will probably not occur or in a different way. Altogether, the start of the erosion process can probably be studied in a good way, whereas the stabilising part will still need wave flume tests. If the initial transport and erosion is chosen as the main interest of study, the wave tunnel seems to be a good option.

Wave tunnel, practical situation

At WL | Delft Hydraulics, a large wave tunnel is available (see Figure 3-2). However, at the moment this tunnel is not operational. Furthermore, international cooperation is probably needed to realize a practical work situation. All this is possible, but not within the time available for this thesis study. When choosing this way of testing, a smaller facility has to be found, to do tests knowing that the scaling problems play a role, and according to the results, make a plan for the large facility. A further study by for instance a next graduate student can comprise testing in the large facility.

3.3.4 Prototype on the coast

With a prototype on the coast, a test type is meant for which a section of a breakwater is placed on the coast, e.g. an existing beach, and thus loaded by the naturally occurring waves. A prototype on the coast is useful to see how a structure behaves under a long term loading, with changing characteristics. The results will probably give more qualitative than quantitative information, as the process can probably not be monitored continuously. The loading cannot be chosen, so continuous data of the waves loading the structure is needed over the long testing period. Different sections with different grain sizes could be made that can be related to different loading

situations during the test. The main disadvantage is that this type of test takes a lot of time.

3.3.5 Choice of test setup: small scale wave flume

The small scale wave flume at the fluid dynamics laboratory of Civil Engineering at TU Delft has been chosen to perform the physical model tests for hydraulic loading variations. This flume is available, the internal processes can be studied by observations through the side walls, a structure resembling a possible prototype cross section can be tested by chosen wave loading situations, the layout of the structure can be altered for different tests and the results of the tests can be compared directly with the results of Uelman (2006). The main disadvantage, the scale effects that occur because of the small scale of the tests, cannot be solved, but an analysis of the scale effects performed in chapter 4 indicates that the magnitude of these effects, although present, is expected to be within reasonable limits. Effects do occur, giving deviations in results, but they do not affect the processes themselves. The erosion processes can be observed and measured to get more insight in the behaviour of hydraulically sand-open filters.

3.4 Objective

The objective of this study is to find relations for the influence of variations of the hydraulic loading, slope steepness and grading of filter material on the stability and erosion patterns of core material in a breakwater configuration with a hydraulically sand-open filter on a sand core, by performing physical model tests in a wave flume. A part of the total problem described in this chapter is to be solved with the observations, results and analysis of these tests. The influence of the variation of hydraulic loading on the erosion of core material is found to be the most effective part of the research possibilities described in section 3.3, in combination with an analysis of scale effects.

3.4.1 Problem definition

Insufficient knowledge

The economically most optimal design of a breakwater could consist of a sand core and a geometrically open and hydraulically sand-open filter construction, thereby accepting a certain amount of loss of core material. Insufficient knowledge about the transport processes involved in this type of breakwater is available in order to predict the behaviour; the amount of loss of core material and deformation of the structure.

The first step has been taken

With the research performed by E.F. Uelman (2006) a first step has been taken towards resolving the problem described above. The results indicate that it is possible to construct a breakwater of this kind that initially experiences loss of material under design conditions, but tends towards an equilibrium state. However, only a limited number of tests have been performed so far, and for instance the effects of irregular waves instead of regular waves, the dependency on wave height, wave period and slope of the breakwater have not been examined yet. Obviously the existing dataset is small because of the limited number of tests performed so far.

Theoretical description

To come to a theoretical description of the erosion and transport of sand in a filter layer loaded by irregular breaking waves, more insight in these processes is needed and more test data are needed to validate theoretical and possibly numerical models.

Design tool for practical applications

When more is known about the occurring processes and more test data are available, design criteria can be formulated and design tools can be constructed for the practical application of breakwaters with open filters on a sand core. Insight in the erosion processes in the breakwater is essential for this.

3.4.2 Ultimate goal of the research

The research into breakwaters with a sand core and hydraulically sand-open filter is aimed at gaining a better understanding of the erosion processes involved in such a structure under wave loading. The ultimate goal is to have a good qualitative and quantitative description of the wave/ water interaction, transport of material and deformation of the structure, and to present a good design tool for the practical application of hydraulically sand-open filters on a sand core.

3.4.3 Objective of this thesis study

The objective of this study is to find relations for the influence of variations of the hydraulic loading, slope steepness and grading of filter material on the stability and erosion patterns of core material in a breakwater configuration with a hydraulically sand-open filter on a sand core by performing physical model tests in a wave flume. The central research question is formulated as:

What is the erosion growth pattern for the erosion of sandy core material through a hydraulically sand-open filter layer in a breakwater under varying wave loading? Does an equilibrium profile occur and if so, when does it occur for both design conditions as for moderate, long term, conditions?

Physical model tests in a wave flume and a theoretical study of the occurring scale effects serve the objective of finding answers to this central question.

Physical model tests

Physical model tests give insight in the erosion growth and stability of the model under selected loading conditions. The loading variation encompasses irregular waves, variation of wave height, period and steepness, but also variation of the slope steepness and grading of the filter material. The results will be analysed for relations between loading and erosion, the development of erosion in time and the establishment of an equilibrium state under various loading situations.

Theoretical study of the scale effects

Scale effects are studied theoretically. The goal of this part is to come to a selection of scaling criteria and quantification of the scale effects between prototype and model, to judge the validity of the model tests. A dimensional analysis of the processes and a literature study of similar projects are applied to reach this goal.

Numerical modelling: preparation

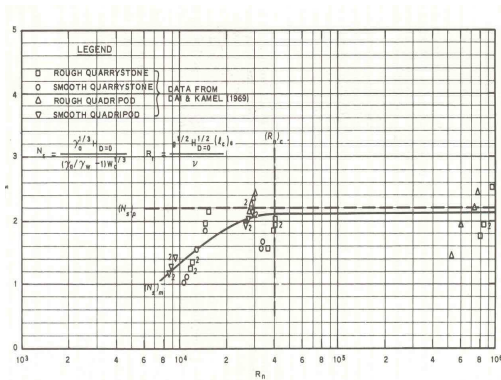
When more data from tests are available, a numerical model could be applied and validated with these data. The preparation for numerical modelling is meant to serve as a starting position for a future study where a numerical model will be constructed for this problem or where an existing model will be modified to fit the configuration.

Scale series and large scale tests: preparation

In order to get a qualitatively and especially quantitatively good description of the occurring processes, leading to a good design tool, the scaling problem has to be solved at some point. Scale series and large scale tests can be the solution for this, but are not feasible within the thesis. However, suggestions can be made as to what tests to perform and with what kind of parameters of interest. The objective of this part is to give a first guideline for large scale tests and scale series tests, as described in section 3.2.1.

Chapter 4

Scale effects



4.1 Dimensional analysis of the processes

4.2 Comparison and quantification of the scale effects

Chapter 4 Scale effects

A theoretical study into the scale effects that occur when a breakwater with hydraulically sand-open filter is scaled down from a prototype to a physical model is described in this chapter. This study is performed to come to a selection of scaling criteria and quantification of the scale effects between prototype and model. The validity of the model tests can be judged and the quantification can be used to define a margin of safety when using the results for practical situations.

4.1 Dimensional analysis of the processes

With a dimensional analysis, a process is described by non-dimensional parameters to be able to see influences of different parameters regardless of the scale or the absolute quantity. The goal is not to come up with an exact formula for the process, but with the essential non-dimensional parameters, which are to be preserved in a scaled model in order to avoid scaling effects. A useful tool within the dimensional analysis is the Pi-theorem²⁴, a systematic way of forming non-dimensional parameters from a set of dimensional parameters describing a process.

According to Ettema et al. (2000), “A *dimensional analysis is a useful tool to formulate the problem and ensure that similitude conditions are taken into account properly.*” In practice however, it can be quite difficult to come to sound results for complicated problems. Nevertheless, it is useful to investigate the problem with a dimensional analysis in order to find important combinations of parameters.

4.1.1 Pi-theorem

The Pi-theorem is a systematic way of forming non-dimensional parameters from a set of dimensional parameters describing a process. It states: “*a dimensionally homogeneous linear equation is reducible to a functional relationship among a set of dimensionless parameters.*” The basic steps are listed below. For more information, see appendix II, part scaling problems.

- List all n relevant physical quantities, expressed in terms of the fundamental dimensions
- Note the number of fundamental dimensions, m
- Select m physical quantities as repeating variables, such that:
 - None is dimensionless
 - No two have the same dimensions
 - Together they do not form a Π parameter
 - They include all fundamental dimensions involved
- Express the terms as the product of the terms selected in step 3
- Solve the unknown exponents

After these steps a dimensionless form of the starting equation is obtained of the form:

$$\Pi_1 = F \{\Pi_2, \Pi_3, \dots\}$$

In which the Pi-terms are dimensionless combinations of the starting equation parameters.

²⁴ Ettema et al. (2000) [9] and Hughes (1993) [26]

Dimensionally homogeneous linear equation

In a dimensionally homogeneous linear equation, the dimension of the left-hand side variable equals the dimension of any of the terms on the right-hand side that stands by itself. E.g.: $x_1 = f(x_2, x_3, x_4, \dots, x_n)$. According to the Pi-theorem, such equation can be rearranged into a new equation expressed in terms of dimensionless products (Pi-terms) as: $\Pi_1 = \Psi(\Pi_2, \Pi_3, \dots, \Pi_{n-r})$.

4.1.2 Application of the Pi-theorem

Various attempts have been made to apply the Pi-theorem to the process of erosion of core material (sand) through an open filter in a breakwater loaded by breaking waves. The procedure for the erosion depth as a function of wave loading and material properties is shown to illustrate this. This process, however, is not easily included into one homogeneous, linear equation. Therefore, different parts of the process are put in separate equations, all examined with the Pi-theorem. They are:

- The hydraulic gradient in the filter as a function of hydraulic loading.
- The filter velocity as a function of gradient and filter material properties.
- The bottom transport at the filter-core interface as a function of core material and filter velocity.
- The erosion depth as a function of the hydraulic loading.
- The erosion area as a function of the hydraulic loading.

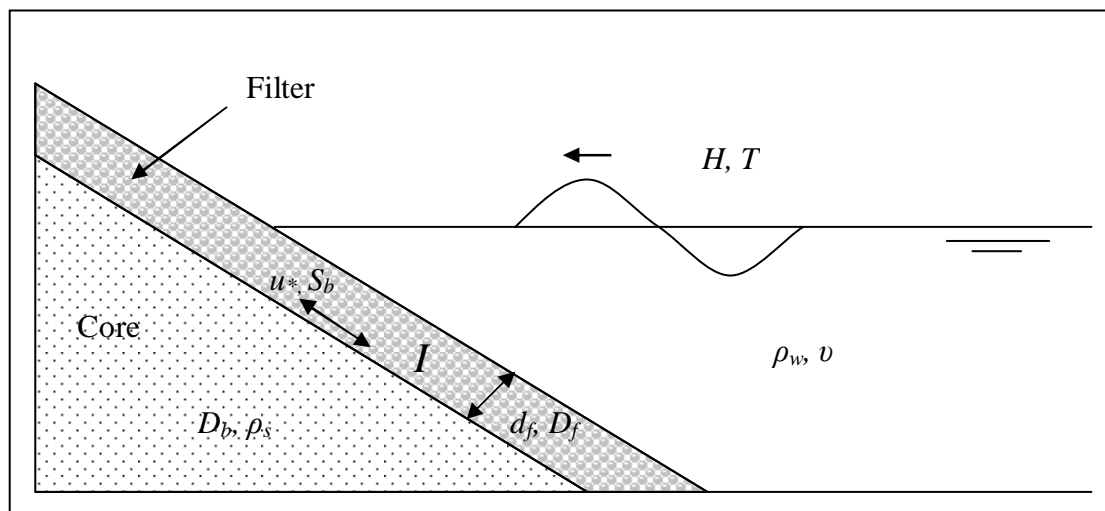


Figure 4-1 Sketch of the breakwater layout with important parameters

Hydraulic gradient in the filter as a function of hydraulic loading

A theoretical equation to quantify the direct relation between the gradient inside the filter layer and the properties of the breaking waves that load the structure does not exist, but it can be stated that the gradient I is a function of the wave properties, the geometric properties and the water properties, for this particular type of structure. In this relation, the used wave properties are height H and period T , the geometric properties are the porosity n_f and the location z (depth below the mean water level), and the water properties are the density ρ_w and the kinematic viscosity ν . Gravity g is an external property. In equation form:

$$I = f(H, T, n_f, \rho_w, \nu, z, g)$$

All the parameters are now written as a combined function with an unknown power x_n for every parameter, and after that written as only the fundamental dimensions Mass, Length and Time, of that parameter, to the same unknown power:

$$\Pi = I^{x_1} H^{x_2} T^{x_3} n_f^{x_4} \rho_w^{x_5} v^{x_6} z^{x_7} g^{x_8}$$

$$\Pi = [-]^{x_1} [L]^{x_2} [T]^{x_3} [-]^{x_4} [ML^{-3}]^{x_5} [L^2T^{-1}]^{x_6} [L]^{x_7} [LT^{-2}]^{x_8}$$

To get a clear overview of the dimensions involved, a table is presented with the powers of the dimensions for every parameter.

	I	H	T	n_f	ρ_w	v	z	g
M	0	0	0	0	1	0	0	0
L	0	1	0	0	-3	2	1	1
T	0	0	1	0	0	-1	0	-2

For the total relation to become dimensionless, all the rows in the table have to add up to be zero, which e.g. means for the first row that $x_5 = 0$, because x_5 is the only power in this row that is not zero. Altogether it means:

$$x_1 = \text{free}; x_4 = \text{free} \rightarrow \Pi_1 = I; \Pi_2 = n_f$$

$$x_5 = 0$$

$$x_2 + 2x_6 + x_7 + x_8 = 0$$

$$x_3 - x_6 - 2x_8 = 0$$

These two equations include five unknown variables, which means that three repeating variables have to be chosen to get values for the other two. As repeating variables, x_6 , x_7 and x_8 have been chosen. Values for these repeating variables are chosen such that one has the value one, the others are zero:

$$x_6 = 1, x_7 = 0, x_8 = 0 \rightarrow$$

$$x_2 = -2 \rightarrow x_3 = 1 \rightarrow \Pi_3 = \frac{Tv}{H^2}$$

For easier comparison, some of the resulting Pi-terms are inverted, giving no real difference as long as the relations between the terms are not fixed. $\frac{H^2}{vT}$ indicates two things. One is that the viscosity plays a role and the other is that the period should be scaled with the same factor as the wave height squared. This also follows from the often applied Froude scaling law.

$$x_6 = 0, x_7 = 1, x_8 = 0 \rightarrow$$

$$x_2 = -1 \rightarrow x_3 = 0 \rightarrow \Pi_4 = \frac{z}{H}$$

$\frac{H}{z}$ suggests that the position under the wave is important, as was also visible in Uelman's test results.

$$x_6 = 0, x_7 = 0, x_8 = 1 \rightarrow$$

$$x_2 = -1 \rightarrow x_3 = 2 \rightarrow \Pi_5 = \frac{gT^2}{H}$$

$\frac{H}{gT^2}$ is a measure for the wave steepness, as the wavelength is a function of gT^2 . This indicates that the wave steepness is to be preserved when scaling down. Again the scale factors for wave height and period as obtained from the Froude scaling law provide this preservation of wave steepness.

Put together, the gradient can be written as a function of the above derived dimensionless terms:

$$I = F \left\{ n_f, \frac{H^2}{vT}, \frac{H}{z}, \frac{H}{gT^2} \right\}$$

The meaning of most Pi-terms has been described above, the other two are the gradient I itself and the porosity n_f , which are dimensionless by itself.

Conclusion Pi-theorem for the hydraulic gradient

The application of the Pi-theorem for the above described relation for the hydraulic gradient shows that in order to preserve the gradient when scaling down, the found dimensionless terms are to be preserved in that process. The Froude scaling law is important for this process, but the viscosity is important as well.

Filter velocity as a function of hydraulic gradient and filter material properties

The same procedure as above has been followed, but not all the steps will be shown and less explanation of the procedure will be given. The used relation is a relation between the filter velocity and the hydraulic gradient, although the gradient is on the left hand side of the equation. This does not make an important difference for the dimensional analysis. The extended Forchheimer relation is used as starting equation:

$I = a \cdot U + b \cdot U \cdot |U| + c \frac{dU}{dt}$. Together with the relations for a , b , and c as used by van Gent²⁵, the following parameter relation was found:

$$I = f(n_f, v, g, D_f, u_f)$$

$$\Pi = I^{x_1} n_f^{x_2} v^{x_3} g^{x_4} D_f^{x_5} u_f^{x_6}$$

$$\Pi = [-]^{x_1} [-]^{x_2} [LT^{-1}]^{x_3} [LT^{-2}]^{x_4} [L]^{x_5} [LT^{-1}]^{x_6}$$

Following the same procedure of the Pi-theorem, this leads to:

²⁵ Van Gent (1995) [14]

$$I = F \left\{ n_f, \frac{u_f D_f}{\nu}, \frac{u_f^2}{g D_f} \right\}$$

Naturally, I and n_f are dimensionless by itself. $\frac{u_f D_f}{\nu}$ is the Reynolds number, a very important parameter in situations where the viscosity of the water might play a role. Inside the filter layer, flow can become less than fully turbulent, causing unwanted scale effects. The other found Pi-term, $\frac{u_f^2}{g D_f}$ is the square of the Froude number, often stated to be the most important parameter for scaling flow properties in general. It should be noted that it is not possible for both the Froude number and the Reynolds number to be preserved simultaneously when scaling down, leading to inevitable scaling effects when scaling down porous flow processes. The magnitude of these effects will be treated in section 4.2.

Bottom transport as a function of the shear velocity in the filter

With bottom transport S_b , here the bed-load type of transport of core-sand over the interface between filter and core is meant. It depends on the shear velocity u_* , the density of the sand grains ρ_s , and the grain size of the core material D_b :

$$\begin{aligned} S_b &= f(u_*, \rho_s, D_b) \\ \Pi &= S_b^{x_1} u_*^{x_2} \rho_s^{x_3} D_b^{x_4} \\ \Pi &= [L^2 T^{-1}]^{x_1} [L T^{-1}]^{x_2} [M L^{-3}]^{x_3} [L]^{x_4} . \end{aligned}$$

Solving this equation leads to:

$$\begin{aligned} x_3 &= 0 \\ 2x_1 + x_2 - 3x_3 + x_4 &= 0 \\ -x_1 + x_2 &= 0 \end{aligned}$$

With repeating variable x_1 this leads to:

$$\begin{aligned} x_1 = 1 &\rightarrow x_2 = -1 \rightarrow x_4 = -1 \rightarrow \Pi_1 = \frac{S_b}{u_* D_b} \\ x_1 = 0 &\rightarrow x_2 = 0 \rightarrow x_4 = 0 \end{aligned}$$

The result is only one dimensionless Pi-term, $\frac{S_b}{u_* D_b}$, which should be preserved in order to keep the bottom transport in the given starting relation preserved in the model. It should be noted that the grain size of the core material, sand, cannot be scaled down when the material is to remain sand; smaller grains than about 0,1 mm get influenced by cohesive forces and become silt instead of sand.

Bottom transport as a function of shear velocity, friction coefficient, water properties and grain properties

The former relationship for bottom transport was deduced from the parameter analysis and process analysis for the configuration of the breakwater as in this research. Other formulas do exist, for instance the Kalinske-Frijlink formula²⁶. This formula relates the bed load (or bottom) transport S_b to the grain size D_b , gravity g , density of sand and water ρ_s and ρ_w , the flow velocity u , the waterdepth h and the friction coefficient k_r . The notation used in van der Graaf (2005) is different and a different friction coefficient, Chezy, is used which can be written as a function of k_r . The formula is not handled here to use it as a formula, but to show the relations for bed load transport in a tested equation. The transport process inside the open pores of the filter is basically the same as the transport process under currents in an open channel or on the foreshore, be it with cyclic loading. The parameters involved are:

$$S_b = f(D_b, g, \rho_s, \rho_w, u, h, k_r)$$

In dimensionless form:

$$\begin{aligned} \Pi &= S_b^{x_1} D_b^{x_2} g^{x_3} \rho_s^{x_4} \rho_w^{x_5} u^{x_6} h^{x_7} k_r^{x_8} \\ \Pi &= [L^2 T^{-1}]^{x_1} [L]^{x_2} [L T^{-2}]^{x_3} [M L^{-3}]^{x_4+x_5} [L T^{-1}]^{x_6} [L]^{x_7} [L]^{x_8} \end{aligned}$$

The results after the performance of the Pi-theorem:

$$\frac{S_b}{u k_r} = F \left\{ \frac{D_b}{k_r}, \frac{g k_r}{u^2}, \frac{h}{k_r}, \frac{\rho_s}{\rho_w} \right\}$$

$\frac{D_b}{k_r}$ and $\frac{h}{k_r}$ are just a length scale divided by a length scale, maybe a trivial result. The relative density $\frac{\rho_s}{\rho_w}$ seems to play a role in this process which can also be expected as the flowing water and the grains express force on each other, influenced by the density. $\frac{g k_r}{u^2}$ is very similar to the inverse of the Froude number, with $Fr = \frac{u}{\sqrt{gh}}$.

Only the power is different and a different length parameter is used. Similarities with Froude scaling appear for most relations and seem to be very important for flow processes.

Erosion depth as a function of hydraulic loading

An attempt has been made to relate the hydraulic loading directly to the erosion depth in the following way:

$$d_s = f(H, T, D_b, D_f, d_f, \tan \alpha)$$

²⁶ Van der Graaf (2005) [15]

The almost trivial result of this was a relation between some dimensionless parameters:

$$\frac{H}{d_s} = F \left\{ \frac{D_b}{d_s}, \frac{D_f}{d_s}, \frac{d_f}{d_s}, \tan \alpha \right\}$$

This indicates that the length scale should not be distorted in the model. Only Length dimensions are found in these results, indicating that the proposed starting relation is not practical for the application of a dimensional analysis for this particular problem as a whole. Therefore, different parts of the process are treated separately as well.

Erosion depth as a function of hydraulic loading for a different relation

In the results above, all the terms are made dimensionless with the erosion depth, which is not practical for the analysis of parameters, because the erosion depth is the dependent parameter. A different approach gives another result, where this time the grain sizes are not taken into account, presuming a fixed combination of grain sizes for which this relation holds. The thickness of the filter layer and the slope steepness are taken into account, as well as the wave height, period and gravitational acceleration:

$$d_s = f(H, T, g, d_f, \tan \alpha)$$

Application of the pi-theorem leads to the following combination of dimensionless parameters:

$$\frac{d_s}{d_f} = F \left\{ \frac{H}{d_f}, \frac{gT^2}{d_f}, \tan \alpha \right\}$$

In this example, the dependent parameter, the erosion depth, as well as the loading parameters, wave height and period, are made dimensionless with the use of the filter layer thickness, an independent variable. This relation is especially useful for the analysis of test results, indicating that a relation between the dimensionless erosion depth and the dimensionless wave height and period should be found in the test results. A variation on this is an extended form of the same parameters:

$$d_s = f(H, T, D_b, D_f, d_f, \tan \alpha, g, \rho_w, \rho_s, \nu)$$

The expectedly most useful result of this in terms of test result analysis:

$$\frac{d_s}{H} = F \left\{ \frac{D_b}{H}, \frac{D_f}{H}, \frac{d_f}{H}, \frac{H}{gT^2}, \tan \alpha, \frac{\rho_s}{\rho_w}, \frac{\sqrt{gHD_f}}{\nu} \right\}$$

From the terms, gT^2 is a measure for the wave length ($L_0 = \frac{gT^2}{2\pi}$) and $\frac{\sqrt{gHD_f}}{\nu}$ is a measure for the Reynolds number inside the pores, with \sqrt{gH} as a flow the velocity.

Erosion area as a function of the hydraulic loading

Besides the erosion depth, also the erosion area is an important measure for the amount of erosion, giving the total volume of sand that is removed by the waves and will have to be supplied as stones if maintenance is required. The same parameters as above yet with A_s instead of d_s , leads e.g. to the following:

$$A_s = f(H, T, D_b, D_f, d_f, \tan \alpha, g, \rho_w, \rho_s, \nu)$$

A combination of dimensionless terms can be made, keeping in mind the parameters that are expected to be important after Uelman's tests, and after a first analysis of parameters:

$$\frac{A_s}{HgT^2} = F \left\{ \frac{d_f}{D_f}, \frac{D_b}{D_f}, \frac{\tan \alpha}{\sqrt{\frac{2\pi H}{gT^2}}}, \frac{\rho_s}{\rho_w}, \frac{\sqrt{gHD_f}}{\nu} \right\}$$

In which the first term of the right hand side equals m , the second is the openness of the filter, the third equals the Iribarren number ξ , the fourth is the density ratio and the fifth the Reynolds number. The left hand side relates the erosion area to the wave height and -length.

Combining relations and introducing the number of waves

Until now only the magnitude of the loading has been used, without the duration. The duration can be expressed in a dimensionless way by using the number of waves, N . Test results of Uelman show that erosion increases gradually during the tests, so the number of waves must have influence. Besides this, a combination of the above is interesting; e.g. the hydraulic gradient used in combination with the erosion area. When assuming an important gradient-driven mechanism, this should result in an interesting relation with a physical relevancy. A possibility for this is:

$$A_s = f(H, T, D_b, D_f, d_f, \tan \alpha, g, \rho_w, \rho_s, \nu, I, N)$$

The result resembles the above closely as well:

$$\frac{A_s}{HgT^2} = F \left\{ I, N, \frac{d_f}{D_f}, \frac{D_b}{D_f}, \frac{\tan \alpha}{\sqrt{\frac{2\pi H}{gT^2}}}, \frac{\rho_s}{\rho_w}, \frac{\sqrt{gHD_f}}{\nu} \right\} = F \left\{ I, N, m, \frac{D_b}{D_f}, m, \xi, \frac{\rho_s}{\rho_w}, \text{Re} \right\}$$

In this relation, parameters are used several times in different ways and loading parameters are used both on the right-hand as on the left-hand side. Nevertheless it might lead to an interesting result in the analysis of Chapter 7.

4.1.3 Conclusions of the dimensional analysis

The application of the Pi-theorem resulted in a number of relations between dimensionless terms being combinations of involved parameters. Because the complex process from hydraulic loading to erosion could not be captured in one single relation, as too many aspects are not well known at this stage, the results of the Pi-theorem should be handled with care and should be compared with known results and relations for similar processes. Some important parameters are found and will be summarized here. The found dimensionless relations are:

$$I = F \left\{ n_f, \frac{H^2}{vT}, \frac{H}{z}, \frac{H}{gT^2} \right\}$$

$$I = F \left\{ n_f, \frac{u_f D_f}{v}, \frac{u_f^2}{gD_f} \right\}$$

$$\frac{S_b}{u_* D_b}$$

$$\frac{S_b}{uk_r} = F \left\{ \frac{D_b}{k_r}, \frac{gk_r}{u^2}, \frac{h}{k_r}, \frac{\rho_s}{\rho_w} \right\}$$

$$\frac{H}{d_s} = F \left\{ \frac{D_b}{d_s}, \frac{D_f}{d_s}, \frac{d_f}{d_s}, \tan \alpha \right\}$$

$$\frac{d_s}{d_f} = F \left\{ \frac{H}{d_f}, \frac{gT^2}{d_f}, \tan \alpha \right\}$$

$$\frac{d_s}{H} = F \left\{ \frac{D_b}{H}, \frac{D_f}{H}, \frac{d_f}{H}, \frac{H}{gT^2}, \tan \alpha, \frac{\rho_s}{\rho_w}, \frac{\sqrt{gHD_f}}{v} \right\}$$

$$\frac{A_s}{HgT^2} = F \left\{ \frac{d_f}{D_f}, \frac{D_b}{D_f}, \frac{\tan \alpha}{\sqrt{\frac{2\pi H}{gT^2}}}, \frac{\rho_s}{\rho_w}, \frac{\sqrt{gHD_f}}{v} \right\}$$

$$\frac{A_s}{HgT^2} = F \left\{ I, N, \frac{d_f}{D_f}, \frac{D_b}{D_f}, \frac{\tan \alpha}{\sqrt{\frac{2\pi H}{gT^2}}}, \frac{\rho_s}{\rho_w}, \frac{\sqrt{gHD_f}}{v} \right\} = F \left\{ I, N, m, \frac{D_b}{D_f}, m, \xi, \frac{\rho_s}{\rho_w}, \text{Re} \right\}$$

Length scale distortions

Many of the Pi-terms found are a combination of two length parameters. This indicates that the length scales should all be scaled with the same factor to avoid

scaling effects. Unfortunately this is not always possible; especially the scaling of sand grain diameters gives problems in this field.

Froude scaling importance

For the process of loading to hydraulic gradient as well as the process of hydraulic gradient to porous flow, the Froude number appeared as one of the Pi-terms. The Froude number is therefore very important for the scaling process, as was expected for processes where flow is important. The Froude scaling law implies that the length scale factor should be the square of the velocity scale factor.

Reynolds scaling importance

For the hydraulic gradient, the kinematic viscosity seems to play a role and for the filter velocity the Reynolds number itself appeared as one of the Pi-terms. As a result, the Reynolds number should be preserved, because it is important for the processes involving porous flow, the processes in the filter layer. Unfortunately, as stated earlier, simultaneous Froude scaling and Reynolds scaling is not possible. A common use is to use the Froude scaling law and to estimate the Reynolds scaling effects as good as possible. Section 4.2 elaborates on this and on how this problem will be dealt with.

Density ratio

The ratio of the densities of water and rock/ sand appears for the dimensional analysis of the Kalinske-Frijlink formula. Although this formula is not designed for this application, the process is very similar to the detailed process of bed load sand transport inside the filter layer, on the small pores-scale. It suggests that the densities of water and other materials should stay in the same ratio. As water is meant to be the used fluid in the model as well as in the real situation (naturally), the density ratio prescribes the same density of sand and rock in prototype and model. The only consideration that might affect this is that in most real situations, the water will be salty, salt water having a density of about 2,5 to 3 percent higher than fresh water, which will be used in the model. This can cause a scale effect.

Initially dimensionless parameters

Parameters that are initially dimensionless, such as the hydraulic gradient, the slope steepness and the porosity, are to be preserved as well.

Comparisons with other processes and known relations

Not all aspects of the total process from hydraulic loading to erosion could be captured in one relation and therefore some important parameters might be missed. In order to handle all the important aspects properly, results of similar studies and known scale effects will be studied and compared with the findings of the dimensional analysis in the next section. Effects like air entrainment in breaking waves, types of wave breaking, extra water properties, sand or stone properties or geometric properties might have additional scaling effects. Another important reason for the comparison with literature is to come to a quantification of the scale effect. With the dimensional analysis only the qualitative effects of parameter combinations are studied and parameters that are to be preserved in order to avoid scale effects are formed. However, because it is impossible to preserve all the important parameters, scale effects will certainly be present. The question remains what the magnitude of the effects is and if the processes themselves are changed or that just the outcomes of the

tests are too high or too low, and to what extent. Section 4.2, quantification of the scale effects elaborates on these questions.

Usefulness for the analysis

The last four of the dimensionless relations are expected to be interesting for the analysis of the test results as done in Chapter 7. All parameters used in these relations are to be measured in the tests, except for the hydraulic gradient. It will be tried to use an estimate of the gradient or to find a relation for it with known parameters. The erosion area and –depth are important parameters for the design of the structure and a formula that relates the erosion to the loading situation with wave parameters, structural parameters and duration will be very useful to the designer.

4.2 Comparison and quantification of the scale effects

It can be concluded from the previous section that scale effects will be present between prototype and model scaled processes. Scale effects and therefore some degree of distortion of the results is inevitable. In this section, the magnitude of these scale effects is studied by comparing the results from the dimensional analysis with literature on similar processes and by comparing the processes for this breakwater layout and configuration with known magnitudes of scale effects for similar situations. The result will be an estimate of the order of magnitude of scale effects rather than an absolute value or percentage. It can serve as an indication for the validity of the experiments and as a guideline for the scaling procedure to be followed. Important literature sources for this are Hughes (1993) [26], Ettema et al. (2000) [9], and Tirindelli et al. (2000) [44].

4.2.1 Comparison of the dimensional analysis with literature

In Hughes (1993), a dimensional analysis for rubble mound breakwaters is presented as performed by Hudson et al. (1979). It should be noted that these tests and analyses are done for structures with a core of quarry run instead of sand and that the main focus is the stability of the armour layer, internal stability being assured by geometrically closed conditions for filter and core layers. Nevertheless, the results are valuable, because the porous flow in the rubble material induced by wave attack is treated and is a very important process for the present research into open filters. Some findings of those studies can be used as indication for the present research. Besides the analysis for rubble-mound structures, also analyses for coastal sediment transport are treated. These are also interesting for the present research as the erosion of core material is similar to the sediment transport process.

Dimensional analysis for rubble mound breakwaters by Hudson et al. (1979)

A large number of involved parameters is listed as follows:

h	-	Water depth at toe of structure
D	-	Percent damage to cover layer
g	-	Gravitational acceleration
H	-	Wave height
l_a	-	Characteristic linear dimension of armour unit
U	-	Water velocity near the cover layer
α	-	Seaside slope angle (from the horizontal)
β	-	Incident wave angle
Δ	-	Shape factor of units
θ	-	Bottom slope seaward of structure
L	-	Wavelength
μ	-	Dynamic viscosity of water
k_a	-	Linear dimension of surface roughness of units
ρ_a	-	Mass density of units
ρ_w	-	Mass density of water

In equation form this becomes:

$$f(U, H, L, h, \beta, \theta, g, \rho_w, \rho_a, l_a, \mu, k_a, \alpha, \Delta, D) = 0$$

After rearrangement of parameters into dimensionless combinations this becomes:

$$F \left\{ \frac{l_a}{h}, \frac{H}{L}, \frac{h}{L}, \alpha, \beta, \Delta, \theta, \frac{U}{\sqrt{gl_a}}, \frac{Ul_a}{\mu/\rho_w}, \frac{k_a}{l_a}, \frac{\rho_w}{(\rho_a - \rho_w)}, D \right\} = 0$$

For complete similitude between model and prototype, all these dimensionless terms should be preserved. The first seven terms are preserved by a geometrically undistorted model. $\frac{U}{\sqrt{gl_a}}$ is the Froude number, $\frac{Ul_a}{\mu/\rho_w}$ is the Reynolds number, $\frac{k_a}{l_a}$ indicates that the roughness of the stones should be scaled in proportion to the length dimension of the stones, $\frac{\rho_w}{(\rho_a - \rho_w)}$ is preserved when the density ratio of water and stone is preserved, and D is the dependent (dimensionless) variable in the analysis. Together, a short list of most important requirements for the scaling of rubble-mound breakwaters is formed:

- Rubble mound structure models must be geometrically undistorted in length scale.
- Flow hydrodynamics in a rubble-mound structure model must conform to the Froude criterion.
- Rubble-mound structure models must have turbulent flow conditions throughout the primary armour layer.
- The surface of structure units is to be made as smooth as possible.
- The ratio of density of stone and water is to be preserved.

All these requirements, except the surface roughness requirement, were also found in the different parts of the dimensional analysis for the breakwater with sand core and very open filter, presented last section.

Dimensional analysis for coastal sediment transport by Kamphuis (1985)

Research and experiments into coastal sediment transport are aimed at different applications than breakwaters with a sand core, but the process of picked up and transported sediment by currents induced by waves, is very similar for the movable bed models and the transport through the relatively very open filter layer. Kamphuis (1985) performed a dimensional analysis for these processes²⁷, of which here only the result is presented:

$$F \left\{ \frac{H}{L}, \frac{h}{L}, \frac{x}{L}, \frac{y}{L}, \frac{z}{L}, \frac{k_s}{L}, t\sqrt{\frac{g}{L}}, \frac{v}{L\sqrt{gL}} \right\}$$

As in the analysis for rubble-mound structures, the first obvious criterion is that the model is to be geometrically undistorted in length scales. The first five dimensionless products lead to this criterion. The sixth dimensionless product suggests that the bottom roughness k_s should be scaled in proportion with the other length scales. The

²⁷ From Hughes (1993) [26]

seventh product indicates that the hydrodynamics are scaled according to the Froude criterion, and the eighth product can be recognized as a flow Reynolds number with \sqrt{gL} representing the velocity. The Reynolds number is to be preserved, or at least turbulent flow in the model is required wherever the flow is turbulent in the prototype. Together, the model should be geometrically undistorted, roughness should be proportional to the length scale and Froude and Reynolds numbers should be preserved.

Bedload dominated sediment transport

For bedload transport, a slightly different approach was used, with sediment parameters D , ρ_s and τ_b , (bottom shear stress) combined with fluid parameters ρ , v and λ (characteristic length, in short wave models taken as the wave amplitude). Also the fall speed, w and the shear velocity, $u_* = \sqrt{\frac{\tau_b}{\rho}}$ were used. The result was the following dimensionless equation in which $\gamma_i = (\rho_s - \rho)g$:

$$\Pi_{S_0} = F \left\{ \frac{u_* D}{v}, \frac{\rho u_*^2}{\gamma_i D}, \frac{\rho_s}{\rho}, \frac{\lambda}{D}, \frac{w}{u_*} \right\}$$

In this equation, the first dimensionless term is the particle Reynolds number, the second is the densimetric Froude number. Together they represent the axes of the Shield's diagram for incipient motion of sediment under flow. The third term is the relative density, the fourth is the relative length and the fifth term is the relative fall speed, the fall speed relative to the shear velocity. The results are similar to the former analyses; some form of Froude and Reynolds number, some form of relative length scale and relative density appear almost every time. The difference here is that the involved parameters affect the process on a very small scale, like the shear velocity acting on a sand particle, or the fall speed of a particle.

Suspended load dominated sediment transport

For suspended load transport, the fall speed is thought to be more important than the shear stress and shear velocity, because the grains are set in motion and kept in suspension by the turbulence of the breaking waves rather than by the shear stress on a grain. Therefore, for suspended load transport, the Dean number or fall speed parameter $\frac{H}{wT}$ is often preserved in the model instead of the Shields parameter or relative shear velocity. The fall speed parameter gives some indication of the importance of suspended load relative to bedload transport, as it can be seen as the ratio of a sediment fall time (H/w) and the wave period. The fall speed parameter is preserved if $n_H = n_w n_T$, so e.g. with $n_w = n_T$ and $n_H = n_T^2$, which is in accordance with $n_{Fr} = 1$ for the scaling of waves. Noda (1978)²⁸ got good results for wave flume tests for equilibrium beach erosion profiles when the fall speed parameter was preserved, and much poorer results when it was not preserved. Dean formulated a list of criteria for geometrically undistorted suspended transport models:

²⁸ From Hughes (1993) [26]

- The model must be geometrically undistorted
- Hydrodynamics should be scaled according to the Froude criterion
- Similarity of the fall speed parameter should be maintained
- The model must be large enough to preclude significant viscous, surface tension, and cohesive sediment effects so that the character of wave breaking is properly simulated
- Sand is preferred as the model material

The above criteria satisfy the Froude hydrodynamic criterion, the ratio of wave steepness H/L_0 , the ratio of fall speed parameter and the ratio of relative density. The drawback is that the Shields parameter is not preserved, leading to scale effects especially if bedload transport also occurs in the model.

4.2.2 Scale effects from other studies

Little quantitative information on scale effects is generally available, results are mostly only suitable for a very specific situation, or results give only qualitative indications and mostly guidelines as to how to avoid scale effects. For the quantitative investigation of scale effects, very often a scale series or comparison with prototype measurements are suggested, non of which are possible within the scope of this study.

Scale effects for wave-structure interactions

Although the primary wave-structure interactions, like armour layer stability, are not the goal of this research, the process is interesting because the porous flow in the filter layer results from the interaction of waves and the structure. In Tirindelli and Lamberti (2000), the following scale effects are brought forward, with Re_c as critical Reynolds number with $U = \sqrt{gH_s}$. The Froude criterion is applied for the scaling.

- Dai and Kamel (1969) found no scale effects on armour damage for $Re_c > 3 \times 10^4$ with $D_{n50} = 20-300$ mm and regular waves.
- Thompson and Shuttler (1975) found no clear dependency of the erosion on Re with $D_{n50} = 20-40$ mm with irregular waves.
- Van der Meer (1988) and others found no significant scale effects on armour stability for $Re_c = 1 \times 10^4 - 4 \times 10^4$ with irregular waves.
- Jensen and Klinting (1983) argued from theoretical considerations that $Re_c > 0,7 \times 10^4$.
- Sharp and Khader (1984) proposed $Re_c = 4 \times 10^5$, but Kajima and Sakakiyama (1994) suggested $Re_c = 3 \times 10^4$ for regular waves.
- Wave run-up can be underestimated in the model. Re_c values are suggested to be the same as for wave impact.
- Van der Meer and Veldman (1991)²⁹ found no significant scale effects for berm breakwater erosion patterns between a 1:7 and a 1:35 scale model. Wave overtopping and reflection were similar, only wave transmission was 10 – 50% higher in the larger model for the largest waves.

Others suggest that the Reynolds number must at least be 4.000 to 10.000. As the Reynolds number gets lower in the model, more viscous scale effects will be

²⁹ Van der Meer and Veldman (1991) [37]

introduced, increasing gradually in magnitude. A sharp boundary does not exist, but effects are thought to be not very large for Reynolds numbers above 10^4 .

Surface tension and viscosity effects for breaking waves

Among others, Tirindelli and Lamberti (2000) indicate that for breaking waves, surface tension and viscous forces give no scale effects as long as the wavelength is greater than 0,5 m and the period greater than 0,5 s. Related to surface tension is a scale effect that does play an important role in breaking model waves: the difference in air entrainment by either fresh or salt water and by smaller scales, leads to scale effects. Air entrained in the wave has a damping effect on the impact of the wave on a structure. Bullock et al. found 10% higher impact values in the model than in the prototype for a Froude scale factor of 1:25³⁰.

4.2.3 Scaling requirements for open filters on a sand core

The configuration of the breakwater for the present research with a hydraulically sand-open filter on a sand core, leads to the occurrence of several different processes that ask for different scaling requirements:

- Incoming waves are successfully scaled with the Froude criterion as long as Reynolds numbers are high enough for the flow to be turbulent.
- Breaking waves are usually scaled with the Froude criterion, but the difference in air entrainment by both fresh or salt water and smaller scales, leads to scale effects.
- Porous flow is scaled successfully for rubble-mound breakwaters with a method that preserves a characteristic value for the hydraulic gradient in the most important points of the cross section³¹.
- Stability tests for rubble-mound structures are scaled with the Froude criterion and additional criteria like geometrically undistorted length scales, turbulent flow in the model, smooth surface of stones and preserved relative density.
- Bedload sediment transport is scaled with the Shields criterion.
- Suspended load sediment transport is scaled with preservation of the fall speed parameter, by which the Shields parameter is not preserved.

It is not possible to satisfy all the requirements for all the processes, which are already compromises for the different aspects of the specific process. Perfect similitude between model and prototype is not possible, nor is it possible to draw one list with scale criteria that can all be satisfied and that satisfy the requirements for all the processes involved. Nevertheless, similarity between the different requirements exists and indications exist that scale effects remain within reasonable limits when certain boundary conditions are fulfilled. The best fit of scale requirements for open filters in breakwaters with a sand core is therefore believed to be as follows:

Scaling requirements for the model in the present research

- The model is recommended to be geometrically undistorted in length scales. Only the grain size of the core material, sand, cannot be scaled according to the overall length scale factor.

³⁰ From Tirindelli et al. (2000) [44]

³¹ Burcharth et al. (1999) [8]

- Hydrodynamics in the model must conform to the Froude criterion.
- The model must have turbulent flow conditions outside and inside the filter layer.
- The surface of filter stones is to be made as smooth as possible.
- The ratio of density of stone and water is to be preserved.
- The sediment grain size can be scaled according to the fall speed parameter preservation.
- The densimetric Froude number (Shields parameter) is to be preserved as much as possible.

The above requirements are a combination of the requirements for the separate processes as described earlier. The first three are found for practically all coastal engineering models and form an important basis. The fourth requirement serves to prevent too high frictional forces in the model. The fifth requirement preserves the relative density, which results from several dimensional analyses. The sixth requirement preserves the fall speed parameter and leads to discussion; the difference between bedload and suspended load sediment transport. The last requirement is closer to a guideline; the Shields parameter should actually be preserved but cannot be by the choice of priority for the sixth requirement.

Discussion of sediment transport and the scaling of sand

The use of the fall speed parameter for the scaling of sediment is desirable for suspended load transport, but compromises the last requirement for the densimetric Froude number, thus leading to scale effects for bedload transport. Both transport modes have been observed by Uelman in his tests. It is therefore difficult to say whether the choice for fall speed parameter preservation gives better results than the choice for Shields parameter preservation. The choice as made in the requirements to give the fall speed parameter the priority, results from practical considerations related to the scaling of sand grains. Following the fall speed parameter scaling, the grain size can be scaled down with the same ratio as the wave period (time scale), which is then the square root of the ratio for the wave height (length scale). This smaller ratio makes it possible to scale down coarse sand in the prototype to fine sand in the model, for usual scaling factors. Scaling with the Shields parameter asks for a higher scaling factor, making it very difficult to use sand as a representative material in the model.

Desired other requirements that are not met

For porous flow in a rubble-mound structure, preservation of the hydraulic gradient is desired, but is not met by the set of requirements. The reasons are of a practical nature: first, the preservation of the hydraulic gradient needs information about the gradient in a prototype situation. The described method by Burcharth³² to do this requires prototype measurements or simulations, none of which are available for this research. Second, preservation of the gradient leads to distortion of other requirements, and choices have to be made. The made choices are mentioned above; scale effects due to not met requirements are estimated as good as possible.

Scaling according to the Froude criterion makes it impossible to satisfy the Reynolds criterion as well. For wave propagation outside the structure this will give no noticeable effects, but for porous flow inside the filter layer, viscous forces easily become too large. This effect will be quantified below. Also the particle Reynolds

³² Burcharth et al. (1999) [8]

number, important for the bedload dominated sediment transport and related to the shear stress, is not preserved. After the tests, an estimate of the particle Reynolds number is to be made in order to see the influence of viscous forces and judge the possible effects associated with this. Also effects due to not properly scaled bottom roughness can be expected. Bottom roughness depends on the grain size.

4.2.4 Quantification of scale effects for this research

Quantification of scale effects for a breakwater remains problematic after the dimensional analysis and comparisons to other research, because only few quantitative results for similar studies have been found. Most guidelines give ranges for certain parameters for which no significant scale effects have been noticed, like for instance a lower boundary for the Reynolds number, above which little viscous effects have been noticed.

In the next chapter, test choices are made. A reference test is chosen as test number 6 by Uelman, where $H = 0,10$ m, $T = 1,2$ s, $D_{f50} = 0,033$ m and $D_{b50} = 0,16$ mm. This reference test is used for the quantification of the scale effects. The following effects and ranges have been found.

Viscous scale effects for porous flow in rubble-mound models

In Hughes (1993), the stability for outer layers is related to the Reynolds number for the same layer. Figure 4-2 shows this relation, where the upper line is the stability number in the prototype and the lower line is the stability number in the model, after Dai and Kamel (1969). This stability number is defined by Hudson (1958)³³ as

$$N_s = \frac{\gamma_s^{1/3} H}{\left(\frac{\gamma_s}{\gamma_w} - 1 \right) W_s^{1/3}}$$

in which $\gamma_s = \rho_s g$ is the specific weight of the stones, W_s is the

weight of the stone and H is the no-damage wave height (threshold of damage).

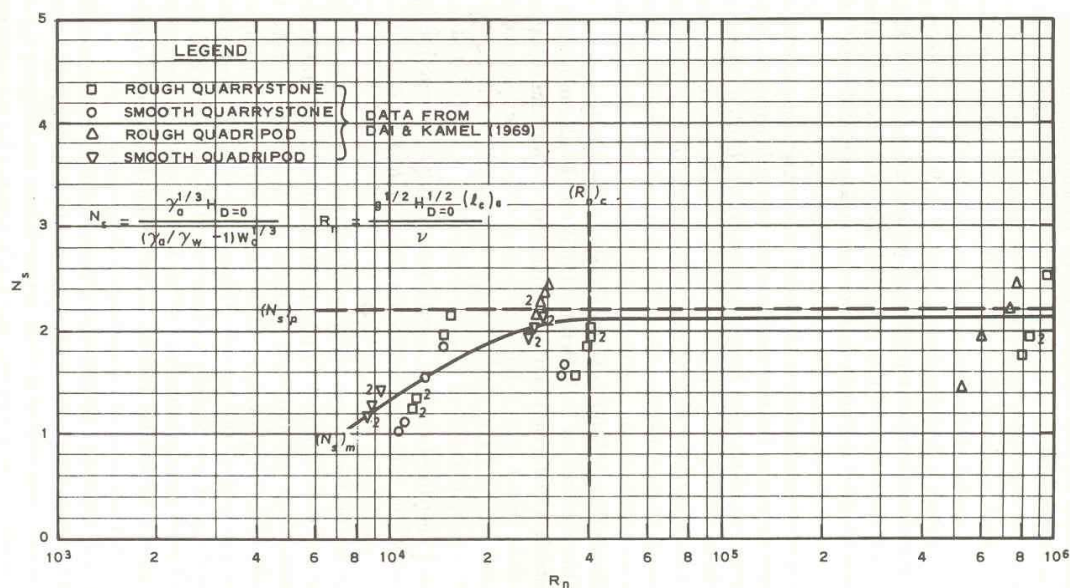


Figure 4-2 Viscous scale effects on rubble-mound stability models (from Hughes 1993)

³³ From Hughes (1993) [26]

The Reynolds number $Re = \frac{\sqrt{gH} D_{50}}{\nu}$ for the reference test is $2,5 \times 10^4$. The figure shows that for $Re = 2,5 \times 10^4$, a scale effect of about 10% occurs. In the model the Reynolds number is lower, thus viscous forces are stronger leading to more resistance to the flow resulting in higher damage because of the higher resistance forces. In other words, for the reference test the damage to the armour layer can be overestimated with about 10% in the model. The stability of the armour layer is not the goal of this research, but it is expected that the viscosity-related scale effect also affects the porous flow in the filter layer in approximately the same way. The velocity is calculated as $U = \sqrt{gH}$ here, the effect is expected to be in the order of the square root of the stability number effect, so the expected underestimation of forces due to viscous effects by the porous flow velocity is in the order of 5%.

Other scale effects related to viscous forces

As discussed in the previous section under ‘wave structure interactions’, different lower boundary values for the Reynolds number are given to avoid scale effects in a Froude-scaled model. From this discussion it is expected that no significant scale effects in wave-structure interaction will occur as long as the Reynolds number exceeds 10^4 . For the reference test, $Re = 2,5 \times 10^4$, so this criterion is met for the reference test. In addition, Thompson and Shuttler (1975) found no clear dependency of the erosion of Re with $D_{n50} = 20-40$ mm with irregular waves. The D_{f50} , the grain size of the filter layer, lies within this range for the reference test.

As a result of overestimated viscous forces, wave run-up can be underestimated in the model. Reynolds boundary-values are suggested to be the same as for wave impact.

For berm breakwaters, Van der Meer and Veldman (1991)³⁴ found no significant scale effects in erosion patterns between a 1:7 and a 1:35 scale model. Wave overtopping and reflection were similar, only wave transmission was 10 – 50% higher in the larger model for the largest waves. This means that more damping occurs at the small scale for which higher forces are necessary. The forces will be overestimated in the model. Wave transmission will hardly occur through the sand core of the present breakwater model, but penetration of the waves through the filter layer is important. The scale effect found by Van der Meer and Veldman holds for transmission through the entire structure, which leads to the hypothesis that the effect for penetration through a relatively thin filter layer is considerably smaller. Therefore it is expected that the 10% overestimation of the damage by the wave height and 5% overestimation of the damage by the filter velocity described above represent the viscous scale effect well enough.

Surface tension effects

For breaking waves, surface tension was not found to give scale effects as long as the wavelength is greater than 0,5 m and the period greater than 0,5 s. In the reference test, the period is 1,2 s and the wavelength is 2,2 m, both well above this limit.

The impact of breaking waves on a structure is affected by surface tension through the amount of entrained air and the size of the air bubbles. A scale effect of 10% has been

³⁴ Van der Meer and Veldman (1991) [37]

found. Bullock et al. (2001) found 10% higher impact pressures in the model than in the prototype for Froude scale factor 1:25 and $H_s = 0,25\text{m}$. It is not known what the effect of this is on the porous flow velocity in the filter layer, but an effect is expected, probably less pronounced than the effect on the impact. By lack of knowledge, a best guess is that the effect will also be 10% on the 'wave height' penetrating the filter, which leads to up to 5% higher velocities.

Density scale effects

If no correction is made to the density of the stones to keep the correct relative density, an estimated scale effect of up to 15% can occur in breakwater stability, where the fresh water is only 3% lighter than the salt water. Hughes (1993) describes a correction method, which could be helpful when scaling up for design purposes.

Summary of quantified scale effects

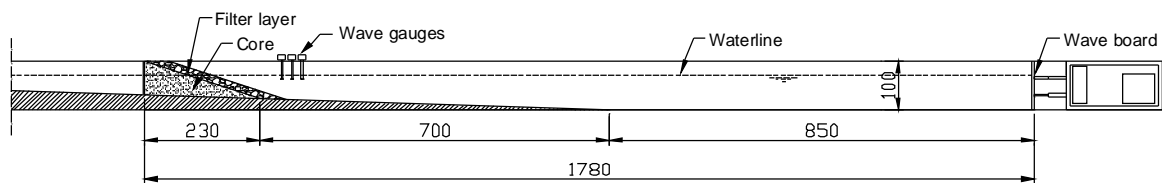
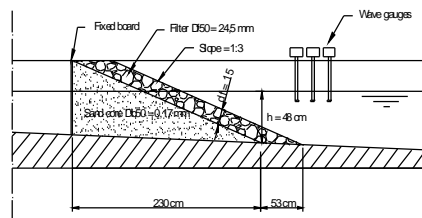
- Viscous effects are expected to cause overestimation of damage in the model by the penetrating wave height of up to 10% and by the maximum porous flow velocity of up to 5% for the parameters of the reference test.
- Differences in air entrainment of breaking waves due to surface tension effects can cause overestimation of wave impact values. An overestimation in the model of up to 10% for the penetrating wave height and up to 5% for the porous flow velocity should be accounted for.
- Density scale effects due to the use of fresh water instead of salt water in the model can be as much as 15% if no correction is made. This correction should therefore be made in the analysis of test results when a prototype situation with salt water is used.

The conclusion from the scale effect quantification is that with a good analysis, the errors of porous flow velocities can be limited to about 5%. The effect of this on the sediment transport and erosion is still not known, but is also limited. The analysis indicates that the test results do not give an exactly quantitatively correct result, but that the errors due to scale effects are limited and therefore the tests give at least a good qualitative picture of the processes at prototype scales.

Chapter 5

Test program for hydraulic variations

Test Number	Parameters Variations	H m	T s	ξ (-)	regularity reg/irreg.	N (-)	DBS/D15 (-)	tan alpha (-)
1	Reference	0.10	1.20	1.58	regular	7200	1.8	0.33
2	Irregular waves	0.10	1.20	1.58	irreg-oneswap	7200	1.8	0.33
3	Varying H	0.08	1.07	1.57	irreg-oneswap	3600	1.8	0.33
4	and N	0.12	1.31	1.57	irreg-oneswap	3600	1.8	0.33
5		0.14	1.42	1.58	irreg-oneswap	7200	1.8	0.33
6	Varying ξ by varying T	0.10	1.00	1.32	irreg-oneswap	3600	1.8	0.33
7		0.10	1.50	1.97	irreg-oneswap	3600	1.8	0.33
8		0.10	2.00	2.63	irreg-oneswap	3600	1.8	0.33
9	Swell waves	0.05	3.00	5.58	regular	9600	1.8	0.33
10	Grading variation	0.10	1.20	1.58	irreg-oneswap	3600	5.0	0.33
11	tan alpha variation	0.10	1.20	1.19	irreg-oneswap	3600	1.8	0.25
12		0.10	1.20	2.37	irreg-oneswap	3600	1.8	0.50



5.1 Parameter adjustments

5.2 Expected relations and parameter variation choices

5.3 Test program

5.4 Measuring techniques

5.5 Test set-up

Chapter 5 Test program for hydraulic variations

Many possibilities exist to test different parameter relations and performance of the structure under different conditions. In this chapter, the choices are made which tests to perform. In order to make these choices, first the possible adjustments of the parameters are described, after which the sensitivity of the relations between the varying parameters and the erosion parameters are estimated. From these relations, choices for the values of the parameters are made.

In chapter 3, the choice for the research direction has been discussed; this chapter elaborates on the made choice for the investigation of the stability of the breakwater configuration as a function of the hydraulic loading by performing tests in the small scale wave flume at the fluid mechanics laboratory of Civil Engineering at TU Delft.

5.1 Parameter adjustments

This section discusses how the different adjustable parameters can be varied by different test setups or different types of tests, and what the expected effects are. In essence, the possibilities for further testing are described.

5.1.1 Loading

Reference test to make comparisons with the tests by Uelman

Before performing tests with varying hydraulic loading, a reference test will be done with for as much as possible the same parameters as used in test number 6 from Uelman. For this test, the wave height was 0,10 m for regular waves, the period was 1,2 s, the D_{f50} was 0,033 m, the D_{b50} was 0,16 mm and the d_f was 0,15 m. The test set up is shown on the figure.

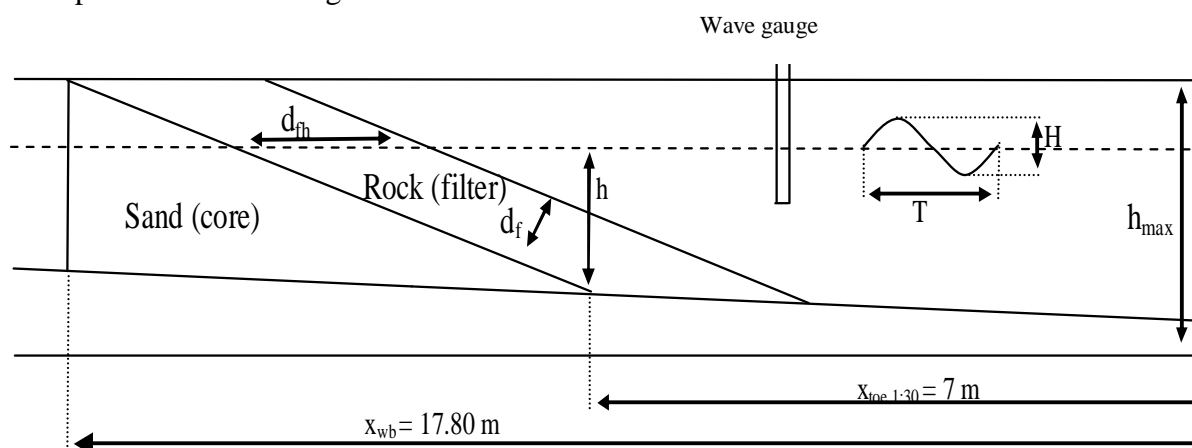


Figure 5-1 Set-up of the flume tests performed by Uelman (from Uelman 2006)

The test set-up is chosen to be the same as the set-up by Uelman to make good comparisons of the results. The set-up will be discussed in a later section of this chapter.

Wave height, period and steepness

The wave height and period in a wave flume can be adjusted by different settings of the wave generator. In the flume, a wave gauge can measure the wave height and

period quite accurately. The wave steepness is a function of the height and period. To make a distinction between wave height variations and period variations, first the wave height will be varied, maintaining the same steepness, after which the period will be varied, maintaining the same wave height. The first wave height variations change the magnitude of the same type of waves, the latter period variations will change the wave steepness as well, so it will change the type of waves with the same steepness.

Regular waves or irregular waves

The regularity of the waves can be adjusted by different settings of the wave generator. In real life, waves are irregular. Therefore, to represent the real situation as good as possible, irregular waves would be better suited. However, when testing, one wants to see connections between loading and effects like erosion, and for regular waves, these connections are easier made because the effects of wave-induced turbulence and the irregularity of the waves can be separated. The tests by Uelman were performed with regular waves. It is expected that irregular waves will show different behaviour of the structure, because the large variation in occurring wave heights. The maximum wave height is about twice the significant wave height for a Jonswap spectrum. To investigate this important difference, tests will be performed with irregular waves, and variations in the significant wave height and period will be made. The Jonswap spectrum is representative for sea states that are being driven by wind. As long as wind is the driving force, sea states resemble this Jonswap spectrum. Therefore this type of wave distribution is representative for storm waves, the design loading for breakwater structures.

Number of waves

To change the number of waves, the duration of the test can simply be lengthened in a wave flume. To see if the erosion pattern stabilizes after a certain number of waves, some tests will be lengthened until this stabilization occurs or until the test shows that it does not occur within a reasonable number of waves. For other tests, the number of waves will be chosen such that a typical design storm event is represented.

5.1.2 Material properties

Core material

The core material is sand, non-cohesive grains in a range of about 100 μm to 2 mm. The variability of the D_{b50} is therefore limited in order to stay within this range. Furthermore, to get all the sand out of a wave flume and replace it takes a lot of work. The variation of the sand grain sizes is not the most practical solution to vary material properties.

Filter grain size

The filter grain size, D_{f50} is easier to change than the core grain size and the possible range is much larger. Former test results indicate a significant effect of the filter grain size on the erosion. The filter grain size will not be varied in the tests, as the choice has been made to vary the hydraulic loading rather than the material. A filter material similar to the chosen reference test of Uelman will be used in the tests.

Filter material grading

The grading of the filter material can be varied by applying different sets of material with different sieve curves. It is expected that a wider graded material results in less erosion of core material. If enough time is available, a widely graded filter material will be tested to study the influence of the grading.

Relative filter thickness

The (relative) filter thickness can easily be changed in a wave flume by applying more filter material. A clear relation between this m and the erosion has been found earlier and is expected to be found again when more tests are carried out. The filter layer thickness has not been chosen as a variable in the tests. However, when results indicate that the applied thickness gives too much erosion to study the hydraulic variation in a good way, a thicker layer will be applied.

5.1.3 Structure layout

Slope steepness

The slope steepness mainly affects the type of wave breaking, and therefore the loading. A milder slope can result in spilling breakers instead of plunging breakers and spreads the energy dissipation over a longer distance, probably resulting in a smaller erosion depth and larger erosion length. On very steep slopes the waves do not break but surge, giving yet another type of loading. In this way the slope steepness affects the loading, and is therefore chosen as a variable parameter in the tests.

Other layout parameters

Other parameters related to the structure layout like the application of a berm or variations of the crest height have not been chosen to study. The expected influences are discussed in chapter 3 in the choice of research direction.

5.2 Expected relations and parameter variation choices

The reference test is expected to show results similar to the test by Uelman with the same parameters. For the other tests, the expected relations between loading and erosion are described per varying parameter. The chosen varying values for the different parameters based on these relations are presented per parameter.

5.2.1 Wave height variation

The wave height H is expected to have a large influence on the erosion. Known relations: E , the wave energy, is proportional to H^2 and in the Van der Meer equations, (Schiereck, 2001) the damage factor S is proportional to H^5 . This S is an area divided by the square of the stone diameter, which is not the same as the erosion area or erosion depth in these tests, but gives an idea of what kind of influence H can have. The expected influence of H on the erosion is in the order of:

- $d_s \propto H^2$, the erosion depth will be in the order of the square root of an area like the area in S , which means a second or third power relationship.
- $L_r \propto H^1$, the erosion length is mainly dependent on the run-down point of the wave, which increases with the wave height. For a slope steepness of 1:3, the erosion length would then increase with 1,5 times the wave height, so $\Delta L_r = 1,5 \cdot \Delta H^1$.
- $Total \cdot erosion \cdot area \propto H^3$, the erosion area is about the depth times the length.

Because the sensitivity of the erosion on the wave height, the wave height will be varied in small steps, from $H_s = 0,10$ m for the first test to $H_s = 0,12$ m and $H_s = 0,14$ m for higher waves, and to $H_s = 0,08$ m for smaller waves. For $H_s = 0,14$ m, the erosion depth is expected to be almost twice as much as for $H_s = 0,10$ m. The variation of the wave height and period will be done with irregular waves.

5.2.2 Number of waves for equilibrium

It is not sure that an equilibrium situation will develop for the design conditions, but if it does, at least a large number of waves is needed for it to be reached.

- For armour layers in the Van der Meer equations, equilibrium is reached after 7500 waves. (Schiereck, 2001).
- Uelman's tests showed a tendency towards equilibrium, but after 2400 waves and even 4600 waves for one of the tests, it was not reached. For test 6, the reference test, equilibrium might be reached after about 4000 waves, based on the erosion growth curve.
- The number of waves for equilibrium is expected to be dependent on the loading (H, T, ζ).

For the reference test, equilibrium is expected after 4000 to 7000 waves, based on erosion growth graphs of Uelman's tests and the above. For this reference test, for the tests with $H_s = 0,10$ m (irregular waves), for the test with $H_s = 0,14$ m and for the test with swell waves, the duration will be extended until equilibrium occurs or until the structure deforms too much and does not function anymore. The number of waves for the other tests will be 3600, representative for a storm of about 12 hours.

5.2.3 Wave period variation

A larger wave period T gives more time for inflow and especially outflow; the flow can develop further, and has more time to start erosion and to transport grains further during one period.

- $\xi \propto T$ and $Rundown \propto \xi^{1 \text{ or } 2(\text{regular})}$ so the rundown and with that the erosion length depends on T , probably to the first order, $L_r \propto T^1$.
- The erosion depth is also influenced by T , but probably less than by H , possibly with a first order relation or similar.
- For swell, relatively low waves with long periods, the results are interesting, but it is difficult to give a good expectation.

With the wave period variation for a preserved wave height of $H_s = 0,10$ m, the wave steepness and with that ξ are varied as well. The erosion is less sensitive on period than on wave height, so a bit larger steps in the wave period T_p can be taken. To stay within realistic steepness values, $T_p = 1,0$ s has been chosen as the shortest wave. $T_p = 1,5$ s and $T_p = 2,0$ s are taken for the longer waves and $T_p = 1,2$ s is tested in the reference test with irregular waves.

5.2.4 Irregular waves: Jonswap

Irregular waves, waves generated by wind have a Jonswap-type spectrum as long as the wind forcing is still active³⁵. During a storm waves are generated in this form. Shallow water or bed forms can influence and deform the spectrum, but breakwaters are often loaded by something similar to a Jonswap spectrum. Therefore it is chosen as loading.

- $H_s \approx 4\sqrt{m_0}$ and $H_{\max} \approx 2H_s$. The average wave height is not so high (lower than H_s), but much higher waves do occur.
- The development of a bar profile is expected, but probably less pronounced, as the higher waves damage the bar.
- The process and therefore the growth of the damage will be more irregular.
- For comparison, $H_s = 0,10$ m, = $H_{\text{reference regular}}$, and $T_p = 1,2$ s have been chosen for a first test to compare the irregularity of the waves with the reference test. Other variations of H_s are described above.

5.2.5 Swell waves

Swell is the result of waves that are generated in a storm that has ceased or that is further away. The waves are transformed to more regular waves with relatively low wave heights, but with long periods. It can be the only form of waves on a calm day, or be superimposed on locally forced waves.

- Proposed here is to do the tests with regular waves, with wave height and period typical for swell, to see the effect of this long period on the erosion.
- It is expected that the relatively low wave height gives low gradients, but that the long period gives a lot of time for the porous flow to develop and to start the transport of sand grains.
- With the very open filter (D_{f50}/D_{b50} of about 200), the critical gradient for the initiation of transport is very low and will probably be exceeded by the swell waves, resulting in a slow but steady transport. The amount of erosion is hard to predict.

³⁵ Holthuijsen (2005) [24]

- The parameters are chosen based on the Froude scale, which gives a possible prototype wave height of 10 m and period of 12 s for the reference test. If for swell $H_{pr} = 5$ m and $T_{pr} = 30$ s is chosen, this would result in $H = 0,05$ m and $T = 3,0$ s with the same scale factor.

5.2.6 Grading variation

It is expected that the D_{f15} is the characteristic size for the performance of the filter, determining the constriction size that occurs regularly throughout the filter layer. It is expected that filter layers with the same D_{f15} show a similar erosion pattern. In the tests it is tried to keep the D_{f50} constant at 33 mm, varying the ratio D_{f85}/D_{f15} to about 5.

Table 5-1 grain sizes grading variation

	D_{f15} (mm)	D_{f50} (mm)	D_{f85} (mm)	D_{f85}/D_{f15}
Reference	27.7	33	35.8	1.3
Wide	10	33	50	5

It is expected that the wide grading will give less erosion than the narrow grading with the same D_{f50} . The smaller stones (D_{f15}) in the wide grading are smaller than in the narrow grading and are expected to decrease the loading inside the filter and increase the resistance for sand grains through the filter. The larger stones can provide more stability against wave attack given that the layer is thick enough for the large stones to be present throughout the whole surface. Constructing the wide graded material can be a problem, as probably three different standard gradings are to be combined to get the wide grading.

5.2.7 Slope steepness variation

$\xi \propto \tan \alpha$, the breaker type depends on the slope steepness. To change the waves with $H = 0,10$ m and $T = 1,2$ s from plunging into fully spilling or surging waves with the variation of the slope is not feasible, because for that end a slope of respectively 1:20 and 1:1 are needed. A slope steepness of 1:2 and 1:4 are more realistic and will therefore be tested.

- From 1:3 to 1:4, the gentler slope is expected to increase L_r with a factor $4/3$, and to decrease the d_s with possibly a factor $3/4$, but probably a bit higher reduction because of the wave breaking change.
- From 1:3 to 1:2, the steeper slope is expected to decrease L_r with a factor $2/3$, and to increase the d_s with possibly a factor $3/2$, but probably a bit more, because the influence of gravity on erosion increases when the slope gets steeper.

5.2.8 Tidal water level variation

Although not included in the proposed tests, the effect of tidal water level variations would be the next parameter of interest, as it is expected to have a large influence on the formation of a bar profile. The attack level of the waves moves up and down with the water level, attacking a bar that was formed with a higher or lower water level. The question is if this gives a much higher erosion in total, as the bar profile for high water levels has to be formed by newly eroded sand every time, and is eroded partly during the low water level loading. On the other hand, the design conditions occur only during a limited amount of time, a storm of e.g. 12 hours, which is about one tidal period. For the design conditions, the development of equilibrium is not strictly necessary as long as the duration is not too long. The scaling of the tidal period and

amplitude is a problem, a time scale factor of 10 and a length scale factor of 100 is used for the swell, and for a period of 12 hours 25 min, and an amplitude of 2 m (4 m variation), a tide in the flume with a period of 75 minutes and amplitude of 0,02 m could be used. This amplitude seems very small in relation to the waterdepth of 0,48 m in the wave flume at the toe of the structure.

5.3 Test program

The variation of parameters is translated into test runs, with a unique combination of parameters for each test. The tests are displayed in Table 5-2. A total number of 12 tests is composed in this way. It is possible that one or two test runs are needed before the reference test gives good results and according to the results of the tests, the program can be adjusted or extended. In total, the number of test runs might be 15 instead of 12 for these reasons.

Table 5-2 Test program

Test Number	Parameters Variations	H m	T s	ξ (-)	regularity reg/irreg.	N (-)	Df85/Df15 (-)	tan alpha (-)
1	Reference	0,10	1,20	1,58	regular	7200	1,8	0,33
2	Irregular waves	0,10	1,20	1,58	irreg-jonswap	7200	1,8	0,33
3	Varying H	0,08	1,07	1,57	irreg-jonswap	3600	1,8	0,33
4	and N	0,12	1,31	1,57	irreg-jonswap	3600	1,8	0,33
5		0,14	1,42	1,58	irreg-jonswap	7200	1,8	0,33
6	Varying ξ by varying T	0,10	1,00	1,32	irreg-jonswap	3600	1,8	0,33
7		0,10	1,50	1,97	irreg-jonswap	3600	1,8	0,33
8		0,10	2,00	2,63	irreg-jonswap	3600	1,8	0,33
9	Swell waves	0,05	3,00	5,58	regular	9600	1,8	0,33
10	Grading variation	0,10	1,20	1,58	irreg-jonswap	3600	5,0	0,33
11	tan alpha	0,10	1,20	1,19	irreg-jonswap	3600	1,8	0,25
12	variation	0,10	1,20	2,37	irreg-jonswap	3600	1,8	0,50

Reference test with regular waves

As a reference test, test number 6 of Uelman was chosen, where $d_f = 150$ mm, $D_{f50} = 33$ mm, so $m = 4,5$. Test number 6 has results in the middle of the range of tests. The result of the reference test will be compared with that of Uelman, to be able to link the datasets. After this, the test will be repeated with irregular waves and then parameters will be varied one by one, to see the influence of that single parameter.

Different filter material for practical reasons

For practical reasons, not the exact same material can be used. The grading with $D_{f50} = 33$ mm and $D_{f85}/D_{f15} = 1,3$ is not available from suppliers and old materials are not kept in the fluid mechanics lab. It is possible to collect the right material from a larger grading, but then at least 4000 kg of stones have to be sorted by hand as two third of that grading is too large and has to be excluded. It would have to be done by hand because a sieve installation is not available at the lab. For the reasons that the tests have the purpose of studying the phenomena of sand erosion through an open filter rather than being stability tests for a specific design, and that a slightly smaller grading still fits within the range of the former tests, a smaller grading has been decided to work with. This material is limestone with a standard 22/40 mm grading, with: $D_{f50} = 26$ mm, $D_{f85} = 29$ mm and $D_{f15} = 22$ mm. The grading parameter D_{f85}/D_{f15} thus becomes 1,3, the same as for Uelman's grading, relatively narrow for the practical standard used gradings in coastal defence works. This filter material will be used in all the tests, except the test with widely graded material, for which a combination of different available sizes will have to be made.

Reference test with irregular waves

The reference test with irregular waves is very similar to the first test, but this time, irregular waves load the structure. The breakwater set-up and geometry is the same.

The waves are irregular according to the well known Jonswap spectrum for the distribution of the energy density. The significant wave height H_s and the peak period T_p are used to identify the spectrum. For the reference test with irregular waves, H_s is the same as H and T_p is the same as T for the reference test with regular waves.

Wave height variations

The wave height is varied in small steps, from $H_s = 0,08$ m, $H_s = 0,12$ m, to $H_s = 0,14$ m, where $H_s = 0,10$ m is tested in the reference test. The wave steepness is kept constant, which means that the wave period changes with the height, from $T_p = 1,07$ to 1,31 to 1.42 s. $\zeta = 1,58$ for these combinations. ζ is not the wave steepness itself, but because the slope steepness is not varied within these tests, it can be used as such.

Wave period variations

The wave period is varied in larger steps than the wave height, because the erosion is expected to be less sensitive to the period than to the height. Values of $T_p = 1,0$ s, $T_p = 1,5$ s and $T_p = 2,0$ s have been chosen as variation on the reference test with $T_p = 1,2$ s. The values of ζ vary from 1,32 for $T_p = 1,0$ s to 1,63 for $T_p = 2,0$ s. The wave height is kept constant in these tests.

Swell waves

A test with waves that are representative for swell conditions will be performed. This test will be done with regular waves instead of irregular waves with a Jonswap spectrum because swell waves are very regular in reality and because the regular waves can give much insight in the occurring processes. A wave height of 0,05 m and a period of 3,0 s have been chosen to represent the swell waves. The number of waves after which equilibrium occurs is expected to be larger than for the reference test, a first estimate is to let N be 9600, four times the number used in the former tests.

Grading variation

A wide grading of $D_{f85}/D_{f15} = 5$ has been chosen to test in order to investigate the influence of a wider grading on the erosion pattern. This material with the $D_{f50} = 26$ mm, the same as for the reference test, will be composed of the filter material and a smaller and a larger graded material. After mixing of the available materials, a grading with $D_{f85}/D_{f15} = 3$ was found to be feasible and has been used in the tests.

Slope steepness variations

Slope steepness of 1:2 ($\tan\alpha = 0,5$) and 1:4 ($\tan\alpha = 0,25$) have been chosen to vary from the steepness of 1:3 in the reference test. The wave height and period are the same as for the reference test, which results in a variation of the Iribarren parameter from $\zeta = 2,37$ for $\tan\alpha = 0,5$ to $\zeta = 1,19$ for $\tan\alpha = 0,25$. The slope steepness will be varied after the other tests have been performed because the whole sand slope has to be adjusted for it, being a lot of work and to be done as little as possible.

5.4 Measuring techniques

In order to get results from tests, the parameters of interest have to be measured in some way. Some techniques are discussed below.

5.4.1 Transport and erosion

Transport

Techniques exist to measure sediment transport in clear water flow, but things get complicated when the transport inside a porous structure is to be measured. The filter stones are obstructing the view of e.g. a laser-Doppler device. Visual observations through the glass sidewall of a flume or tunnel give qualitative results, but no absolute quantitative values. Besides, the wall-effect, flow deviations near the side walls, will distort the process. The wall effect is expected not to be very large, from visual observation during the former tests. A possibility is to measure the erosion periodically to get the time-averaged net transport.

Erosion

Erosion measurements in a wave flume are difficult for two reasons: the above mentioned wall-effect distorts measurements through the side wall, and when one tries to remove the filter stones to measure the sand profile, the sand profile is easily disturbed by the removal of the stones. The idea is to very gently remove stones after a test, to judge the importance of the wall-effect, and validate the side wall measurements with that.

Visual observation with a digital photo camera

A digital camera placed on a tripod next to the flume makes pictures of the internal slope of the core material, in essence of the interface between core and filter layer. The deformation of this slope displays the erosion of core material through the filter layer. After every 300 waves a photo will be taken, or sooner when during the test the erosion grows very fast. These photos will be processed into a graph with x,y coordinates of the internal sand slope. From these graphs, the erosion depth, erosion length and erosion surface can be determined. From these results, an erosion growth curve in time can be constructed for each test.

Photos from two sides

Due to asymmetry of the breakwater setup or imperfection of the incoming waves, a difference might occur over the width of the flume. To see this difference, photos from both sides can be taken and be compared. When the difference is large, the validity of the tests and the measurements has to be judged.

Visual observation with a video camera

The process of erosion of core material by the waves can be recorded with a video camera. From these images, little quantitative information can be determined, but they give insight in the processes and the possibility to review the process after the tests have been performed. The relative amount of transport can be measured and the type of transport can be determined from video images.

Polystyrene balls to measure the wall effect

A possibility to measure the importance of the wall effect is to put small expanded-polystyrene (EPS) balls inside the core layer at a depth that will come to the surface due to the erosion. A row over the width of the flume with differently coloured balls at the area where considerable erosion is expected can serve this goal. The balls have to be small enough to easily travel through the filter layer. When the erosion depth at the location of the ball is reached, the ball will float up through the filter layer and become visible in the water column. The difference in time between the appearances of the different balls is a measure for the wall effect, for the difference in erosion growth.

5.4.2 Loading

Wave measuring

Waves can be measured with a wave gauge. Placed at the toe of the breakwater, it measures the height of the waves the moment they arrive at the breakwater. These are the waves loading the structure. The surface elevation versus time is the output of a standard wave gauge. Placed in series of three instruments, the reflection of the waves at the breakwater can be calculated from the results. Especially when irregular waves are used in the tests, it is important to know what the reflection is, because it did not load the structure and does turn up in the wave gauge output.

Porous flow

The porous flow is difficult to measure as devices easily affect the flow itself. The best option seems to put a pressure meter in some of the filter stones or in the pores, positioned at important places in the filter layer. The question remains what is measured exactly in this way, a pressure fluctuation at the surface of a filter stone. This is not the velocity in the middle of a pore. The most valuable information will probably be the pressure fluctuations rather than the absolute values.

5.5 Test set-up

The basic setup of the tests is shown in Figure 5-2. On the far right the wave maker is visible, an electronic wave machine with an electrically driven wave board and automatic reflection compensation. Despite the reflection compensation, some reflection can still occur and waves that are reflected by the breakwater pass the wave gauges before they reach the wave board and will therefore have to be filtered out of the time series recorded by the wave gauges. To be able to do that, three wave gauges are positioned close to each other. The combined time series will be analysed afterwards and reflection will be excluded in order to get the wave properties of the waves that actually loaded the structure. The wave gauges are placed close to the structure to measure the waves that attack the structure, after possible deformation by the 1:30 slope in front of it.

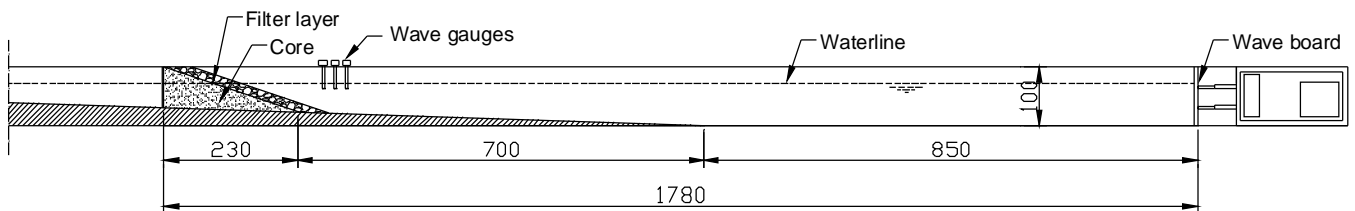


Figure 5-2 Test setup in the wave flume (dimensions in cm)

A solid slope with a steepness of 1:30 is present in the flume (hatched in Figure 5-2). It begins 8,50 m from the mid-position of the wave board and ascends from there. 9,30 m from the beginning of this slope and 17,80 m from the wave board, a solid board is placed vertically in the flume, blocking the entire cross-section. The sand slope is constructed against this board and the stones of the filter layer are placed on the sand slope.

5.5.1 Setup of the reference test

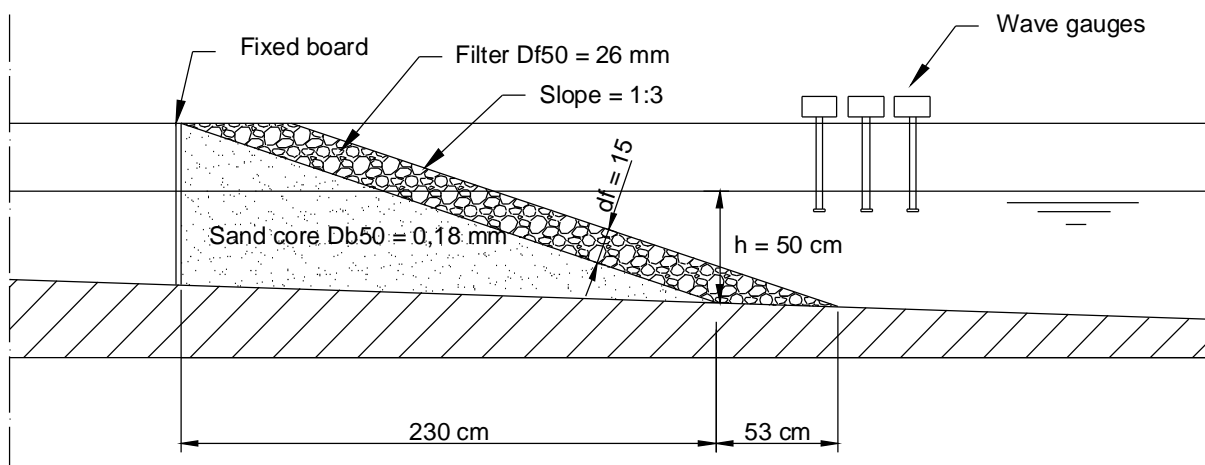


Figure 5-3 Setup of the reference test

The setup of the reference test is shown in more detail in

Figure 5-3. For this test, the steepness of the slope is 1:3, or in other words $\tan\alpha = 0,33$. The thickness of the filter layer is 15 cm, with a grading of rock with a D_{f50} of

24,5 mm. The core material is sand, with a D_{b50} of 0,17 mm, or 170 μm . This test setup is representative for most of the tests; only tests 10, 11 and 12 of the test program differ from this. In tests 10 and 11 different slope steepness is used and in test 12 a different grading of the filter material is used.

5.5.2 Measurement devices

For the measurements different devices are used: wave gauges to measure the surface elevation, photo cameras to measure the erosion profile of the internal sand slope, a video camera to study the transport mechanism of sand through the filter layer and polystyrene balls to study the importance of the wall effect in the erosion of core material.

Wave gauges

The used wave gauges are standard wave gauges with a standard accuracy of 99,5%. The gauges measure the electrical resistance through two wires that are put in the water. The water surface connects the electric loop; the higher the water level, the lower the resistance. At the bottom end of the wires, another electrode performs a reference measurement under water to compensate for differences in the electrical resistance caused by differences in for instance the density, temperature or salinity of the water.

Digital photo camera

The used camera is a digital camera with a resolution of 6 Megapixel, with autofocus and manual setting possibilities. The pictures are taken without flash to avoid reflection in the glass side wall of the flume. The resulting pictures give an accurate view at a small scale; the sand contour is clearly visible when zoomed-in.

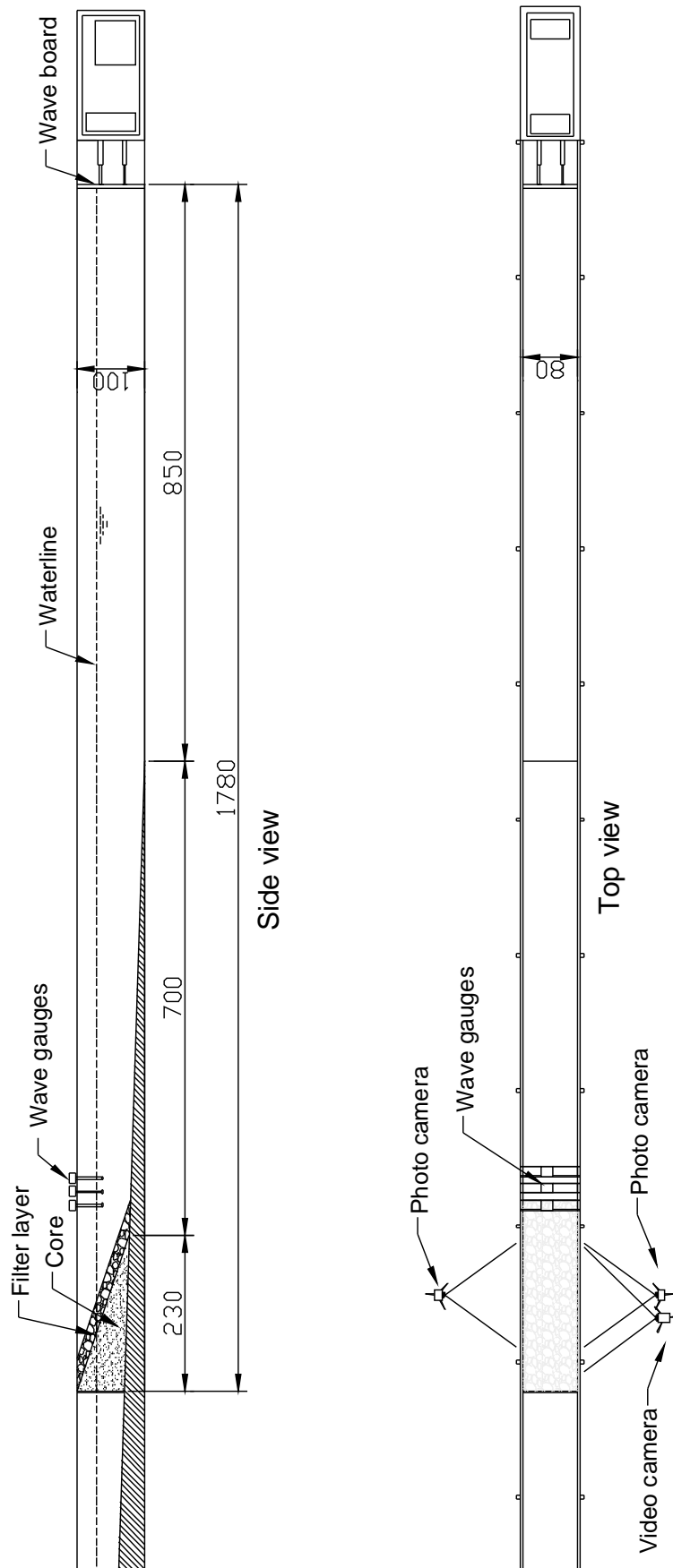
Video camera

The used video camera provides moving images of the wave breaking and sand transport. For each test, overview takes and zoomed-in takes are filmed. The results are digitalised with Windows Movie Maker, providing films and snap shots. The snap shots have a lower resolution than the photos, but still give an accurate picture on a small scale.

Polystyrene balls

The expanded-polystyrene balls have to be able to fit through the pores of the filter layer and float up to the surface. The material will float because of its low density and the size will have to be considerably smaller than the porosity n_f times the D_{f15} of the filter material, which is $0,42 \times 22 = 9,3$ mm. Balls with a diameter of 2 to 3 mm are used in the tests.

Figure 5-4 Setup of the wave flume with measurement devices



5.5.3 Measurement setup

The setup of measurement devices is shown in Figure 5-4. The wave gauges are placed close to the breakwater in order to measure the waves that actually load the structure and the cameras are placed on both sides of the flume to measure the side view of the internal sand slope in the breakwater.

5.5.4 Granular materials

For the core and the filter, granular materials are used.

Core material: sand

The core material is sand S80 quartz-sand with the following properties:

$D_{b50} = 180 \mu\text{m}$, $D_{b15} = 140 \mu\text{m}$ and $D_{b85} = 230 \mu\text{m}$. The density is $\rho = 2650 \text{ kg/m}^3$. The sieve curve is shown in Figure 5-5.

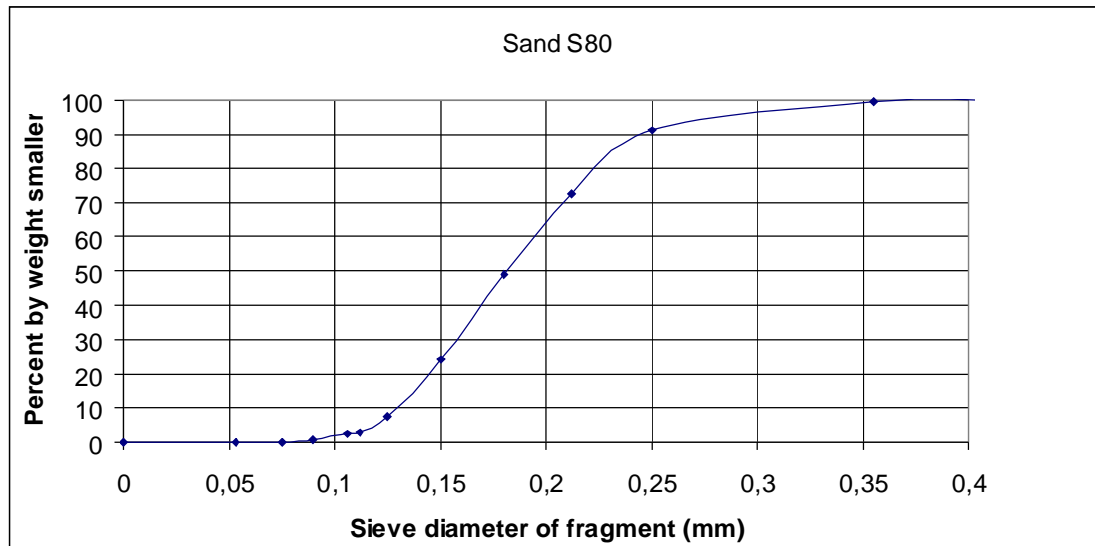


Figure 5-5 Sieve curve of the used sand S80

Filter material: quarry stone

The filter material is quarry stone of the standard grading 22/40 mm. the properties of this grading are:

$D_{f50} = 26 \text{ mm}$, $D_{f15} = 22 \text{ mm}$ and $D_{f85} = 29 \text{ mm}$. The density is $\rho = 2650 \text{ kg/m}^3$ and the porosity is $n = 0,42$. The sieve curve is shown in Figure 5-6.

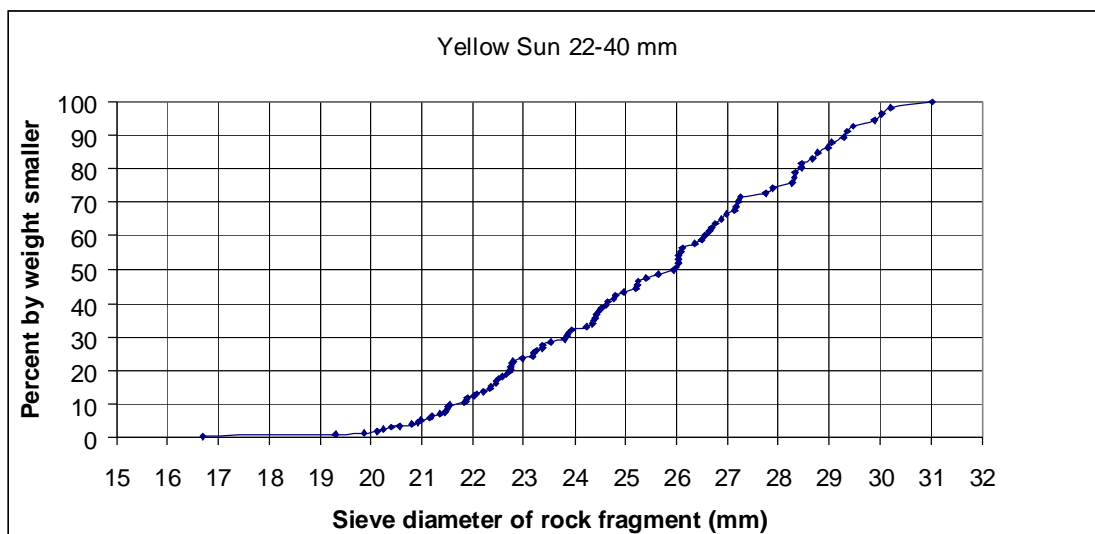


Figure 5-6 Sieve curve of the used filter material

Filter material with wide grading: combination of yellow sun and larger stones

The wide grading filter material is a combination of available gradings. The properties of this grading are:

$D_{f50} = 26$ mm, $D_{f15} = 16$ mm and $D_{f85} = 48$ mm. $D_{f85}/D_{f15} = 3$. The density is $\rho = 2710$ kg/m³ and the porosity is $n = 0,37$. The sieve curve is shown in Figure 5-7.

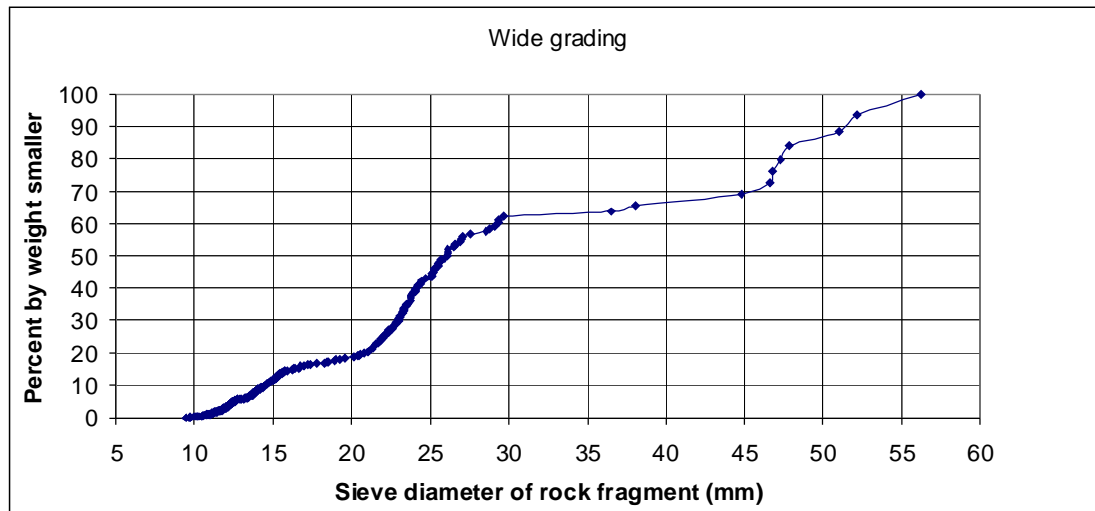


Figure 5-7 Sieve curve of the used filter material



Figure 5-8 samples of the standard filter grading (left) and wide grading (right)

5.5.5 Placement of the core and filter

The sand is dropped into place from a level at the top side of the flume. To construct a straight 1:3 sand slope, a structure with two beams and a plate that rolls underneath these beams is used, see Figure 5-9. The plate attached to the rollers is pushed up along the beams over the sand slope, straightening the surface of the sand. The sand is not removed between the tests, but the top layer is mixed and the surface is straightened again before each test.

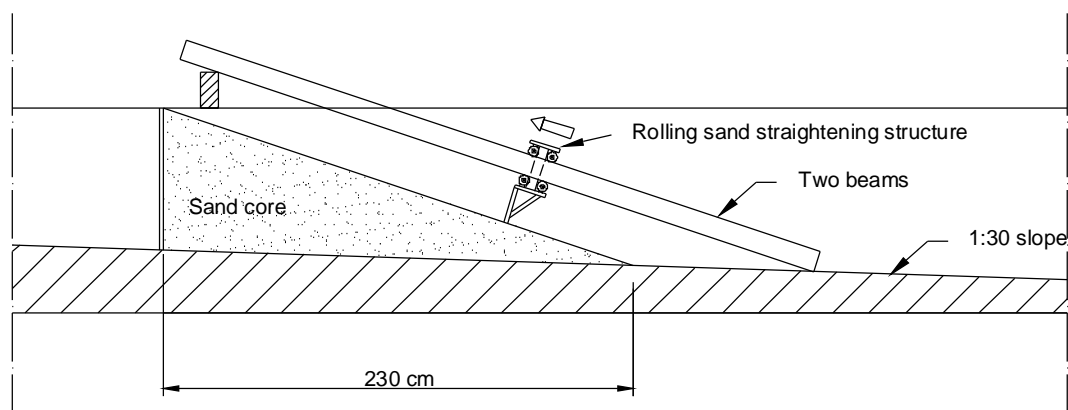
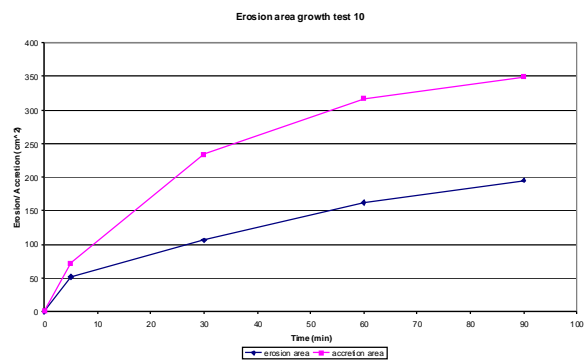
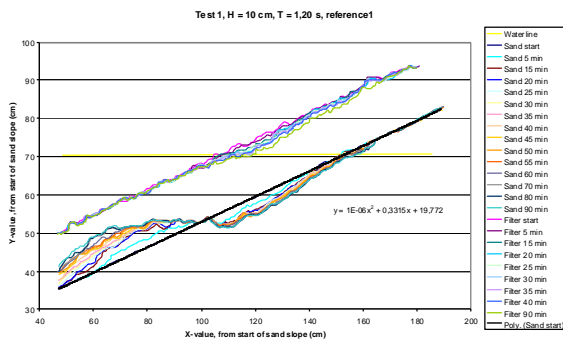


Figure 5-9 Sand profiling structure

The filter stones are dropped manually onto the sand from the level of the waterline. For the first test, the placement of core and filter will be done in the dry flume, but for the other tests the replacement of the sand and stones will be done in the flume filled with water, because the water is too turbid after the tests to flow into the general laboratory reservoir system. All the wave flumes, flow flumes and the wave basin are connected to this system. The system water has to remain clean and the water in these tests becomes too turbid for this because of small fractions of fines from the sand and eroded dust from the stones. If necessary the water is let out into the sewer system.

Chapter 6

Test results and observations



6.1 Results of test 10

6.2 Observations

6.3 Results of all the tests

6.4 Validity of the tests

Chapter 6 Test results and observations

In this chapter the results of the tests are presented. First the results of test 10 are shown with explanation of the photos and graphs as presented. Then the detailed qualitative observations of test 10 and less detailed observations of other tests are described, after which the results of all the tests are shown in the same form. Test number 10 has been described in detail because the water movement and sand transport were clearly visible in this test with relatively long wave periods. During testing extra tests have been added to the program, as shown in Table 6-2 on page 98.

6.1 Results of test 10

Test number	10
Type of waves	Jonswap
$H_{s,input}$	10 cm
$H_{s,measured}$	9,7 cm
$T_{p,input}$	2,0 s
$T_{p,measured}$	1,96 s
ζ	2,62
L_0	6,0 m
Duration	90 min
N	2755
d_f	15 cm
D_{f50}	25 mm
D_{f85}/D_{f15}	1,3
D_{b50}	180 μm
m	6
$\tan\alpha$	0,33



Figure 6-1 setup of test 10 at the start

Test 10 was done with irregular waves with the normal wave height of $H_s = 10$ cm, and with a relatively long period of $T_p = 2,0$ s. The structure layout was the same as for the reference tests and the hydraulic variations tests. Test 10 is the test with the longest period within the period variation test series. The longer period gives the waves much more power to run up and down the slope than shorter periods. The run-up level is much higher than in the reference test with a period of 1,2 s. The flow velocities through the filter seemed to be much higher and the sand transport intensity larger than in the reference test. Figure 6-2 shows the run-up and rundown of a large wave and Figure 6-3 shows the erosion growth during the test in a series of photos. The sand transport is described in detail in section 6.2, observations.



Figure 6-2 run-up (left) and rundown (right) of a large wave in test 10

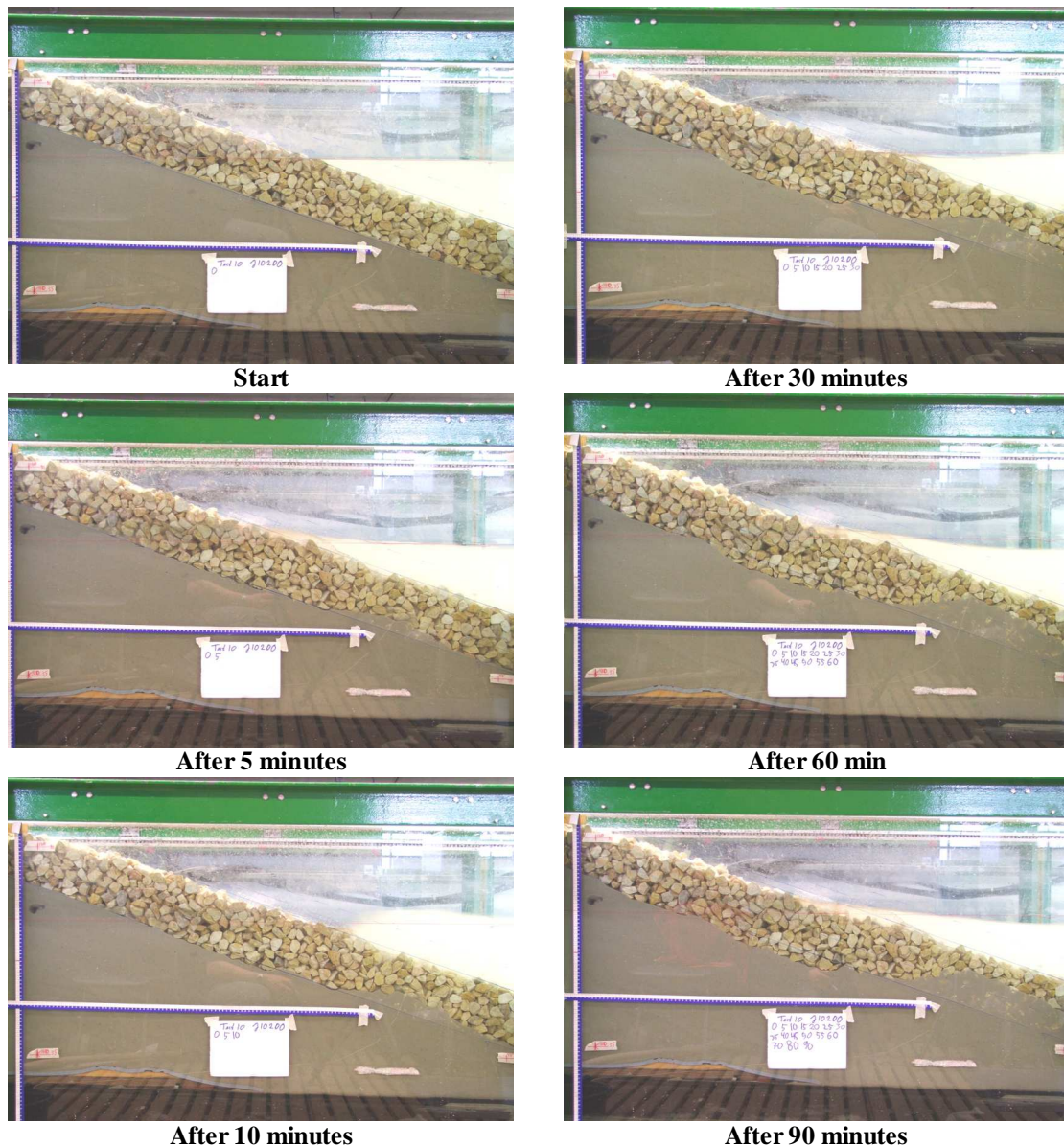


Figure 6-3 photo series of test 10

Before the start, the sand is levelled smoothly on the 1:3 slope and the stones are gently dropped onto it. After 5 minutes of wave attack, a thin erosion area and a bit larger accretion are visible already, but more pronounced after 10 minutes. After 30 minutes the erosion area is clearly visible over a long erosion length and after 60 minutes only the erosion depth and accretion height have increased considerably. After 90 minutes, the erosion depth and accretion height have grown only a little bit, the amount of erosion decreasing in time. In this last part of the test, the erosion depth grows slowly but steady over the whole erosion area, and the accretion area is mostly extended downward, sand is deposited lower on the slope. The accretion height grows only very slow at this stage. After 90 minutes, the accretion height is more than $\frac{2}{3}$ of the filter thickness and sand is leaving the filter in high waves. The test was stopped here.

Extracted graphs of the sand and filter slope

In Figure 6-4, the graph is shown that indicates the level of the sand slope (lower lines) and of the filter slope (higher lines). Every line represents the slope after certain duration in the test, from the start up to 90 minutes. The slopes are in mirror image compared to the photos because the toe of the sand slope has been defined as $x = 0$, progressing up the slope. The graphs have been constructed from the photos shown in Figure 6-3 with the software Getdata, which enables x - y -value extraction from an imported picture. The x - y -values were imported in Excel to analyse, calculate erosion parameters, compare tests and plot the results of a test in one figure.

Test 10 $H_s = 10$ cm, $T_p = 2,00$ s, varying T

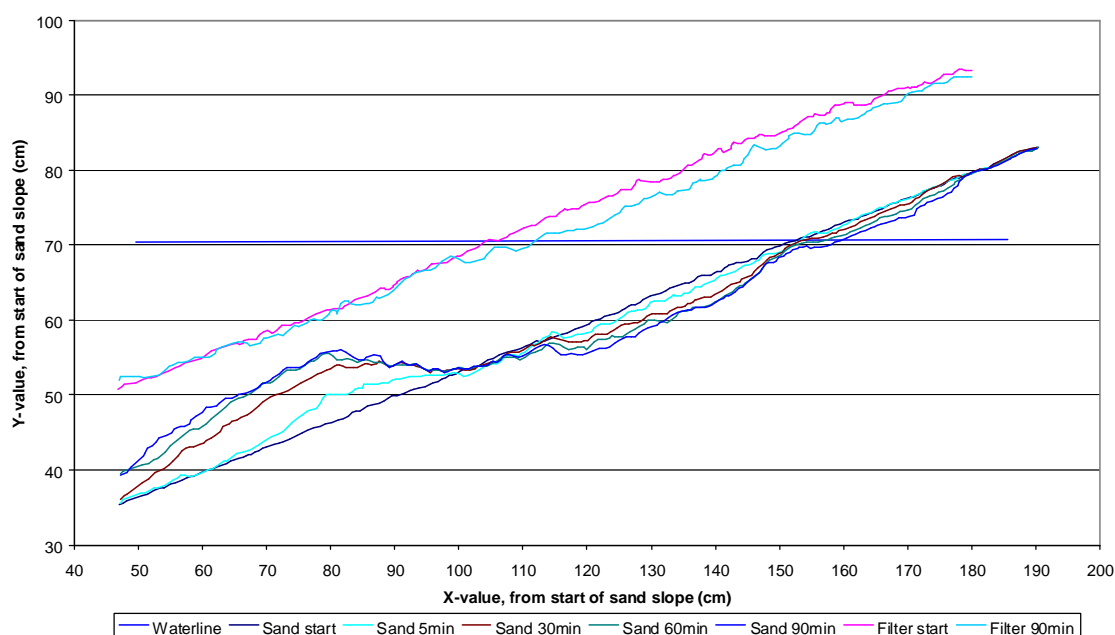


Figure 6-4 graph of the sand slope and filter slope of test 10

Erosion of the sand

It is visible in the figure that the erosion pattern is already present after 5 minutes, gradually expanding from there. Most of the erosion and accretion occur in the first 30 minutes of the test, the rate of erosion decreases considerably after 30 minutes. The area below the waterline shows the most erosion, above the waterline a less deep erosion area occurs. Around the waterline less erosion is visible. At the downward end of the erosion area, a part of about 15 cm stays relatively stable, with very little erosion. The point where the accretion area starts is stable throughout the whole test. This point has been found in all the tests.

Settling of the filter layer

If the sand is washed away from under the filter layer stones, the stones settle and go down with the sand slope. This is visible in Figure 6-4; above the whole erosion area, the filter layer has settled after 90 minutes. The settlement of the filter layer is more spread-out over the erosion area, with less difference between maximum and minimum erosion depth. It is also visible that the filter stones are not lifted up by the sand in the accretion area; the sand clearly settles in-between the stones, in the pores.

Growth of the erosion- and accretion area

The surfaces of the total erosion- and accretion area have been calculated and are shown in Figure 6-5 at the different points in time. The figure shows how the areas grow in time and the relation between erosion and accretion. Both grow fast in the beginning of the test, the growth rate decreasing as time progresses. After 90 minutes, although the trend seems to go towards equilibrium, no steady equilibrium state has developed; the erosion process is still going on. The surface of the erosion area should be about 42% of the surface of the accretion area, as the eroded sand is deposited in the pores between the stones that occupy about 42% of the volume. This is not exactly the case, the accretion area seems too small. The reason for this is that the glass of the flume is only 1,5 m wide, after which a pole is located. Behind this pole a part of the accretion area is invisible and not taken into account here. In the next chapter this will be treated further and the total accretion area will be calculated to get a solid comparison. Researchers experience is that erosion and accretion areas never balance in the physical tests (e.g. experience of ir. G. Smith).

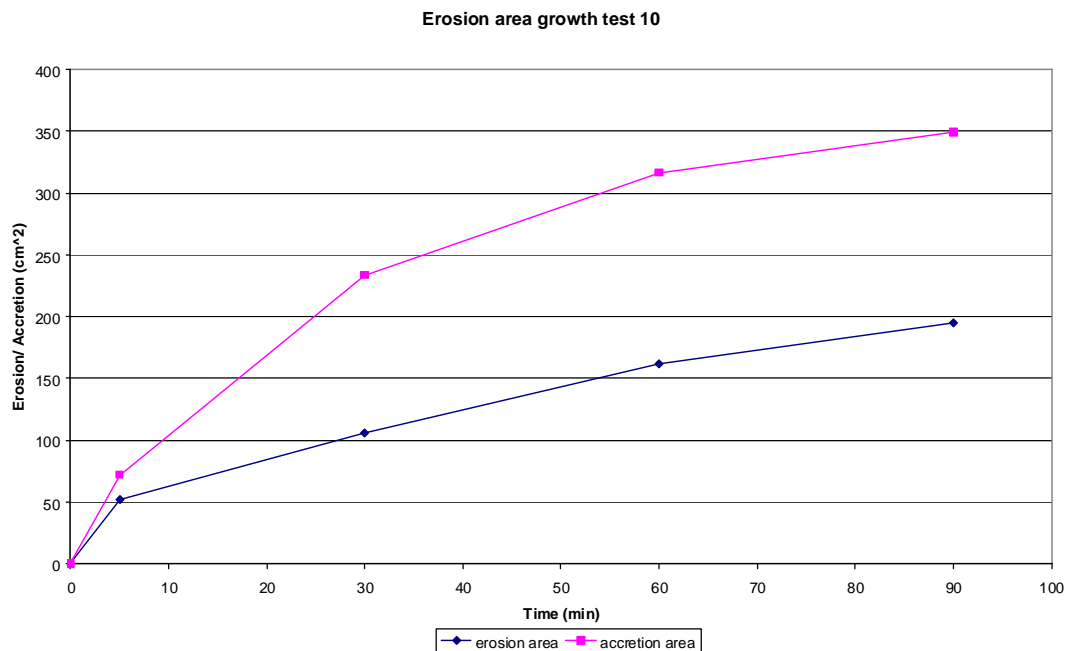


Figure 6-5 erosion- and accretion area growth of test 10

Remarkable in Figure 6-5 is that the erosion grows very fast in the beginning of the test and grows slower and slower as time progresses. After 5 minutes, already a significant amount of erosion can be seen, more than 25% of the total erosion in 90 minutes, in only 6% of the time. After 90 minutes, no equilibrium has been reached; the erosion is still going on. The test was stopped however, because the accretion area almost reached the top of the filter layer, some suspended sand was already transported out of the filter layer and an equilibrium situation was not to be expected.

Polystyrene (EPS) balls

The EPS balls that were put inside the core in an area where erosion was expected turned out to stick to the filter stones. Hardly any of the balls floated up through the filter and became visible. No valuable information resulted from this technique.

6.2 Observations

This section gives descriptions of the visual observations during the tests. These observations give a qualitative view on the different processes and mechanisms that occur during the different tests. Quantitative indications in these observations are only relative indications, comparisons with other tests, or with for instance smaller or larger waves within the same test. Test 10 is described in great detail as it is a test suited for this. The relatively long wave period ($T_p = 2,0$ s) makes that the processes are better visible than in other tests. Observations of tests 13, 14, 15 and 16 are described more briefly to illustrate the differences in water motion and transport, occurring in these tests with respectively very low waves, very high waves, swell-waves and a gentler slope. Analysis of the results and observations is done in the next chapter.

6.2.1 Water motion

Waves are generated by the wave board and travel through the flume towards the breakwater setup. During the passage from the wave board to the structure no changes in the wave shape or height are visible with the eye. When the waves reach the outside of the structure, they feel the toe of the slope and start to break. Throughout the different tests, different types of waves with varying heights and periods have been used, making the type of breaking different. Most used waves have values of the breaker parameter around $\xi = 1,6$ and therefore break in a plunging way as expected. The longer, less steep waves of the tests for swell do not break but surge over the filter slope and the relatively long waves of test 10 are at the transition between surging and collapsing breaker types. All the non-swell waves break on the filter layer, generating a lot of turbulence and air entrainment on the outside of the filter layer.



Figure 6-6 three stages of a breaking wave in test 14

Internal wave

However, on the interface between filter and core, the sand slope, the waves do not break at all. Here the wave just runs up and down the sand slope. The amplitude of this internal wave is much smaller than that of the external wave that drives it, while the period is the same. The internal wave has a phase lag in comparison with the external wave with a magnitude depending on the wave characteristics.

Disconnection

A disconnection has been observed between the water surface outside and inside the filter. As mentioned above, the internal wave has a phase lag to the external wave, occurring over the whole thickness of the filter. At the interface of the outside of the

filter, this leads to a disconnected water surface. Practically this is visual as a very sharp gradient between the outside of the filter and the inside. When for instance the external wave is at its lowest point and the internal wave still high, a part of the leap in water surface is overcome by a thin water layer just over the filter and a part by a sharp gradient just inside the filter. The internal water level has a less steep gradient through the whole filter layer, which is necessary for the internal wave to follow the movement of the outside water level.

Internal setup

The mean water level inside the filter is higher than outside the filter. This phenomenon is called internal setup and is attributed to the fact that during the wave run-up, a thicker layer of water flows on the outside of the filter layer than during rundown, which means that during rundown more water has to flow through the filter; therefore the velocity needs to be higher and with that the resistance increases. A higher water level in the filter develops to provide the extra pressure gradient that the water needs to overcome the higher resistance. Figure 6-6 shows the thicker water layer when the wave runs up the slope (left and middle picture) and the much thinner water layer when the wave is running down (right picture). When the wave front is breaking on the outside of the filter (left picture), the water through a large part of the filter is still running down. The porous flow close to the sand slope uses a longer part of the period for the rundown than for the run-up, up to $\frac{3}{4}$ of the period. The down-running porous flow has time to develop and accelerate, being able to transport a lot of sand downward. Transport is described in detail in sections 6.2.3 and 6.2.4.

6.2.2 Stability of the filter layer

The stones of the filter layer have a D_{f50} of 26 mm and a nominal diameter D_{n50} of 22 mm, and they are attacked directly by the waves. According to the van der Meer equations and using the parameters of the reference test for irregular waves, test 4, these stones will become unstable when H_s exceeds 8 cm. The tests, however, show no considerable instability of stones for test 4, where the measured H_s was 9,0 cm. Some stones moved a little bit into a more stable position and some stones kept wiggling during the test, but no real damage occurred. In test 6 with $H_s = 11,0$ cm, some stones began to roll during the test. The stones were not completely stable in this test, but the filter layer as a whole was not washed away and the thickness did not decrease considerably. Individual stones were removed causing only a very local slightly thinner spot. For tests 7 and 14, with $H_s = 13,0$ cm and 14,8 cm respectively and for test 10 with $H_s = 9,7$ cm but $T_p = 1,96$ s, a thin wire mesh was placed over the filter layer and anchored in the sand, at the place where the waves break. This wire mesh was meant to keep the stones in place to keep the thickness of the filter layer constant during the tests. This worked well. In all the other tests, no extra measures were necessary, hardly any displacement of filter stones occurred.

6.2.3 Transport of sand, two mechanisms

Sand, the core material, is transported over the sand slope, through the pores of the filter layer during the tests. Most of the sand stays within the filter layer, only a small amount leaves the filter when the waves are high enough. The sand is redistributed over the slope by the effects of the waves. Two transport mechanisms have been observed during the tests: bedload transport and suspended-load transport.

Bedload sand transport

When the internal wave runs down over the sand slope, bedload sand transport can be observed. A thin layer of sand up to a few grains thick travels over the sand slope in downward direction. The amount of bedload transport increases when the steepness of the slope increases locally and also when the height or the period of the down-running wave increases. For waves with smaller heights than about 4 to 5 cm (of the external wave), no transport is visible.

Suspended-load sand transport

Both during run-up and run-down of the internal waves, suspended-load sand transport can be observed, provided that the waves are large enough. A cloud of sand is picked up by the water motion caused by the wave and travels with the wave. For average waves this cloud of sand can be up to 1 cm high, travelling just over the sand slope. For higher waves the height of the cloud increases and for the highest waves a cloud (with low concentration) can even reach the outside of the filter layer at some places during some tests. This happens in tests with large waves like tests 7, 14, 9 and 10. Above the area where the accretion area is the highest, the suspended sand cloud reaches the top of the filter layer and sand is leaving the filter towards the water column. In tests with lower waves, this phenomenon is not clearly visible; if some sand is leaving the filter in these tests, it can only be a small amount.

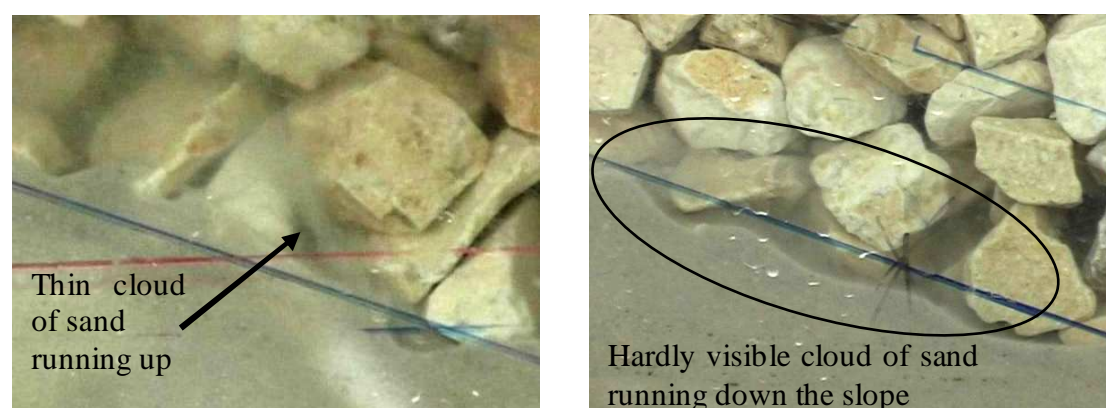


Figure 6-7 suspended-load sand transport during wave run-up (left) and rundown (right)

When a wave is running up, the cloud of sand tends to move under an upward angle, rather than parallel to the sand slope. The duration of this is short, about a quarter of the total wave period or even less. When a wave is running down, the suspended sand from the up-running wave, or newly picked up sand or a combination of both, moves down with the water flow over the sand slope. This cloud of sand does move parallel to the sand slope, and it stays close to the slope. Higher waves cause a higher cloud of sand. The concentration of sand is high close to the sand slope and decreases higher in the cloud. A sequence of larger waves increases the amount of sand in suspension and the height of the sand cloud. In this case, the sand does not seem to have time to settle and stays in suspension in the next wave, which also picks up new sand.

6.2.4 Observations test 10, $H_s = 10$ cm, $T_p = 2,00$ s

The observations of test 10 are described in close detail per distinctive point in the erosion-profile. The waves were distributed according to the Jonswap spectrum, meaning that different waves have different sizes. In the description, a distinction is made between large and small waves from this spectrum. The large waves have

heights in the order of H_s , whereas the small waves have heights of about half that value. Test 10 was done with long waves with a large run-up and run-down. The long period gives the flow over the sand interface time to develop and to transport a relatively large amount of sediment per wave.

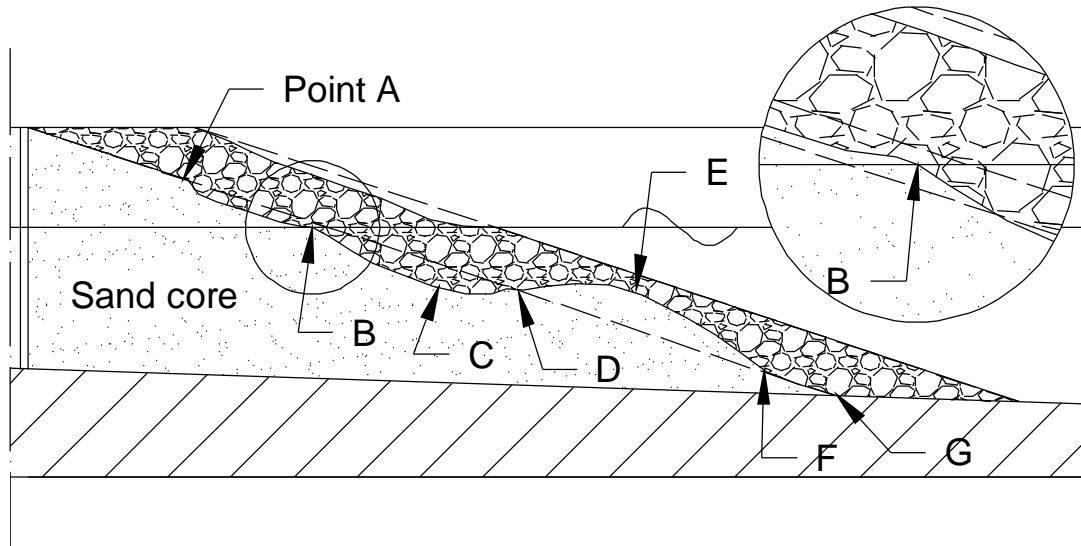


Figure 6-8 sketch of the erosion pattern after test 10 with point definitions

Point A, highest erosion point

Point A is the highest part of the slope where erosion occurs. It is the point up to where the wave runs up.

- The wave runs up quickly, stirring up a thin layer of sediment. This sediment is transported up as a suspended load, settling again at the end of the wave run-up.
- During the wave run-down, which lasts longer than the run-up, the flow over the sand-interface has time to develop and accelerates in time. This downward flow picks up sediment and transports it to a lower part of the slope. First some bedload transport can be observed, a thin layer of a few grains thick slides and bounces downward over the sand slope, and a bit later, when the flow velocity has increased, also suspended-load transport can be observed. The suspended-load transport can transport a layer of sediment of a few mm high downward with high velocities, leading to a relatively large amount of transport.
- It is to be noted that no cliff-erosion is visible, a sharp steep edge in the erosion pattern undermined by the up-running waves as seen in tests with regular waves, is not present. The reason for this can be the irregularity of the waves. The different waves have different run-up levels and therefore the highest point of erosion is smoothed over a larger part of the slope than in the case of regular waves, where all the waves reach the same run-up level and attack the slope at the same point.

During both run-up and run-down transport is observed, but during run-down a bit more than during run-up, resulting in a slow net erosion of the area around point A.

Point A marks the highest point of the erosion area and shifts higher up the slope as the test progresses.

Point B, waterline SWL

Point B is the point at the sand slope where the still water level (SWL) crosses the slope. The wave runs up above this point and runs down below this point.

- Small wave running up: a little bit of suspended-load transport is visible, a thin cloud of stirred up sediment is moved up a short distance in a short time span.
- Small wave running down: some bedload transport is visible. The amount of transport is not large, but more sediment is transported than during run-up, because of a slightly higher intensity and a longer duration.
- Large wave running up: a large amount of suspended-load transport is visible; a cloud of sediment is stirred up and moves up with the wave in a short time span.
- Large wave running down: a large amount of sediment is transported as a combination of bedload and suspended-load. The time span of this transport is considerably larger than that of the run-up transport.

At point B, more sediment is transported during the run-down than during the run-up of the wave. However, the sand slope itself seems to be more or less in equilibrium, only a very small amount of erosion is visible. The higher downward transport is mostly caused by sediment that is eroded from the area between point A and B and passes point B in downward direction.

Point B does not shift up or down the slope as it is defined as the intersection of the still water level and the (eroded) sand slope. B only shifts horizontally with the erosion of the sand.

Point C, maximum erosion point

Point C is at the location on the sand slope where the depth of the erosion area has its maximum. This point is always submerged; the internal waves do not run down below this point.

- Small wave running up: a little bit of sediment is stirred up, but hardly any transport is visible.
- Small wave running down: a moderate amount of bedload transport is visible during the run-down, in combination with a little bit of suspended-load transport.
- Large wave running up: a moderate amount of suspended-load transport is visible.
- Large wave running down: a large amount of suspended-load transport is visible during a relatively long time span.

At point C, a steady but ongoing erosion of the sand is visible, and sand is also passed on from higher up the slope to lower down the slope. The amount of transport in downward direction during run-down of the wave is considerably larger than the amount of transport in upward direction during run-up.

A sequence of larger waves, a number of larger waves following-up on each other, increase the downward erosion, probably due to the higher internal set-up in the filter layer which grows in a sequence of larger waves and is an important driving force for the downward water flow through the filter layer over the sand slope.

The location of point C on the slope does not change much. It tends to shift down a bit towards point D as the test progresses; the maximum erosion depth first occurs about halfway between B and D and shifts down towards D towards the end of the test.

Point D, transition from erosion to accretion

Point D is the point on the sand slope where the erosion area ends and the accretion area begins. At this point the net erosion is zero, sand is only passed on. In the tests with regular waves this point is clearly visible as one single point where the instantaneous sand slope line crosses the original sand slope line from the start of the

test, but in the tests with irregular waves this point D is more like an area with a length of some 10 cm (about 15 cm in test 10), over which the instantaneous sand slope is more or less at the same level as the original sand slope.

- Small wave running up: no transport is visible.
- Small wave running down: a little bit of bedload transport is visible.
- Large wave running up: a small amount of suspended-load transport is visible.
- Large wave running down: a large amount of suspended-load transport is visible.

Point D is stable; a dynamic equilibrium can be seen. Sand is passed on in downward direction, from the erosion area to the accretion area. An area of about 15 cm length of the sand slope is stable and stays at the level of the original sand slope. The upper edge of this area is located under the point where the SWL-line crosses the outside of the filter layer and the lower edge is located under the point to where the relatively large waves ($H \approx H_s$) run down over the outside of the filter layer.

Point D stays at the same location during the whole test, both vertically and horizontally, but the area over which no net erosion takes place decreases slightly from about 15 cm to about 10 cm over the duration of test 10.

Point E, maximum accretion point

Point E is the point on the sand slope where the accretion has its maximum. Here the sand settles in the pores between the stones of the filter layer, making the level of the sand slope increase in this area.

- Small wave running up: a little bedload transport and a tiny amount of suspended-load transport are visible.
- Small wave running down: a moderate amount of both bedload and suspended-load transport can be observed.
- Large wave running up: a large amount of suspended-load transport can be seen; in a sequence of large waves the sand stays in suspension, partly leaving the filter into the water column.
- Large wave running down: a large amount of suspended-load transport can be seen as well. Sand brought in suspension by the up-running wave stays in suspension and extra sand is also picked up from the bottom.

At point E more sand is settling than is transported away because the sand level grows in time. Sand is transported to the area around point E from higher up the slope, partly settling and partly passing point E in the direction of point F. In large waves, and especially in a sequence of large waves, some sand is stirred up high enough to leave the filter. This amount of lost sand increases when the effective filter layer thickness decreases by the growth of the sand slope level.

Point E shifts a bit downwards over the slope with the growth of the accretion area, but the maximum (E) stays relatively close to point D. E is closer to D than to F during the test.

Point F, end of accretion area

Point F is where the accretion area ends and the original sand slope stays more or less in place. The water is deeper at this location lower on the slope and waves are expected to have less influence at this point and further down.

- Small wave running up: no visible transport.
- Small wave running down: a tiny amount of bedload transport.
- Large wave running up: a little suspension transport is visible.

– Large wave running down: a moderate amount of bedload transport is visible. Since point E grows and point F stays at the same level, the slope between E and F becomes steeper. It seems that on the steeper slope the downward bedload transport is more easily triggered by the water motion from the wave than on the original, gentler slope. As sand is supplied from E, the amount of sand in the low part of the accretion area increases and the accretion area becomes larger. Point F shifts further down the slope when this happens.

Point F shifts down over the sand slope with the growth of the accretion area. The accretion area grows gradually, starting from D which stays at the same location, and expands in downward direction.

Point G, end of the sand slope

Point G is where the sand slope ends and reaches the bottom of the flume. Here the waves have no direct influence, no transport is visible. In the area between F and G, a little bit of bedload transport can be observed when the highest waves of the spectrum are passing. The slope is hardly affected by the waves and keeps its original level and shape.

6.2.5 Observations test 13, $H_s = 5$ cm, $T_p = 0,85$ s

Test 13 is the test with the smallest irregular waves used. H_s is measured to be 4,4 cm, so most of the waves are smaller than 4,4 cm and some of the waves are higher.

- Hardly any movement of the sand has been observed at all in test 13. The total amount of erosion after 420 minutes is zero, with only very locally some small perturbation of the original sand slope.
- The height of the internal wave is less than 1 cm and the internal setup not more than a few mm, apparently not enough to generate sand transport.
- For waves lower than about 5 cm (visual estimate), no movement of sand was observed at all; for larger waves, some movement of individual grains can be observed. For these waves, grains roll or slide over the slope over a short distance; the transport can not be called collective. The waves with a height of 5 cm seem to be at a threshold value for this wave-type with $\zeta \approx 1,6$.

6.2.6 Observations test 14, $H_s = 16$ cm, $T_p = 1,52$ s

Test 14 is the test with the highest waves used. It is the test in the wave height variation series with the largest waves. In these series, only the wave height has been varied, and the period adjusted such that the breaker parameter stays constant, $\zeta = 1,6$. The most remarkable observations are mentioned here.

- A sequence of a few large waves pushes the internal water level at the sand slope interface up to about 9 cm above SWL, after which the back-flowing water transports a lot of sand downward, both as bedload and as suspended-load. The suspended-load transport starts a few cm lower than the highest water level.
- The highest observed water level at the sand slope is 11 cm above SWL, after a sequence of large waves.
- The large waves of test 14 are large enough to directly cause a little bit of bedload transport at the toe of the sand slope, whereas most waves in most tests are not able to do this.

6.2.7 Observations test 15, $H = 3$ cm, $T = 2,0$ s

Test 15 was done with regular waves with a height of 3 cm and a period of 2,0 s, to represent swell waves. Earlier, test 11 was also executed with regular waves to represent swell, but the wave height of 5 cm and the period of 3,0 s were apparently too large for the particular test setup, as the test showed a rapidly growing erosion area over a long erosion length, an unwanted situation for swell waves that can occur during quite a long time. Therefore a test was added to the program with lower swell waves, to see if this type of wave could be resisted long enough by the structure. The erosion growth was indeed much slower. Interesting observations are mentioned here:

- As regular waves are used, no size-difference between the individual waves occurs; therefore no distinction is to be made between large and small waves.
- The internal wave has a height of 2 cm, the water level varying from SWL to SWL + 2 cm. In other words, the internal setup of the mean water level is 1 cm, the amplitude of the internal wave also 1 cm.
- The internal wave has a phase lag of almost 180 degrees compared to the external wave, both waves being almost in opposite phase.
- Most of the sand transport in this test is bedload transport; only high up the slope, from the run-up height of the internal wave to 6 cm lower, small clouds of suspended-load transport can be observed.
- The run-down of the wave lasts longer than the run-up. The downward water flow has more time to develop and seems to transport more sand than the upward flow.
- The relatively long period gives the flow over the sand slope time to develop, leading to a relatively strong flow for the small wave height of only 3 cm.
- In the area from $x = 80$ to 100 cm, accretion occurs. A little bedload transport can be seen, more during rundown than during run-up (see Figure 6-38 graph of the sand- and filter slope of test 15).
- In the area from $x = 100$ to 130 cm, erosion occurs. Hardly any transport is visible during run-up; bedload transport can be seen during rundown. Sometimes a tiny cloud of suspended-load transport is visible during rundown as well.
- In the area from $x = 130$ and higher up the slope, a little erosion occurs. Bedload transport and a little bit of suspended-load transport are visible; a bit more transport during rundown than during run-up.

6.2.8 Observations test 16, $H_s = 10$ cm, $T_p = 1,2$ s, $\tan\alpha = 1:4$

Test 16 has the same wave characteristics as test 4, the reference test for irregular waves, with as difference the slope steepness of 1:4 for test 16, instead of 1:3 for the other tests. The gentler slope is expected to spread the energy dissipation over a longer area of the slope and to reduce the wave run-up and rundown, leading to less erosion. Some interesting observations:

- The internal wave reaches a run-up level of 3 cm above SWL.
- During small waves, no transport is visible during run-up, and a little bedload transport is visible during rundown.
- During large waves running up, small clouds of suspended-load transport are visible over the whole slope and a little bit of bedload transport occurs.
- During large waves running down, bedload transport is visible, and some suspended load transport at the accretion area.
- As expected, the erosion was considerable less for the 1:4 slope than for the steeper 1:3 slope.

6.3 Results of all the tests

In Chapter 5 the test program was constructed, consisting of 12 tests. The original program is shown again in Table 6-1. While executing the actual tests, in total five tests were added to the program, of which two were reruns of the reference test, two were extra wave height variation tests and the last was an extra swell-wave test. The test program as executed is displayed in Table 6-2. The test numbers in this table are used in the results and analyses to refer to the specific test.

Table 6-1 original test program

Test Number	Parameters Variations	Hs m	Tp s	ξ (-)	regularity reg/irreg.	N (-)	Df85/Df15 (-)	tan alpha (-)
1	Reference	0,10	1,20	1,58	regular	7200	1,8	0,33
2	Irregular waves	0,10	1,20	1,58	irreg-jonswap	7200	1,8	0,33
3	Varying H	0,08	1,07	1,57	irreg-jonswap	3600	1,8	0,33
4	and N	0,12	1,31	1,57	irreg-jonswap	3600	1,8	0,33
5		0,14	1,42	1,58	irreg-jonswap	7200	1,8	0,33
6	Varying ξ by varying T	0,10	1,00	1,32	irreg-jonswap	3600	1,8	0,33
7		0,10	1,50	1,97	irreg-jonswap	3600	1,8	0,33
8		0,10	2,00	2,63	irreg-jonswap	3600	1,8	0,33
9	Swell waves	0,05	3,00	5,58	regular	9600	1,8	0,33
10	tan alpha	0,10	1,20	1,19	irreg-jonswap	3600	1,8	0,25
11	variation	0,10	1,20	2,37	irreg-jonswap	3600	1,8	0,50
12	Grading variation	0,10	1,20	1,58	irreg-jonswap	3600	5,0	0,33

Table 6-2 test program as executed with measured wave heights and periods

Test Number	Parameters Variations	Hs m	Tp s	ξ (-)	regularity reg/irreg.	Duration min	N = Duration / Tp (-)	Df85/Df15 (-)	tan alpha (-)
1	Reference	0,095	1,20	1,62	regular	90	4500	1,3	0,33
2	Reference 2	0,095	1,20	1,62	regular	120	6000	1,3	0,33
3	Reference 3	0,096	1,20	1,61	regular	180	9000	1,3	0,33
4	Irregular waves	0,090	1,20	1,66	irreg-jonswap	180	9000	1,3	0,33
5	Varying H	0,071	1,10	1,72	irreg-jonswap	600	32727	1,3	0,33
6	and N	0,110	1,32	1,66	irreg-jonswap	90	4091	1,3	0,33
7		0,130	1,39	1,60	irreg-jonswap	90	3885	1,3	0,33
8	Varying ξ by varying T	0,081	1,02	1,49	irreg-jonswap	90	5294	1,3	0,33
9		0,096	1,47	1,97	irreg-jonswap	90	3673	1,3	0,33
10		0,097	1,96	2,62	irreg-jonswap	90	2755	1,3	0,33
11	Swell waves	0,051	3,00	5,52	regular	90	1800	1,3	0,33
12	Grading variation	0,090	1,23	1,71	irreg-jonswap	120	5854	3,5	0,33
13	Varying H	0,044	0,84	1,65	irreg-jonswap	420	30000	1,3	0,33
14	Varying H	0,148	1,48	1,59	irreg-jonswap	90	3649	1,3	0,33
15	Swell waves low	0,030	2,00	4,76	irreg-jonswap	240	7200	1,3	0,33
16	tan alpha	0,090	1,23	1,28	irreg-jonswap	180	8780	1,3	0,25
17	variation	0,090	1,23	2,56	irreg-jonswap	90	4390	1,3	0,50

Five tests were added: test 2 and test 3 are reruns of the reference test, with slight differences in the test setup. Test 13 and 14 were added to extend the wave height variation test series, to get a better view on possible relations between erosion and wave height. Test 15, finally, was added as an extra swell-waves test because test 11, the original swell-waves test, gave unexpected results. Test 15 was added to be able to say more about the behaviour of low long waves loading the structure.

General test parameters

d_f	15	cm	These parameters are the same for all tests, with three exceptions: $\tan\alpha = 0,25$ in test 16 and 0,50 in test 17, and $D_{f85}/D_{f15} = 3$ in test 12. In the next paragraphs, all the tests are described with a photo after 5 minutes, a photo at the end of the test and the graph of the sand- and filter slope during the test. A short explanation of the test and remarkable observations is given.
D_{f50}	25	mm	
D_{f85}/D_{f15}	1,3		
D_{b50}	180	μm	
m	6		
$\tan\alpha$	0,33		
h at toe	0,50	m	

6.3.1 Test 1 reference test regular waves

Test number	1	
Type of waves	Regular	
$H_{s,input}$	10	cm
$H_{s,measured}$	9,5	cm
$T_{p,input}$	1,2	s
$T_{p,measured}$	1,20	s
ζ	1,62	
L_0	2,25	m
Duration	90	min
N	4500	
$\tan\alpha$	0,33	

Test 1 is the reference test with regular waves, included to be able to compare the results of the tests with Uelman's results. A photograph was taken every 5 minutes during the first 60 minutes and every 10 minutes during the rest of the test. x - y coordinates were extracted for the sand slope of every photo and for the filter slope of most of the photos, all displayed in Figure 6-10.



Figure 6-9 test 1 after 5 minutes (left) and after 90 minutes (right)

The erosion and accretion area are visible already after 5 minutes and after 90 minutes the accretion area has a height of $\frac{2}{3}$ of the filter layer thickness. The erosion area is less deep than the accretion area is high. Two reasons for this are: 1, the erosion is spread over a longer distance and 2, the accretion area has to be larger because the eroded sand can only settle in-between the pores of the filter stones.

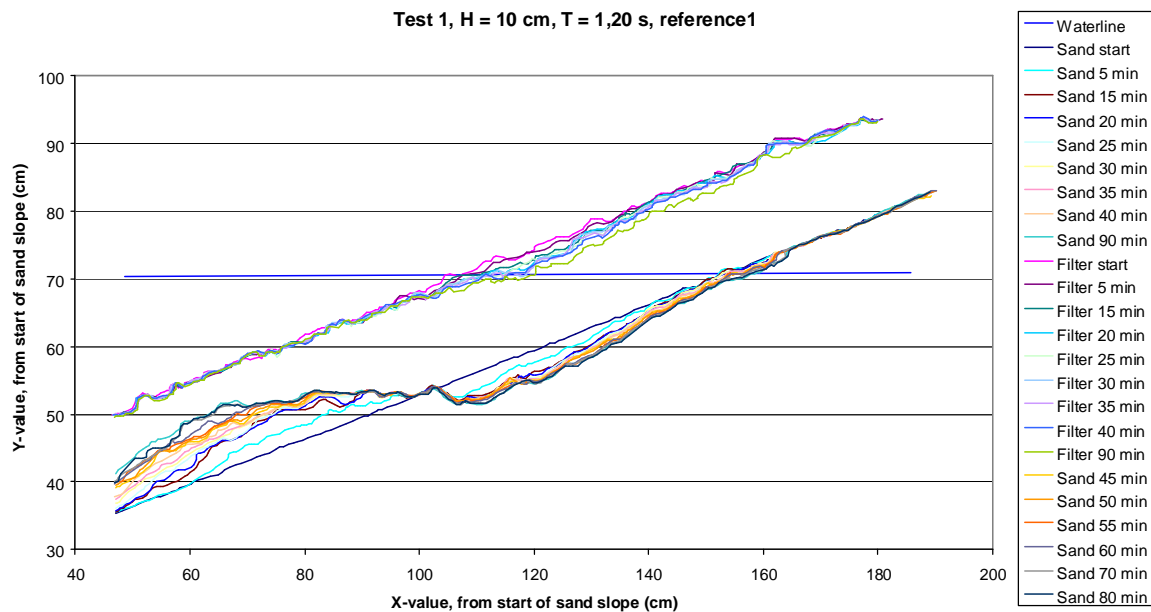


Figure 6-10 graph of the sand- and filter slope of test 1

6.3.2 Test 2 rerun reference test regular waves

Test number	2
Type of waves	Regular
$H_{s,input}$	10 cm
$H_{s,measured}$	9,5 cm
$T_p,input$	1,2 s
$T_p,measured$	1,20 s
ζ	1,62
L_0	2,25 m
Duration	120 min
N	6000
$\tan\alpha$	0,33

Test 2 is a rerun of the reference test, included to see if the test result can be reproduced. The result was indeed very similar to that of test 1, with locally some variations. A reason for the differences might be that the sand was not fully saturated or less densely packed in the first test. This comparison will be treated further in the next chapter. The duration of test 2 was extended to 120 minutes, to see if the erosion would decay further as time progresses. This seemed to be the case.



Figure 6-11 test 2 after 5 minutes (left) and after 120 minutes (right)

It is visible in the graph that the sand slope was not perfectly straight at the start of the test. Experience with the sand levelling had yet to be gained. In the calculation of erosion area and other parameters, this has been taken into account by adding a second order trendline to the start-line of the sand, calculating the erosion from there.

Test 2, H = 10 cm, T = 1,20 s, reference2

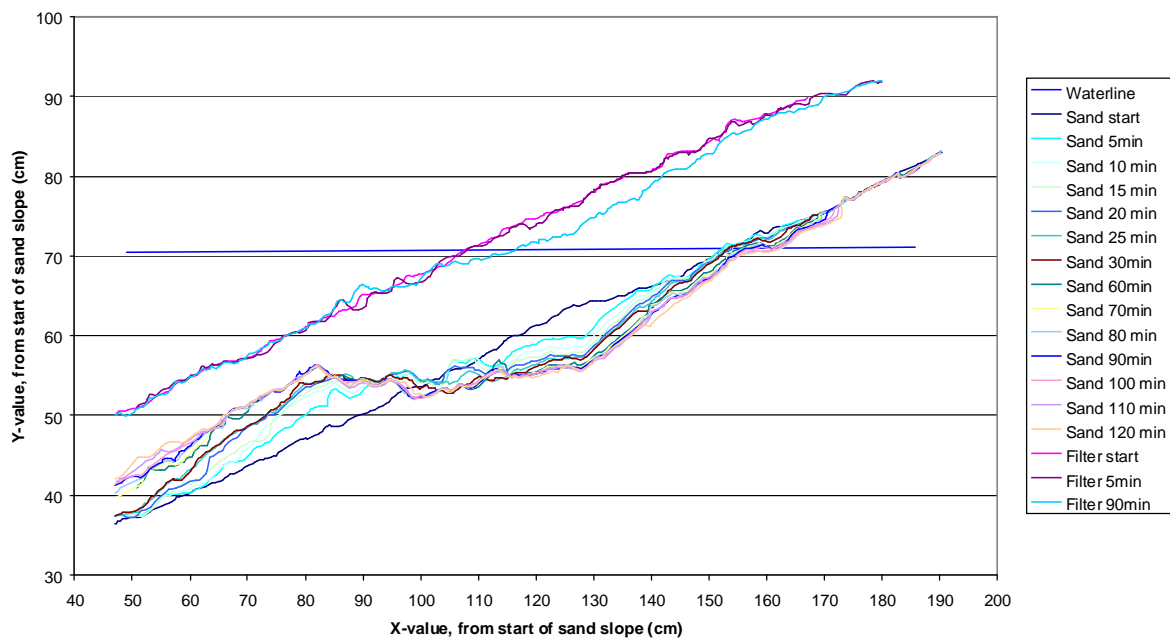


Figure 6-12 graph of the sand- and filter slope of test 2

6.3.3 Test 3 reference test regular waves

Test number	3
Type of waves	Regular
$H_{s,input}$	10 cm
$H_{s,measured}$	9,6 cm
$T_p,input$	1,2 s
$T_p,measured$	1,20 s
ζ	1,61
L_0	2,25 m
Duration	180 min
N	9000
$\tan\alpha$	0,33

Test 3 is the third run of the reference test with regular waves, included to see the influence of a thin mesh wire under the stones for easier removal of the stones. As shown in Figure 6-43, the wire mesh only influenced the erosion high up the slope (point A), the run-up point of the internal wave. Besides this effect, the erosion pattern of test 2 was reproduced very well.



Figure 6-13 test 3 after 5 minutes (left) and after 180 minutes (right)

It can be seen from the photos and the graph that this test, like test 1 and 2, produces a clear bar-profile in the sand slope, with the filter layer only settling in the erosion area. The transition between erosion and accretion, point D, is a well pronounced point that stays in the same spot throughout the whole test. The transition between erosion and accretion is sharp and can easily be defined in this one spot.

Test 3, H = 10 cm, T = 1,20 s, reference3

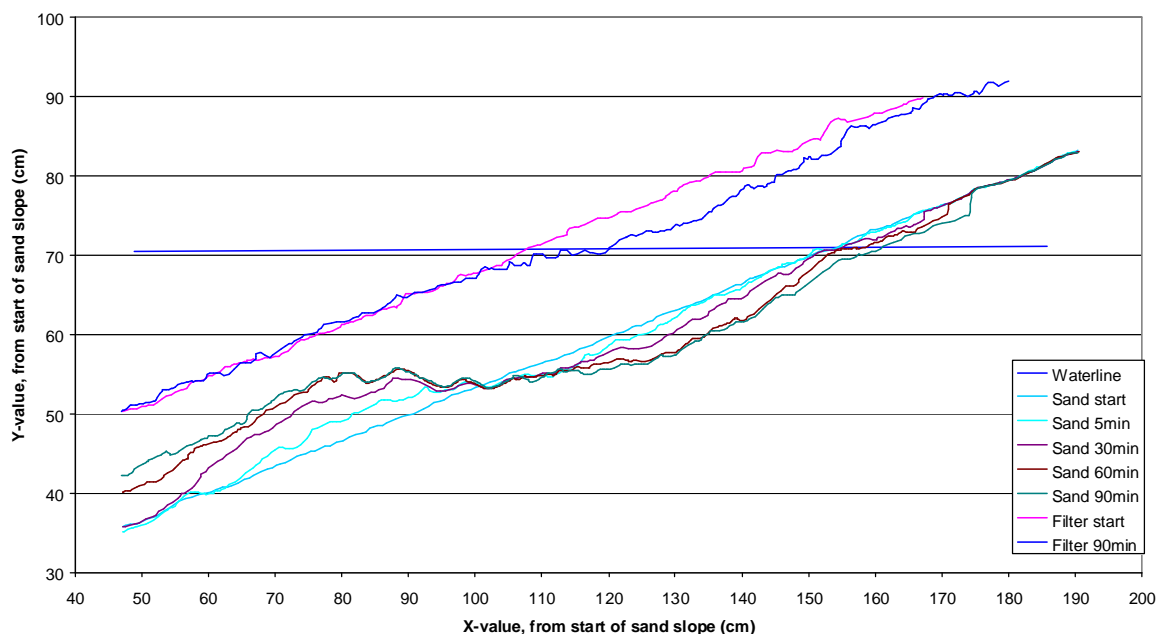


Figure 6-14 graph of the sand- and filter slope of test 3

6.3.4 Test 4 reference test Jonswap waves

Test number	4
Type of waves	Jonswap
$H_{s,input}$	10 cm
$H_{s,measured}$	9,0 cm
$T_{p,input}$	1,2 s
$T_{p,measured}$	1,20 s
ζ	1,66
L_0	2,25 m
Duration	180 min
N	9000
$\tan\alpha$	0,33

Test 4 is the reference test with Jonswap waves, included to be able to compare the results of the regular waves with those of the irregular waves. Because a relation was not known, H_s has been compared with $H_{regular}$ and both have been set the same. Expected was a more or less equal or a bit higher amount of erosion with the irregular waves, because of the irregularity and the presence of larger waves ($H_{max} \approx 2H_s$ for Jonswap). Surprisingly, the amount of erosion was less in test 4. The difference is clearly visible in the photos.



Figure 6-15 test 4 after 5 minutes (left) and after 180 minutes (right)

The overall erosion pattern is very similar to that of tests 1-3, with two differences: at point A, high up the slope, a sharp edge (cliff) is not visible, only a bit after 90 minutes, and at point D, the transition between erosion and accretion is spread over an area of about 10 cm rather than being one single point as in tests 1-3.

Test 4, $H_s = 10$ cm, $T_p = 1,20$ s, Jonswap reference

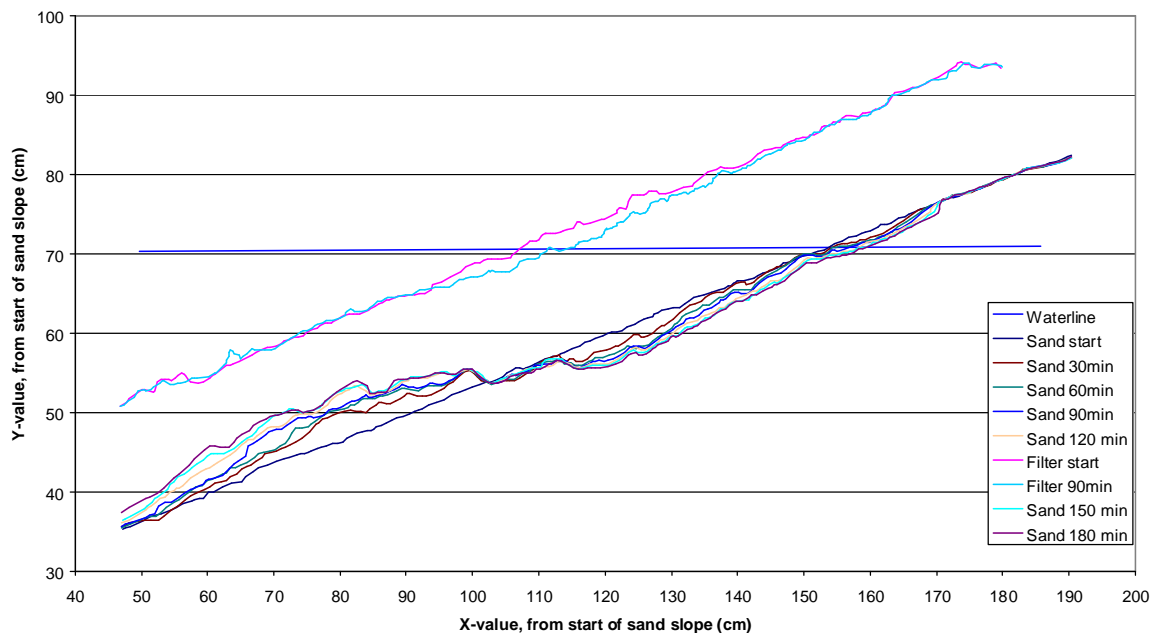


Figure 6-16 graph of the sand- and filter slope of test 4

6.3.5 Test 5 variation of H

Test number	5
Type of waves	Jonswap
$H_{s,input}$	8 cm
$H_{s,measured}$	7,1 cm
$T_{p,input}$	1,07 s
$T_{p,measured}$	1,10 s
ζ	1,72
L_0	1,89 m
Duration	600 min
N	32727
$\tan\alpha$	0,33

In test 5, the wave height is lower, and the period is set such that the ζ is maintained at 1,6. As visible on the left, the measured parameters differ from the input. Reasons for this can be found in two things: the wave board does not produce the exact wave that is put in, especially when the reflection is large, and the waves are measured just before the toe of the structure, after the wave has travelled about 15 m. The measured wave is used in the analysis for it is what loaded the structure.



Figure 6-17 test 5 after 5 minutes (left) and after 600 minutes (right)

The same erosion pattern, a bar-profile, is visible in test 5, but the erosion process went much slower. The test was extended to 600 min, (10 hours) to see if an equilibrium situation would develop. The erosion grew very slow in the end, but did not stop, not even after 600 minutes. The total erosion after 600 minutes was still less than the erosion of test 4 after 180 minutes.

Test 5, $H_s = 8$ cm, $T_p = 1,07$ s, varying H

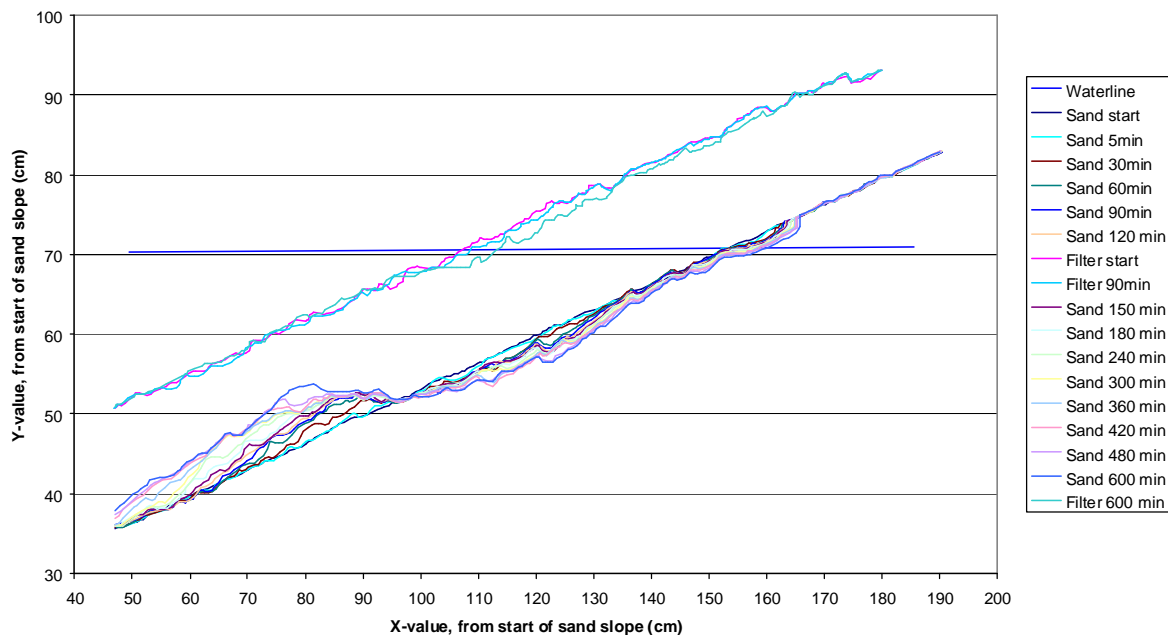


Figure 6-18 graph of the sand- and filter slope of test 5

6.3.6 Test 6 variation of H

Test number	6
Type of waves	Jonswap
$H_{s,input}$	12 cm
$H_{s,measured}$	11,0 cm
$T_p,input$	1,31 s
$T_p,measured$	1,32 s
ζ	1,66
L_0	2,72 m
Duration	90 min
N	4091
$\tan\alpha$	0,33

In test 6, the waves were higher than in test 4. The waves were high enough to let the filter stones roll a little, without actual damage to the filter layer. A few stones were moved, but mostly stones were only wiggling and rolling a bit in the same place. It seemed that this was the maximum wave height that could be resisted by the filter layer without extra protection and without real damage and loss of layer thickness.



Figure 6-19 test 6 after 5 minutes (left) and after 90 minutes (right)

The erosion in test 6 clearly went faster than in test 4, after 90 minutes it had already exceeded the amount of erosion of test 4 after 180 minutes. The erosion profile does not differ; the same bar-profile can be recognized.

Test 6 $H_s = 12$ cm, $T_p = 1,31$ s, varying H

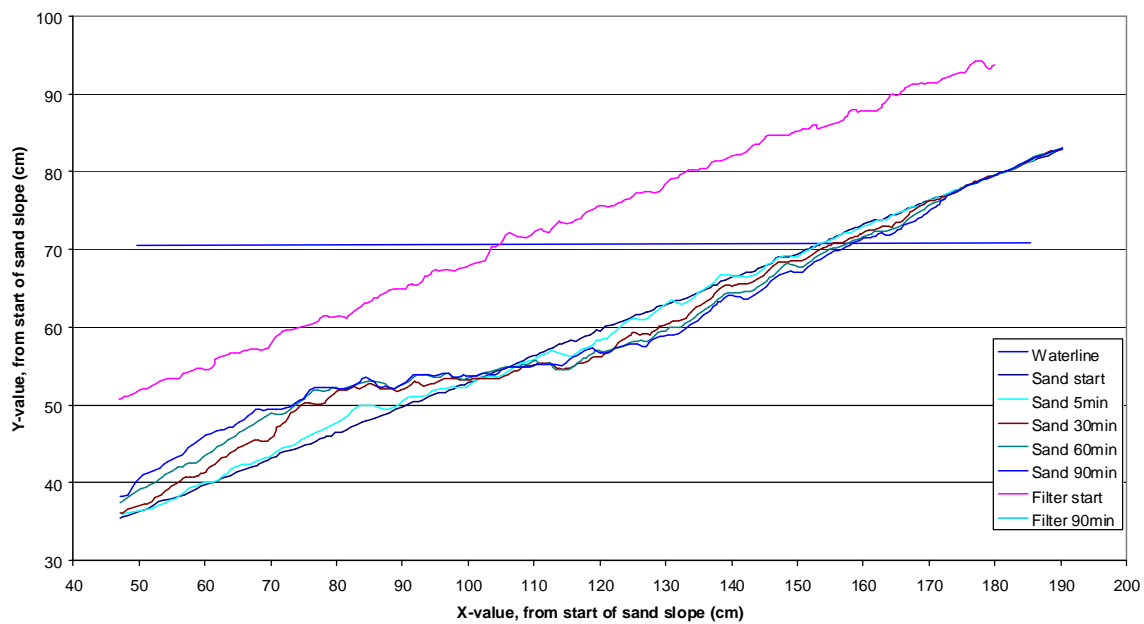


Figure 6-20 graph of the sand- and filter slope of test 6

6.3.7 Test 7 reference test regular waves

Test number	7
Type of waves	Jonswap
$H_{s,input}$	14 cm
$H_{s,measured}$	13,0 cm
$T_p,input$	1,42 s
$T_p,measured$	1,39 s
ξ	1,60
L_0	3,02 m
Duration	90 min
N	3885
$\tan\alpha$	0,33

In test 7, the wave height was increased to $H_s = 14$ cm, leading to an even more severe attack of the structure. To exclude the effects of a decreasing filter layer thickness, a thin wire mesh was put over the stones around the waterline, anchored into the core with four steel pins. This wire mesh prevented the stones from being washed away by the waves, without disturbing the water motion processes. The wire mesh was very thin and flexible, the same as used under the stones.



Figure 6-21 test 7 after 5 minutes (left) and after 90 minutes (right)

The higher waves clearly cause a larger amount of erosion and accretion. The bar-profile is still the same and again the erosion-growth rate decreased during the test. The larger waves run higher up the slope, making the length of the erosion area larger (L_a = absolute erosion length).

Test 7 $H_s = 14$ cm, $T_p = 1,42$ s, varying H

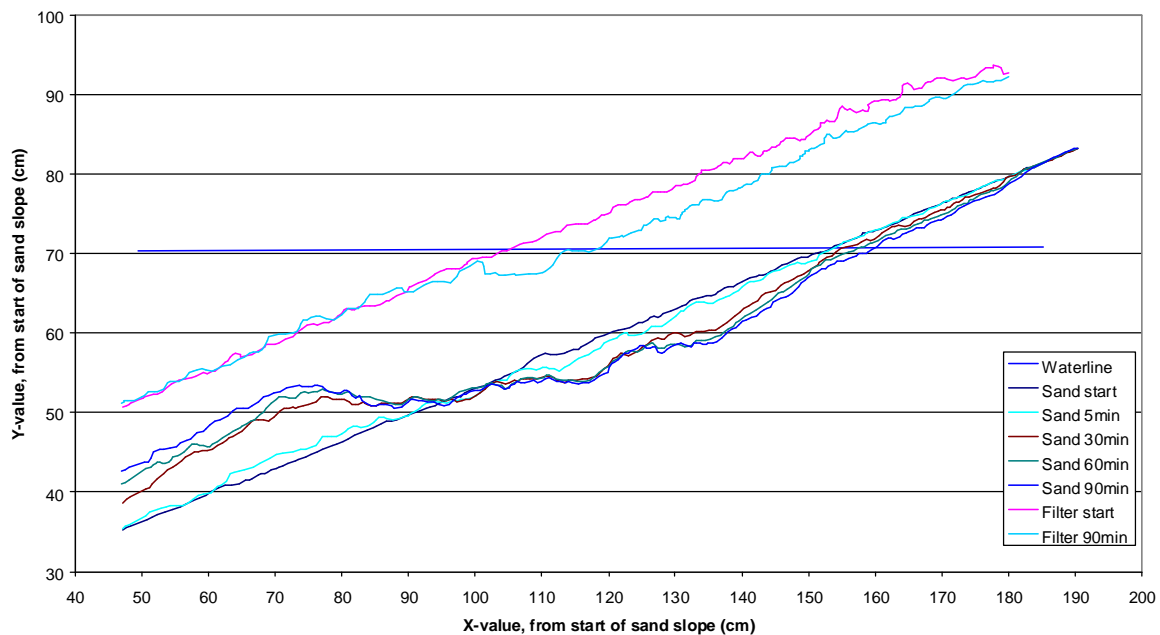


Figure 6-22 graph of the sand- and filter slope of test 7

6.3.8 Test 8 variation of T

Test number	8
Type of waves	Jonswap
$H_{s,input}$	10 cm
$H_{s,measured}$	8,1 cm
$T_{p,input}$	1,0 s
$T_{p,measured}$	1,02 s
ζ	1,49
L_0	1,63 m
Duration	90 min
N	5294
$\tan\alpha$	0,33

In test 8 the wave period is varied, the wave height maintained at $H_s = 10$ cm like in test 4. The period was $T_p = 1,0$ s. These relatively steep waves were difficult for the waveboard to generate; the machine produced a few loud bangs and stopped once during the test. The input wave height of 10 cm was not reached, only 8,1 cm was measured for H_s . Steeper waves were not used in the test series. The breaker-type of test 8 was still plunging waves.



Figure 6-23 test 8 after 5 minutes (left) and after 90 minutes (right)

The amount of erosion is clearly less than in test 4, with a lower erosion-depth and length. The bar-profile does occur, being less pronounced because the total erosion is less. The erosion-growth pattern is also similar to test 4, as can be seen in the analysis in Chapter 7.

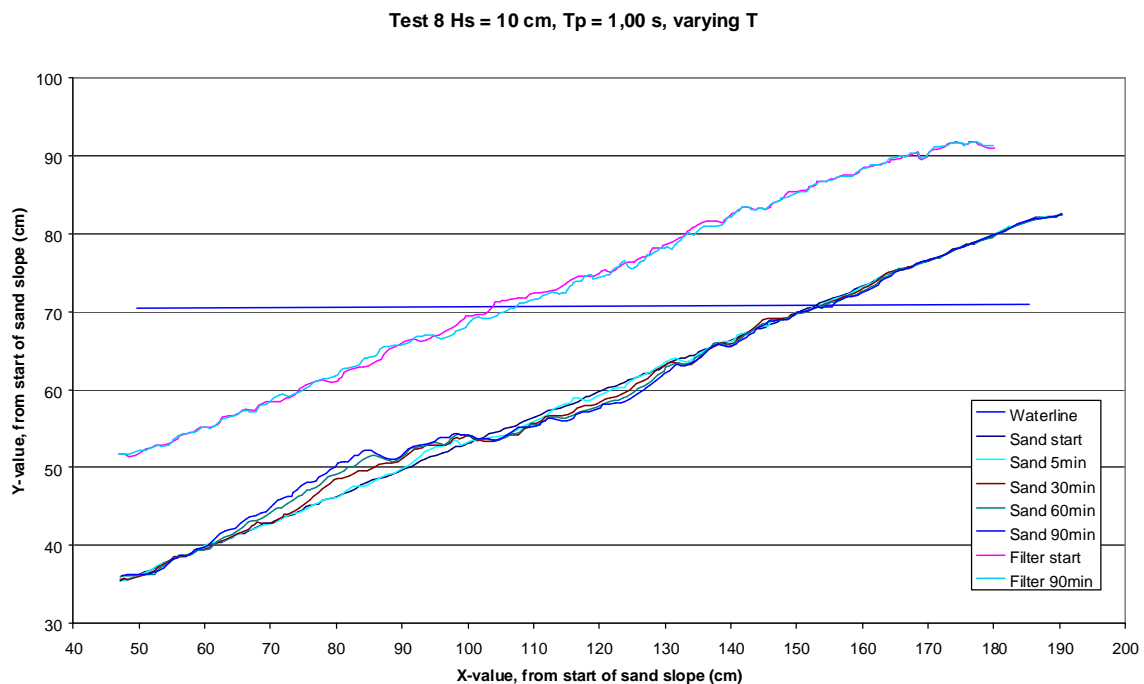


Figure 6-24 graph of the sand- and filter slope of test 8

6.3.9 Test 9 variation of T

Test number	9
Type of waves	Jonswap
$H_{s,input}$	10 cm
$H_{s,measured}$	9,6 cm
$T_{p,input}$	1,5 s
$T_{p,measured}$	1,47 s
ζ	1,97
L_0	3,38 m
Duration	90 min
N	3673
$\tan\alpha$	0,33

In test 9, the wave period was 1,5 s, larger than in test 4. The longer waves have a larger run-up and rundown height and seem to give the porous flow inside the filter layer more time to develop. The internal setup is higher, the internal wave over the sand slope runs-up higher and has a higher average level than with shorter waves. The waves break in a plunging way.



Figure 6-25 test 9 after 5 minutes (left) and after 90 minutes (right)

The amount of erosion is larger than in test 4, with the same basic pattern. The erosion-growth pattern is also the same, fast growth in the beginning, slowing down as time progresses.

Test 9 $H_s = 10$ cm, $T_p = 1,50$ s, varying T

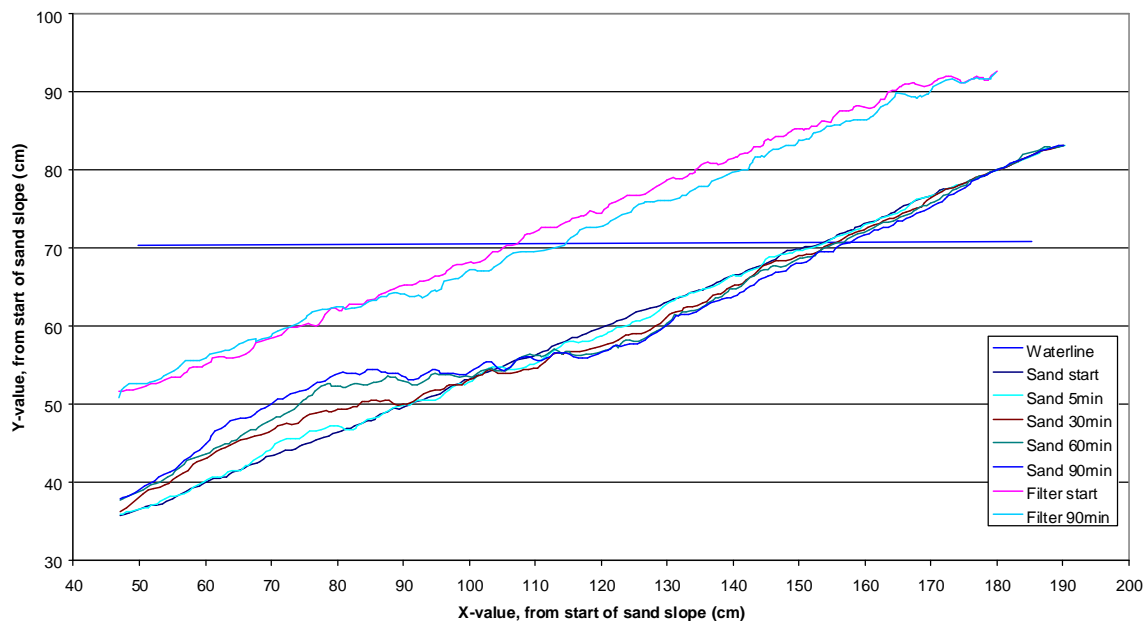


Figure 6-26 graph of the sand- and filter slope of test 9

6.3.10 Test 10 variation of T

Test number	10
Type of waves	Jonswap
$H_{s,input}$	10 cm
$H_{s,measured}$	9,7 cm
$T_{p,input}$	2,0 s
$T_{p,measured}$	1,96 s
ζ	2,62
L_0	6,00 m
Duration	90 min
N	2755
$\tan\alpha$	0,33

In test 10 the waves are even longer than in test 9, with a period of 2 s. These longer waves cause an even larger run-up and rundown height and a larger internal setup. The long period gives time for the development of high porous flow velocities running down the sand slope. The sand transport mechanisms of test 10 have been described in detail in section 6.2.4.



Figure 6-27 test 10 after 5 minutes (left) and after 90 minutes (right)

Especially the erosion-length is very large in test 10, the total amount of erosion is also quite large. The length of the area at point D over which the net-erosion is practically zero is larger as well, from about 10 cm in test 4 to over 15 cm in test 10.

Test 10 $H_s = 10$ cm, $T_p = 2,00$ s, varying T

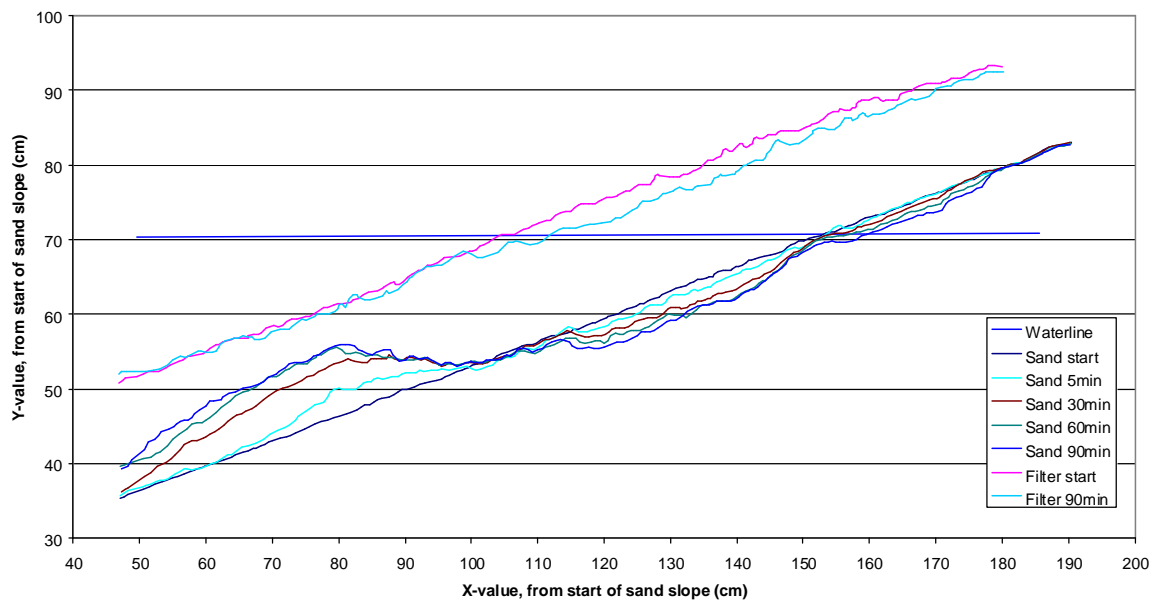


Figure 6-28 graph of the sand- and filter slope of test 10

6.3.11 Test 11 swell waves

Test number	11	Test 11 was done with regular waves to simulate the effect of swell waves, with the expectation that the erosion would grow slowly because of the small wave height. However, the effect of the long period was underestimated and the erosion went very fast instead.
Type of waves	Regular	
$H_{s,input}$	5 cm	
$H_{s,measured}$	5,1 cm	
$T_{p,input}$	3,00 s	
$T_{p,measured}$	3,00 s	
ζ	5,52	The long waves with a height of only 5 cm have a larger run-up and rundown than the waves of test 1 with a twice as large wave height. Test 15, with lower swell waves was included to the program for comparison.
L_0	14,06 m	
Duration	90 min	
N	1800	
$\tan\alpha$	0,33	



Figure 6-29 test 11 after 5 minutes (left) and after 90 minutes (right)

The long waves do not break at all, but surge over the filter slope. The difference in amplitude between the external and internal wave is much smaller than for shorter waves. The up-running wave takes some sand with it, but during the long run-down, porous flow velocities develop to a high level, being able to transport a large amount of sand over a long distance down the slope.

Test 11 H = 5 cm, T = 3,00 s, regular waves, swell

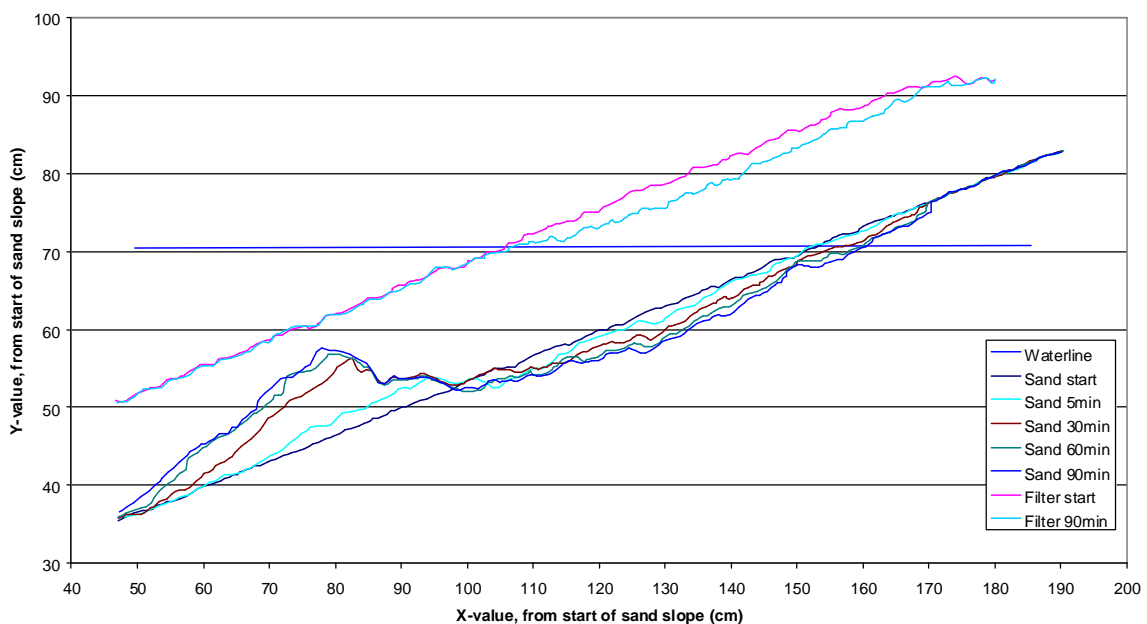


Figure 6-30 graph of the sand- and filter slope of test 11

6.3.12 Test 12 wide grading

Test number	12
Type of waves	Jonswap
$H_{s,input}$	10 cm
$H_{s,measured}$	9,0 cm
$T_{p,input}$	1,2 s
$T_{p,measured}$	1,23 s
ζ	1,71
L_0	2,36 m
Duration	120 min
N	5854
$\tan\alpha$	0,33

In test 12 a different filter material was used; a mixed grading from three existing materials, to get a widely-graded material. The small stones can fill a part of the pores between the large stones, leading to smaller pores and a lower porosity. The smaller pores were expected to decrease the amount of erosion by reducing the load and giving more resistance to the porous flow. However, after 90 minutes the amount of erosion was exactly the same as in test 4 with the narrow grading. The porosity was measured after the tests and the difference turned out to be small: $n = 0,42$ for the other tests, $n = 0,37$ for test 12.



Figure 6-31 test 12 after 5 minutes (left) and after 120 minutes (right)

As in the other tests, the bar-profile is clearly visible. A difference between test 12 and test 4 is that in test 12 the erosion area above SWL is much less pronounced; only a very little erosion above SWL is visible. The rest of the profile is very similar.

Test 12 $H_s = 10$ cm, $T_p = 1,2$ s, Jonswap, Wide grading

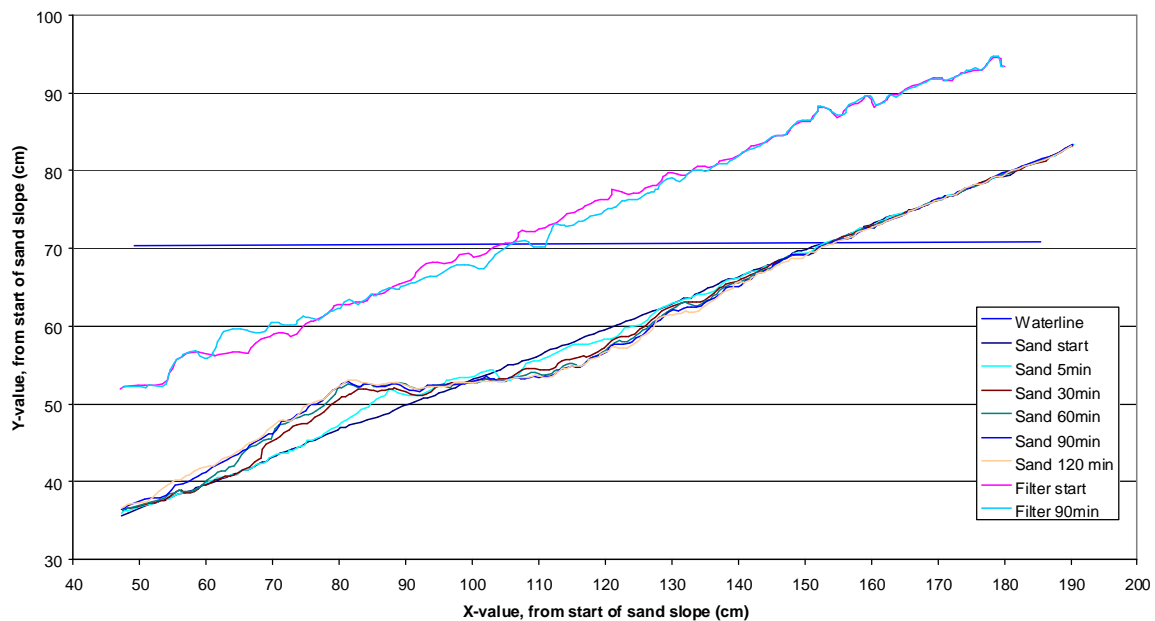


Figure 6-32 graph of the sand- and filter slope of test 12

6.3.13 Test 13 variation of H

Test number	13
Type of waves	Jonswap
$H_{s,input}$	5 cm
$H_{s,measured}$	4,4 cm
$T_p,input$	0,85 s
$T_p,measured$	0,84 s
ζ	1,65
L_0	1,10 m
Duration	420 min
N	30000
$\tan\alpha$	0,33

Test 13 was added to the program to get an extra data point in the wave height variation test series. The relation between erosion and wave height did not seem to be linear for the tests, and to have more data to find a relation, test 13 and 14 were added. The low wave height of $H_s = 5$ cm was expected to give little erosion, with the possibility of finding an equilibrium situation. Indeed the amount of erosion was small; no real erosion did even occur at all, only some very local sand motion.



Figure 6-33 test 13 after 5 minutes (left) and after 420 minutes (right)

Clearly the amount of erosion is practically zero, leading to a threshold in the wave height below which no erosion occurs. It was visible in the test that the larger waves in the test did cause some sand movement, a tiny bit of local bedload transport, while waves lower than about 5 cm did not cause any visible transport at all.

Test 13 $H_s = 5$ cm, $T_p = 0,85$ s Jonswap, varying H

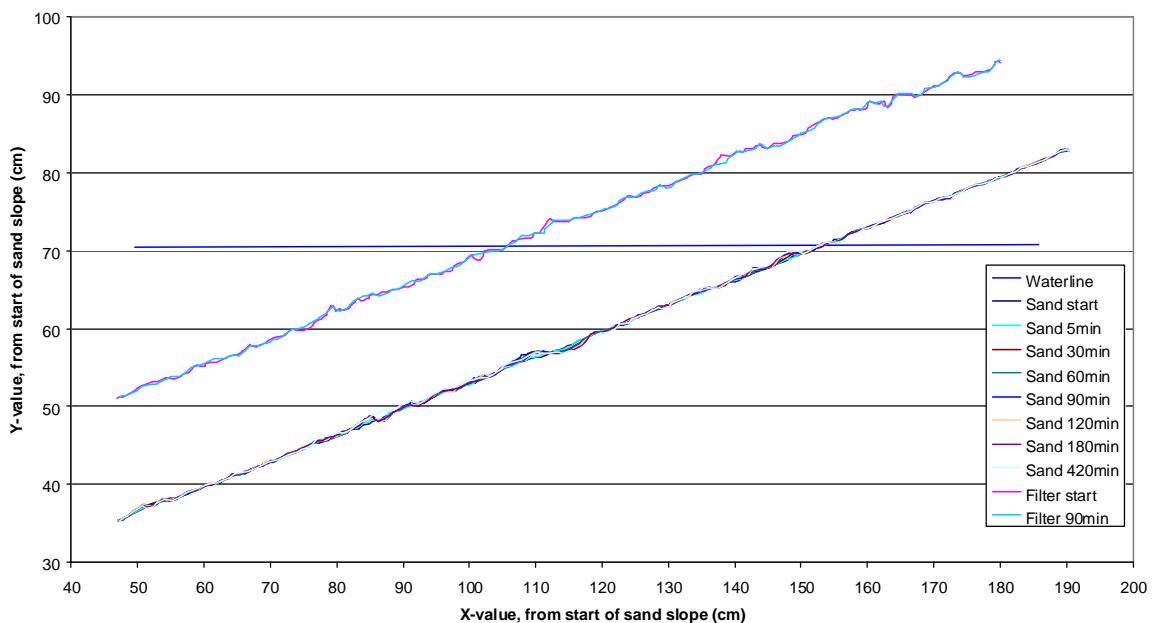


Figure 6-34 graph of the sand- and filter slope of test 13

6.3.14 Test 14 variation of H

Test number	14
Type of waves	Jonswap
$H_{s,input}$	16 cm
$H_{s,measured}$	14,8 cm
$T_p,input$	1,52 s
$T_p,measured$	1,48 s
ζ	1,59
L_0	3,42 m
Duration	90 min
N	3649
$\tan\alpha$	0,33

In test 14, the highest waves of the whole test series were used. Again a wire mesh was put over the stones to prevent them from rolling away, this time also stabilized with two heavy bars, put lengthwise in the flume to influence the wave motion as little as possible. As expected, the amount of erosion was larger than for lower waves and the erosion area grew faster. The larger waves seemed to have more power than smaller waves, creating stronger flow and more sand transport.



Figure 6-35 test 14 after 5 minutes (left) and after 90 minutes (right)

The shape of the erosion profile is more or less the same as in e.g. test 12, with the difference that the erosion is spread a little better over the erosion area, with less difference in erosion depth over the area. The accretion area is high, reaching towards the top of the filter layer. Sand was leaving the filter in high waves.

Test 14, $H_s = 16$ cm, $T_p = 1,52$ s, Jonswap, varying H

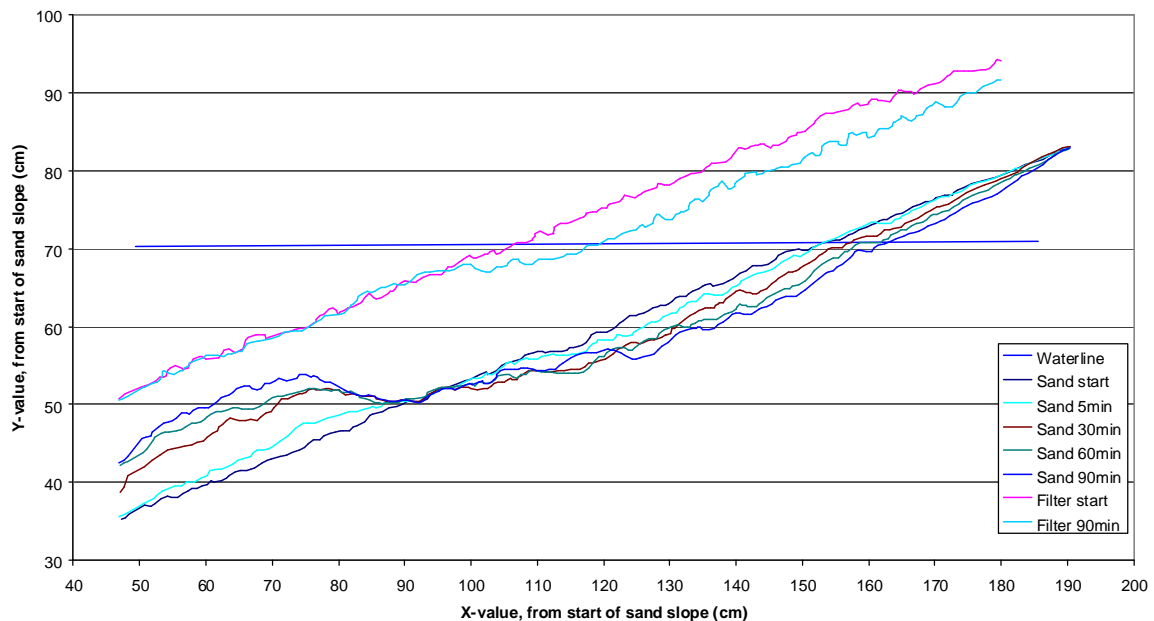


Figure 6-36 graph of the sand- and filter slope of test 14

6.3.15 Test 15 swell waves low

Test number	15
Type of waves	Regular
$H_{s,input}$	3 cm
$H_{s,measured}$	3,0 cm
$T_p,input$	2,00 s
$T_p,measured$	2,00 s
ζ	4,76
L_0	6,25 m
Duration	240 min
N	7200
$\tan\alpha$	0,33

The wave height in test 15 is only 3 cm, the lowest waves used. Yet some erosion does occur, in contrast to test 13 where no erosion occurred for waves of 5 cm high. The difference lies in the period, which is larger in test 15. The amount of erosion is much less than in test 11, with larger swell-waves. Test 15 was run for 240 minutes, (4 hours), after which the amount of erosion was still small compared to test 11 after 90 minutes.



Figure 6-37 test 15 after 5 minutes (left) and after 240 minutes (right)

Like in the other tests with regular waves, a sharp edge or cliff develops at point A, high up the slope, slowly eroding upward. Point D is visible, but less clear than in other tests, as the whole erosion and accretion area are less pronounced and the total amount of erosion is small.

Test 15 H = 3 cm, T = 2,00 s, regular waves, swell

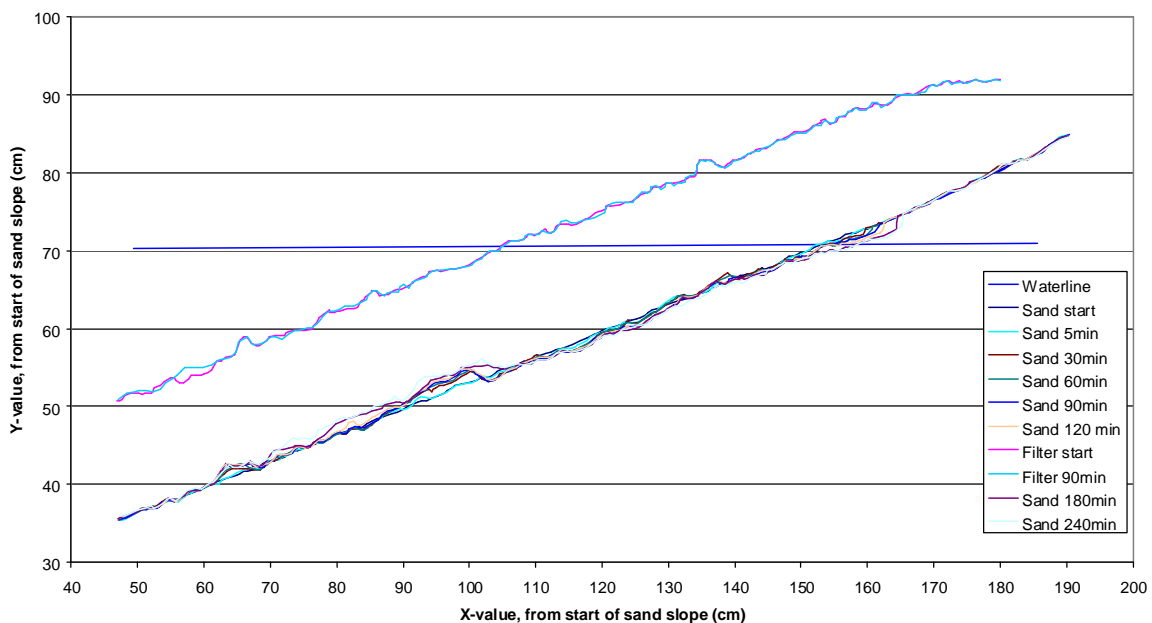


Figure 6-38 graph of the sand- and filter slope of test 15

6.3.16 Test 16 slope steepness variation

Test number	16
Type of waves	Jonswap
$H_{s,input}$	10 cm
$H_{s,measured}$	9,0 cm
$T_p,input$	1,2 s
$T_p,measured$	1,23 s
ζ	1,28
L_0	2,36 m
Duration	180 min
N	8780
$\tan\alpha$	0,25

In test 16, the slope of the structure was changed to 1:4 instead of 1:3 in the other tests. The wave parameters equalled those of test 4. It was expected that the wave dissipation would be spread over a longer part of the slope, plus that the gentler slope is more stable, both leading to less erosion. Indeed, the amount of erosion was considerably less. Which of the mentioned mechanisms was most important for this will be elaborated on in the next chapter.



Figure 6-39 test 16 after 5 minutes (left) and after 180 minutes (right)

Hardly any erosion is visible above SWL; the wave action does not seem to reach high enough to cause strong enough porous flow high up the slope. The bar-shaped profile is visible on the rest of the slope.

Test 16, $H_s = 10$ cm, $T_p = 1,2$ s, slope 1 : 4

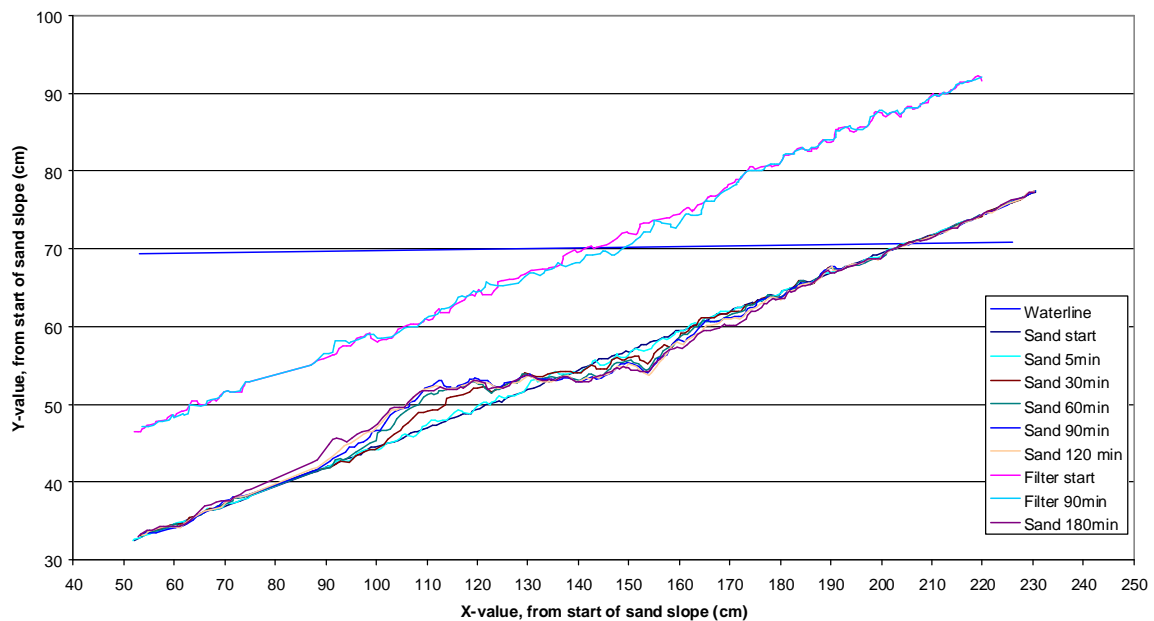


Figure 6-40 graph of the sand- and filter slope of test 16

6.3.17 Test 17 slope steepness variation

Test number	17	In test 17 the slope was steeper instead of gentler; 1:2.
Type of waves	Jonswap	The opposite effects of test 16 were expected; a shorter distance over which the wave energy is dissipated and
$H_{s,input}$	10 cm	less stability of the sand by the steeper slope. The sand
$H_{s,measured}$	9,0 cm	had to be levelled very carefully as the sand had the
$T_p,input$	1,2 s	tendency to slide down with only little disturbance of
$T_p,measured$	1,23 s	the levelling board. The amount of erosion was indeed
ζ	2,56	large and the erosion grew fast in test 17.
L_0	2,36 m	
Duration	90 min	
N	4390	
$\tan\alpha$	0,50	



Figure 6-41 test 17 after 5 minutes (left) and after 90 minutes (right)

As in all tests, the bar-profile is visible. Remarkable in this test is the very large cliff at point A. The vertical edge is more than 5 cm high after 30 minutes and it was clearly visible during the test that the up-running waves undermine this cliff by eroding sand from the base of it.

Test 17, $H_s = 10$ cm, $T_p = 1,2$ s, slope 1 : 2

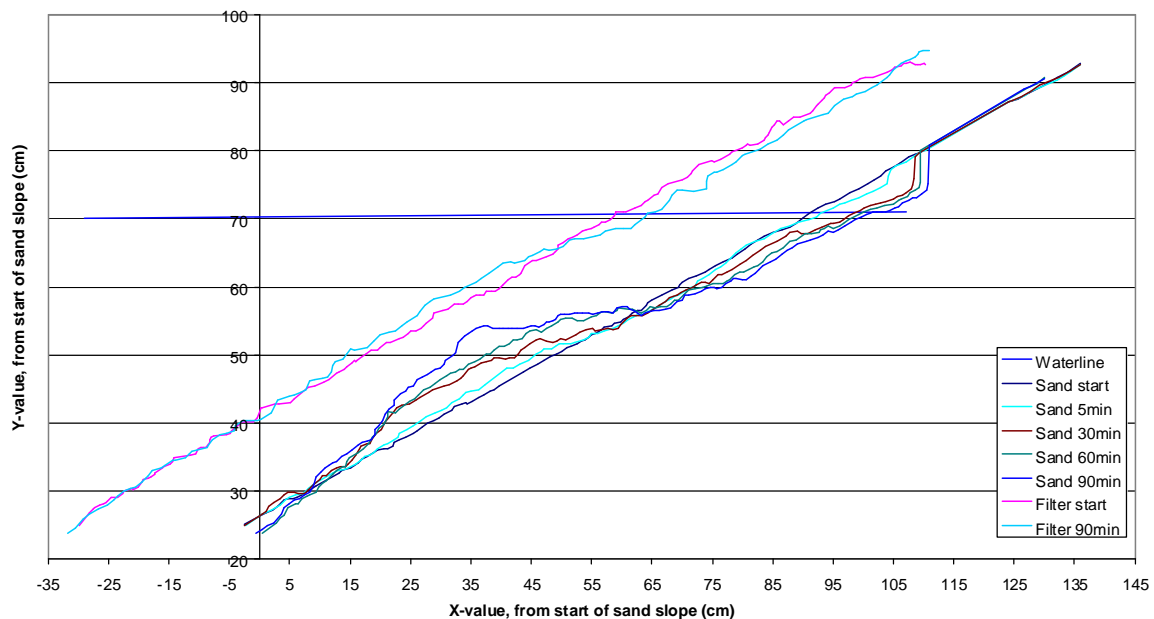


Figure 6-42 graph of the sand- and filter slope of test 17

6.4 Validity of the tests

The tests were performed in the long sediment transport flume of the fluid mechanics laboratory of the faculty of Civil Engineering at Delft University of Technology. This flume has a length of 42 m, a width of 0,80 m and a depth of 1,00 m. The electrically driven wave board with automatic reflection compensation can never give the exact wave that was put in, and differences of up to 10 % have been measured between the input and the actual wave that arrived at the structure. However, because the analysis is done with the measured wave parameters, the errors due to this difference do not influence the results. If for some reason they do, it will be mentioned in the analysis of the particular situation.

6.4.1 Setup of the structure

Tests 2 and 3 are reruns of the reference test with slight differences in the test setup. In test 3, a thin mesh wire was placed under the filter layer, on the sand slope. With this mesh wire, the stones are much easier removed after the test, and the thin wires sink easily into the sand without interference of the tests. Nevertheless, test 3 showed that the mesh wire does have influence high up the slope, where a steep edge develops. Here the wire cannot follow the sharp bend in the slope and keeps the stones of the filter too high above the sand. The result is an open space underneath the stones where the up-running wave has more space and therefore more power to erode the steep edge. To avoid this influence in the other tests, the mesh wire was only used on the lower part of the slope, where no influence was measured. Figure 6-43 shows this difference between test 2, without mesh wire and test 3, with the mesh wire. High up the slope, where point A is defined, a larger and higher (further eroded) sharp edge or cliff can be seen for test 3 than for test 2. At the rest of the slope, the erosion after 90 minutes is practically the same for both tests.

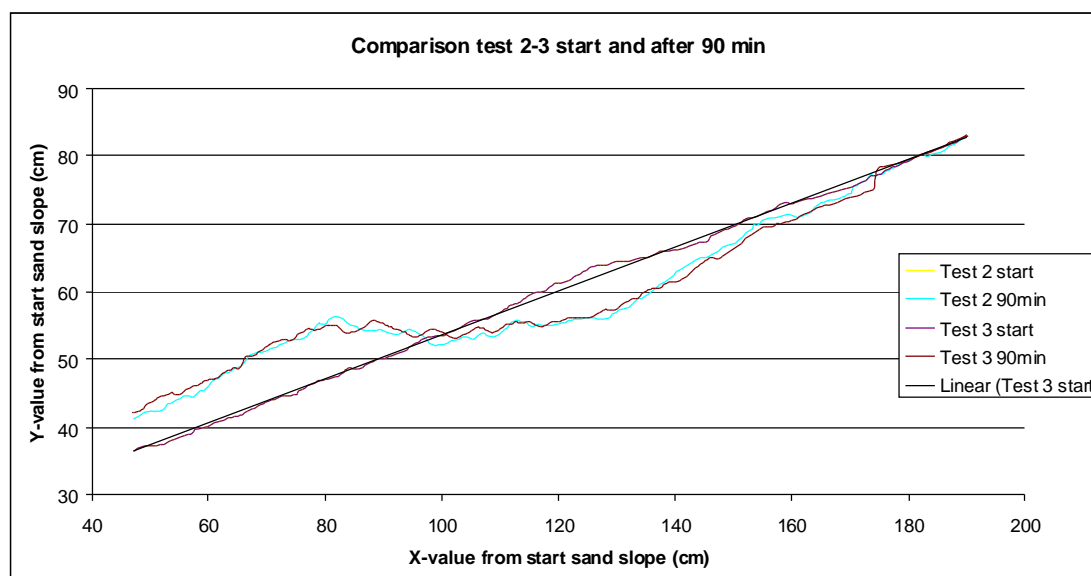


Figure 6-43 comparison of the erosion after 90 minutes of test 2 and test 3



Figure 6-44 photo of the space under the mesh wire in test 3

6.4.2 Reproducibility of the tests

Most tests have different loading parameters, making a repeatability study difficult. Nevertheless, tests 1, 2 and 3 have been done with the same waves loading the structure and principally the same setup of the structure. Differences are that the structure for test one was built in the dry flume and for the other tests in the flume filled with water. For the first test, the sand may have been less densely packed and not completely saturated. The only difference between tests 2 and 3 is the application of the thin mesh wire in test 3 as described above.

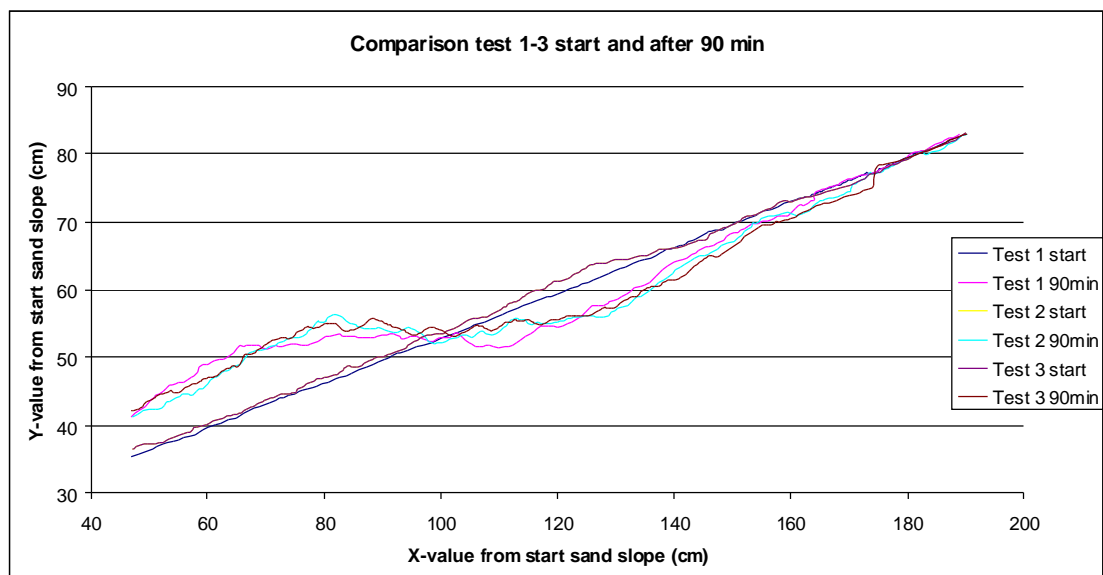


Figure 6-45 erosion of the sand profile of test 1 to 3 at the start and after 90 minutes

Test 1 shows deviations in the erosion profile

Figure 6-45 shows the erosion of the sand profile of tests 1-3 at the start and after 90 minutes of testing. It is visible that the erosion of test 1 after 90 minutes deviates from that of test 2 and 3; higher on the slope the erosion is less, towards point D the erosion is more and the accretion area is first a bit lower and later a bit higher than that of tests

2 and 3. These deviations are expected to be due to the difference in packing and saturation of the sand in test 1 as described above.

Tests 2 and 3 show good similarity

Test 2 and 3 show much less deviation; despite the use of the mesh wire in test 3, the erosion profiles after 90 minutes almost coincide with only very local differences. These differences are expected to be local scour holes around single filter stones or due to local differences in porosity of the filter stones.

Reproducibility based on tests 2 and 3

Based on the observations of test 2 and 3 it can be said that the tests are reproducible in a qualitatively good way. Small local disturbances do not induce large deviations in the overall erosion profile.

6.4.3 Measurement errors

Some devices were used to measure for instance wave heights or distances in the structure. All measurements have a certain accuracy and hence a certain error.

Wave gauges

The used wave gauges have a standard error of 0,5%. The gauges measure the electrical resistance through two wires that are put in the water. The water surface connects the electric loop; the higher the water level, the lower the resistance. At the bottom end of the wires, another electrode performs a reference measurement under water to compensate for differences in the electrical resistance caused by differences in for instance the density, temperature or salinity of the water.

Photographs of the sand profile

Photos were taken with a 5 megapixel digital camera, on which differences of half a mm are still visible. The graphs were constructed manually from the photos with the software Getdata, for which an error of 0,5 mm is to be expected as well. This way, the measurements of the sand profile have an error of up to 1 mm.

Measurements with a measure-tape

For the construction of the breakwater cross-section, a measure-tape was used with a mm scale. The error in these measurements is about 1 mm, which is the thickness of the lines drawn on the glass of the flume.

6.4.4 Laboratory effects

A wall effect can be expected at the glass sidewalls of the flume, causing an error in the measured profile. Also an asymmetry in the erosion pattern over the width of the flume has been observed.

Wall effect error

At the wall, the irregular structure of the filter stones is disturbed. The straight wall changes the shape and size of the pores between the stones at the wall compared to the pores deeper in the filter layer. Pores at the wall are usually larger, expectedly causing higher porous flow velocities. This will lead to more erosion at the wall than in the middle of the structure. To investigate this difference, filter stones have been removed very gently after a number of tests, and the sand surface has been measured for deviations.

Table 6-3 deviations of erosion and accretion over the width of the flume in mm

Test number	6	7	9	10	11	14	Average
Waterline	0	0	0	2	2	1	0,83
Erosion 1	2	2	1	2	3	3	2,17
Erosion 2	2	5	2	0	0	0	1,50
Max erosion	5	5	3	2	2	1	3,00
Erosion 4	3	2	1	1	2	2	1,83
Point D	1	3	3	3	0	2	2,00
Accr. 1	2	1	1	4	1	3	2,00
Max accr.	1	3	2	2	2	0	1,67
Average	2,00	2,63	1,63	2,00	1,50	1,50	1,88
Maximum	5	5	3	4	3	3	3

In Table 6-3 these deviations are shown. The numbers indicate the amount of mm that the sand-slope-level at the wall differs from that in the middle of the flume. As expected, a somewhat deeper erosion and higher accretion area developed in most tests, with deviations of 2 mm on average, and locally a maximum of 5 mm for tests 6 and 7. These maxima were measured at places where local scour around a stone had deepened the erosion. The overall sand slope did not change over the width of the flume, only these very local differences were present. In the calculation of the erosion area (150 cm² on average), these deviations can cause an error of 1% maximum.

Asymmetry error

Due to asymmetry in either the wave generation, the shape of the flume, the shape of the fixed 1:30 slope or the shape of the breakwater cross section, an asymmetry in the erosion between the front- and backside of the flume has been found.

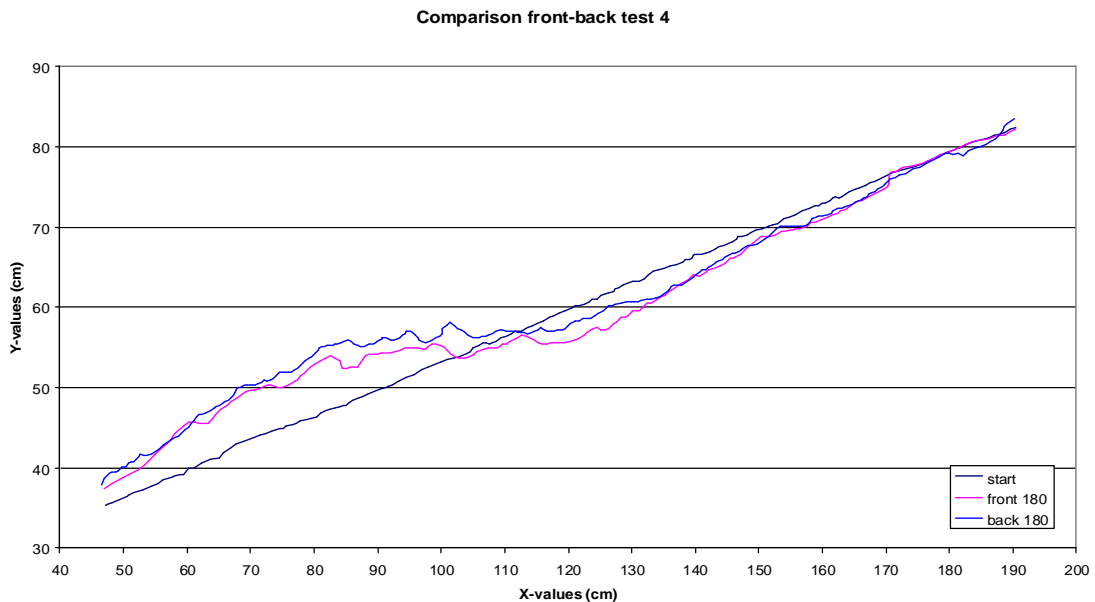


Figure 6-46 comparison of the sand slope after 180 min from the front- and backside for test 4

In Figure 6-46, the lines of the sand slope as extracted from a photo from the front side and one from the backside after 180 minutes of test 4, are plot simultaneously. In the erosion area, the two lines lie close to each other, but in the accretion area and around point D, differences are clearly visible. The amount of erosion does not deviate much in total and over the largest part of the erosion area the lines lie close. However, point D lies higher up the slope at the backside of the flume and the

accretion area is higher in this area. The same plot has been made for tests 5, 6, and 7, and the same pattern occurred for all these tests; very little differences in the erosion area, but a higher point D and a higher sand slope around D and between D and E (accretion max) at the backside of the flume.

Table 6-4 deviations in cm between the front- and backside of the flume

Test number	4	5	6	7	Average	Maximum
Erosion average	0	0	0	0	0,00	0,00
Erosion max	2	1,5	1	1	1,38	1,50
Accretion average	1	1	1	3	1,50	3,00
Accretion max	3	3	3	4	3,25	4,00

In Table 6-4 the differences in sand slope level are displayed for tests 4 – 7, divided into an average and a maximum value over the erosion area and over the sand slope. It should be noted that these differences are in cm, instead of the mm used to display the deviations between the middle and the sides to indicate the wall effect. The deviations due to asymmetry effects are one order higher than the wall effect-deviations. As mentioned above, different reasons could be responsible for these asymmetry effects, but without the necessary data, no conclusions can be drawn. The overall average asymmetry effect is about 1,5 cm.

6.4.5 Conclusions on the errors

Different types of errors have been described: setup errors by the wire mesh under the stones, measurement errors by the wave gauges, digital photos and measured distances, and laboratory effects being a wall effect and an asymmetry over the width of the flume.

Relative importance of the errors

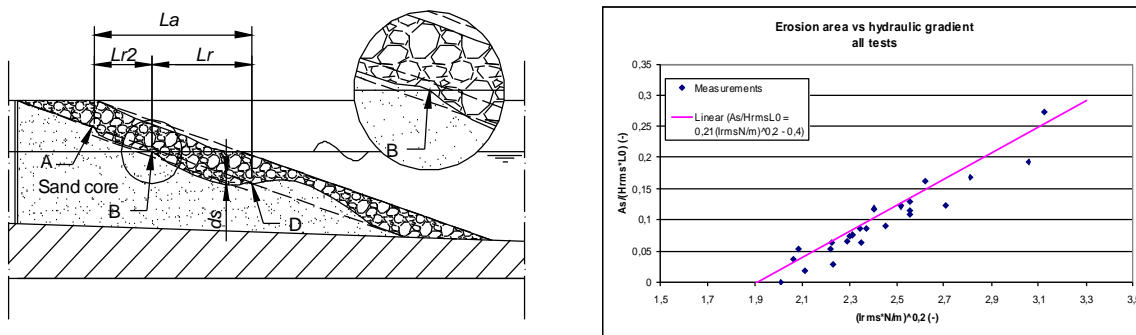
The error by the wire mesh has been countered by only applying it where no influence was found, so this error does not influence the analysis. The measurement errors do not exceed 1 mm, which is in the order of 1% of the typical length scales in the structure, and leads to errors in the order of 0,3% in the calculation of the erosion area. The wall effect gives a somewhat higher error, about 2% in the length scales, but the error due to the asymmetry in the flume-erosion-process gives the highest error, of up to 10% in the erosion area and even 20% in the accretion area.

Handling the errors

Errors by the wire mesh and measurements are negligible because they are an order smaller than asymmetry errors and irregularities in the test results. The wall effect errors are also small compared to the other effects and never underestimate the erosion, which might lead to unsafe design formulas, so they are not taken into account in the further analysis, other than being noticed and recognized. The asymmetry error is much larger, and must be handled with care. Because the same pattern of deviations occurs at all the investigated tests, regularity to some degree in these deviations is expected. The amount of erosion and the erosion depth do not change much, and the influence in relations between loading and erosion is expected to be very limited as the error seems relative to the amount of erosion. Absolute values can be influenced by this type of error, and case-specific physical model tests will be recommended to eliminate this type of error when designing breakwaters with hydraulically sand-open filters.

Chapter 7

Analysis of the test results



7.1 Calculation of parameters

7.2 Sand balance for erosion and accretion area

7.3 Comparisons with Uelman's tests

7.4 Relations between loading and erosion

7.5 Existing open filter design criteria and Shields

7.6 Turbulence-dominance or porous-flow-dominance

7.7 Dimensionless parameter relations

7.8 Up-scaling to a possible prototype

7.9 Evaluation of the analysis

Chapter 7 Analysis of the test results

In chapter 7 the results of the tests are analysed. Relations between parameters are investigated and interpreted, and explanations are searched for. First interesting parameters, such as erosion depth and –length, are calculated, after which the sand balance for the erosion and accretion area is explained. Then the results are compared with the results of the tests done by Uelman³⁶, and relations between loading- and erosion parameters are investigated. The dominant loading force is identified from observations and the dimensionless parameter combinations found in Chapter 4 are used to find useful dimensionless relations suitable for the understanding and design of breakwaters with open filters on a sand core. The chapter ends with up-scaling to a prototype scale and an evaluation.

7.1 Calculation of parameters

The computation of the erosion area has already been mentioned earlier; from the photos through the glass side wall of the flume, graphs were extracted using the software Getdata. This program creates x - y -coordinates when dots are placed (manually) in the picture. These sets of coordinates are imported in Excel, to plot graphs and calculate interesting parameters.

Erosion and accretion area

Because the lines after different times for one test have different x - y -values, they cannot be subtracted or added at once. Therefore a second order polynomial was added to the start line as a trendline and the differences were calculated from the resulting function, see Figure 7-1. The erosion area is the surface between the start line and the particular line of interest of the sand slope.

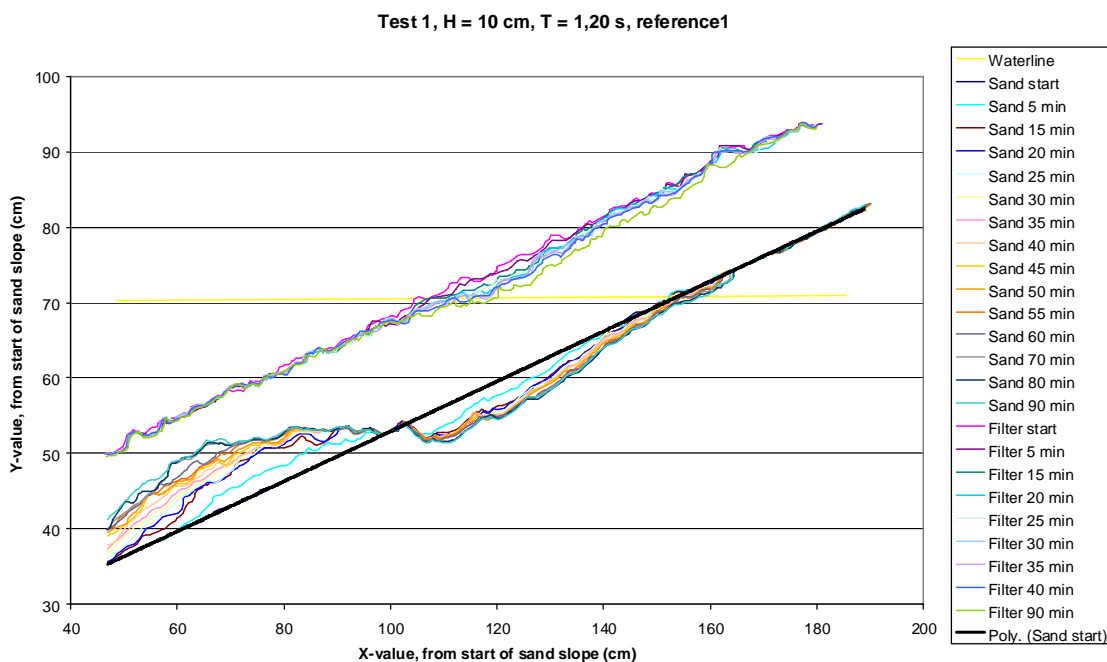


Figure 7-1 example of an extracted graph with trendline at the start

³⁶ Uelman (2006), [49]

Erosion length and -depth

The erosion length is defined as the horizontal length (x -values) between point A where the erosion starts, and point D where the erosion ends. This is the absolute erosion length L_a , divided into the relative erosion length L_r from D to the waterline (point B), and the relative erosion length 2, L_{r2} from point A to point B.

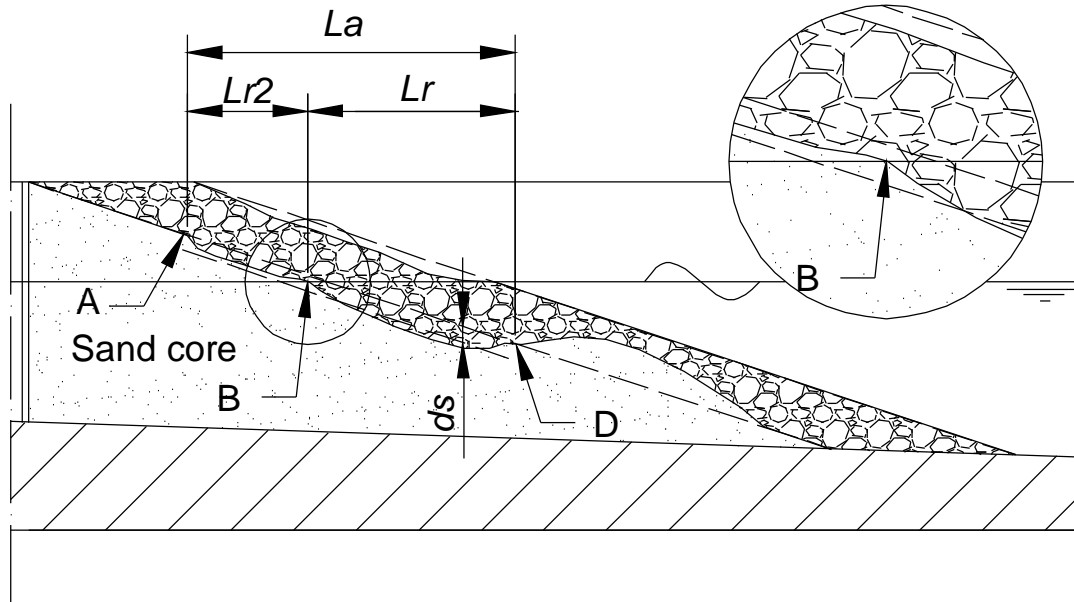


Figure 7-2 definition sketch of erosion length and -depth

The erosion length values were calculated from the x - y coordinates, and the erosion depth was calculated by dividing the erosion area by the absolute erosion length, $d_s = \frac{A_s}{L_a}$. This is the average vertical erosion depth. The average depth is used instead of the maximum depth to minimize the influence of the local wall effects and to be able to compare the quantitative results with those of Uelman. The erosion area, the different erosion length parameters and the erosion depth are shown in Table 7-1 for all tests after 90 minutes.

Table 7-1 erosion parameters of all tests

Test Number	Parameters Variations	H m	T s	ξ (-)	Erosion area 90 min cm ²	La 90 min cm	Lr 90min cm	Lr2 90min cm	ds 90min cm
1	Reference	0,095	1,20	1,62	247,65	64,10	59,09	5,01	3,51
2	Reference 2	0,095	1,20	1,62	231,97	75,24	60,45	14,79	3,08
3	Reference 3	0,096	1,20	1,61	279,73	73,80	60,64	13,17	3,79
4	Irregular waves	0,090	1,20	1,66	96,10	65,17	55,36	9,81	1,47
5	Varying H	0,071	1,10	1,72	52,03	67,30	48,19	19,11	0,77
6	and N	0,110	1,32	1,66	159,50	68,21	55,58	12,63	2,34
7		0,130	1,39	1,60	257,22	87,87	66,02	21,86	2,93
8	Varying ξ by varying T	0,081	1,02	1,49	56,09	61,27	53,59	7,67	0,92
9		0,096	1,47	1,97	133,26	71,44	53,45	17,99	1,87
10		0,097	1,96	2,62	194,73	76,72	58,85	17,87	2,54
11	Swell waves	0,051	3,00	5,52	206,97	73,39	56,11	17,29	2,82
12	Grading variation	0,090	1,23	1,71	94,56	64,92	55,89	9,03	1,46
13	Varying H	0,044	0,84	1,65	-2,52	0,00	0,00	0,00	0,00
14	Varying H	0,148	1,48	1,59	293,05	93,20	71,25	21,95	3,14
15	Swell waves low	0,030	2,00	4,76	35,70	72,20	53,48	18,72	0,49
16	tan alpha	0,090	1,23	1,28	56,11	80,49	72,14	8,35	0,70
17	variation	0,090	1,23	2,56	184,85	48,07	38,98	9,08	3,85

Maximum erosion depth

The maximum erosion depth is located at a very local scour hole around a filter stone at the glass side wall of the flume. This depth is not particularly relevant for the behaviour or the design of the structure because this local scour hole is evened out by the filter layer above it. The filter layer settles to fill the erosion area with its stones and averages the erosion of the sand over the whole erosion length. Therefore, the average erosion depth as used in the analysis does have a physical meaning and is relevant for the behaviour of the structure as a whole.

Example of loading-erosion relations

From the data in Table 7-1, relations between loading parameters and erosion parameters can be plot and investigated. As an example, total erosion area is shown in Figure 7-3 versus the wave height, for all tests.

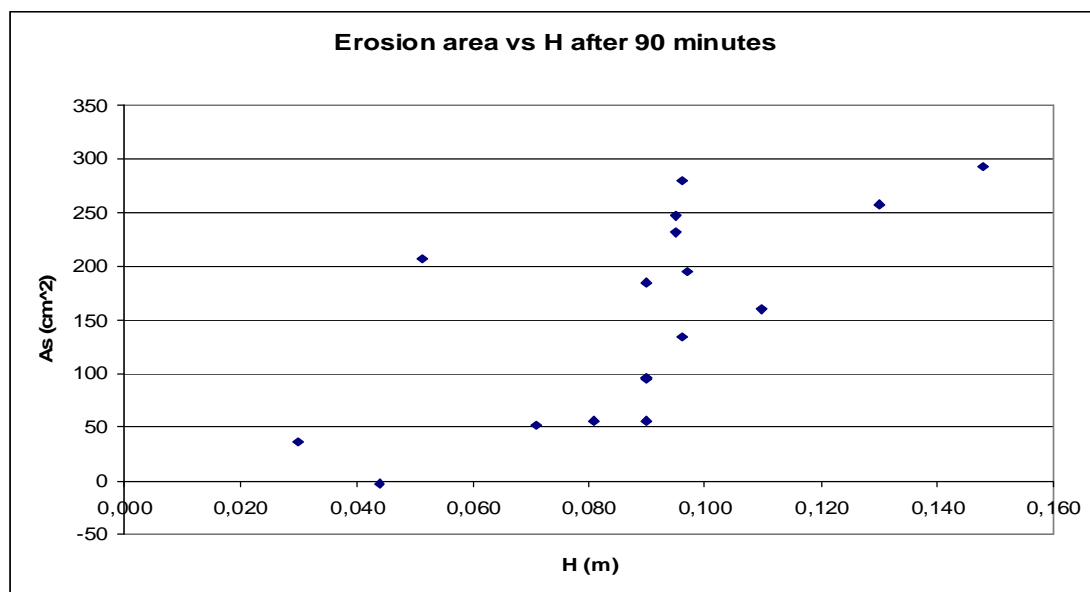


Figure 7-3 chart of the erosion area versus the wave height for all tests

In the chart all the tests have been put, showing no single relation between the amount of erosion and the wave height. In section 7.4 relations are shown per subset of the tests, for instance wave height variation tests, and different combinations of parameters are used to find important relations.

7.2 Sand balance for erosion and accretion area

At the end of most tests, a zoomed-out photo has been taken of the whole slope to be able to calculate the total accretion area correctly, beyond the green pole of the flume. The results are shown in Table 7-2, with the ratio of the erosion area over the accretion area. Theoretically, this ratio should equal the porosity, n , which has been measured to be 0,42 for the used filter stones.

Table 7-2 comparison of erosion- and accretion area

Test number	Erosion area cm ²	Accretion area cm ²	Ratio erosion/accretion	porosity -
4	-159,71	283,37	0,56	0,42
5	-135,98	221,19	0,61	0,42
6	-164,53	289,12	0,57	0,42
7	-268,02	458,54	0,58	0,42
8	-140,29	303,84	0,46	0,42
9	-138,34	289,48	0,48	0,42
10	-202,64	401,36	0,50	0,42
11	-206,05	312,98	0,66	0,42
14	-305,19	502,84	0,61	0,42

Clearly, the erosion area is smaller than the accretion area, but larger than the 42% that it should be theoretically, with values of the ratio ranging from 46% to 66%. This is unexpectedly high; possible reasons are listed below.

- The measured porosity is the internal porosity between the filter stones. At the edges, on the flat sand bed and at the glass side walls, the porosity is different. This can be explained when looking at a sphere that just fits inside a cubical. The volume of the sphere is $V_{sphere} = \frac{4}{3}\pi r^3$, and the volume of the cubical is $V_{cube} = (2r)^3 = 8r^3$. A layer of spheres on a e.g. a flat bottom thus has a porosity of $n = 1 - \frac{V_{sphere}}{V_{cube}} = 1 - \frac{4/3\pi}{8} = 0,48$. The stones of the filter layer are not perfect spheres, but the porosity at the edges is close to 0,48 for the first layer with a thickness of about half a stone diameter. For example, this effect increases the average porosity over the accretion area of test 11 to 0,45.
- A part of the finest fraction of the sand will not settle in the accretion area, but leave the filter as wash load. After the tests, about one bucket could be filled with fine sediments that had settled on the bottom of the dried flume. Per test, this cannot be more than about 2/3 litre, or about 20 cm² of the measured accretion area (the porosity and flume width taken into account). Some of the even finer sand fractions may have left the flume with the water when it was emptied, but the amount is not known.
- Some sand might stick within pores of the filter stones, not being measured as accretion area. Furthermore, after most of the tests, some sand was found at the toe of the filter slope, between the stones on the flume floor. The amount is difficult to estimate as the removal of filter stones had affected it at the time it was observed. Both mentioned effects together are expected to add less than 10 cm² to the accretion area.

- The wall effect as explained in section 6.4.4, could have an effect, but it must be very small, because where local scour around stones increases the erosion area slightly, the accretion area is increased as well, because the effect in this area is reverse with local extra sedimentation at the wall.
- The asymmetry that was observed over the width of the flume can have a larger effect. Especially in the accretion area an asymmetry was observed, with a tendency that the accretion area at the back of the flume is larger than at the front-wall. For test 11, this effects even leads to a ratio of erosion/ accretion of 0,33 at the backside of the flume, less than the porosity.

The effects mentioned above partly explain the difference between measured and theoretical erosion/ accretion ratio. As an example, test 11 is looked at for it is the test with the highest ratio. The edge-effect increases the porosity to 0,45. The accretion area can be increased with 20 cm² for the fine fractions that left the filter and with maximum 10 cm² for the other effects, resulting in an accretion area of 343 cm². With the erosion area of 206 cm², this leads to a ratio of 0,60. Still, the accretion area remains about 125 cm² smaller than expected for test 11. The asymmetry does play an important role; measured from the backside of the flume, a ratio of 0,33 is found. As no better information is available, the average between front and back has been taken, resulting in a ratio of 0,47, closer to the 0,45 that it should be. The remaining difference can be due to measurement errors or sand that left the flume with the exiting water.

For the other tests, a similar comparison between front and backside leads to comparing results. For instance, test 4 shows a ratio at the backside of 0,31, a ratio at the front side of 0,56, leading to an average of 0,44, the same as expected with the edge-effect taken into account. Test 5 shows a result of 0,45. Test 6 leads to 0,50, still higher than expected, and test 7 to 0,45. For the other tests, no clear data are available containing the total erosion area at the backside of the flume.

Altogether, for most tests the different possible reasons as mentioned answer the question to where the eroded sand has gone after erosion. Perhaps even more important than the balance between erosion and sedimentation, is the observation that asymmetry and other effects mainly affect the accretion area. The erosion area shows little asymmetry and little disturbances over the tests by various mentioned effects. It is the erosion area that determines the deformation of the structure as a whole and with that the applicability of the filter in a practical situation.

7.3 Comparisons with Uelman's tests

Evert Uelman performed tests with the same model setup in the same wave flume. He used regular waves with a height of 10 cm and a period of 1,2 s for all his test, varying the filter layer thickness and the grain size of the filter layer. His most important results, detailed observations and relations between erosion parameters and the dimensionless filter layer thickness $m = \frac{d_f}{D_{f50}}$, are compared to the results of the present study.

7.3.1 Observations

Uelman has made a similar detailed description of observations as was made for test 10. In his tests, the waves were always the same and regular, so the observations are representative for all his tests and no distinction was made between large and small waves. Remarkable similarities and differences are mentioned here.

Water motion

The same water motion has been observed by Uelman; the wave breaks on the outside of the structure and an internal wave with an amplitude of 1 to 2 cm develops in the filter layer. In Uelman's tests the internal setup is a few cm.

Sand transport types

As in the present tests, two types of sand transport have been observed; bedload and suspended-load transport. The bedload transport is described as a blanket of up to 10 grains thick moving over the slope, the same as the present observations. The suspended-load transport is described as transport of individual grains; where in the present tests a cloud of grains was observed rather than individual grains, which are too small to be followed clearly with the eye. However, the transport mode is the same.

Point to point description of the transport

At point A the cliff-erosion process is described. Uelman observed this in all his tests; in the present tests it was observed clearly for regular waves, steep structure slopes and tests where the height-differences were small; but less clearly or not at all for tests with irregular waves with a significant difference between larger and smaller waves. The waves with different heights also have different run-up heights on the sand slope, smoothing the erosion at point A over a larger area.

At point B, a combination of bedload and suspended-load transport is observed, moving up and down the slope. This is very similar to the present tests. Remarkable is that the share of the total transport being bedload transport increases when the filter layer thickness increases or the filter grain size decreases. In other words, a filter that reduces the wave loading more lets the bedload transport increase relative to the suspended-load transport. In the present tests, the same was observed; smaller waves show only bedload transport and larger waves show suspended-load transport or a combination of both.

At point C the bedload transport is dominant, only when the filter layer is thin or the grains large, suspended-load transport has been observed. This is similar to small waves in the present tests, where bedload transport with a little suspended-load transport is visible. However, two differences are found; in Uelman's tests bedload

transport is described also for up-running waves whereas hardly any bedload transport during wave run-up has been found in the present tests, and in the present tests, large waves do cause a considerable amount of suspended-load transport at point C, especially during rundown. The amount of suspended-load transport at point C seems to be sensitively dependent on the degree of loading.

At point D the observations are similar, again with a larger share of suspended-load transport for the larger waves of the present tests. As described in the observations of test 10, point D is one single point in tests with regular waves while it is spread over a distance of about 10 cm in tests with irregular waves. Uelman found a stable point D defined in a single point in his tests with regular waves, directly below the point on the outside of the filter to where the wave runs down.

At point E, Uelman describes the tendency of the slope to become horizontal during the tests, and a lot of suspended-load transport and sand eventually leaving the filter for high loading situations. The same has been observed in the present tests as well.

At point F, a small amount of transport is described, mainly bedload transport. The same was found in the present tests.

Point G, finally, shows no transport at all in both Uelman's tests and the present tests.

7.3.2 Parameter relations

The parameters that can be compared are the erosion area, –length and –depth, in relation to the dimensionless filter layer thickness, $m = \frac{d_f}{D_{f50}}$, which is 5,8 in all the

present tests. Uelman compared all his tests after 2400 waves, which is different than the 90 minutes after which the present tests are compared. The parameters were recalculated to represent the value after 2400 waves. Comparisons are made for tests 1-3 because they have the same wave parameters as Uelman's tests and test 4 to compare the influence of irregular waves for which holds: $H_s = H_{regular}$ and $T_p = T_{regular}$.

Table 7-3 erosion parameters after 2400 waves for $m = 5,8$

Test number	A_s cm ²	L_r/D_{f50} -	L_{r2} cm	d_s cm
Expected by Uelman	200	20	16	3,4
1	210	20	8,5	3,5
2	190	22	15	2,7
3	195	22	13	2,8
4	67	20	14	1,0

Erosion area

For the present tests, the erosion area for tests 1-3 is 210 cm², 190 cm² and 195 cm² respectively. For test 4 this is 67 cm². For Uelman's tests, the erosion area should be about 200 cm² for $m = 5,8$. For test 1-3, the differences are small, order 5. In test 1, erosion might be more because the sand might have been less densely packed as it was built dry. For test 4, the difference is large, the erosion area being about a third of the erosion area expected from Uelman's results. Test 4 was done with irregular waves, which apparently cannot be compared with regular waves when $H_s = H_{regular}$ and $T_p = T_{regular}$. Figure 7-4 shows a graph of the relation between the total erosion area after 2400 waves and the relative filter layer thickness for Uelman's tests, with the reference tests for regular waves (tests 1-3) and the reference test for irregular waves (test 4) added. Tests 1-3 seem to fit nicely in the results of Uelman; test 4

shows much less erosion. The spreading (deviations from the expected value) of tests 1-3 seems to be in the same order as the spreading of Uelman's tests.

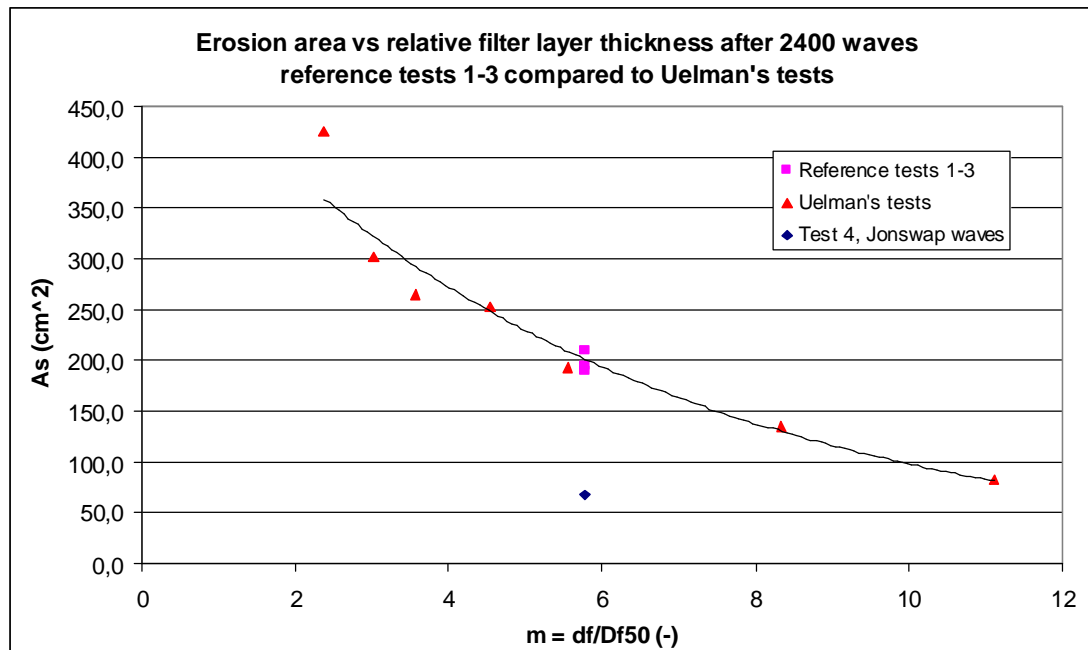


Figure 7-4 comparison of tests 1-4 with Uelman's tests, A_s versus m

Erosion length

The relative erosion lengths L_r and L_{r2} are shown in relations with m by Uelman; with the expectations for $m = 6$ of $L_r/D_{f50} = 20$ and $L_{r2} = 16$ cm. For the present tests, dimensionless erosion length is practically the same with values of 20 and 22, and the relative erosion length 2 is a bit smaller, 13 to 15 cm, with the exception of test 1, for which it is only 8,5 cm. Test 1 shows a different erosion pattern in both erosion area and -length. Only the erosion depth is almost the same as was found by Uelman.

Erosion depth

The erosion depths of the present tests are considerably smaller than Uelman's results, except for test 1. Tests 2 and 3 have an erosion depth 20% smaller than Uelman, and test 4 even 70% smaller. Test 4 was done with irregular waves, and, as mentioned before, cannot be compared with regular wave tests. Tests 2 and 3 give low values compared to Uelman, but still seem to fit reasonably within his results, as the data through which his trend has been plotted have a bandwidth of about 20% as well.

7.3.3 Conclusions of the comparisons

The erosion of tests 2 and 3 fits very well within the results of Uelman's test series, only the erosion depth is a bit less than would be expected. Test 1 gives results that are further away from the expectations and also from tests 2 and 3. The reason is probably that the sand was either less saturated or less densely packed as the structure was built in the dry flume before test 1. The results of test 4 are clearly different, indicating that when using $H_s = H_{regular}$ and $T_p = T_{regular}$, no comparison can be made. The relations found by Uelman are affirmed when the same waves are used, but should be handled with care when different waves are loading the structure.

The observations of Uelman show general consistency with the present tests, with small deviations in mainly the importance of one type of sand transport. The type of transport is strongly dependent on the loading of the sand slope. In general, when the waves are larger in the present tests, or better reduced by the filter in Uelman's tests, the type of transport shifts from mainly suspended-load to mainly bedload. This effect is similar to sediment transport under flow as described e.g. by Van der Graaf³⁷, where bedload transport occurs when the flow-induced bottom shear stress is larger than a certain threshold value and where suspended-load transport is added to this and increasing when the shear stress increases further.

Regular waves lead to a clear sharp edge in the slope at point A (eroding cliff) and to a point D in a single point, whereas irregular waves spread the erosion at point A over a larger area and spread point D over a larger area as well. The difference is due to the fact that the irregular waves of the Jonswap spectrum have varying wave heights and periods, giving them varying run-up and rundown levels. These levels determine the points A and D and if the levels are different for each wave, the specific point is also different for that wave, resulting in a spreading of A and D for a series of waves.

³⁷ Van der Graaf (2005) [15]

7.4 Relations between loading and erosion

In Table 7-1 (copied as Table 7-5) the erosion parameters of all tests are shown, but also different loading parameters can be distinguished. The irregular waves are from the Jonswap spectrum, until now only specified with a significant wave height and peak period, can also be studied by for instance the root mean squared wave height H_{rms} or the mean wave height H_m , or the period by the $T_{m-1,0}$ which is an alternative for the mean period. These values are shown in Table 7-4. Many combinations between loading- and erosion parameters can be made with all these data, the most interesting are shown in the following sections.

Table 7-4 important loading parameters for all tests

Test Number	Parameters Variations	H m	m0 m ²	Hm m	Hrms m	T s	Tm-1,0 s	ξ (-)	regularity reg/irreg.	Duration min	N = Duration / Tp (-)
1	Reference	0,095				1,20		1,62	regular	90	4500
2	Reference 2	0,095				1,20		1,62	regular	120	6000
3	Reference 3	0,096				1,20		1,61	regular	180	9000
4	Irregular waves	0,090	0,00051	0,057	0,064	1,20	1,13	1,66	irreg-jonswap	180	9000
5	Varying H	0,071	0,00032	0,045	0,051	1,10	1,02	1,72	irreg-jonswap	600	32727
6	and N	0,110	0,00075	0,069	0,078	1,32	1,23	1,66	irreg-jonswap	90	4091
7		0,130	0,00105	0,081	0,092	1,39	1,23	1,60	irreg-jonswap	90	3885
8	Varying ξ by varying T	0,081	0,00041	0,051	0,057	1,02	0,99	1,49	irreg-jonswap	90	5294
9		0,096	0,00058	0,060	0,068	1,47	1,38	1,97	irreg-jonswap	90	3673
10		0,097	0,00059	0,061	0,069	1,96	1,84	2,62	irreg-jonswap	90	2755
11	Swell waves	0,051	0,00032	0,045	0,051	3,00	3,00	5,52	regular	90	1800
12	Grading variation	0,090	0,00051	0,056	0,064	1,23	1,14	1,71	irreg-jonswap	120	5854
13	Varying H	0,044	0,00012	0,027	0,031	0,84	0,82	1,65	irreg-jonswap	420	30000
14	Varying H	0,148	0,00136	0,092	0,104	1,48	1,42	1,59	irreg-jonswap	90	3649
15	Swell waves low	0,030				2,00		4,76	regular	240	7200
16	tan alpha	0,090	0,0005	0,056	0,064	1,23	1,14	1,28	irreg-jonswap	180	8780
17	variation	0,090	0,00051	0,056	0,064	1,23	1,14	2,56	irreg-jonswap	90	4390

Table 7-5 copy of the erosion parameters

Test Number	Parameters Variations	H m	T s	ξ (-)	Erosion area 90 min cm ²	La 90 min cm	Lr 90min cm	Lr2 90min cm	ds 90min cm
1	Reference	0,095	1,20	1,62	247,65	64,10	59,09	5,01	3,51
2	Reference 2	0,095	1,20	1,62	231,97	75,24	60,45	14,79	3,08
3	Reference 3	0,096	1,20	1,61	279,73	73,80	60,64	13,17	3,79
4	Irregular waves	0,090	1,20	1,66	96,10	65,17	55,36	9,81	1,47
5	Varying H	0,071	1,10	1,72	52,03	67,30	48,19	19,11	0,77
6	and N	0,110	1,32	1,66	159,50	68,21	55,58	12,63	2,34
7		0,130	1,39	1,60	257,22	87,87	66,02	21,86	2,93
8	Varying ξ by varying T	0,081	1,02	1,49	56,09	61,27	53,59	7,67	0,92
9		0,096	1,47	1,97	133,26	71,44	53,45	17,99	1,87
10		0,097	1,96	2,62	194,73	76,72	58,85	17,87	2,54
11	Swell waves	0,051	3,00	5,52	206,97	73,39	56,11	17,29	2,82
12	Grading variation	0,090	1,23	1,71	94,56	64,92	55,89	9,03	1,46
13	Varying H	0,044	0,84	1,65	-2,52	0,00	0,00	0,00	0,00
14	Varying H	0,148	1,48	1,59	293,05	93,20	71,25	21,95	3,14
15	Swell waves low	0,030	2,00	4,76	35,70	72,20	53,48	18,72	0,49
16	tan alpha	0,090	1,23	1,28	56,11	80,49	72,14	8,35	0,70
17	variation	0,090	1,23	2,56	184,85	48,07	38,98	9,08	3,85

7.4.1 Erosion growth as a function of the number of waves

During the tests, the erosion area grows. Observations show that the growth-rate decreases during the tests, but without reaching an equilibrium state. Figure 7-5 shows the erosion area growth as a function of time for all the tests. Two parameters are interesting for the growth: time and number of waves. The difference between the two is the wave period. An advantage of using the number of waves is that it is a dimensionless parameter that is preserved in the scaling procedures. To represent a design storm, usually a storm of e.g. 1000 or 2400 waves is used, applying the number of waves. Often the square root of the number of waves, \sqrt{N} is an important measure for erosion processes. The erosion growth curves seem to resemble a square root

function as well, and to come to a representative relation the erosion growth is investigated as a function of \sqrt{N} .

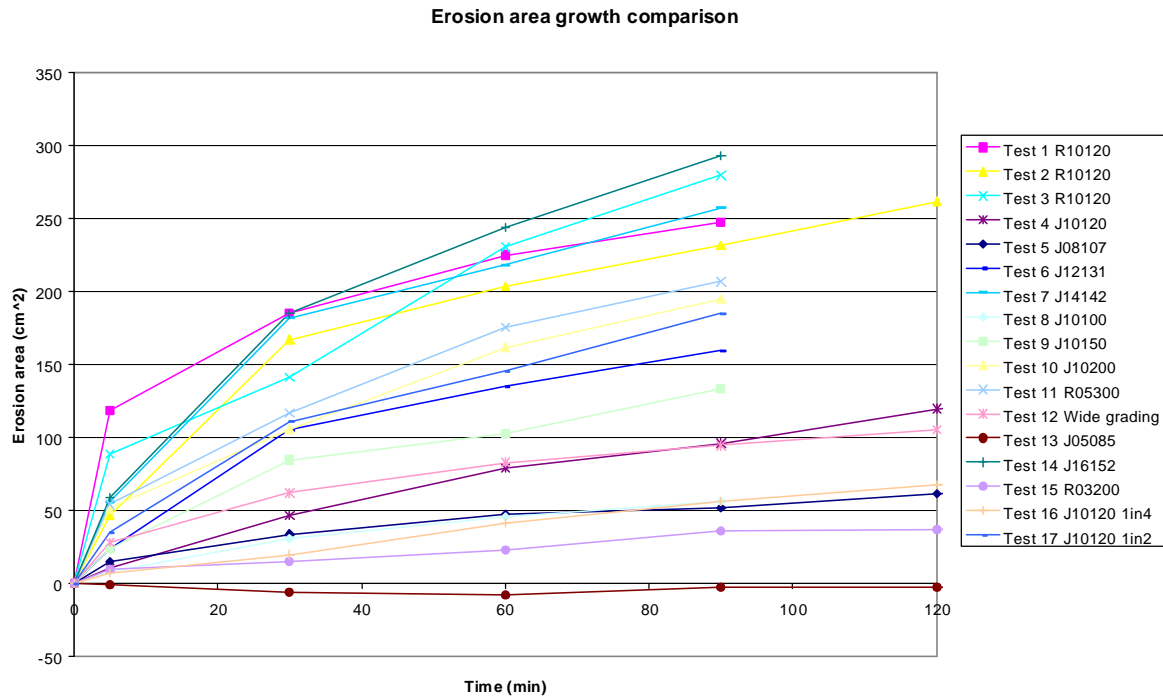


Figure 7-5 erosion area growth in time during the tests

Erosion growth related to \sqrt{N}

The erosion growth decreases as time progresses during a test, and a good fit has been found between the erosion growth and \sqrt{N} . For all tests, the relation is linear, starting from the origin. In other words, the erosion area is a constant factor times \sqrt{N} for all tests. This factor is constant within the test, but changes for the different tests. Two erosion growth curves are shown to illustrate the relation, for test 4 with a reasonable fit and for test 10 with a very good fit. The other tests show comparing results.

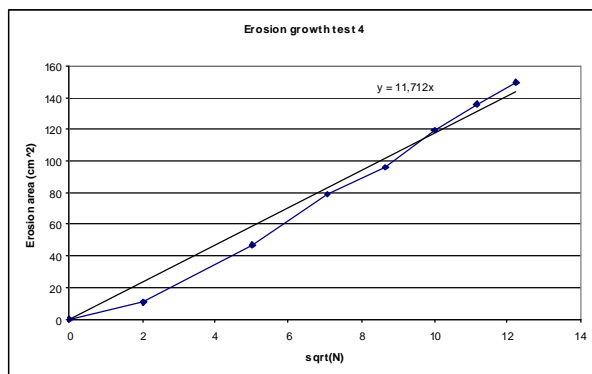


Figure 7-6 A_s vs \sqrt{N} of test 4

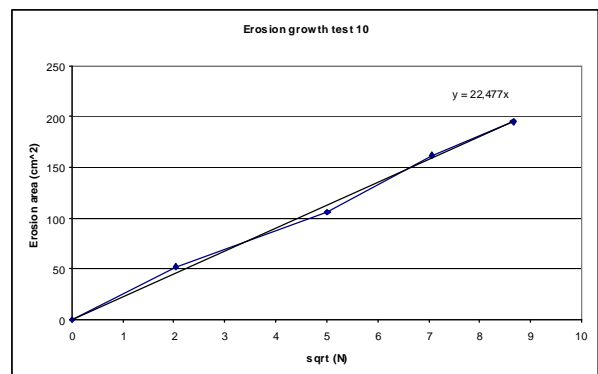


Figure 7-7 A_s vs \sqrt{N} of test 10

The results indicate that: $A_s \propto \sqrt{N}$, with a constant factor that is different for each test. No straightforward function for this factor has been found.

7.4.2 Erosion area relations

The erosion area is of first interest as it is the first parameter to be calculated and an important measure for erosion. It represents the total amount of core material that has been moved from its original place. As a first study to see what kind of relations might be interesting, the erosion area is plotted versus the significant wave height (regular wave height for the tests with regular waves).

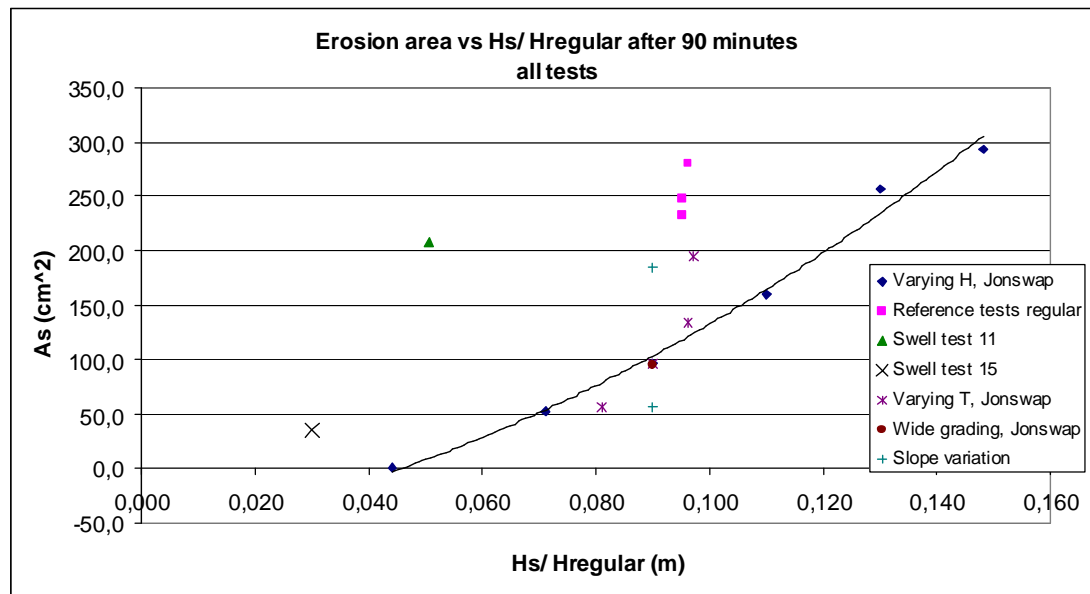


Figure 7-8 erosion area versus significant wave height for wave height variation tests

Wave height relations

In Figure 7-8 all the tests are included. The most important tests to evaluate on the wave height are naturally the wave height variation tests (tests 4 to 7, 13 and 14) and the reference tests 1 to 3 to see the difference in erosion between regular and irregular waves. The wave height variation tests clearly show a relation with increasing erosion for increasing wave height. This relation does not seem to be linear but rather a second order function with a threshold value for the wave height. In other words, for the wave height variation tests with irregular waves, $A_s \propto H_s^2$ for $H_s \geq H_{threshold}$. The trendline in the figure shows the relation, in which the tests with regular waves do not fit.

Test 12 (wide grading) was added to Figure 7-8 to show that the wide grading does not influence the erosion; the datapoint overlaps with test 4. Tests 11 and 15 (swell waves) were added to show that relatively low waves ($H = 5$ or even $3,0$ cm) can give a lot of erosion when the period is very large ($2,0$ to $3,0$ s). The swell waves do not fit the other results in a wave height comparison, indicating that the wave height is not the only important parameter in the processes. The period variation tests and the slope steepness variation tests are included to show that the results are consistent with the other tests; the data points surround the trendline of the wave height variation tests. It is evident that the results do not fit this trend because the wave height has been kept constant for all these tests. The results show that other parameters like wave period and slope steepness do change the amount of erosion in a test.

Using the root-mean-squared wave height H_{rms}

The erosion area seems to be related to the square root of the wave height. This indicates that the underlying processes rely on the wave height in a second order relation. The complexity of the processes prevents a simple explanation of this relation, however, considering the found relation the second order dependence can be assumed. The expectations of section 5.2 assume a third order relation between wave height and erosion area, based on the known relations for armour stability. The stability of armour stones depends on the direct forces from the breaking waves, dominated by turbulent processes. Test observations indicate that for these tests, the porous flow is the dominant forcing mechanism rather than turbulence induced by the wave-breaking (see also section 7.6). Flow processes usually have a lower order of dependence on the wave height than turbulence processes. Considering this, the found squared relation seems more relevant than the a-priori expected higher order relation.

Since a squared relation with the wave height seems to hold for the irregular wave tests, the root-mean-squared wave height H_{rms} can be more interesting than the H_s , because it is related to square values of the wave heights as well. H_{rms} is the root of the average of the individually squared wave heights. In general, in relations between regular and irregular waves, H_m (mean) is important for linear processes, H_{rms} is important for squared-related processes and H_s is important for higher order processes. Therefore H_{rms} is expected to be a better representative. The erosion area is plot versus H_{rms} to see if this assumption is valid for the wave height variation tests.

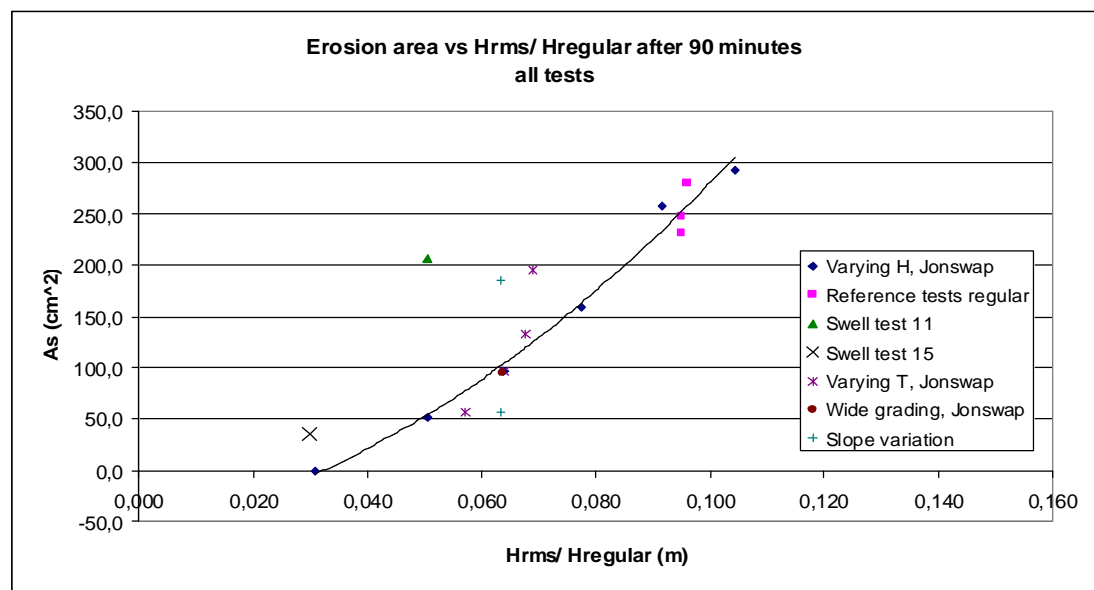


Figure 7-9 erosion area versus root mean squared wave height

Figure 7-9 shows the relation with H_{rms} . Indeed the comparison with regular waves looks promising, the second order polynomial trendline touches the point of test 1 and tests 2 and 3 are surrounding it closely. Again a second order relation gives the best result. The values of H_{rms} are lower than the values of H_s of the same tests. Tests other than the wave height variation tests do not fit the relation, although they seem to lie closer to it than in the relation with significant wave height. The tests for which the relation holds have in common that the Irribarren parameter ζ is the same, where it is different in the other tests. The result indicates that:

$$A_s \propto H_{rms}^2 \text{ for } H_{rms} \geq H_{threshold}, \text{ and } \zeta = const.$$

To see the influence of other parameters and to find relations for the not-fitting tests, relations with the wave period and slope steepness are investigated next.

Wave period relations

For the wave period, first the peak period has been used to study the relations. Tests 4, 8, 9 and 10 have been done within the wave period variation test series, and the results are plotted in Figure 7-10 together with the results of the other tests. The line is a linear trendline through the data of the wave period variation tests.

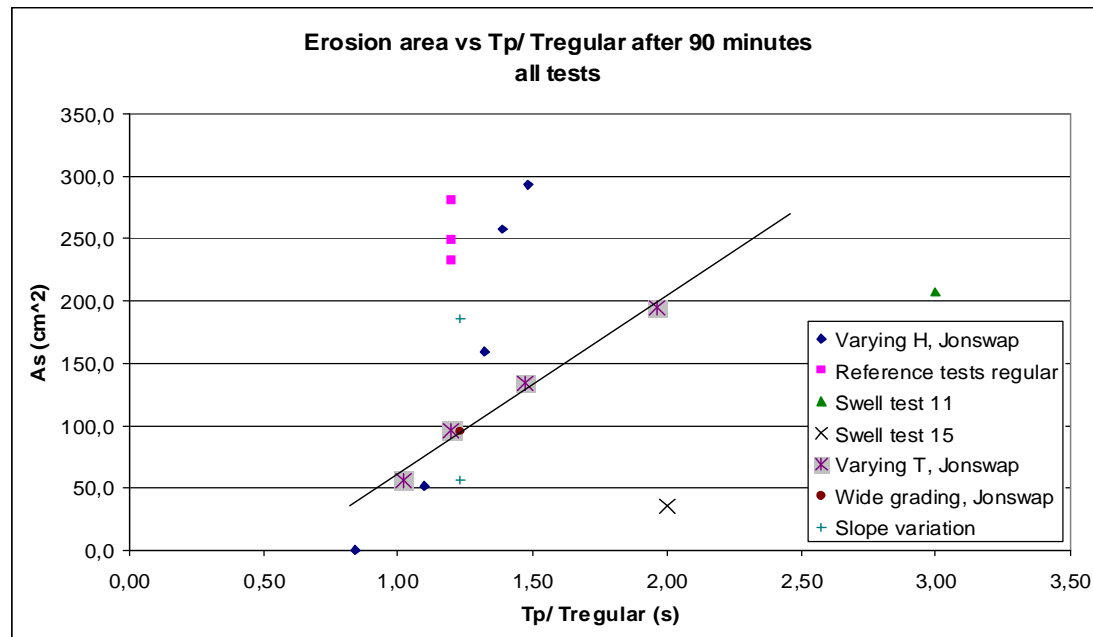


Figure 7-10 erosion area versus peak period of the wave period variation tests

The linear trendline is added to the results since the points seem to be linearly related. It should be noted that the lowest point, test 8, had a too low wave height in the tests. In the period variation series, the wave height was kept constant at 10 cm. For test 8, the resulting waves were relatively steep and the wave machine had difficulty generating them, resulting in a H_s of only 8,1 cm where the other tests had a H_s of 9,0 to 9,7 cm. If the wave height of test 8 would have been the same as for the other tests, the erosion area is expected to be about 30 to 40 % higher based on the relations found for wave height variations. This would put the result of test 8 close to the linear line, or just above it. The other test series clearly show no coherence to the linear relation. As expected, the wave period is not the only interesting parameter. Nevertheless, it can be seen that an increasing wave period increases the erosion area as well. This holds for the T -variation tests, the H -variation tests as well as the swell tests. A linear trend is visible for tests with the same wave height:

$$A_s \propto T_p \text{ for } H = \text{const.}$$

Using $T_{m-1,0}$ instead of T_p

With the wave height relations, H_{rms} appeared to be a better parameter than H_s . For the wave period, an alternative exists as well, the $T_{m-1,0}$. This period is an alternative for the mean period and is especially interesting for double peaked spectra or other complex spectra, as it is not dependent on the peak of the spectrum. In the executed tests, only single peaked spectra have been used, nevertheless it is interesting to see

the influence of the alternative wave height on for instance the comparison between regular and irregular waves. Figure 7-11 shows the resulting relation.

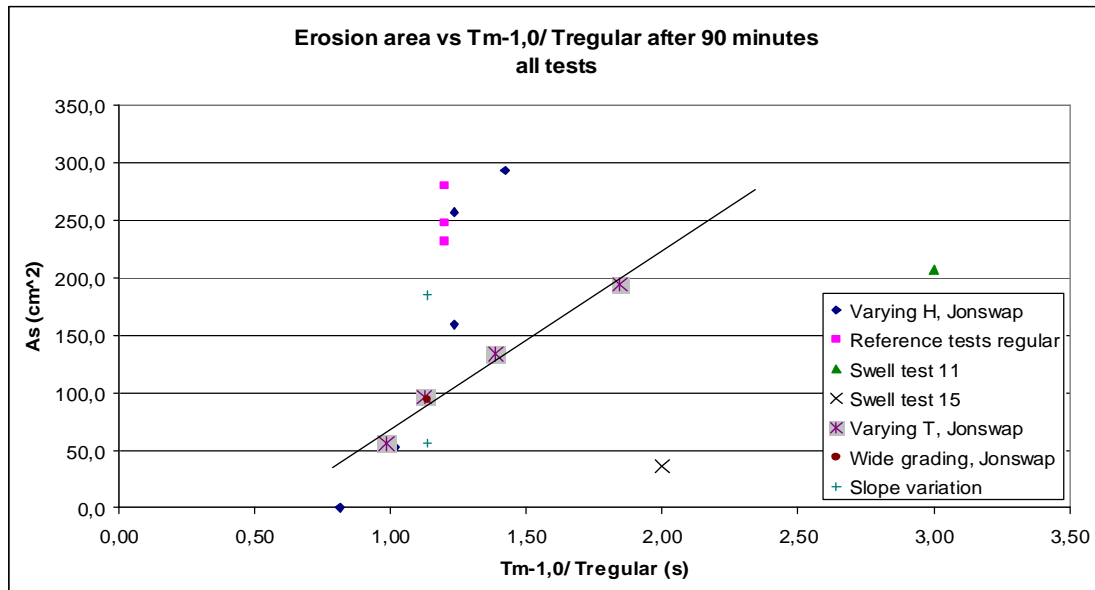


Figure 7-11 erosion area versus $T_{m-1,0}$

The results do not differ much from the relations with the peak period; regular wave tests do not fit the relation, the relation itself does not look different, only the values of the wave period have changed a bit. Based on this figure and the lack of a theoretical reasoning to use another period than the peak period, no reason has been found to do so. The peak period will still be used.

Slope steepness relations

Figure 7-12 shows the relation between the erosion area and the slope steepness. Only the tests of the slope steepness variation series are included (tests 4, 16 and 17) because the other tests all have a slope of 1:3 and hence cannot show a sound relation. The points are in line in the figure; the relation is almost perfectly linear.

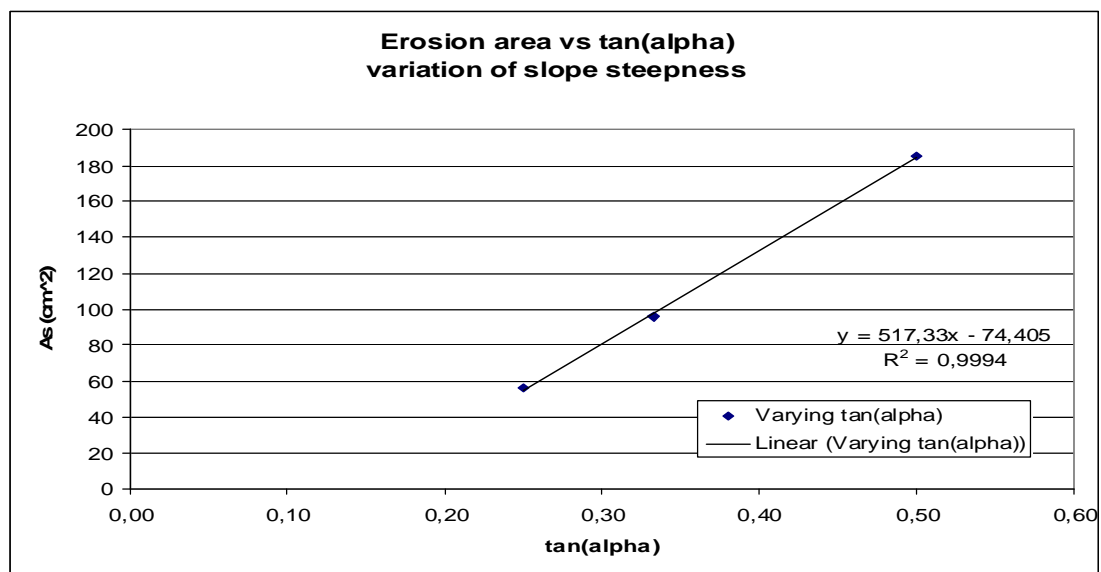


Figure 7-12 erosion area versus $\tan\alpha$ for only the slope steepness variation tests

There are a number of reasons for increasing erosion with increasing slope steepness:

- The type of wave breaking is affected and the energy of the breaking wave is dissipated over a shorter distance on a steeper slope. The first reason, the breaker type, probably has little influence as all three tests have values of ζ within the plunging breaker area, be it that 2,56 of the steepest slope is close to the collapsing breaker area.
- The second reason, the shorter dissipation distance, is expected to have some influence, especially on the erosion length and –depth, but actually not on the erosion area. The waves dissipate their energy over a longer distance, which would logically let the erosion length increase and the erosion depth decrease, but let the erosion area (the product of the other two) be about the same in size.
- Observation of the movies of the tests showed a probable third reason for increasing erosion with increasing steepness: the horizontal component of the filter layer thickness is much smaller for a 1:2 slope than for a 1:4 slope. This horizontal layer thickness is thought to be very important since the waves travel horizontally through the filter layer. The wave amplitude is damped in horizontal direction as well; therefore the internal wave amplitude in the 1:4 test is much smaller than in the 1:2 test. The horizontal layer thickness is 34 cm for the 1:2 test, 47 cm for the 1:3 test and 62 cm for the 1:4 test. This varies a factor 1,8, whereas the erosion area varies a factor 3,3 for the same tests. The horizontal filter layer thickness is expectedly important, but will not be the only reason for the large variation in erosion area.
- A fourth reason is the fact that sand on a steep slope has less resistance against sliding down than sand on a milder slope. Gravity helps the downward directed transport more effectively as the slope gets steeper.

Altogether, four reasons have been found of which the horizontal filter layer thickness and the gravity-effect on grains on a steep slope are thought to be the most important. However, the question why the relation is in fact linear cannot be answered by this information. Result: $A_s \propto \tan \alpha$, for $H = const.$, and $T = const.$

Relations after 2400 waves instead of 90 minutes

The wave periods are not the same for the different tests, so there is a difference between the erosion after a fixed time span and the erosion after a certain number of waves. To study this difference, the wave height variation tests are plotted versus H_{rms} , and the period variation tests versus T_p , after 2400 waves. Figure 7-13 shows the wave height relation and Figure 7-14 the wave period relation. The graphs are very similar to Figure 7-9 and Figure 7-10, which show the same relations after 90 minutes. The absolute values are different, but a squared relation with a threshold value for the wave height variations and a linear relation for the wave period variations are found here as well. No structural differences have been found between the relations after 90 minutes or after 2400 waves.

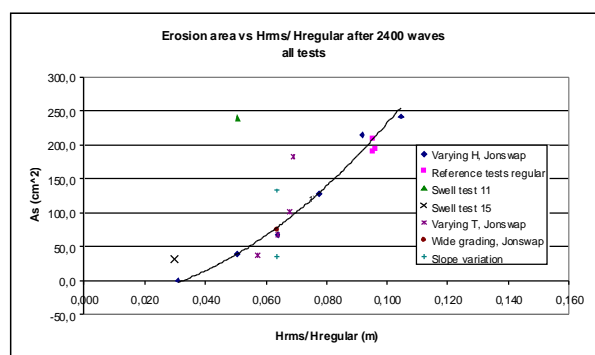


Figure 7-13 A_s vs H_{rms} after 2400 waves

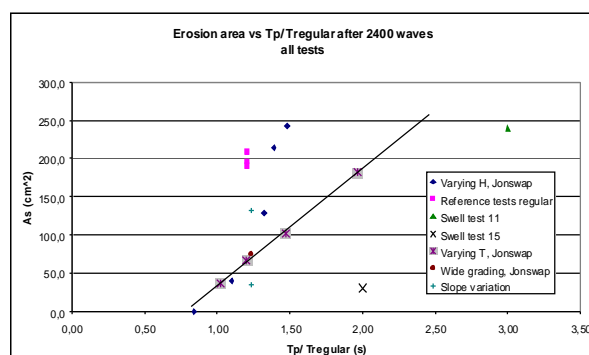


Figure 7-14 A_s vs T_p after 2400 waves

7.4.3 Erosion length and –depth relations

The erosion length, the horizontal distance between point A and point D on the slope, gives information about the spreading of the erosion over the slope. In the test results, indications were found that points A and D are related to the run-up and rundown locations of the waves. The erosion depth, the average thickness of the erosion area, is defined as the ratio of the erosion area and the absolute erosion length. It gives information about the spreading of the erosion as well and is especially interesting as an indicator of how much the filter layer might settle due to the erosion, for purposes of maintenance of the structure. Relations between these parameters and the loading parameters are studied in this section.

Absolute erosion length in relation to the wave height

The absolute (total) erosion length is the horizontal distance between points A and D as defined in the observations. From the observations it was concluded that point A is related to the internal run-up height of the higher waves and that point D is related to the external rundown level of the higher waves, probably about H_s . Considering these observations, the significant wave height is expected to be more interesting than the root-mean-squared wave height. Both are shown in Figure 7-15 and Figure 7-16. Both relations show a relatively small variation in erosion length for the relatively large variation in wave heights. No single relation can be drawn through either of the figures data collections. In general, a higher wave height seems to induce a larger erosion length. For the wave height variation tests, this trend is clearest; the wave period variation fits this trend quite well.

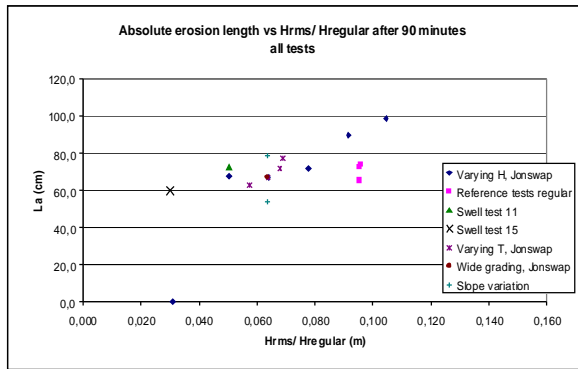


Figure 7-15 Absolute erosion length vs H_{rms}

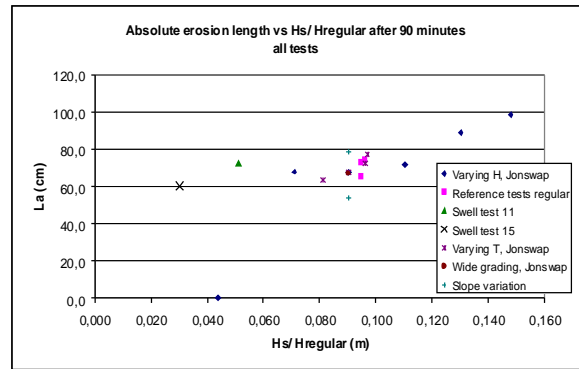


Figure 7-16 Absolute erosion length vs H_s

The main difference between the relations with H_{rms} and H_s is the comparison between regular and irregular wave tests. When H_{rms} is used, tests 1-3 are outside all the other data ranges. When H_s is used however, the points of tests 1-3 are in the middle of the range of the wave height variation tests, with whom they are to be compared. The points are close to test 4, which has the same H_s as the $H_{regular}$ of the regular wave tests. As was expected, the significant wave height is an important measure for the erosion length. The large variation in the other test series (especially in the swell tests) indicates that there is no generally valid relation between L_a and H . The result of this analysis: H_s is an important measure for the absolute erosion length.

Relative erosion lengths L_r and L_{r2} in relation to the wave height

The relative erosion length L_r is the horizontal distance from B to D, from the intersection of the sand slope with the mean water level to the lowest point of the erosion area. The observations suggest that the external rundown level of the waves determines the point low on the slope. Figure 7-17 shows the relation between the relative erosion length and the significant wave height. H_s is preferred here and with the relative erosion length 2 for the same reason as with the absolute erosion length; a better comparison between regular and irregular wave tests. Figure 7-17 shows a result similar to Figure 7-16; no clear relation, only a larger length for higher waves.

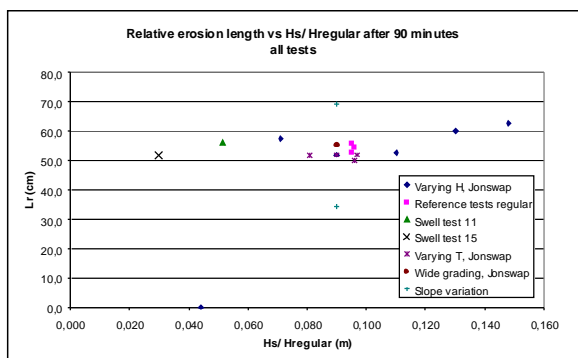


Figure 7-17 Relative erosion length vs H_s

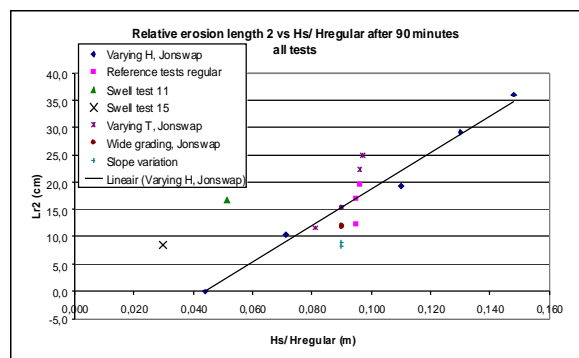


Figure 7-18 Relative erosion length 2 vs H_s

Figure 7-18 shows a different image. The relative erosion length 2 L_{r2} , the horizontal distance between points A and B or in other words the length of the erosion area above the mean water level, is shown versus H_s . Not one single relation for all the tests can be found, nevertheless a clear linear relation can be found for the wave height variation tests. The plotted line is a linear trend through the points of the wave height variation tests with irregular waves. This line also crosses tests 1-3, indicating

that again the significant wave height is important for the comparison of regular and irregular wave tests. Like in the comparison between erosion area and wave height, a threshold value is found here and the tests have a constant ξ in common. Result:

$$L_{r2} \propto H_s \text{ for } : H_s \geq H_{\text{threshold}}, \text{ and } : \xi = \text{const.}$$

Erosion length in relation to the wave period

Relations between the different erosion length parameters and the wave period give no extra interesting information. A large spreading is visible; only reasonable linear relations for only the wave period variation tests can be found. The graphs are not shown here.

Erosion depth in relation to the wave height and period

The erosion depth is defined as the erosion area divided by the absolute erosion length. As was found earlier in the analysis, the erosion area depends on the root-mean-squared wave height, while the erosion length depends on the significant wave height. For the erosion depth, both are expected to be important, with the largest influence of the erosion area and thus the root-mean-squared wave height. Both have been tried but only the relation with H_{rms} has been plot in Figure 7-19 to prevent a total overload of graphs in this analysis. Result:

$$d_s \propto H_{rms} \text{ for } : H_{rms} \geq H_{\text{threshold}}, \text{ and } : \xi = \text{const.}$$

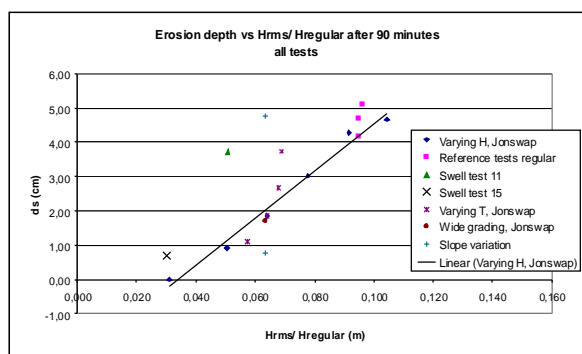


Figure 7-19 Erosion depth vs H_{rms}

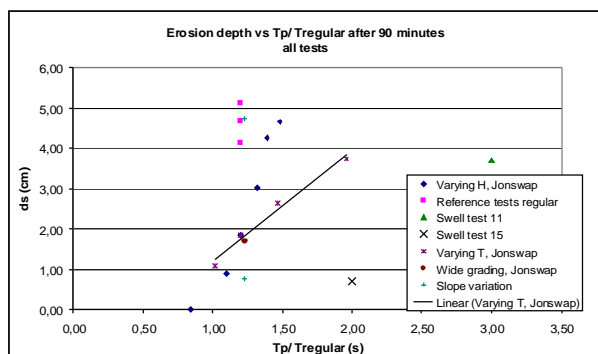


Figure 7-20 Erosion depth vs T_p

Figure 7-20 shows the relation with the wave period. A linear relation between the erosion depth of the wave period variation tests and the peak period is visible, although the other tests do not match this relation. No match between regular and irregular wave tests was found. The wave period is important for the erosion depth, but not the determining parameter. Using $T_{m-1,0}$ instead of T_p does not make a significant difference.

Variation in erosion length and –depth

The analysis of erosion length and –depth relations shows that the variation in values of the erosion length is only small compared to the erosion depth or –area. To illustrate this, Figure 7-21 shows the relation between the erosion area and the erosion depth. A linear correlation is relatively strong, with an outlier on the right below the line, from test 17 with the steep slope of 1:2, which leads to an extra large erosion depth. The figure illustrates that the spreading in erosion length is small; the erosion length is the erosion area divided by the –depth, and therefore the direction of the line through the origin and the respective data point in the figure. The points are almost aligned, indicating that the values of the erosion length vary only very little.

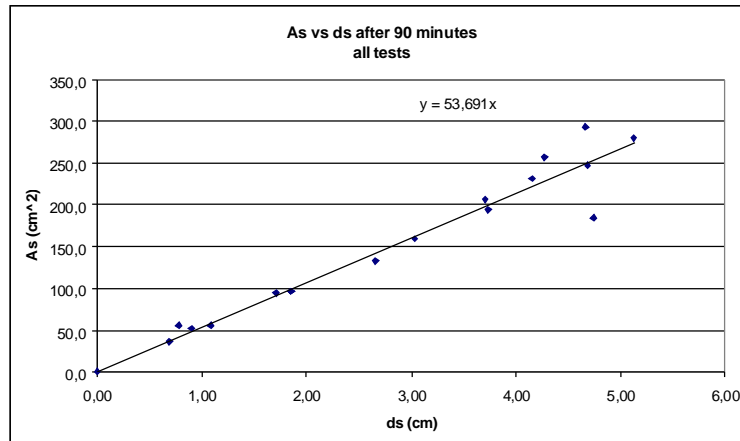


Figure 7-21 Erosion area versus erosion depth after 90 minutes

Wave run-up and –down related to the erosion length

The observations of chapter 6 indicate that the erosion length is determined by the wave run-up and rundown levels. To investigate this, the run-up and –down level of the waves have been calculated using the common formulae as presented in Schiereck³⁸. In the table the values are presented.

Table 7-6 wave run-up and rundown parameters

Test Number	Parameters Variations	H m	ξ (-)	regularity reg/irreg.	La 90min cm	Lr 90min cm	Lr2 90min cm	ds 90min cm	ds 90 visual cm	run-up m	rundown m	run-up+down m
1	Reference	0,095	1,62	regular	65,3	52,9	12,4	3,79	5	0,12	-0,02	0,14
2	Reference 2	0,095	1,62	regular	72,9	55,8	17,1	3,18	6	0,12	-0,02	0,14
3	Reference 3	0,096	1,61	regular	74,1	54,6	19,5	3,78	5	0,12	-0,02	0,14
4	Irregular waves	0,090	1,66	irreg-jonswap	67,4	52,0	15,4	1,43	4,5	0,14	-0,05	0,19
5	Varying H	0,071	1,72	irreg-jonswap	67,8	57,4	10,4	0,77	2,5	0,12	-0,04	0,16
6	Varying H and N	0,110	1,66	irreg-jonswap	71,8	52,6	19,2	2,22	4	0,18	-0,06	0,24
7		0,130	1,60	irreg-jonswap	89,4	60,2	29,2	2,88	5,5	0,20	-0,07	0,27
8	Varying ξ by varying T	0,081	1,49	irreg-jonswap	63,3	51,7	11,6	0,89	2,5	0,12	-0,04	0,16
9		0,096	1,97	irreg-jonswap	72,4	50,1	22,3	1,84	3,5	0,18	-0,06	0,25
10		0,097	2,62	irreg-jonswap	77,1	52,1	25,0	2,53	4	0,24	-0,08	0,33
11	Swell waves	0,051	5,52	regular	72,6	55,9	16,7	2,85	4,5	0,10	-0,08	0,18
12	Grading variation	0,090	1,71	irreg-jonswap	67,2	55,2	12,0	1,41	3,5	0,15	-0,05	0,20
13	Varying H	0,044	1,65	irreg-jonswap	0,0	0,0	0,0	0,00	0	0,07	-0,02	0,09
14	Varying H	0,148	1,59	irreg-jonswap	98,9	62,8	36,1	2,96	6	0,23	-0,08	0,30
15	Swell waves low	0,030	4,76	regular	60,1	51,6	8,5	0,59	1	0,06	-0,05	0,10
16	tan alpha	0,090	1,28	irreg-jonswap	78,7	69,1	8,4	0,71	2,5	0,11	-0,04	0,15
17	variation	0,090	2,56	irreg-jonswap	54,1	34,2	9,1	3,42	6	0,16	-0,08	0,24

A relation between the run-up level and the relative erosion length L_{r2} and between the rundown level and the relative erosion length are expected. The run-up and –down levels are vertical distances and the erosion lengths are horizontal distances, so the slope and the filter thickness determine the difference between the parameters. Besides, the external run-up has been calculated, whereas point A depends on the internal run-up level. No calculation method is available to calculate the internal run-up in a good way, but internal and external levels must be related, so the external level must be related to point A as well. The relations are shown in Figure 7-22 and Figure 7-23 respectively.

The relation between the run-up and L_{r2} shows a general trend with increasing L_{r2} for increasing run-up, with a linear relation for the wave height variation tests. The

³⁸ Schiereck (2001), [42]

reference tests 1-3 lie slightly above the line and especially tests with high values of ξ are outliers (swell tests and test 10). Logically, test 17 with the steep slope does not fit because the slope influences the relation as stated above. Test 16 with the mild slope does fit, probably by coincidence. Result:

$$L_{r2} \propto \text{Run-up}, \text{ for } : \text{Run-up} \geq \text{Run-up}_{\text{threshold}}, \text{ and } : \xi = \text{const.}$$

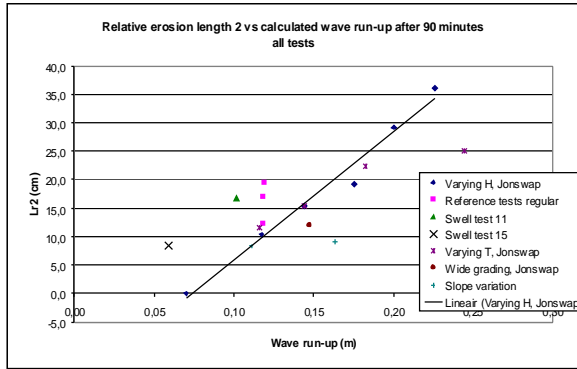


Figure 7-22 L_{r2} vs wave run-up

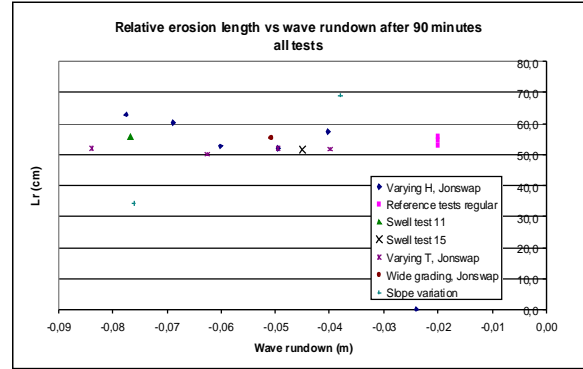


Figure 7-23 L_r vs wave rundown

The relation between the rundown and L_r shows no relation, as the values of L_r are almost constant showing little variance over the tests. Furthermore, the calculation of the rundown level is not very straightforward. For the run-up level, a lot of research has been done, resulting in good empirical formulae with reduction factors for e.g. rubble mound slopes as used in the tests. However, for the rundown, only a formula for smooth slopes has been found. The rubble mound filter layer does influence the rundown level significantly, as the back-flowing water flows through and does not hinder the new up-running wave as much as back-flow over a smooth slope. Better estimates of the rundown level of waves on rubble mound slopes could help the understanding of the erosion length development. This will be treated in the recommendations for further research.

A comparable relation for the absolute erosion length was studied but is not shown here for it resembles Figure 7-23 closely, with a higher average value of the erosion length. $L_a = L_r + L_{r2}$. Values of L_r are much larger than those of L_{r2} , so the spreading of the latter has a relatively small influence on the total spreading.

7.5 Existing open filter design criteria and Shields

In the test results, a threshold value of the loading has been found below which no erosion occurs. This threshold is expectedly the critical loading for a geometrically open filter that is still hydraulically sand-tight. Shields³⁹ developed a method for determining a critical velocity above which sand grains start to be transported by the flow. The pores of the hydraulically sand-open filter are so large that this Shields criterion for open channel flow is expected to apply. Based on the same assumption and experimental research, geometrically open (yet hydraulically sand-tight) filter design criteria have been developed in the 1990's. The findings are compared to the found threshold of motion in the performed tests.

7.5.1 Comparison to open filter design formulae

Design formulae for geometrically open filters do exist, but not for hydraulically sand-open filters. The existing formulae are based on the threshold of motion; the gradient in the filter should not exceed a critical value above which core material starts to be moved. Klein-Breteler⁴⁰ constructed a practical graph for the design (Figure 7-24) and De Grauw⁴¹ presents a graph with comparisons between calculated results from De Grauw and measurements (Figure 7-25).

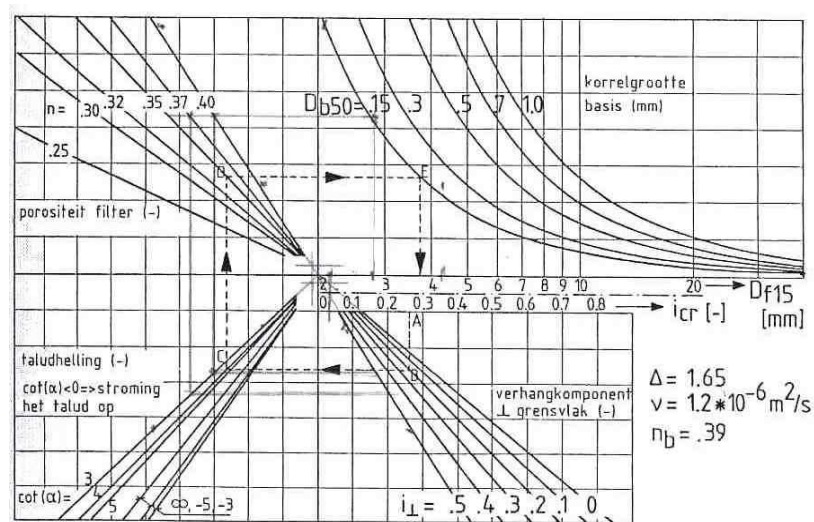


Figure 7-24 Open filter design criteria by Klein Breteler

In the graph of Klein-Breteler the critical parallel hydraulic gradient is found from the filter grain size or vice versa, following the dashed lines with arrows. The grain size of the bed material, the porosity of the filter, the slope steepness and the perpendicular gradient are asked as input.

³⁹ Schiereck (2001) [42]

⁴⁰ Klein Breteler et al. (1990) [31]

⁴¹ De Grauw et al. (1984) [16]

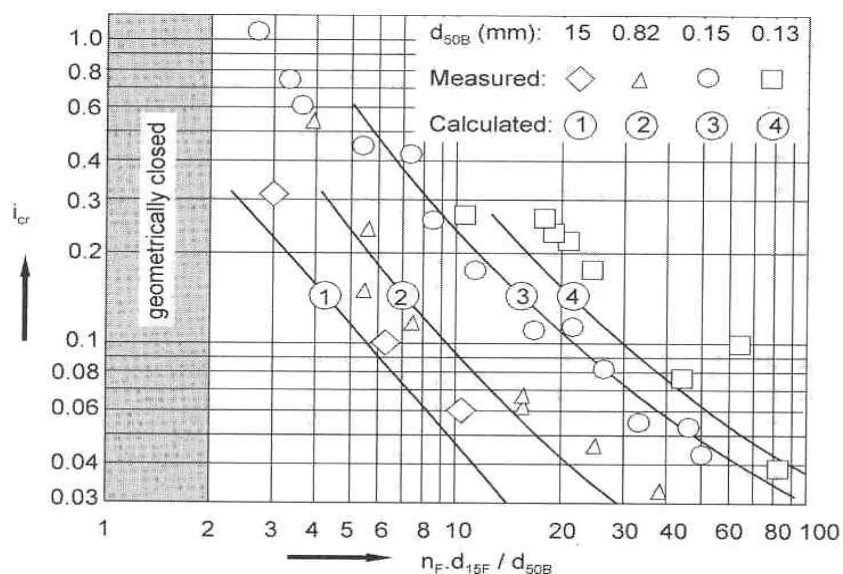


Figure 7-25 Open filter design by De Grauw

Both use the D_{f15} , d_f , D_{b50} and Klein-Breteler also $I_{perpendicular}$ and $\cot(\alpha)$ as input, resulting in the critical gradient I_{cr} . The input of the used materials from the model tests leads to a I_{cr} of 0,03 according to Klein-Breteler and 0,048 according to De Grauw. A comparison with the present tests can be made. Test 13 showed no erosion, only some movement for the highest waves in the spectrum, therefore the occurring gradient should be in the order of the critical gradient as calculated. No measurements are available, but visual observations show that the maximum internal setup (setup of the mean water level) is about 1 cm, the run-down of the wave over the filter slope about 1 cm, and the horizontal distance between these points 47 cm. The gradient resulting from this is $2/47 = 0,042$, which is well in-between the calculated points.

The formula by De Grauw, $I_{cr} = \left(\frac{0.06}{n_f^3 D_{f15}^{4/3}} + \frac{n_f^{5/3} D_f^{1/3}}{1000 D_{b50}^{5/3}} \right) U_{*cr}^2$, can be used to

calculate the critical gradient, and gives the same result of $I_{cr} = 0,042$ as the measured gradient in test 13. This is a confirmation of the idea that a threshold of motion is present in the breakwater setup with hydraulically sand-open filter. As a threshold value, the critical value of the existing design criteria for geometrically open filters can be used.

A note should be made: the estimated gradient from the test is not the parallel gradient, but has an angle of about 15 degrees with the parallel interface between filter and core. The real parallel gradient cannot be observed as no movement of sand is visible. The difference is expected to be small.

Tests with a little higher erosion, tests 5 (Jonswap $H_s = 8$ cm and $T_p = 1,07$ s) and 15 (Regular $H = 3$ cm, $T = 2,0$ s), do have a higher occurring gradient, about 0,09 from visual observations. The amount of erosion for these tests is limited, the smallest of all the tests apart from test 13. Dependency of the amount of erosion by the magnitude of the occurring hydraulic parallel gradient is expected after these observations.

7.5.2 Comparison to the Shields criterion

The Shields criterion⁴² gives a value of the critical flow at the threshold of motion of bed material. The used relations are the general Shields formula:

$$\Psi_c = \frac{\tau_c}{(\rho_s - \rho_w)gd} = \frac{u_*^2}{\Delta gd} \quad \text{and the applied formula: } d_{n50} = \frac{u_c^2}{\Psi_c \Delta C^2}$$

Ψ_c is a function of the particle Reynolds number Re_* as shown in Figure 7-26.

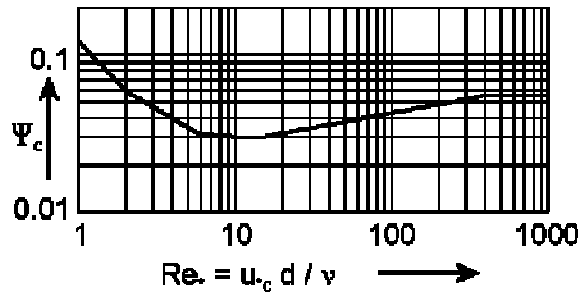


Figure 7-26 Critical Shields parameter as function of Re_*

For the used sand on a 1:3 slope, the critical shear velocity $u_{*c} = 0,013$ m/s, and the critical average velocity in the filter is $u_c = 0,12$ m/s, with as hydraulic radius $R = n_f * D_{f15} = 0,011$ m. To compare this with the occurring flow velocities in the tests, the movies of test 13 have been observed. Test 13 only showed some sand movement for its highest waves, in other words it should be around the threshold of motion as meant by Shields. Flow velocities in the filter could not be measured; therefore an estimate is made using the amplitude of the internal wave. The height of the internal wave is about 1,5 cm for the higher waves of the test, which means with a sine-wave approach the water level runs up and down with a maximum velocity of 0,055 m/s, so the occurring filter velocity is lower than the Shields criterion suggests. However, the average velocity through the filter is lower than the velocity in the pores, which is acting on the sand grains. The average pore-velocity can be estimated by dividing the average filter velocity with the porosity: $U_{pore,max} = U_{f,max}/n_f = 0,13$ m/s, in fact very close to the found Shields velocity. The visual estimate is not very precise; nevertheless the outcome is quite good. The design rules for geometrically open filters, which gave a similarly good result for the threshold parallel gradient in the filter, is, through another method, based on the critical shear velocity and thus on the Shields criterion as well.

The Shields criterion for flow seems to apply as a threshold of motion for the transport of sand grains for the filter velocity in the pores, caused by the internal wave.

7.5.3 The threshold of motion explained

The comparisons of the test results with the existing design formulae and with the Shields criterion show that indeed for the very open filter as used in the tests a threshold value of loading applies that coincides with the geometrically open, hydraulically sand-tight filter criteria.

⁴² Schiereck (2001), [42]

7.6 Turbulence-dominance or porous-flow-dominance

Breaking waves generate a lot of turbulence, which is linked to the stirring up of sediment in the swash zone by various researchers. A generally existing idea is that turbulence from breaking waves can stir up sand in the swash zone on a beach-coast and keep the sand in suspension, by which only a small current is needed to transport the sand. The small current would not be able to pick-up the sand itself, as the shear stress on the grains would not exceed the threshold of motion. In the present study, a layer of stones lies between the direct wave action and the sand, reducing the wave loading. The question remains whether the turbulence generated by the breaking waves is still the dominant forcing mechanism or that the parallel porous-flow running through the filter layer is dominant.

Turbulence intrusion

Movies were made of the tests with close ups of varying interesting areas. For test 4, the reference test for irregular waves, close ups of the wave-breaking on the filter layer have been studied for the intrusion of turbulence generated by the waves. It is clearly visible that a lot of air is entrained in the plunging breaker-jets of the waves, leading to a lot of small air bubbles in the up-running wave front. In the upper part of the filter layer, a part of these small air bubbles is still visible, indicating that the breaking-wave turbulence is still active in this part. However, lower than about $2 D_{f50}$ (estimated) inside the filter layer, no air bubbles have been seen, and the internal water level only rises quickly with a large gradient from the outside of the filter layer (high) to the core-interface (low).

Parallel porous flow and parallel gradient

The water inside the filter layer runs up and down the sand-slope of the core. The internal water level runs-up very quick and rundown takes much longer. As described in section 6.2.1, an internal setup of the water level develops because more water has to flow through the filter during rundown than during run-up. The internal setup contributes to the parallel hydraulic gradient, which drives the down-running porous flow.

The rundown-time is up to $\frac{3}{4}$ of the wave period, leaving only $\frac{1}{4}$ for the run-up. During run-up, the water reaches a high speed for a very short time, picking up small clouds of sediment into suspension. It looks like turbulence has a part in this, since the sediment does not flow parallel to the slope, but departs the slope under an angle or with a circular movement. This turbulence, however, does not seem to be caused by the wave-breaking, but rather by the local high flow velocities. The flow acceleration is locally high. During rundown the flow does run parallel to the slope and has time to build up, pick up sand (first as bedload and after that as suspended-load if the velocity is high enough) and transport the sand downward.

Altogether, the accelerating flow seems to be dominant for transport during run-up, where the gradient-induced, steadier parallel porous flow is dominant during rundown. For the erosion, the rundown and therefore the parallel hydraulic gradient is expected to be dominant. These observations affirm the expectation that the amount of erosion depends on the gradient, explained in section 7.5.1.

7.7 Dimensionless parameter relations

The relations between loading and erosion found in section 7.4 give interesting results indicating dependencies of erosion parameters on certain loading parameters, but always with either a very poor correlation, or a strict limitation for e.g. one test series. One parameter that seemed to be important in this is the Iribarren number ζ which is a dimensionless combination of wave height, -length and slope steepness. In chapter 4, dimensionless relations have been constructed with the relevant parameters in a dimensional analysis. Furthermore, observations and analysis of the threshold of motion indicate that the parallel hydraulic gradient is another important parameter. In this section, these dimensionless parameters are used to find more generally applying dimensionless relations between loading and erosion.

7.7.1 Relations with ζ

The surf similarity parameter or Iribarren number, ζ , is the ratio of the slope steepness and the square root of the wave steepness, $\zeta = \frac{\tan \alpha}{\sqrt{H/L_0}}$ with $L_0 = \frac{gT^2}{2\pi}$. It has an important influence in many wave-breaking related processes and is studied as an interesting parameter because it appeared as a condition in a number of the found relations. ζ has been kept constant in the wave height variation tests, but changes in the period variation tests. In Figure 7-27 the erosion area is shown versus ζ for all tests.

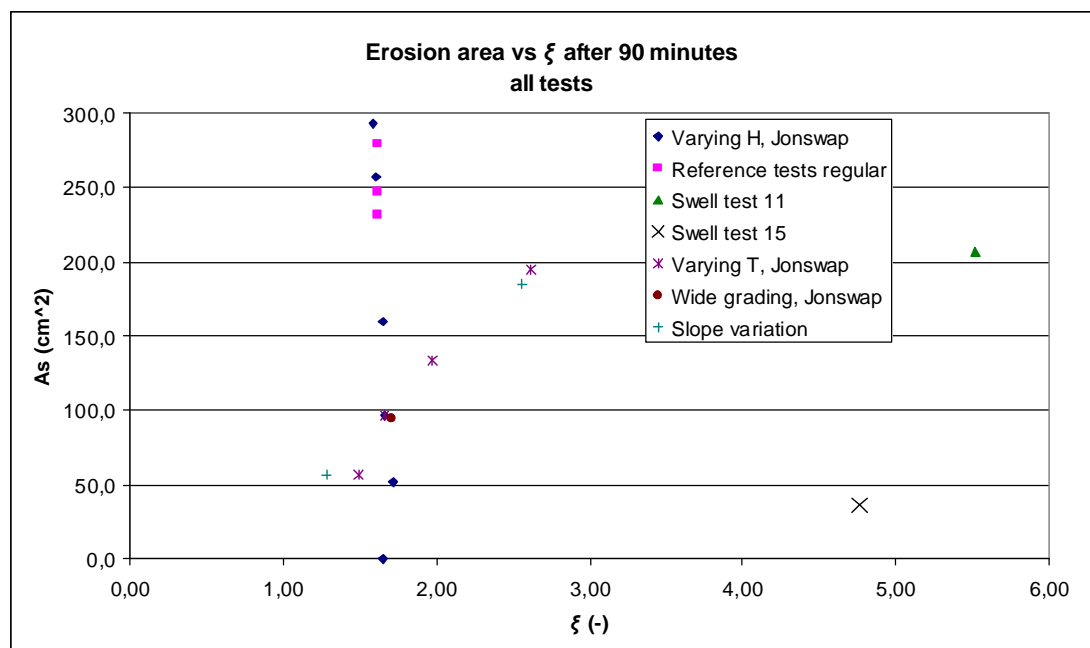


Figure 7-27 erosion area versus ζ

The figure shows three clear directions of the data-spreading, one with an almost constant ζ , one for the wave period variation tests and one at the high ζ -values of the swell tests. Clearly, ζ is not the dimensionless parameter that forms the connection between all tests. It will be used in other relations further in the analysis as part of a solution.

7.7.2 Relations from the dimensional analysis

In section 4.1, dimensionless parameter combinations have been formulated of which the following were expected to be interesting for the analysis:

$$\frac{d_s}{d_f} = F \left\{ \frac{H}{d_f}, \frac{gT^2}{d_f}, \tan \alpha \right\}$$

$$\frac{d_s}{H} = F \left\{ \frac{D_b}{H}, \frac{D_f}{H}, \frac{d_f}{H}, \frac{H}{gT^2}, \tan \alpha, \frac{\rho_s}{\rho_w}, \frac{\sqrt{gHD_f}}{v} \right\}$$

$$\frac{A_s}{HgT^2} = F \left\{ \frac{d_f}{D_f}, \frac{D_b}{D_f}, \frac{\tan \alpha}{\sqrt{\frac{2\pi H}{gT^2}}}, \frac{\rho_s}{\rho_w}, \frac{\sqrt{gHD_f}}{v} \right\}$$

$$\frac{A_s}{HgT^2} = F \left\{ I, N, \frac{d_f}{D_f}, \frac{D_b}{D_f}, \frac{\tan \alpha}{\sqrt{\frac{2\pi H}{gT^2}}}, \frac{\rho_s}{\rho_w}, \frac{\sqrt{gHD_f}}{v} \right\} = F \left\{ I, N, m, \frac{D_b}{D_f}, m, \xi, \frac{\rho_s}{\rho_w}, Re \right\}$$

The first relation, $\frac{d_s}{d_f} = F \left\{ \frac{H}{d_f}, \frac{gT^2}{d_f}, \tan \alpha \right\}$, was expected to be an interesting basis

for the comparison of erosion and loading. Figure 7-28 shows that this is clearly not the case; the data are spread in two directions and a lot of data have the same loading parameter like the wave height, but a very different erosion depth. Other relations have to be found that combine the influences of different parameters in one.

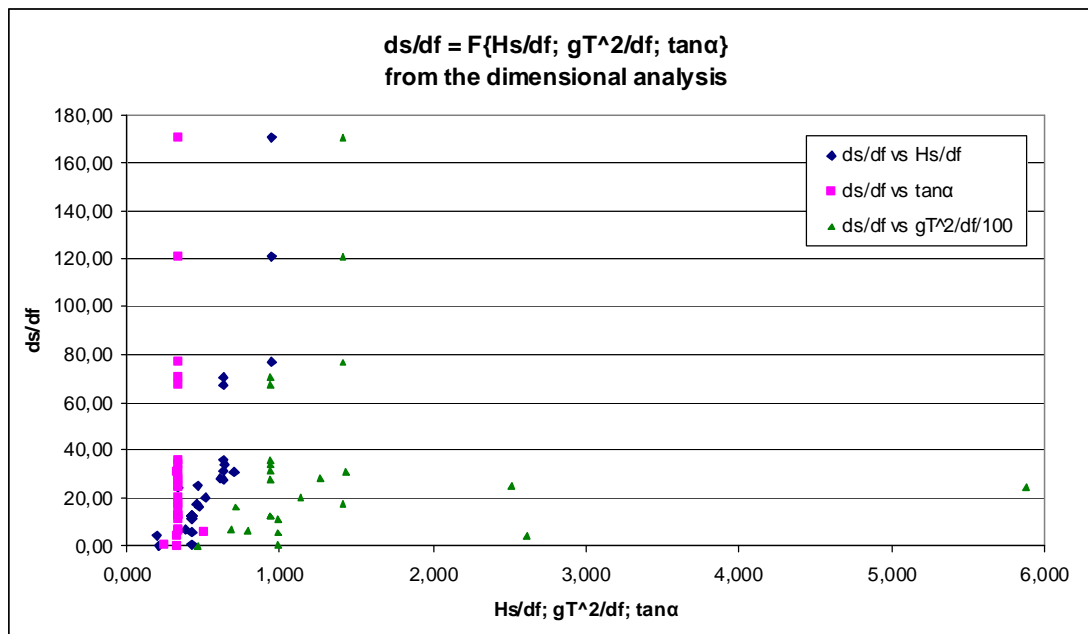


Figure 7-28 graph of the relations from the dimensional analysis

The second relation, $\frac{d_s}{H} = F \left\{ \frac{D_b}{H}, \frac{D_f}{H}, \frac{d_f}{H}, \frac{H}{gT^2}, \tan \alpha, \frac{\rho_s}{\rho_w}, \frac{\sqrt{gHD_f}}{v} \right\}$, was expected to give more insight in the erosion process.

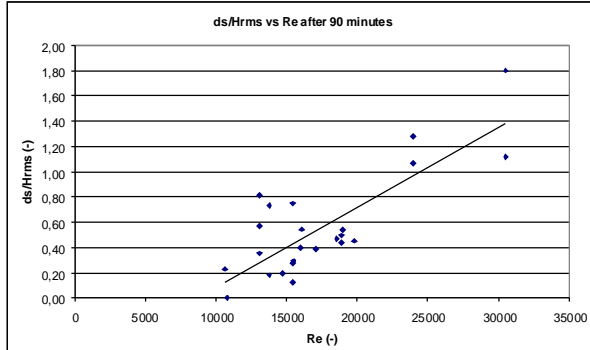


Figure 7-29 d_s/H_{rms} vs $Re = \frac{\sqrt{gHD_f}}{v}$

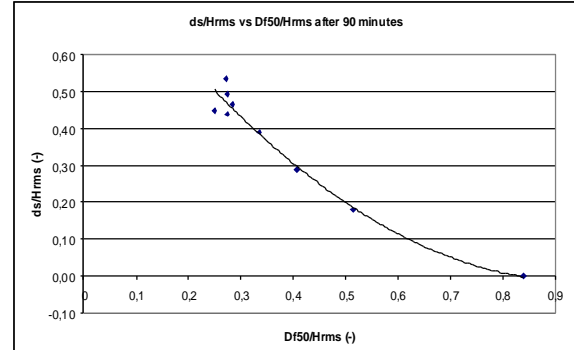


Figure 7-30 d_s/H_{rms} vs D_{f50}/H_{rms}

Figure 7-29 shows one of the resulting interesting relations. d_s/H_{rms} shows a tendency to increase with an increasing Reynolds number. Here the Reynolds is expressed as $Re = \frac{\sqrt{gHD_f}}{v}$. All tests, including those of Uelman, have been used for the figure. The correlation is poor and only the tendency for a positive relation seems relevant from this graph. Figure 7-30 shows another relation: d_s/H_{rms} versus D_{f50}/H_{rms} for only the wave height variation tests and the reference tests 1-3. A mirror image of the direct relation between erosion and wave height appears and the graph is dominated by the same parameters, in a different order. D_{f50} is constant for these tests. The same graph with other values on the x -axis appears when d_s/H_{rms} is plot versus D_{b50}/H_{rms} or versus d_f/H_{rms} for the same tests. These are all basically the same relations, since D_{f50} , D_{b50} and d_f all three are constant within these tests. Expanding these three relations to the other tests leads to three uncorrelated clouds of points. The relation with H/gT^2 gives no correlation, $\tan \alpha$ has only been varied in two tests and the density ratio has not been varied at all, not leading to interesting relations for all three. The main result of this part is an increasing dimensionless erosion depth for increasing Re .

The fourth relation,

$$\frac{A_s}{HgT^2} = F \left\{ I, N, \frac{d_f}{D_f}, \frac{D_b}{D_f}, \frac{\tan \alpha}{\sqrt{\frac{2\pi H}{gT^2}}}, \frac{\rho_s}{\rho_w}, \frac{\sqrt{gHD_f}}{v} \right\} = F \left\{ I, N, m, \frac{D_b}{D_f}, m, \xi, \frac{\rho_s}{\rho_w}, Re \right\},$$

the next interesting combination since the third relation is exactly a part of this. In this analysis, $L_0 = \frac{gT^2}{2\pi}$ is used instead of gT^2 because the wave length has more physical meaning and the difference is only a constant factor. For N , a square-root relation is expected as was shown in section 7.4.1.

The dimensionless parameters used in this equation are shown in Table 7-7. The values of $I_{max}^*(H_{rms}/H_s)$ are used in the next section. The values of the hydraulic gradient, I_{max} , have been estimated from the movies of the tests, for the present tests as

well as Uelman's tests of which movies are available as well. The gradient is defined as the vertical distance between the internal run-up point and the external rundown point divided by the horizontal distance between those points. This is not the exact parallel gradient but will resemble is closely as it is the head difference over the horizontal difference at the moment the internal wave is at its highest point.

Table 7-7 Dimensionless parameters of all tests

Test Number	Parameters Variations	As/Hrms*L0	I _{max}	I _{max} *(Hrms/Hs)	N 90min	Df/Db	m = df/Df50 (-)	ξ (-)	wave-Re
1	Reference	0,116	0,14	0,14	4500	144	5,77	1,62	18872
2	Reference 2	0,109	0,14	0,14	4500	144	5,77	1,62	18872
3	Reference 3	0,130	0,14	0,14	4500	144	5,77	1,61	18971
4	Irregular waves	0,067	0,12	0,09	4500	144	5,77	1,66	15485
5	Varying H	0,054	0,09	0,06	4909	144	5,77	1,72	13761
6	and N	0,075	0,15	0,11	4091	144	5,77	1,66	17069
7		0,093	0,17	0,12	3885	144	5,77	1,60	18547
14	Varying H	0,082	0,20	0,14	3649	144	5,77	1,59	19780
13	Varying H	0,000	0,04	0,03	6429	144	5,77	1,65	10777
8	Varying ξ by varying T	0,060	0,11	0,08	5294	144	5,77	1,49	14663
4	Irregular waves	0,067	0,12	0,09	4500	144	5,77	1,66	15485
9		0,058	0,14	0,10	3673	144	5,77	1,97	15947
10		0,047	0,16	0,11	2755	144	5,77	2,62	16072
11	Swell waves	0,029	0,18	0,18	1800	144	5,77	5,52	13772
12	Grading variation	0,063	0,12	0,08	4390	144	5,77	1,71	15441
15	Swell waves low	0,019	0,09	0,09	2700	144	5,77	4,76	10605
4	Irregular waves	0,067	0,12	0,09	4500	144	5,77	1,66	15485
16	tan alpha	0,037	0,07	0,05	4390	144	5,77	1,28	15433
17	variation	0,123	0,19	0,13	4390	144	5,77	2,56	15440
Evert 3	Uelman's	0,086	0,13	0,13	4500	100	8,33	1,62	13065
Evert 4	tests	0,053	0,10	0,10	4500	100	11,11	1,62	13065
Evert 5		0,123	0,18	0,18	4500	100	5,56	1,62	13065
Evert 6		0,162	0,13	0,13	4500	183	4,55	1,62	23953
Evert 7		0,194	0,18	0,18	4500	183	3,03	1,62	23953
Evert 8		0,170	0,14	0,14	4500	233	3,57	1,62	30486
Evert 9		0,273	0,16	0,16	4500	233	2,38	1,62	30486

Two of the relations are shown in Figure 7-31 and Figure 7-32. $A_s/(H_{rms} * L_0)$ versus I_{max} shows a cloud of points with little cohesion. $A_s/(H_{rms} * L_0)$ vs Re, the other relation, shows a trend very similar to Figure 7-29: Increasing erosion for increasing Re. It should be noted that this Reynolds number is not the exact Reynolds number inside the pores, because the velocity used for it is not the pore velocity, but \sqrt{gH} .

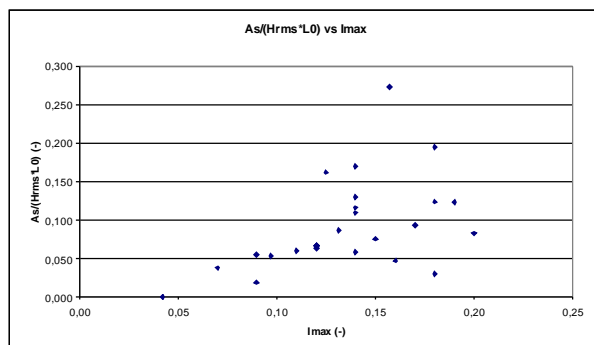


Figure 7-31 $A_s/(H_{rms} * L_0)$ vs I_{max}

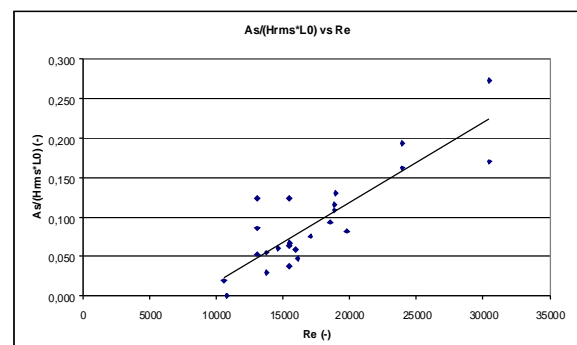


Figure 7-32 $A_s/(H_{rms} * L_0)$ vs Re

The other relations between parameters of this combination show less correlation. The studied relations are combinations between the left-hand term and one of the right-hand terms. The left-hand term, in this case $A_s/(H_{rms} * L_0)$, is actually expected to depend on all the terms of the right-hand side of the equation. The analysis done here is interesting to see influences of single terms; the next step is to find combinations

that are generally valid for all tests. The next section presents the relations that have been found with the available data. These relations are interesting for design purposes.

7.7.3 Combined relations

The former section shows relations between dimensionless parameters found in the dimensional analysis. In this section combinations are shown, the influence of as many relevant dimensionless parameters as possible taken into account. A shear infinite number of empirical relations can be thought of and tried. Here, the partial results as found in the analysis so far are used to come up with relations that are expected to have potential, with some adjustments of powers of terms to give the best fit. Not all results are shown; only results leading to useful relations interesting for the understanding and design of breakwaters with open filters on a sand core are presented. Two interesting results have been found, one from the reasoning above and one from further curve fitting.

I_{rms} ; using a substitute for the root-mean-squared gradient

The parallel hydraulic gradient, shortly called gradient, was estimated from the movies. For this, the maximum observed value was used during a relatively short part of the tests for which the camera was zoomed in at the right area. This value is expected to resemble the gradient that relates to the significant wave height, being the wave height that is usually observed in a visual observation. During the observation period, this can very well be the maximum wave height, as the absolute maximum will occur maybe only once or twice during the whole test. The significant wave height is the average of the highest one third of the waves. The gradient that was observed and probably related to this wave has been called I_{max} , the maximum gradient. It was found in the analysis that the root-mean-squared wave height rather than the significant wave height dominates the erosion process and as such is related to the amount of erosion. For this reason, it is expected that a gradient related to the H_{rms} is a better representative of the loading that induces a total amount of erosion. The root-mean-squared gradient could be estimated by observing all the individual gradient levels and taking the root-mean-square of those values. This is not possible as the movie material does not allow this and would be very time consuming if at all possible. As an alternative, the found I_{max} has been multiplied with the ratio of H_{rms}/H_s to find a representative for the root-mean-squared gradient. This gradient has been called $I_{rms} = I_{max} * H_{rms}/H_s$, although it should be noted that is not the observed root-mean-square of the occurring gradients. Results show that this value indeed gives a clearer relation between erosion area and loading.

The best result found from the partial results

The partial analysis of dimensionless parameter relations shows increasing erosion for increasing I , increasing Re , decreasing m , increasing \sqrt{N} , increasing D_f/D_b and

decreasing ξ . A relation with the form of $\frac{A_s}{H_{rms} L_0} \propto \frac{I_{rms} \sqrt{N} \frac{D_f}{D_b} Re}{m \xi}$ would be expected

from these results. This relation is shown in Figure 7-33 to illustrate the reasonable agreement of all the data points (all tests including Uelman's) to it. The four points on the right-hand side of the figure are four of Uelman's tests, with a high openness of the filter, the highest point on the far-right is of Uelman's test 9, with the thinnest filter layer and the largest stones giving the least reduction. $D_{f50}/D_{b50} = 233$ for this test.

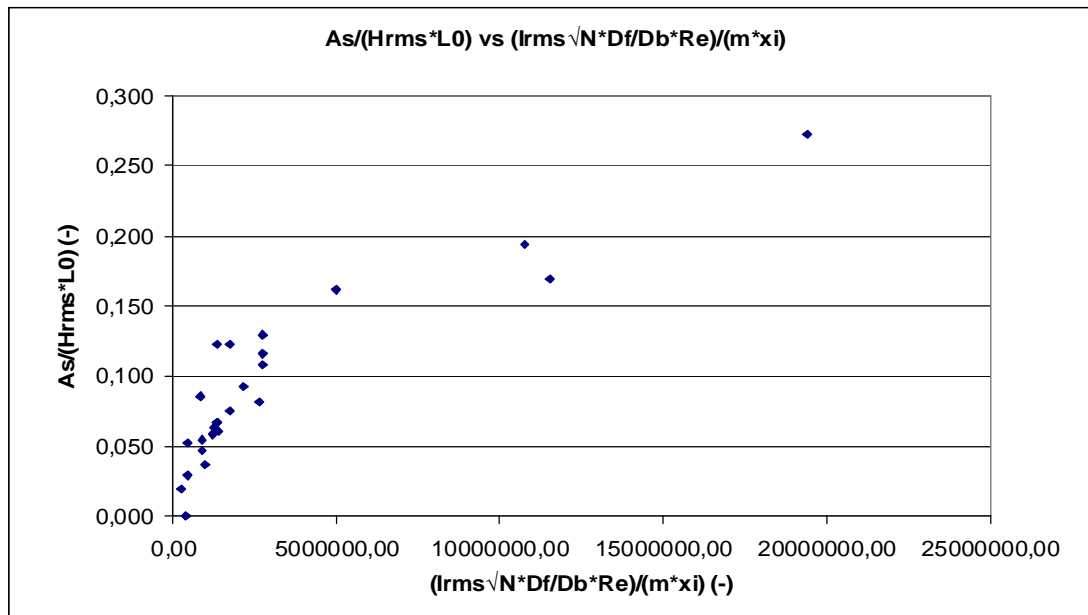


Figure 7-33 Relation between erosion area and gradient from the partial results

To further investigate the process and to come up with a useful relation, various combinations of parameters have been tried. The best result found from this is the relation shown in Figure 7-34, with a linear line drawn through it. Most of the measurements lie below this line, to get only a small possibility that erosion exceeds the found value. In this relation, Re , D_f/D_b and ζ have not been used. The gradient, however, is not independent of these parameters. The influence of the three mentioned parameters is expected to affect the erosion through the gradient. Re as it is used here is mainly a function of wave height and filter grain size, the openness of the filter is so high that the porous flow transports the sand as if it were open channel flow and is only affecting the flow through the gradient and ζ (slope steepness/ wave steepness) increases or decreases the gradient.

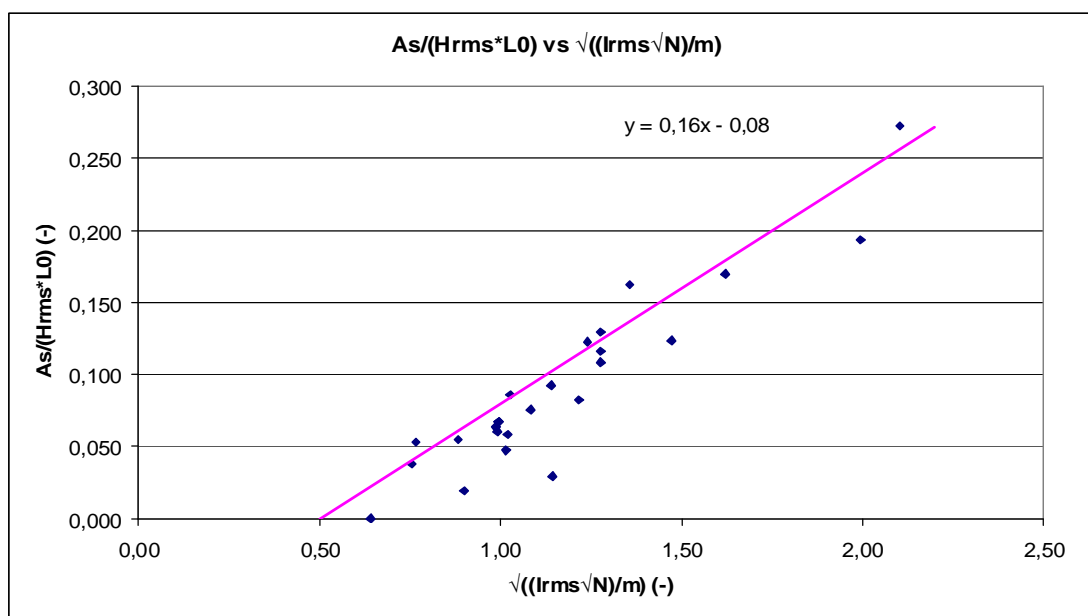


Figure 7-34 Dimensionless relation between erosion area and gradient

The relation shown in the figure (pink line) yields:

$$\frac{A_s}{H_{rms} L_0} = 0,16 \sqrt{I_{rms}} \frac{\sqrt{N}}{m} - 0,08.$$

The relation between the gradient and the parameters it depends on is still open for further research as no good relation has been found yet.

The best result found by curve-fitting

Observations of the tests showed a large influence of the parallel downward porous flow velocity on the sand transport. The parallel porous flow is driven by the parallel hydraulic gradient in the filter layer, which has been estimated for all the tests, including Uelman's, from the movies that were made during the tests. The values are shown in Table 7-7. The relation presented here in Figure 7-35 is the result of further elaboration on and curve-fitting of the above relation (Figure 7-34). The same parameters have been used with different powers to fit the measurements better.

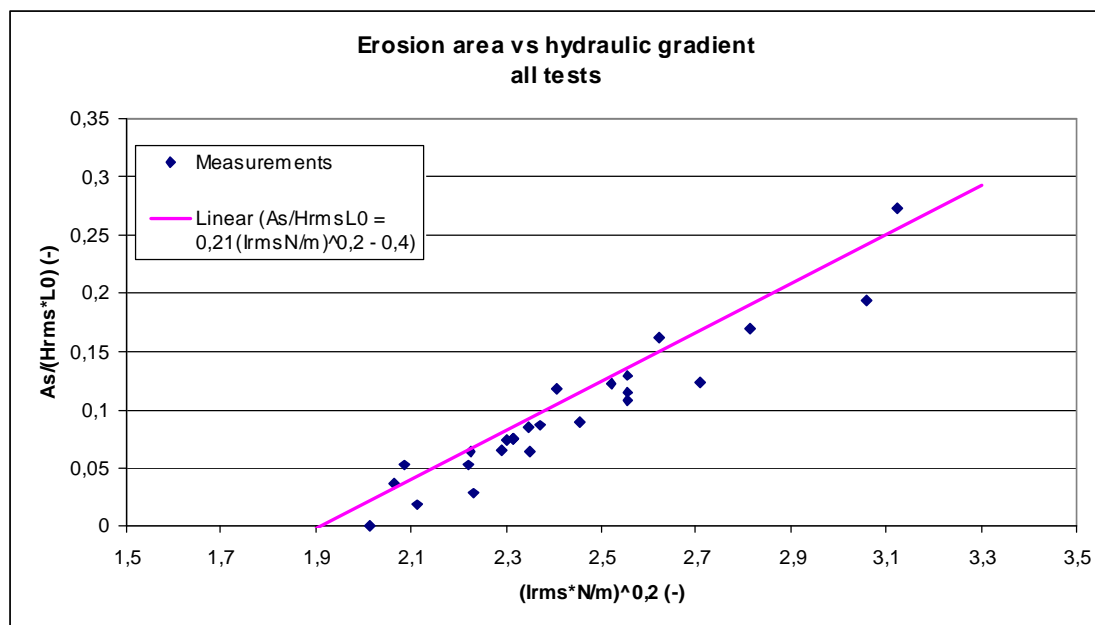


Figure 7-35 Alternative dimensionless relation between erosion area and gradient

Figure 7-35 shows the relation with the solid line as a recommended line with most of the data points lying below. The erosion area is divided by the wave height and – length, to get a dimensionless parameter that relates the amount of erosion directly to the wave characteristics. The gradient was multiplied by the number of waves because erosion grows with it, and divided by the relative filter layer thickness since a thicker filter gives less erosion. The power of 0,2 was found by optimising the fit. A fifth order relation between the velocity and the amount of sediment transport under currents is found as well when elaborating the Engelund-Hansen⁴³ formula for total load transport under currents, suggesting that the fifth order relation between gradient, which is partly linearly related to the velocity, and erosion, which is the integrated transport, might be valid. In formula form, the solid line in Figure 7-35 is:

⁴³ Van der Graaf (2005), [15]

$$\frac{A_s}{H_{rms} L_0} = 0,21 \left(I_{rms} \frac{N}{m} \right)^{0,2} - 0,4$$

This formula has the best fit with the test data and is therefore recommended as the most useful formula for design purposes. Caution with the application of it is needed because the relation has only limited physical explanation and only a theoretical analysis of occurring scale effects has been performed. Scale series tests will be recommended for further research. Besides these considerations, three remarks have to be made on this formula:

- The hydraulic gradient is difficult to estimate directly from the wave- and geometry characteristics, making the formula difficult to use. A good relation between gradient and loading parameters still has to be developed.
- The wave height and –period have influence on both sides of the equation; directly on the left-hand side and through the gradient on the right-hand side. This is not an ideal situation, but not a real problem. Examples of proven formula with the same drawback exist, e.g. the well-known Van der Meer equations for the stability of armour layers.
- The grain size of the core material is not in the formula, although it is evidently important for the transport of it. It was not varied in the tests, so no predictions can be made for other grain sizes based on this relation alone. The threshold of motion has been related to the grain size through the Shields criterion, but the amount of transport above this threshold remains uncertain without some form of scale-testing.

7.7.4 Found relations and remaining uncertainties after analysis

To give an overview of all the relevant relations that were found in this chapter, the relations are listed. First the dimensional relations of section 7.4, then the partial dimensionless relations of sections 7.7.1 and 7.7.2, and finally the combined dimensionless relations of section 7.7.3 are listed. For explanation and background information, the reader is referred to the respective section.

Dimensional relations between loading and erosion

The relations with dimensional parameters lead to a lot of conditional relations; it is valid for only a certain number of tests for which the conditions apply.

$$A_s \propto \sqrt{N}$$

$$A_s \propto H_{rms}^2 \text{ for } : H_{rms} \geq H_{threshold}, \text{ and } : \xi = const.$$

$$A_s \propto T_p \text{ for } : H = const.$$

$$A_s \propto \tan \alpha, \text{ for } : H = const., \text{ and } : T = const.$$

$$L_{r2} \propto H_s \text{ for } : H_s \geq H_{threshold}, \text{ and } : \xi = const.$$

$$d_s \propto H_{rms} \text{ for } : H_{rms} \geq H_{threshold}, \text{ and } : \xi = const.$$

$$L_{r2} \propto Run - up, \text{ for } : Run - up \geq Run - up_{threshold}, \text{ and } : \xi = const.$$

Dimensionless relations from partial parameter combinations

These relations did not result in consistent formulae, but did affirm that the combination of dimensionless parameters from the dimensional analysis is interesting:

$$\frac{A_s}{HgT^2} = F \left\{ I, N, \frac{d_f}{D_f}, \frac{D_b}{D_f}, \frac{\tan \alpha}{\sqrt{\frac{2\pi H}{gT^2}}}, \frac{\rho_s}{\rho_w}, \frac{\sqrt{gHD_f}}{v} \right\} = F \left\{ I, N, m, \frac{D_b}{D_f}, m, \xi, \frac{\rho_s}{\rho_w}, \text{Re} \right\}$$

Combined dimensionless relations

Combinations of the dimensionless terms lead to the reasoning that a relation with the

form of $\frac{A_s}{H_{rms} L_0} \propto \frac{I_{rms} \sqrt{N} \frac{D_f}{D_b} \text{Re}}{m \xi}$ should

give interesting results. The results are:

$$\frac{A_s}{H_{rms} L_0} = 0,16 \sqrt{I_{rms} \frac{\sqrt{N}}{m}} - 0,08 \text{ and}$$

$$\frac{A_s}{H_{rms} L_0} = 0,21 \left(I_{rms} \frac{N}{m} \right)^{0,2} - 0,4.$$

The former has the best physically founded reasoning, the latter the best fit to the test results.

Remaining uncertainties after analysis

Interesting relations have been found, however some questions remain after the analysis of the test results.

- The parallel hydraulic gradient is important for the erosion process. The way it depends on the loading parameters and structural parameters still has to be found in further research.
- Scale effects have been analysed theoretically. It is however uncertain how this type of structure will exactly behave on a larger scale because the analysis could only be done with the available information of relevant but yet different situations.
- The grain size of the core material has not been varied in the tests and it remains uncertain how the amount of erosion will be affected by another grain size. For the threshold of motion this can be calculated using the Shields criterion or the easier applicable design criteria for geometrically open filters, but for the amount of erosion it remains uncertain.
- Other interesting parameters such as Structural layout variations, oblique incident waves, (longshore sand transport), breakwater head/ crest/ berm stability and tidal variations will practice an unknown effect on the erosion process and study of it will be recommended for further research.

Conclusions and recommendations will be treated further in Chapter 8.

7.8 Up-scaling to a possible prototype

In the model tests, the highest waves had an H_s of 16 cm, whereas in real situations, the design wave height can be in the order of 2 to 10 m, depending on the location and circumstances. A theoretical up-scaling of the model is applied to show some possibilities and to indicate a range of loading conditions for which this type of breakwater setup is interesting.

7.8.1 Up-scaling with general Froude scaling factors

As was pointed out in section 4.2, the Froude scaling law is the most important for this structure-type. When Froude scaling is applied, viscous effects and air entrainment effects are expected to cause scale effects of up to 10 % in the penetrating wave height. Froude scaling implies that all length dimensions are linearly scaled, with a factor that is the square of the time scale factor.

Table 7-8 scaling with fixed Froude scaling factors

Scaling:	model	(-)	prototype nL = 20	prototype nL = 50	prototype nL = 100
Db50	0,00018	m	0,0036	0,009	0,018
Df50	0,026	m	0,52	1,3	2,6
df	0,15	m	3	7,5	15
H	0,1	m	2	5	10
T	1,2	s	5,4	8,5	12,0
Hmoderate	0,05	m	1,0	2,5	5,0
Tmoderate	0,85	s	3,8	6,0	8,5
Hextreme	0,16	m	3,2	8,0	16,0
Textreme	1,52	s	6,8	10,7	15,2
L0	2,25	m	45,0	112,5	224,9
As	0,01	m ²	4,86	30,39	121,55

Table 7-8 shows the results for three length scale factors: 20, 50 and 100. All length scales are multiplied by these factors; the wave period, the only time scale, is multiplied with the square root of the factor. The factor of 100 was chosen for it was used as a reference factor for some calculations in the test program. The results, however, show unrealistic values for the grain sizes, filter thickness and erosion area. Waves of 16 m are in fact extremely high, and this type of structure is not recommended for such extreme conditions. The lower factors give slightly more realistic values, the factor of 20 the most realistic, with a filter thickness of 3 m with D_{f50} of 0,5 m. The problem with this theoretical prototype is that the grain size of the core material of 3,6 mm, lies outside the range of sand. The use of sand was one of the basic principles of the whole setup; therefore even this prototype is of little value. A different scale factor for the sand than the overall scale factor is necessary. The effect of this distorted scaling is not exactly known yet as indicated in section 7.7.4. further research has to validate the found relations for the amount of erosion for large scales and different grain sizes of the sand.

7.8.2 Up-scaling for two layers from core to armour to loading

In the tests, only one single layer of stones was used, to keep out the complicating hydraulic effects of a double-layered system. However, an armour layer on top of the filter layer will be necessary in some cases to get a realistic design. The large armour stones keep the filter in place; the filter reduces the wave loading far enough to limit the core-erosion to acceptable values. Now the structure can be scaled as follows:

– $n_l = 5$, so $D_{b50} = 0,9$ mm, still in the range of sand. $D_{f50} = 130$ mm to keep the same openness of the filter, and $d_f = 0.75$ m, to keep the same m . A standard grading of 80/200 mm could be used as filter material to meet the requirements.

– On the filter, an armour layer is placed. Using the Terzaghi filter rule $\frac{D_{A15}}{D_{f85}} \leq 5$

(D_A is the armour grain size), with D_{f85} estimated to be 150 mm, leads to a D_{A15} of 0,75 m, and a D_{A50} of about 0,9 m, the nominal diameter of $D_{nA50} = 0,75$ m and a weight of $W_{A50} = 1100$ kg. A standard grading of 1000/3000 kg could be applied. The thickness of the armour layer is recommended to be 3 times D_{nA50} instead of the usual 2 times, because the filter layer will settle due to the erosion of core material and the armour layer has to follow this deformation without weakening. Because of this thicker layer, a relatively high damage level is accepted in the wave height calculation.

– The waves that can be handled by this armour layer are estimated using the van der Meer equation for plunging breakers, with $\Delta = 1,65$; $D_{n50} = 0,75$ m; $P = 0,5$; $S = 5$; $N = 3600$ and $\zeta = 1,62$. The resulting maximum critical $H_s = 3,24$ m. The corresponding period is $T_p = 6,8$ s.

– The amount of erosion that would occur is the most difficult part to estimate. The total layer thickness of filter and armour is $0,75 + 3 * 0,75 = 3$ m. The wave run-up over the slope is 3,6 m, calculated with formula 7.15 in Schiereck (2001), with $H_{rms} \approx 0,71 * H_s = 2,3$ m. The internal run-up is expected to be 0,4 times this value, as found in the model tests, leading to 1,4 m. The rundown is calculated with formula 7.18 (Schiereck) to be 1,2 m over the armour slope. The gradient over the armour/filter layer is then $\Delta h/\Delta x = (1,4m + 1,2m)/(9,5m + 3*1,4m) = 0,19$. The relation found in the analysis in Figure 7-35,

$$\frac{A_s}{H_{rms} L_0} = 0,21 \left(I_{rms} \frac{N}{m} \right)^{0,2} - 0,4;$$

leads to a total erosion area of the cross section of the core of $3,5$ m², with the above used values and $m = 6$. The total erosion length is estimated as the horizontal component of the internal run-up and the external rundown: $(1,4+1,2)*3 = 7,8$ m, leading to an erosion depth of $3,45/7,8 = 0,44$ m.

– The threshold wave height below which no erosion is expected, is calculated backwards in the same way as the erosion area, leading to $I_{rms} = 0,042$ and $H_s = 0,15$ m.

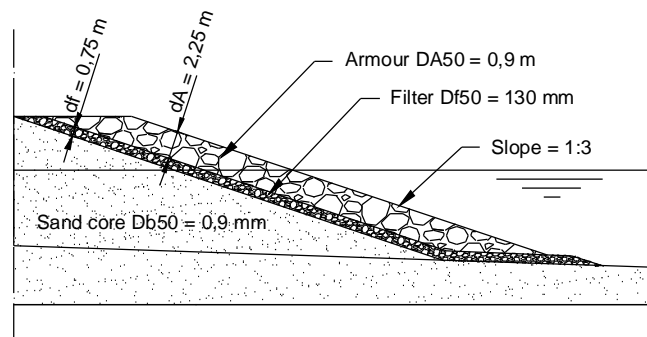


Figure 7-36 sketch of the scaled-up prototype

For this calculation, the core has been scaled to a grain size within the sand range, the filter has been scaled with the same factor, the armour has been added with the Terzaghi rules for geometrically closed filters, the core-erosion after 3600 waves that can just be handled by the armour has been calculated with the relation found in the

analysis and the threshold wave height has been calculated backwards with the same relation. The result is a structure with only one filter layer between the armour stones of 0,9 m and the sand of 0,9 mm. Waves with a significant height of 3,24 m can be resisted by the structure, leading to 0,44 m of erosion depth after 3600 waves. This all seems interesting; the drawback of the presented layout is the threshold wave height value of only 0,15 m. Higher waves are expected to give some erosion, so this layout is in fact only interesting for a structure in a mild wave climate or a situation where erosion can be accepted in the normal conditions. Since no equilibrium has been found in the tests, this last option is not recommendable without more knowledge about long-term behaviour of such a structure.

The relation that was used for the calculation of the erosion has to be handled with care; as indicated in section 7.7, the grain size of the core material is not in it, which can cause errors. The grain size in the prototype is larger than in the model, therefore an overestimation of the amount of erosion is expected. Scale effects as studied in Chapter 4 also indicate that the erosion is overestimated slightly. Still no good way of calculating the occurring gradient is available.

7.8.3 Up-scaling with the Shields criterion

Using the method found in section 7.5.2, a threshold value of the wave height for no transport was calculated for the up-scaled prototype. Using the same filter parameters as in the two-layer up-scaling above, but with a filter of 2 m thick, the result is a maximum pore velocity of 0,17 m/s and a maximum average filter velocity of 0,07 m/s. The maximum allowed amplitude of the internal wave at the interface that gives this velocity is about 1 cm. The problem is to calculate the external wave that drives an internal wave of 2 cm high ($H = 2 * \text{ampl.}$). Using the method presented by Helgason⁴⁴ for the exponential damping of pore pressures inside rubble mound structures and as input the amplitude of the external wave, the amplitude of the internal wave at the core-interface has been calculated. The expression

is $p_{\max}(x) = p_{0,\max} \exp\left[-\delta \frac{2\pi}{L'} x\right]$, with $\delta = 0,0141 \frac{\sqrt{n}L^2}{H_s b}$, with $L' = 0,85L$ and b is the

horizontal filter layer thickness, 3,13 times d_f for a slope of 1:3. With as input the data of test 13, it results in $\text{ampl}_{\max}(x) = \text{ampl}_{0,\max} \exp[-2,989x]$, leading to an amplitude of 0,0075 m at the interface ($x = 0,47$ m) from an impute amplitude of 0,03 m. In other words, a wave of 6 cm height results in an internal wave of 1,5 cm high. The same was estimated from the observations; 1,5 cm internal wave height for the higher waves of the spectrum (about 6 cm). The intention was to use this relation for the up-scaling of the threshold wave height to a larger scaled prototype, however, no reduction was found for a thicker filter because the increase of x is countered exactly by the decrease of δ by the higher b . This method does not work for the up-scaling procedure. It is expected that a thicker filter does reduce the internal wave height but the extend remains uncertain. No good estimate of the maximum wave height can be made based on this method with the available knowledge.

⁴⁴ Helgason (2004), [21]

7.8.4 Conclusions after up-scaling

Three attempts have been made to scale-up the model test results to a prototype situation. Two main problems prevent successful up-scaling:

- The core material sand cannot be scaled with the overall scale factor. The distortion has not been solved with the available knowledge yet. The effect of sand-scaling on the amount of erosion remains uncertain.
- The relation between the hydraulic gradient and the wave height, wave period, slope steepness, filter thickness and grain size remains unknown. This relation is necessary because it is the dominant loading parameter for sand transport and the input in the found design relations.

For these reasons no good up-scaling can be done. The potential of this type of structure is not represented in a good way by the found scaled-up prototype examples. Further research will be necessary to resolve these problems.

7.9 Evaluation of the analysis

After the analysis, an evaluation is relevant to see if the expected relations on which the test program was based have been found in the tests as well and to see if the findings of the analysis answer the questions and goals of the objective.

7.9.1 Evaluation of the expected relations

In section 5.2, the expected relations between loading and erosion are given. After the tests, they can be compared to the measured relations.

Wave height relations

It was expected that the erosion area would be related to the wave height to the power 3: $A_s \sim H_s^3$. A quadratic relationship between the erosion area and the root-mean-squared wave height was found in the results; $A_s \sim H_{rms}^2$. For the erosion depth, a relation of an order lower was found than expected as well: $d_s \sim H_{rms}$ was found where $d_s \sim H_{rms}^2$ was expected. For the erosion length, the expected linear relation was found indeed, be it that the relation for L_r was not very clear, but for L_a it was. $L_r \sim H_s$ was expected where $L_a \sim H_s$ was found. The differences are due to a different dominant loading mechanism; in the expectations a dominance of the wave generated turbulence was expected, where the occurring parallel gradient in the filter layer was found to be the dominant loading mechanism.

Wave period relations

For the variation of wave periods, linear relations between erosion length and –depth and wave period were expected and found indeed, and the relation between erosion area and period was found to be linear as well. The influence by the period was larger than expected; longer periods give much more erosion.

Number of waves for equilibrium and threshold of motion

An equilibrium state in the erosion pattern was expected for a large enough duration. No equilibrium state was found however; the erosion growth showed to follow a square root function of the number of waves nicely, and kept on growing. The longest test was done for 600 minutes, 33000 waves, and showed a decrease of the growth during the whole test, but the erosion did not stop. Instead, a threshold of motion was found: test 13 showed no erosion at all for waves lower than 5 cm. The threshold depends not only on the wave height but also on the period, as test 15 did show erosion with a wave height of only 3 cm but a long period of 2,0 s.

Irregular Jonswap waves

It was expected that Jonswap waves would result in a similar bar-profile as with regular waves, with a more irregular growth process. H_s was expected to give a similar erosion as $H_{regular}$. The results showed a bar-profile that was indeed very similar to that of regular wave tests, with two differences: the cliff-erosion at point A did not occur; point A was spread over a larger distance, and the neutral zone at point D was spread over a larger distance, whereas it was a single point with regular waves. The erosion-growth was very similar to regular waves, but the amount of erosion after N waves was less when H_s was compared to $H_{regular}$. A good result was found when H_{rms} was compared to $H_{regular}$.

Swell waves

It was expected that swell waves would result in a low gradient and thus a slow erosion process. The opposite was found: waves with a height of only 5 cm gave a very high erosion compared to the other tests, caused by the long period of 3,0 s. the wave run-up level was very high, which resulted in a high gradient and the long period gave the downward porous flow time to build-up and transport a lot of sand. The influence of the period was underestimated. Swell waves with a height of 3 cm and a period of 2,0 s gave much less erosion, being more representative for the type of swell that could be handled by the structure.

Grading variation

A test with a wide grading was expected to give less erosion for the same D_{f50} than a narrow grading. It was expected that the D_{f15} was dominant for the amount of erosion as it determines the pore-sizes in the filter. In the results, no significant difference was found; the amount of erosion after 90 minutes was almost exactly the same as in the test with a narrow grading. Perhaps the porosity is dominant, which was 0,37 in the wide grading test versus 0,42 in the reference test, or the grading was not wide enough to lead to visible differences. On the basis of the results, no reduction by a wider grading is expected and D_{f50} is expected to be more important than D_{f15} .

Slope steepness variation

For the slope steepness variation, a more or less linear relation with the amount of erosion was expected; an almost perfectly linear relation was found. The slope steepness influences ζ , the breaking distance and the horizontal filter layer thickness. Which of these is dominant is not known, but a very important influence of the horizontal filter layer thickness is expected as it is important for the parallel gradient in the filter, which has been found to be a dominant parameter in the amount of erosion.

7.9.2 Evaluation of the objective

The objective of this study was to study the influence of variations of the hydraulic loading, slope steepness and grading of filter material on the stability and erosion patterns of core material in a breakwater configuration with a hydraulically sand-open filter on a sand core by performing physical model tests in a wave flume. The central research question was formulated as:

What is the erosion growth pattern for the erosion of sandy core material through a hydraulically sand-open filter layer in a breakwater under varying wave loading? Does an equilibrium profile occur and if so, when does it occur for both design conditions as for moderate, long term, conditions?

Physical model tests

Physical model tests in the wave flume have been carried out after a theoretical study of the scale effects for these model tests. Relations between loading, slope steepness and grading on the one hand and the amount of erosion and its growth on the other have been found. A complete theoretical description of all the occurring processes and mechanisms inside the hydraulically sand-open filter layer of a breakwater has not been found, although a threshold of motion and a dominance of the parallel hydraulic gradient in the filter layer are clearly shown. The expected equilibrium has not been

found; with the present knowledge the erosion is expected to go on slowly as a function of \sqrt{N} .

Theoretical study of the scale effects

Scale effects have been studied theoretically. Scaling criteria have been selected for the actual situation and an estimate of the magnitude of the scale effects has been made. A few examples of up-scaling of the test results to a prototype situation have been presented and comments on the different followed procedures are given. The scaling procedures will have to be validated with other test data in further research.

Numerical modelling: preparation

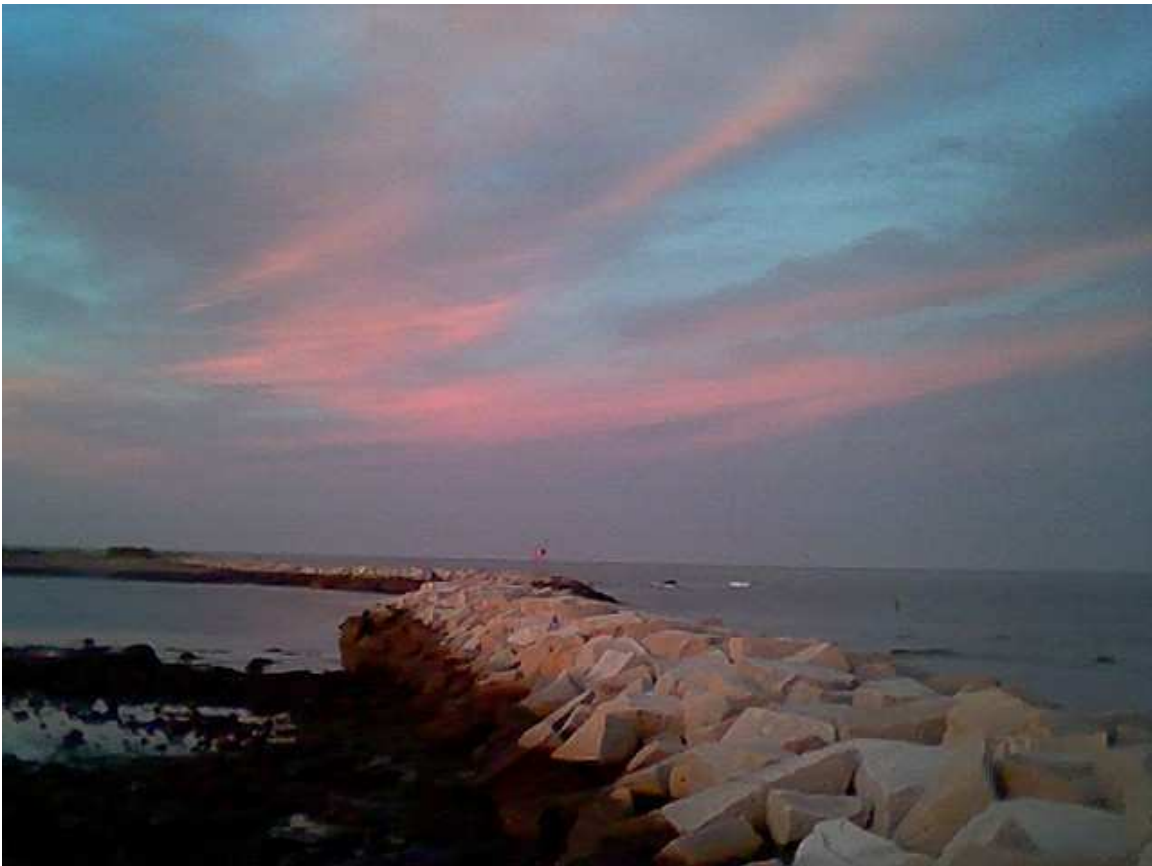
Chapter 2 explains the present state of available models for this type of processes. Numerical models are able to calculate breaking waves quite good. Porous flow gives more problems; average flow velocities give good results, but the actual velocity inside the pores is still problematic. Porous sand transport depends on these velocities and is therefore still difficult to predict. Nevertheless, a wave model (e.g. Volume Of Fluid-based) can be coupled to a porous flow model (e.g. based on Navier-Stokes equations with Forchheimer resistance terms) to calculate velocities averaged in space but not in time. To connect this to the amount of sand transport, the results of the done physical model tests can be used to calibrate relations that are for instance based on the Kalinske-Frijlink formula explained in section 4.1.2 for bedload transport. This process is complicated because the underlying processes are complicated and not yet fully understood.

Scale series and large scale tests: preparation

As indicated in section 7.7.4 it is still uncertain how this type of structure will behave exactly at a larger scale. Especially the behaviour of the core material sand is uncertain at a larger scale. Sand is meant to be used in the prototype as well, meaning that the scale factor for the core material is much smaller than the overall length-scale factor. The threshold loading can be calculated with the existing criteria for geometrically open filters but the amount of transport remains uncertain. To investigate this, two options of physical modelling exist: large scale testing and scale series. Large scale testing has the advantage that certainty about large scale behaviour is obtained. The disadvantages are the high costs and limited availability of the few large scale wave flumes (in the Netherlands, the Delta Flume could be used for this). Scale series are done at a smaller scale. For instance, some of the present tests are done at twice and three times the length-scale, so with grain sizes, structure sizes and waves are scaled all with the same length-scale. The results are compared and extrapolated towards the desired prototype scale. With this way of testing, no absolute certainty of the large scale behaviour is obtained since extrapolation always leaves some uncertainty. The advantage is the possibility to use smaller facilities. With a clever choice of parameters, such a procedure is possible to perform in the flume used for the present tests; up to twice the scale of the present tests can be executed in this flume. A form of scale-series tests will be recommended for further research.

Chapter 8

Conclusions and recommendations



8.1 Conclusions

8.2 Recommendations for further research

Chapter 8 Conclusions and recommendations

This chapter gives an overview of the findings of the study, with an evaluation to the objective. These conclusions do not present new information of findings but summarize the findings of the different sections. Recommendations for further research are presented based on the conclusions of what important information is missing to come to a good description of erosion processes and a useful design tool for breakwaters with an open filter on a sandy core.

8.1 Conclusions

Hydraulically sand-open filters in breakwaters with a sand core form a useful alternative for conventional designs of breakwaters. The results of this study indicate that they can be applied successfully when designed properly. Knowledge of the erosion processes inside this type of breakwater has increased and interesting relations have been found.

8.1.1 Evaluation of the objective

The objective of this study was to find relations for the influence of variations of the hydraulic loading, slope steepness and grading of filter material on the stability and erosion patterns of core material in a breakwater configuration with a hydraulically sand-open filter on a sand core by performing physical model tests in a wave flume.

Physical model tests

Physical model tests in the wave flume have been carried out after a theoretical study of the scale effects for these model tests. Relations between loading, slope steepness and grading on the one hand and the amount of erosion and its growth on the other hand have been found. The expected equilibrium profile has not been found; with the present knowledge the erosion is expected to go on slowly as a function of \sqrt{N} .

Theoretical study of the scale effects

Scale effects have been studied theoretically. Scaling criteria have been selected for the actual situation and an estimate of the magnitude of the scale effects has been made. The scaling procedures will have to be validated with other test data in further research.

Numerical modelling: preparation

Numerical models are able to calculate breaking waves quite good. Porous flow gives more problems. Porous sand transport depends on the porous flow and is therefore still difficult to predict. Suggestions have been made on what type of models could be coupled to get a representation of the erosion process induced by the waves. This combined modelling is complicated because the underlying processes are complicated and not yet fully understood.

Scale series and large scale tests: preparation

Sand is meant to be used in the prototype as well as in the model, meaning that the scale factor for the core material is much smaller than the overall length-scale factor. To investigate the effects of this, two options of physical modelling exist: large scale testing and scale series. Considerations show that scale series testing is a good option.

8.1.2 Concept of the processes after analysis

The breakwater configuration that is the subject of study is schematised as a sand core with a slope, loaded by incoming waves. The filter layer reduces the loading of the waves, which break on the filter and dissipate their energy. The filter stones absorb this turbulent energy and what remains deeper inside the filter is flow through the pores of the stones. The water level runs up and down in the filter layer over the sand slope with the same period as the external wave but with a smaller amplitude and without breaking.

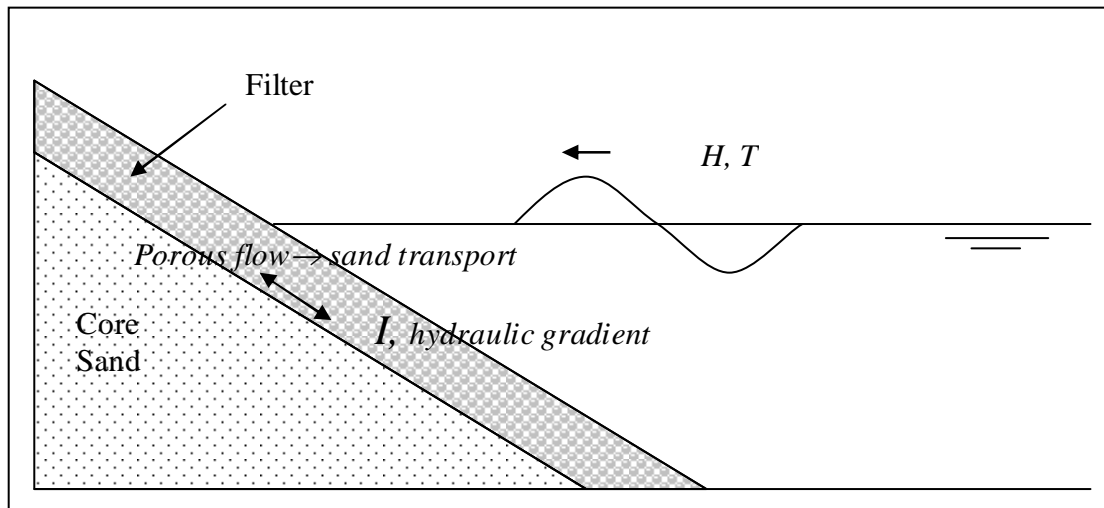


Figure 8-1 Concept of the breakwater configuration

The external waves induce an internal setup and an internal wave. The internal water level is still high when the external water level is at its lowest point (rundown point external wave). A hydraulic parallel gradient sets in from the high internal water level to the lowest external water level. This gradient drives the downward porous parallel flow, which induces the transport of sand through the filter layer downwards over the sand slope. An erosion area occurs where this flow is strong, in the part of the slope where the wave is active. The transported sand settles lower on the slope between the filter stones, forming an accretion area. The barred erosion profile that develops in this way has a stabilizing effect; the amount of erosion decreases in time without a decreasing loading. The erosion does not stop but decreases gradually with a square-root function of the number of waves. When the waves are low enough, the induced hydraulic gradient is not strong enough to drive a porous flow that transports sand. In other words, a threshold of loading has been found below which no erosion takes place. This concept is based on the observations and analysis of the tests.

8.1.3 Conclusions from observations and analysis

- Parallel downward porous flow is the dominant loading process rather than turbulence by the breaking waves. The turbulence has been observed to die out in the upper part of the filter layer. Porous flow has been observed to develop during the wave rundown, picking up sand when the velocity is high enough.
- The parallel downward porous flow is driven by the hydraulic gradient that sets in from the internal setup- or run-up level to the external rundown level.
- The amount of erosion grows with the square-root of the number of waves. An equilibrium state has not been found during the relatively long tests, but a gradual decrease of the erosion rate is evident.

- A threshold value for the loading has been found below which no erosion takes place. This threshold coincides with the existing design criteria for geometrically open filters. These criteria can be used to determine the maximum hydraulic gradient that does not lead to erosion for a designed structure.
- The amount of erosion was found to depend on the wave height and length (function of period), the hydraulic gradient, the number of waves and the relative filter layer thickness. The hydraulic gradient is a complex function of wave parameters (height, period, run-up, rundown, steepness) and structure parameters (filter grain size, thickness, porosity and slope steepness).
- The erosion area and erosion depth are both related to the square of the root-mean-squared wave height. The regular wave height of tests with regular waves can be compared to this H_{rms} .
- The erosion length is related to the significant wave height. These are the higher waves in the spectrum. The wave run-up and rundown which determine the erosion length are a function of these higher occurring waves.
- The wave period has a large influence on the erosion process. Longer waves result in high run-up levels and thus a high gradient. The downward flow has time to develop and to transport a lot of sand.
- The open filter structure is sensitive to swell waves because the long periods cause a large amount of sand transport.

8.1.4 Relations between loading and erosion

Besides qualitative results, quantitative relations have been found between loading and erosion. They are the results of the analysis of Chapter 7.

Dimensional relations between loading and erosion

The relations with dimensional parameters have lead to a lot of conditional relations; they are valid for only a certain number of tests for which the conditions apply.

$A_s \propto \sqrt{N}$; the amount of erosion is a constant factor times the square root of the number of waves. The factor is different for each test.

$A_s \propto H_{rms}^2$ for: $H_{rms} \geq H_{threshold}$, and: $\xi = const.$; for waves with the same Iribarren number, the erosion area was found to be linearly related to the square of the root-mean-square wave height. This relation starts at a threshold for H_{rms} for which $A_s = 0$. The relation holds for both regular and irregular waves; H_{rms} is the relevant wave height parameter.

$A_s \propto T_p$ for: $H = const.$; for Jonswap tests with a constant wave height the erosion area is linearly related to the peak period. The relation is not valid for other tests.

$A_s \propto \tan \alpha$, for: $H = const.$, and: $T = const.$; the erosion area is linearly dependent on the slope steepness, for tests with the same waves.

$L_{r2} \propto H_s$ for: $H_s \geq H_{threshold}$, and: $\xi = const.$; the erosion length depends on H_s instead of H_{rms} . The erosion length depends on the internal run-up level and the external rundown level, determined by the higher waves.

$d_s \propto H_{rms}$ for: $H_{rms} \geq H_{threshold}$, and: $\xi = const.$; the erosion depth depends on the erosion area and –length. The erosion area was found to be dominant, and with that the erosion depth depends on H_{rms} .

$L_{r2} \propto Run-up$, for: $Run-up \geq Run-up_{threshold}$, and: $\xi = const.$ The external run-up level can be calculated quite accurately from known relations. L_{r2}

depends on the run-up; nevertheless a relation with the external run-up was found. External and internal run-up are related.

Dimensionless relations for the erosion area

Combinations of the dimensionless terms lead to the reasoning that a relation with the

form of $\frac{A_s}{H_{rms} L_0} \propto \frac{I_{rms} \sqrt{N} \frac{D_f}{D_b} Re}{m \xi}$ should give interesting results. The results are:

$$\frac{A_s}{H_{rms} L_0} = 0,16 \sqrt{I_{rms} \frac{\sqrt{N}}{m}} - 0,08 \text{ and}$$

$$\frac{A_s}{H_{rms} L_0} = 0,21 \left(I_{rms} \frac{N}{m} \right)^{0,2} - 0,4.$$

The former has the best physically founded reasoning, the latter the best fit to the test results. These relations can be used as an indication of the amount of erosion to be expected. However, the results should be handled with care and have to be validated with e.g. design-specific tests. These relations have not been validated on a large scale and the grain size of the core material is not in it as a variable. The calculation of the occurring hydraulic gradient from wave- and structure parameters is still a problem.

8.1.5 Lacking knowledge after analysis

Interesting relations have been found, however some questions remain after the analysis of the test results.

- The parallel hydraulic gradient is important for the erosion process. The way it depends on the loading parameters and structural parameters still has to be found in further research.
- Scale effects have been analysed theoretically. It is however uncertain how this type of structure will exactly behave on a larger scale because the analysis could only be done with the available information of relevant but yet different situations.
- The grain size of the core material has not been varied in the tests and it remains uncertain how the amount of erosion will be affected by another grain size. For the threshold of motion this can be calculated using the Shields criterion or the easier applicable design criteria for geometrically open filters, but for the amount of erosion it remains uncertain.
- Other interesting parameters such as structural layout variations, oblique incident waves, (longshore sand transport), breakwater head/ crest/ berm stability and tidal water level variations will exert unknown effects on the erosion process and study of it will be recommended for further research.

8.2 Recommendations for further research

This study is part of the research into hydraulically sand-open filters in breakwaters. Understanding of the processes has increased and interesting relations between loading and erosion have been found but not enough knowledge is available to construct a good design tool and to give a full theoretical description of the erosion process. Section 8.1.5 describes the lacking knowledge after the analysis of test results; this section gives recommendations on how the lacks can be filled in further research.

8.2.1 Relations for the parallel hydraulic gradient

The parallel hydraulic gradient that develops during rundown of the wave was found to be the dominant forcing of the porous flow and with that the erosion process. It is recommended to search for the relation between this gradient and the parameters that it depends on. These parameters are expected to be:

- Wave height
 - Wave period
 - Slope steepness
 - Filter thickness
 - Filter grain size
 - Filter porosity
- } Iribarren number ζ }
- } wave run-up/ rundown }

It is recommended to search for good estimates of the wave rundown on rubble mound slopes and to combine that with the wave run-up and relate it to the gradient. The data of the performed tests can be used to validate the results. When more data of the occurring gradient is necessary, wave flume tests can be performed with a setup similar to the performed tests. Pressure sensors can be installed throughout the filter layer to measure the distribution of pressures in the filter during wave attack. The results can be analysed for a relation between gradient and loading parameters.

8.2.2 Prototype scale validation

The model tests were performed at a small scale. Scale effects were estimated theoretically but certainty about large scale behaviour is still insufficient. To investigate this, two options of physical modelling exist: large scale testing and scale series. Large scale testing has the advantage that certainty about large scale behaviour is obtained. The disadvantages are the high costs and limited availability of the few large scale wave flumes (in the Netherlands, the Delta Flume could be used for this). Scale series are done at a smaller scale. For instance, some of the present tests are done at twice and three times the length-scale, so with grain sizes, structure sizes and waves all scaled with the same length-scale. The results are compared and extrapolated towards the desired prototype scale. With this way of testing, no absolute certainty of the large scale behaviour is obtained since extrapolation always leaves some uncertainty. The advantage is the possibility to use smaller facilities. With a clever choice of parameters, such a procedure is possible to perform in the flume used for the present tests; up to twice the scale of the present tests can be executed in this flume.

It is recommended to perform a scale series test program, if possible in the same wave flume. The reference test for irregular waves, test 4 of the present study, can e.g. be

done at a length scale factor of 1,5 and 2. The wave height H_s would then be 20 cm, still feasible in the flume. The waterdepth will only be relatively smaller; effects of this have to be considered. If a larger facility is available larger scale factors can be used. The larger the scale, the more reliable the extrapolation towards prototype scale.

8.2.3 Influence of the core grain size

The grain size of the core material has not been varied in the tests and it remains uncertain how the amount of erosion will be affected by another grain size. It is recommended to perform wave flume tests with varying grain sizes of the sand in the core. This can easily be combined with the recommended scale series tests by extending the program. For the scale series, already different grain sizes for both filter and core are necessary to determine only the scale effects of the geometrically undistorted up-scaling. When core grain size variation is added (for constant filter properties) valuable information on the relation between erosion and core grain size can be found. This information is necessary to be able to design properly at prototype scale with a distorted grain size scale factor compared to the present tests.

8.2.4 Influence of structural layout and local circumstances

A number of parameters associated with the layout of the structure or local circumstances influence the behaviour of the breakwater:

- Slope steepness
- Use of a berm in the outer slope
- Low crest or submerged crest
- Special situation around the breakwater head (curved structure, high wave intensity)
- Tidal water level variations and wind setup
- Oblique incidence of waves
- Combination of waves and (parallel) currents

Of these parameters only the slope steepness has been studied. The influence of the other parameters is unknown and can be studied in model tests.

It is recommended to perform physical model tests in the wave flume to study the influence of a berm, low/ submerged crest and water level variations. The flume used for the present tests is a possibility for this.

To study the influence of oblique incident waves, the behaviour of the breakwater head and the combination of waves and currents it is recommended to perform tests in a wave basin. The two-dimensional wave flume is not suited for this. In a wave basin more possibilities exist to place a breakwater under an angle with the waves, to build a breakwater head or to add a current. Special attention has to be paid to the scale effects since the tests probably have to be performed at a smaller scale than in the wave flume.

References

- [1] Adel H. den *'Transportmodel voor filters dl 1 Samenvatting'*. 1992
- [2] Adel H. den *'Transportmodel voor filters dl 2 loodrechte stroming'*. 1992
- [3] Adel H. den *'Transportmodel voor filters dl 3 parallelle stroming'*. 1992
- [4] d'Angremond K., & van Roode F.C., *'Breakwaters and closure dams.'* Delft University Press, 2001
- [5] Bakker K.J., Verheij H.J. & de Groot M.B. *'Design of Geometrically open Filters in Hydraulic Structures'*. Filters in Geotechnical and Hydraulic Engineering, Balkema, the Netherlands, 1993
- [6] Bakker K.J., Verheij H.J. & de Groot M.B. *'Design Relationship for Filters in Bed Protection'*. Journal of Hydraulic Engineering Vol 120, No 9, 1994
- [7] Bezuijen A., Klein Breteler M. & Bakker K.J. *'Design Criteria for Placed Block Revetments and Granular Filters'*. 2de copedec, Beijing, China, 1987
- [8] Burcharth H.F., Liu Z. & Troch P. *'Scaling of Core Material in Rubble Mound Breakwater Model Test'*. Coastal and Port Structures, South Africa, April, 1999
- [9] Ettema R., Arndt, R., Roberts, P., Wahl, T., *'Hydraulic Modelling – Concepts and Practice'*. American Society of Civil Engineers, 2000
- [10] Foster M. & Fell R. *'Assessing Embankment Dam Filters that do Satisfy Design Criteria'*. Journal of Geotechnical and Geo environmental Engineering, May, 2001
- [11] Gent M.R.A. van *'Porous flow through rubble mound material'*. Journal of Waterway, Port, Coastal & Ocean Engineering, May/June 1995
- [12] Gent M.R.A. van *'The Modelling of Wave Action on and in Coastal Structures'*. Elsevier, Coastal Engineering 22 311-339, 1994.
- [13] Gent M.R.A. van, Tönjes P., Petit H.A.H. & van den Bosch P. *'Wave Action on and in Permeable Structures'*. Coastal Engineering 125, 1994
- [14] Gent M.R.A. van *'Wave interaction with permeable coastal structures'*. Thesis, 1995
- [15] Graaf J. van der *'Coastal morphology and protection'* Lecture notes CT5309, TU Delft, 2005
- [16] Grauw A. de, van der Meulen T. & van der Does de Bye M. *'Granular Filters: Design Criteria'*. Journal of Waterways, Port, Coastal and Ocean Engineering, 1984
- [17] Groot M.B. de, Bezuijen A., Burger A.m. & Konter J.L.M. *'The Interaction between Soil, Water and Bed or Slope Protection'*. Modelling Soil-Water-Structure Interactions, the Netherlands, Balkema, 1988
- [18] Groot M.B. de, Yamazaki H., van Gent M.R.A. & Kheyri Z. *'Pore Pressure in Rubble Mound Breakwaters'*. Coastal Engineering 124, 1994
- [19] Hagerty D.J. & Parola A.C. *'Seepage Effects in some Riprap Revetments'*. Journal of Hydraulic Engineering, July, 2001
- [20] Halter W., *'The behaviour of erosion filters under the influence of wave loads'*, MSc thesis, Delft University of Technology, 1999
- [21] Helgason E., Burcharth H.F. & Grúne F. *'Pore Pressure Measurements inside Rubble Mound Breakwaters'*. International Conference on Coastal Engineering, Lisbon, 2004
- [22] Hoeven M.A. van der *'behavior of a falling apron'*. Msc thesis TuDelft, 2002
- [23] Hólscher P., de Groot M.B. & van der Meer J.W. *'Simulation of Internal Water Movement in Breakwaters'*. Modelling Soil-Water-Structures Interactions, Balkema, The Netherlands, 1988
- [24] Holthuijsen L.H., *'Wind waves'*, lecture notes of Civil Engineering course CT5316, Delft 2005

- [25] Hsu T.-J., Sakakiyama T. & Liu P.L.F. '*A Numerical Model for Wave Motions and Turbulence Flows in Front of a Composite Breakwater*'. Elsevier, Coastal Engineering 46 25-50, 2002
- [26] Hughes S.A., '*Physical models and laboratory techniques in coastal engineering*'. World Scientific, 1993
- [27] Indraratna B. & Radampola S. '*Analysis of Critical Hydraulic Gradient for Particle Movement in Filtration*'. Journal of Geotechnical and Geo environmental Engineering, April 2002
- [28] Indraratna B. & Vafal F. '*Analytical Model for Particle Migration within Base Soil-Filter System*'. Journal of Geotechnical and Geo environmental Engineering, February, 1997
- [29] Jansens R., '*Turbulent velocity fluctuations in filterlayer due to wave action*', MSc thesis, Delft University of Technology, 2000
- [30] Jong W. de, Verhagen H.J. & Olthof J. '*Experimental Research on the Stability of Armour and Secondary Layer in a Single Layered Tetrapod Breakwater*'. International Conference on Coastal Engineering, Lisbon, 2004
- [31] Klein Breteler M., Bakker K.J. & den Del H. '*New Criteria for Granular Filters and Geotextile under Revetments*'. Coastal Engineering, 1990
- [32] Lara J.L. '*A Numerical Wave Flume to Study the Functionality and Stability of Coastal Structures*'. PIANC Magazine AIPCN, no 121, October 2005
- [33] Liu P.L.F., Lin P., Chang K.A. & Sakakiyama T. '*Numerical Modelling of Wave Interaction with Porous Structures*'. Journal of Waterway, Port, Coastal & Ocean Engineering, 1999
- [34] Locke M., Indraratna B. & Adikari G. '*Time-Dependent Particle Transportation through Granular Filters*'. Journal of Geotechnical and Geoenvironmental Engineering, June 2001
- [35] Lone M.A., Hussain B. & Asawa G.L. '*Filter Design Criteria for Graded Cohesionless Bases*'. Journal of Geotechnical and Geoenvironmental Engineering ASCE, February, 2005
- [36] Martín F., Martínez C., Lomónaco P. & Vidal C. '*A new Procedure for the Scaling of Core Material in Rubble Mound Breakwater Model Tests*'. International Conference on Coastal Engineering, Cardif, 2002
- [37] Meer J.W. van der & Veldman J.J. '*Singular points at berm breakwaters: scale effects, rear, round head and longshore transport*'. Coastal Engineer 17 (1992), Elsevier Amsterdam, 1991
- [38] Os P., '*Hydraulic loading on a geometrically open filter structure*', MSc thesis, Delft University of Technology, 1998
- [39] Oumeraci H. & Partenscky H.W. '*Wave-Induced Pore Pressure in Rubble Mound Breakwaters*'. Coastal Engineering, Ch 100, 1990
- [40] Oumeraci H. '*Role of Large-Scale Model Testing in Coastal Engineering -Selected Examples Studies performed in GWK Hannover*'. Towards a Balanced Methodology in European Hydraulic research, Budapest, May 2003
- [41] Rouck J. de & van Damme L. '*Overall Slope Stability Analysis of Rubble Mound Breakwaters*'. International Conference on Coastal Engineering, Orlando Florida, 1996
- [42] Schiereck G.J., '*Introduction to bed, bank and shore protection*' Delft, 2001
- [43] Schiereck G.J., Fontijn H.L., d'Angremont K. & Steijn B. '*Filter Erosion in Coastal Structures*'. International Conference on Coastal Engineering, Sydney, 2000
- [44] Tirindelli M. & Lamberti A. '*Wave Action on Rubble Mound Breakwaters: the Problem of Scale Effects*'. DELOS EVK3-CT-2000-00041

-
- [45] Troch P. 'VOFbreak, *'A Numerical Model for Simulation of Wave Interaction with Rubble Mound Breakwaters'*. Environmental and Coastal Hydraulics, 1996
- [46] Troch P., De Rouck J. & Burcharth H.F. *'Experimental Study and Numerical Modelling of Wave induced Pore Pressure Attenuation inside a Rubble Mound Breakwater'*. International Conference on Coastal Engineering, Cardiff, 2002
- [47] Troch P., De Rouck J. *'Development of Two-Dimensional Numerical Wave Flume for Wave Interaction with Rubble Mound Breakwaters'*. International Conference on Coastal Engineering, Copenhagen, 1998
- [48] Troch P., de Somer M., de Rouck J., van Damme L., Vermeir D., Martens J.P. & van Hove C. *'Full Scale Measurements of Wave Attenuation inside a rubble Mound Breakwater'*. International Conference on Coastal Engineering, Orlando, Florida, 1996
- [49] Uelman E.F., *'Granular geometrically open filters in breakwaters with a sand core'* MSc thesis, Delft University of Technology, 2006
- [50] Vries M. de *'Waterloopkundig onderzoek college handleiding b 80'*. Delft, 2004
- [51] Watanabe A, *'A Sheet-Flow Transport Rate Formula for Asymmetric, Forward-Leaning Waves And Currents'*, International Conference on Coastal Engineering, Lisbon, 2004
- [52] Wörmann A. *'Riprap Protection without Filter Layers'*. Journal of Hydraulic engineering Vol 115, no. 12, 1989
- [53] Zhao Q., Armfield S. & Tanimoto K. *'Numerical Simulation of Breaking Waves by Multi-Scale Turbulence Model'*. Elsevier, Coastal Engineering 51 53-80, 2004

Appendix I Study Report Evert Uelman

A study of Evert's report to get familiar with the subject, the global theory and directions to other sources of knowledge.

- Breakwaters with a sand core can be more economic
- More flexibility with geometrically open filters
- No proper design tool available
- Objective:
 - o Insight in transport of sand out of the core
 - o Relations between
 - Transport
 - Initiation of transport
 - Grain size filter / core material
 - Thickness filter
 - Hydraulic loading

Experiments: $H = 10\text{cm}$, $T = 1,2\text{s}$, $d_f = 10/15/20\text{cm}$, $D_f = 1,8/3,3/4,2\text{cm}$. Regular waves, no scaling. Observed:

- Decreasing $d_f \rightarrow$ shift from bottom transport to suspension transport Increasing $D_f \rightarrow$ shift from bottom transport to suspension transport.
- Upper part: erosion (A-D). Lower part: accretion
- Increasing $m \rightarrow$ less erosion, lower erosion depth d_s , lower erosion length L_{r2} ($m = d_f/D_{f50}$)
- Erosion decreases in time, but after 2400 waves no equilibrium was reached.

Theory open filter processes

Area of interest: $2,5 < (n_f * D_{f15}/D_{b50}) < 6 \text{ à } 7$. Lower values: geometrically closed, higher values: fluidization/ no filter working.

Occurring mechanisms:

- Grains arrive in larger pores with lower water velocities and slow down and stop moving further.
- Arching: small grains form arches. Cyclic loads (waves) destroy arches and have a lower critical gradient.

The critical gradient is a function of:

- Core- and filter material characteristics
- Flow type (filter velocity, physical properties of water)

Empirical formula with flow parallel to the interface:

$$\text{De Grauw: } I_{cr} = f\left(D_b, \frac{D_f}{D_b}, n_f\right) \rightarrow I_{cr} = \left(\frac{0.06}{n_f^3 D_{f15}^{4/3}} + \frac{n_f^{5/3} D_f^{1/3}}{1000 D_{b50}^{5/3}}\right) U_{*cr}^2$$

If the pore spaces of the filter are large relative to the grain size of the core material, the critical shear stress at the interface is assumed to be equal to that at the bottom of an open channel (bed material equals core material). Klein Breteler: used Shields criteria to relate the critical filter velocity to the D_{50} of the core material (p.20)

For turbulent flow parallel to the interface at a horizontal bed: $I_{fcr} = \frac{C_7 \psi_b \Delta_b D_{b50}}{\kappa^2 D_{f15}}$

Wörmann: single layer of riprap protection around bridge piers: acts as a moderator of the erosion process due to the hydraulic filter effect. Important parameters: $\frac{U^2}{g \cdot d_f}$ and

$$\frac{D_{b85}}{D_{f15}} \text{ (p.21)}$$

Transport

Adel: for perpendicular flow, the type and magnitude of transport depends on the gradient in the core. Collective transport, no single grains. A sharp boundary between penetration in filter or not.

For parallel flow, transport is governed by independent movement of grains. Movement along the interface in a thin layer for low velocities. Higher velocity: thicker layer. $U_{\text{grain}} \approx \frac{1}{2} U_{\text{water}}$.

Waves and water motion

Wave energy: $E_t = E_d + E_r + E_i$.

Porous flow: laminar/ inertial/ turbulence resistance. Through sand: only laminar. Gravel/ rubble mound structures: also inertial/ turbulence. Flow depends on Reynolds number. (p.26)

Non-stationary porous flow: Forchheimer equation: $I = a \cdot U + b \cdot U \cdot |U| + c \frac{dU}{dt}$ (p.26)

– Terms: first = laminar, second = turbulence, third = inertial

Disconnection with wave loading: friction $\rightarrow U_f > U_{\text{core}} \rightarrow U_{\text{internal phreatic surface, f}} > U_{\text{internal phreatic surface, b}} \rightarrow$ A discontinuity can exist between core and filter. (p.28)

Internal set-up: water table inside the breakwater is higher than the still water level outside. Outflow mainly happens in the lower part, the water has to flow through a smaller surface than during inflow. This requires a higher pressure gradient, realized by a higher water level inside.

Numerical models

ODIFLOCS: a hydraulic model simulating the external flow, coupled to a porous flow model with the extended Forchheimer equation. (p.28)

VOFbreak²: describes wave induced flows and pressures in porous structures. (p.29). Better wave induced velocity field, but no turbulence.

VARANS: also small scale turbulence in porous media can be modelled.

All give an averaged velocity field.

Scaling

Geometric/ kinematic (velocities)/ dynamic (forces) similarity

Froude-scaling: $n_{Fr} = 1 \rightarrow n_t = n_u = n_l^{1/2} = n_p^{1/2}$.

Reynolds-scaling: $n_{Re} = 1 \rightarrow n_t = n_l^2$
 $n_u = n_l^{-1}$
 $n_p = n_l^{-2}$

Burcharth: keep the hydraulic gradient the same inside the breakwater core. (p.31)
 Problem: the gradient varies in time, so a characteristic gradient is used. The deviation of this characteristic gradient and velocities remains a problem.

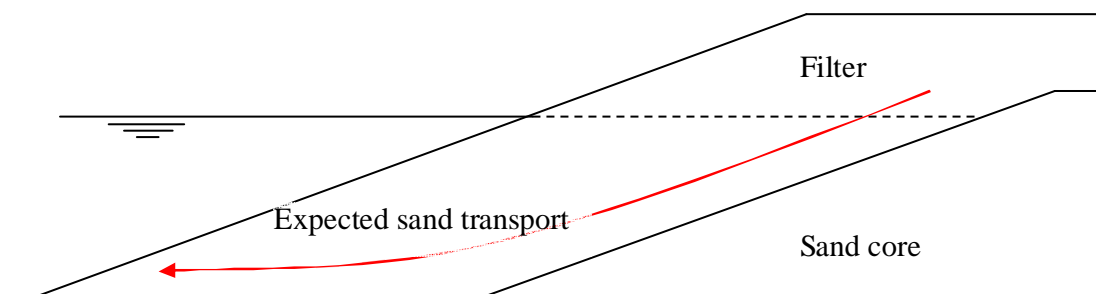
Experiments

Objectives/focus: (p.34)

- Transport of sand through a very coarse filter under non-stationary loading
- Amount of transport out of the core
- Transport rate

Concept/ expectations: (p.36)

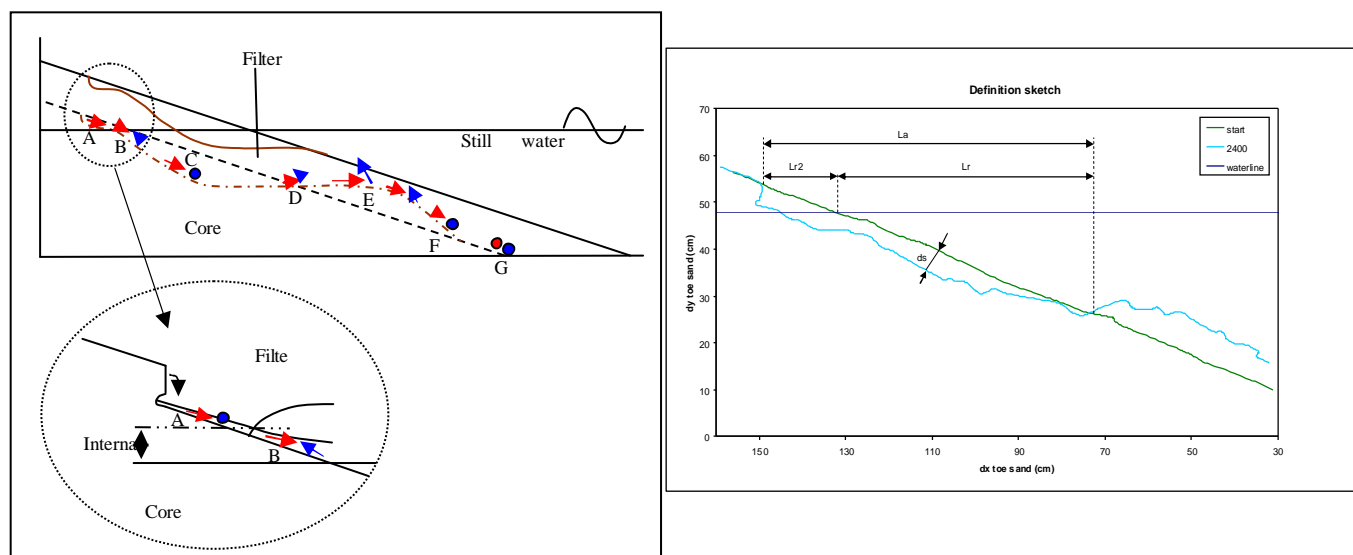
- The filter will reduce H exponentially when moving inside the filter, so $d_f \uparrow \rightarrow$ transport \downarrow .
- A thicker filter slows down the wash out.
- Wave breaking causes a lot of turbulence, which gives pressure fluctuations that, when directly above the interface, will lift grains out of the core.
- A larger D_b means less transport.
- A smaller D_f means less transport.
- A smaller D_f/D_b means less transport.
- The way of breaking of the waves might be important
- Uniformity of the filter material: more uniform means easier transport
- The shape of the material (roundness/ roughness)
- Density of the material, can have effects in both more and less transport



Schematization of expected sand transport in breakwater

Model set up: (p.38)

- A process based model test is chosen (no scaling of a larger model) because of the problems with scaling described above and the problem that sand cannot be scaled down, it becomes silt.
- Parameters: variable: D_f and d_f . the rest is set at a representative value. (p.41)
- Regular waves have been used
- H and T typical for wind waves, $H = 10$ cm, $T = 1,2$ s.
- Number of waves: typical for a storm of 8 hours with a T of 12 s.
- D_b is chosen small to get erosion
- Only one layer is used as filter/ armour.



Observations: (p.48)

- A profile develops resembling a bar profile on a sandy beach.
 - Both bottom (sheet flow) and suspension transport have been observed.
- A: erosion, an almost vertical slope develops and is undermined by the up running wave.
- B: sand is moving up and down by the reduced wave, not in phase with the outside wave.
- C: erosion, mainly bottom transport during wave run-down, less transport during wave run-up, but also suspension transport.
- D: net erosion = zero. Run-down: mainly bottom tr. Run-up: mainly susp. tr.
- E: sedimentation, a lot of suspension-transport.
- F: only transport during run-down, first both types, later only bottom transport.
- G: no transport.
- Internal setup ranging from 0 or 1 to 3 cm for different tests.
 - Between A and B a small wave in the filter layer develops, running up and down the sand slope.
 - Between C and F: the outside water layer is much thicker with the up-running wave than with the down-running wave, so more water has to flow through the filter during run-down than during run-up. The result is a higher filter velocity during run-down.

Analysis: (p.55)

- The erosion in A is discontinuous, hard to tell if it is decreasing in time or not.
- At B and C the erosion is decreasing in time.
- At E the sedimentation is decreasing in time.
- After 2400 waves there is still erosion, but it is decreasing in time
- A dependency on m is clearly visible from the results (p.58), a smaller m ($=d_f/D_f$) means less erosion.
- L_r increases with increasing filter thickness, probably because point D stays directly under the run-down point of the wave, which shifts further down.
- L_r increases with increasing D_f , because larger stones give less wave reduction.
- L_{r2} decreases with increasing m and with increasing d_f and with decreasing D_f .
- Erosion depth d_s ($=$ erosion after 2400 waves / L_a) (p.66). A larger D_f and a smaller d_f give a larger d_s . Both were to be expected.

- d_s vs m gives a possible linear relation: $d_s \approx 0.058 - 0.4 \times m$. d_s decreases with increasing m , so more layers of filter grains reduce the erosion depth.

Recommendations

Conclusions:

- The erosion, d_s and L_{r2} depend on m ($=d_f/D_{f50}$). All decrease with increasing m . This relation is more sensitive for $2 < m < 4$ than for $m > 5$.
- A “sandy beach bar-profile” develops with a fixed turning point D .
- Erosion length also dependent on the wave run-down point.
- Sheet flow- and bottom transport of core material.
- Water movements: main wave and small internal wave ($H \approx 1$ cm).
- Run-up mainly on the outside; run-down mainly through the filter.
- Erosion decreases but does not become zero in 2400 waves

Recommendations:

1. The data set obtained in this thesis should be extended
2. The erosion should be related to the wave parameters and the slope steepness of the breakwater. Suggested is to perform process-based experiments.
3. Model tests should be executed with irregular waves
4. Insight in the water movement inside the filter layer must be obtained.
5. A theoretical description of the transport of sand inside a filter layer under influence of a wave load should be developed.

Remarks:

- The scaling problem should be handled and sorted out at some point, possibly by repeating a few essential tests in the Delta flume and comparing the results. The conclusions for the small scale tests might be corrected if possible.
- Suggestion by Greg Smith: first perform tests with irregular waves and study the differences.

Comparison test profile with beach erosion profile

Based on the results of Uelman’s tests, a comparison between the erosion profile of the tests and that of sandy beaches has been made. This was done after the literature study and did not lead to clear relations, but it is shown in the appendices for information and because the comparison does give interesting indications.

For beach slopes under wave attack, an equilibrium beach profile is normally reached, with $z = px^{0,78}$ (Schierck, 2001). For sand of 0,16 mm, p is about 0,1. When plotted together with the profile from the test, a resemblance can be observed in the slope of the upper side of the occurring bar in the tests and the average slope of the equilibrium profile. Without a filter layer, the sand takes the purple profile, and with the filter, this profile seems to take form at a larger depth, the slope around the waterline-slope intersection is much steeper. See Figure 8-2. The test profile lies about one wave height (0,10 m) lower than the equilibrium profile that starts at the waterline intersect. It might be possible that the filter is in the way of the development of such an equilibrium profile, but that a part of the profile occurs in the upper bar area, where a sort of free sand surface develops within the filter layer. Comparison with more test data can give more insight.

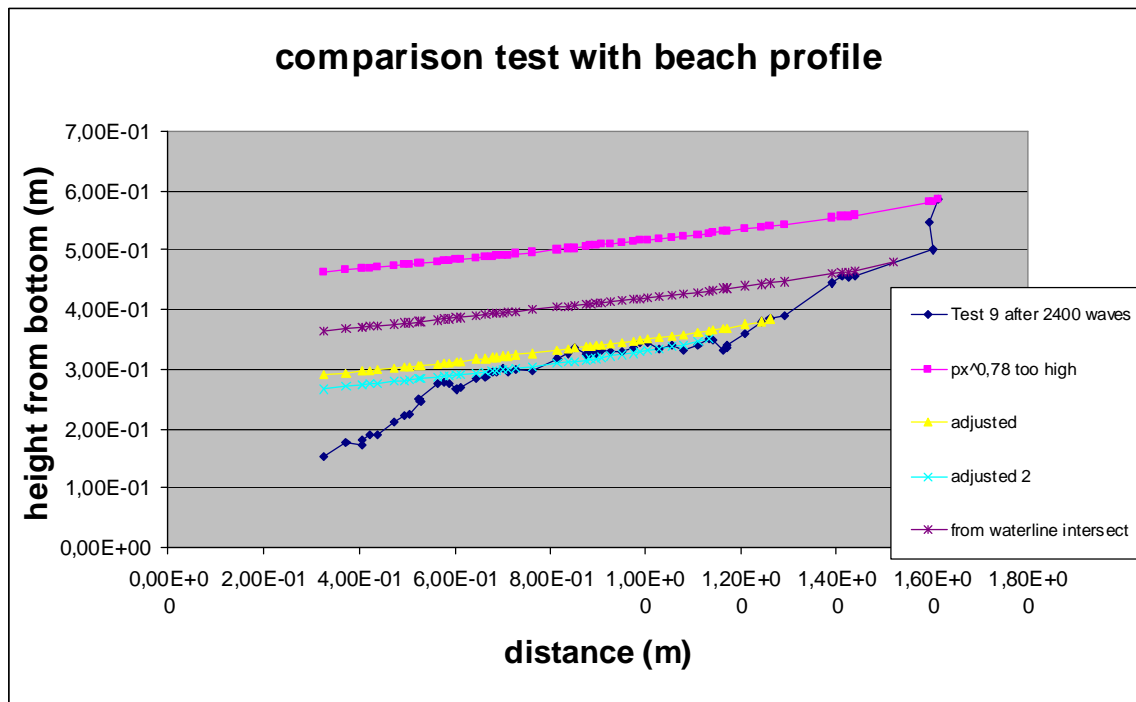
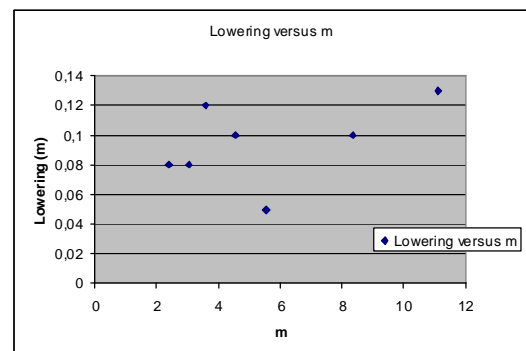
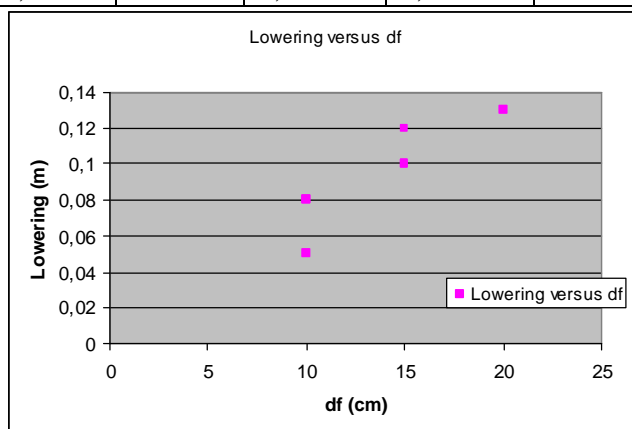
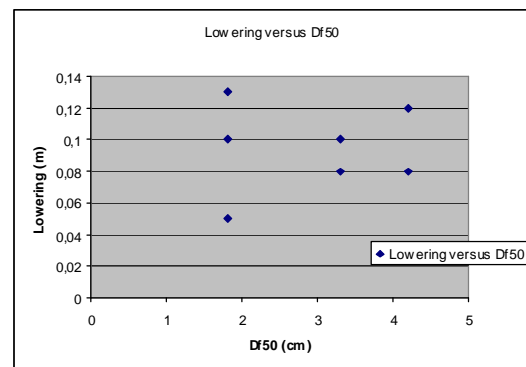


Figure 8-2 comparison of tests and equilibrium beach profile

Comparison with the other tests shows a similarity: after 2400 waves the erosion profile shows a slope resembling the lowered beach profile. For some of the tests this resemblance is clearer than for others. The distance over which the beach profile is lowered to fit the test profile differs from test to test and varies from 0,05 to 0,13 m. This distance seems to depend mostly on the thickness of the filter layer, and increases with an increasing filter layer thickness.

Df50	df	lowering	m	Test no.
1,8	10	0,05	5,555556	5
1,8	15	0,1	8,333333	3
1,8	20	0,13	11,111111	4
3,3	10	0,08	3,030303	7
3,3	15	0,1	4,545455	6
4,2	10	0,08	2,380952	9
4,2	15	0,12	3,571429	8



Appendix II Literature study

Articles, publications of research, give detailed information on specific subjects. They are used to get deeper into a subject pointed out and described in a book.

Porous flow

van Gent M.R.A. 'Porous flow through rubble mound material'. Journal of Waterway, Port, Coastal & Ocean Engineering, May/June 1995

- Laminar resistance in sand, also turbulence and inertial resistance in rubble material.
- In small scale physical models none of the three can be neglected.
- Oscillatory flow probably causes more turbulence than stationary flow, which causes a higher b-coefficient in the Forchheimer equation. This is the highest term of the equation in all the tests.
- KC-number \approx (influence of turbulence) / (influence of inertia). KC is put in the relation for b.
- The c-coefficient is also dependent on the flow field, on the Ac number (acceleration). Added mass has been taken into account: the amount of momentum needed to accelerate a certain volume of water is higher in porous media than in free flow. This can be seen as more mass that has to be accelerated.

Van Gent M.R.A. 'Wave interaction with permeable coastal structures'. Thesis, 1995

- A Reynolds number for porous medium is presented as $Re = \frac{\hat{U}D}{nv}$. Here \hat{U} is the velocity amplitude (maximum velocity), D is the particle size, n is the porosity and v is the kinematic viscosity. This form of the Reynolds number differs from the normal Reynolds number in that the characteristic length scale is $\frac{D}{n}$ instead of just D or h . This implies that the length scale is larger for a smaller porosity, resulting in a larger Reynolds number, which seems to be illogical. It would be expected that a higher porosity, larger pores, leaves more room for turbulent eddies, and gives less resistance for the turbulent flow.
- Chapter 3, porous media flow, explains the Forchheimer relation and all its parts. After that, results of permeability measurements are treated and some remarks are made on scaling problems. Table 3.4 gives Reynolds numbers that can be used for comparisons.

Criteria and processes for filter design

de Grauw A., van der Meulen T. & van der Does de Bye M. 'Granular Filters: Design Criteria'. Journal of Waterways, Port, Coastal and Ocean Engineering, 1984

- A summary of design criteria for granular filters and tests with parallel/perpendicular flow with steady and cyclic loading.
- Laminar flow for $Re < \text{about } 4$ ($Re = u_f \cdot D/v$) for which Darcy's law is valid, turbulent flow for $Re > 600 - 1000$, for which $u_f \propto I^{1/2}$.
- Cyclic flow parallel to the interface: the I_{cr} is of the same order as for steady flow ($T > 2$ s.).

- Cyclic parallel flow may cause gradients perpendicular to the interface, causing perpendicular transport.
- LARGER CORE MATERIAL GIVES A LOWER I_{cr} !!??
- Formula derived to link I_{cr} to the critical Shields velocity (6).
- Internal stability:
- Very widely graded materials are less permeable.
- Interesting article.

Klein Breteler M., Bakker K.J. & den Del H. '*New Criteria for Granular Filters and Geotextile under Revetments*'. Coastal Engineering, 1990

- Geometrically open, but hydrodynamic sand tight filters.
- Criteria based on a hydrodynamic limit, assuming similarity between open channel flow and flow in the pores at the interface, because the pores of the filter are much larger than the grains of the core. The Shields critical shear stress is applied here.
- Relation for parallel flow derived between the critical filter velocity and Shields, the soil properties, the slope angle and the perpendicular hydraulic gradient.
- Forchheimer relation is used to relate the filter velocity to the filter material.
- A design diagram for granular filter interfaces is given. Suitable for practical use, but, for breakwaters, special attention has to be paid to the dynamic effects of the flow in between the large elements, and, the hydraulic loading conditions have to be known.
- Interesting article, still, information about very open filters is not present.

Bakker K.J., Verheij H.J. & de Groot M.B. '*Design of Geometrically open Filters in Hydraulic Structures*'. Filters in Geotechnical and Hydraulic Engineering, Balkema, the Netherlands, 1993

- Hydraulic sand tight instead of geometrically sand tight criteria.
- Section 3: load transformation from waves to external pressure head, to internal pressure head, to the response of the structure. These steps are not easy, but necessary for a good geometrically open filter design. Also for sand-open filters these are very important.
- Examples are presented, using the diagram of Klein Breteler 1990, design steps are explained.

Bakker K.J., Verheij H.J. & de Groot M.B. '*Design Relationship for Filters in Bed Protection*'. Journal of Hydraulic Engineering Vol 120, No 9, 1994

- Derivation of I_{cr} of the top layer, and of the filter layer, from the shear stress, Shields and Bezuijen et al. (1987).
- A comparison with the filter ratio of Wörmann (1989) has been made, resulting after some modifications and averaging (!) in $\frac{D_{f15}}{D_{b50}} = 0,50 \frac{R}{D_{r50}}$. This implies that a bigger hydraulic radius R (\approx waterdepth) and a smaller top-layer grain size result in a higher possible filter ratio. Caution with this formula is needed.

Bezuijen A., Klein Breteler M. & Bakker K.J. '*Design Criteria for Placed Block Revetments and Granular Filters*'. 2de copedec, Beijing, China, 1987

- The hydraulic gradient in these filter layers is often so small, that less strict than sand-tight rules can be applied. The filter layers discussed in the paper are,

however, covered by a placed block revetment, so this is not directly applicable for filters without cover layers.

de Groot M.B., Bezuijen A., Burger A.m. & Konter J.L.M. *'The Interaction between Soil, Water and Bed or Slope Protection'*. Modelling Soil-Water-Structure Interactions, the Netherlands, Balkema, 1988

- Scaling: the ratio of the flow resistances in the model and in nature should be constant, irrespective of location and time (forces requirement). And: the ratio between discharge in the model and in nature should be constant (continuity requirement).
- Froude scaling is possible, but scaling down reduces the Reynolds number. This gives problems.
- Internal set-up: the increase in level of the internal phreatic surface above the average level of the external phreatic surface.
- Internal storage is not important if the cover layer is very permeable.

Wörmann A. *'Riprap Protection without Filter Layers'*. Journal of Hydraulic engineering Vol 115, no. 12, 1989

- Stationary, turbulent flow experiment, with sand covered by one layer of stones around a cylinder.
- A thicker protection layer reduced the flow velocities near the interface and reduced the erosion depth for the same hydraulic loading.
- The used core material is quite large for sand; smaller grains can give different mechanisms (cohesion).
- The riprap layer acts as a moderator of velocities and turbulent vortices, reducing the erosion depth. The shape of the scour hole is similar to that with an unprotected bed.
- The thickness of the riprap layer determines the reduction of scour.
- $\frac{U^2}{g \cdot d_f} \approx 6 \frac{D_{b85}}{D_{f15}}$ if $\frac{D_{b85}}{D_{f15}} < 0.1$. for larger ratios the coefficient increases asymptotically, towards geometrically closed criteria (Terzaghi: ratio > 0,2).
- A larger gradation in the riprap material is preferred to get a well functioning, but relatively thin filter layer. This, however, can give problems in construction: separation has to be avoided.

Schiereck G.J., Fontijn H.L., d'Angremont K. & Steijn B. *'Filter Erosion in Coastal Structures'*. International Conference on Coastal Engineering, Sydney, 2000

- Overview of some of the topics above, with additional tests.
- Tests show that velocity fluctuations hardly reduce further inside the filter layer, so the reduction in erosion by a thicker filter is most probably due to the longer path grains have to follow to leave the filter.

Foster M. & Fell R. *'Assessing Embankment Dam Filters that do Satisfy Design Criteria'*. Journal of Geotechnical and Geo environmental Engineering, May, 2001

- Tests with filters for perpendicular flow, tested for the no-erosion boundary and the coarsest filter grain size boundary, for which the filter sealed itself after initial erosion. The ratio between no-erosion and coarsest filter sealed, ranging from 1,6 to 24.

- Interesting to see the differences in the boundaries for different soils (e.g. different clay content), but no relation with wave loading, and the tests do not say a lot about the physical small scale processes.
- It can be interesting to compare the D_{f85}/D_{b15} ratios with the results of Evert and coming results, to see if there is coherence between this flow-type and wave-loading.

Numerical modelling of filter processes

van Gent M.R.A. *'The Modelling of Wave Action on and in Coastal Structures'*. Elsevier, Coastal Engineering 22 311-339, 1994.

- ODIFLOCS: One Dimensional Flow on and in Coastal Structures: a hydraulic model is coupled to a porous flow model.
- The hydraulic model uses the long wave theory, with hydrostatic pressures, depth-averaged velocities, a single layer of water, and wave-breaking simulation like a bore.
- The porous flow model uses the extended Forchheimer equation and the long wave equations. u is replaced by u/n e.g.. Constant values have been used for the coefficients.
- The slope is divided into three areas with different treatment; from the part overlapped by the hydraulic model, the part with infiltration through a partly saturated area, to the part with no exchange to the outside.
- Disconnection is taken into account and internal set-up can be calculated.
- Run-up can be calculated accurately, run-down within $2 < \xi < 3$.
- The model works well, but is only one-dimensional and does not take turbulence generation-dissipation into account.

van Gent M.R.A., Tönjes P., Petit H.A.H. & van den Bosch P. *'Wave Action on and in Permeable Structures'*. Coastal Engineering 125, 1994

- A numerical model to simulate plunging waves on breakwaters, with the VOF- (Volume Of Fluid) method to solve the 2D-V Navier-Stokes equations.
- The model gives a detailed flow description of breaking waves on permeable structures.
- Turbulent generation-dissipation and air-extrusion are not in the model, neither are irregular waves (yet).

Troch P. *'VOFbreak, A Numerical Model for Simulation of Wave Interaction with Rubble Mound Breakwaters'*. Environmental and Coastal Hydraulics, 1996

- VOFbreak²: a coupling of the VOF-model for external water motion (based on the Navier-Stokes equations) to a porous flow model using the Forchheimer resistance terms instead of the viscosity terms in the Navier-Stokes equations.
- The same remarks as for van Gent (1994) (above) hold.

Troch P., De Rouck J. *'Development of Two-Dimensional Numerical Wave Flume for Wave Interaction with Rubble Mound Breakwaters'*. International Conference on Coastal Engineering, Copenhagen, 1998

- Further elaboration on the VOFbreak² model, in order to construct a numerical wave flume.
- 2D velocity field calculations.

- No Turbulent generation-dissipation is taken into account.
- It would be interesting to try to repeat some of Uelman's tests numerically and evaluate the differences, but the wave breaking is still difficult, and how to incorporate the actual transport of sand from the core?

Hólscher P., de Groot M.B. & van der Meer J.W. '*Simulation of Internal Water Movement in Breakwaters*'. Modelling Soil-Water-Structures Interactions, Balkema, The Netherlands, 1988

- Wave attenuation in porous media, simulated with the Hadeer computer program. It was found that the phenomena of disconnection and internal set-up are important for the behaviour of the structure.
- The effect of wave breaking is lacking.

Liu P.L.F., Lin P., Chang K.A. & Sakakiyama T. '*Numerical Modelling of Wave Interaction with Porous Structures*'. Journal of Waterway, Port, Coastal & Ocean Engineering, 1999

- The introduction gives a clear overview of the research done previous to this.
- The external wave field is described by the Reynolds averaged Navier-Stokes (RANS) equations, the effects of the turbulence field by an improved k- ϵ model, and the free surface by the VOF method.
- The internal flow field is derived from the Navier-Stokes equations, and averaged over length scale l_p , which is larger than the pores but smaller than the characteristic length scale of the physical problem.
- A well working model for wave action on and in the armour layer is presented, interaction with a core is not included.

Hsu T.-J., Sakakiyama T. & Liu P.L.F. '*A Numerical Model for Wave Motions and Turbulence Flows in Front of a Composite Breakwater*'. Elsevier, Coastal Engineering 46 25-50, 2002

- "An accurate prediction of turbulence under a breaking wave is an ongoing and challenging research object". The wave breaking process, the turbulence generation inside the boundary layer near the bottom and the turbulence flow in the porous media are all three important factors for the interaction between breaking waves and structures.
- The model of Liu and Lin (1999) has been improved and extended, using the VARANS equations, Volume-Averaged, Reynolds-Averaged Navier-Stokes equations, along the k- ϵ turbulence closure model. This combination can describe flow both inside and outside the porous medium.
- The internal flow field is still volume-averaged.
- The model shows improvements, but wave breaking is still difficult to calculate in all cases.

Zhao Q., Armfield S. & Tanimoto K. '*Numerical Simulation of Breaking Waves by Multi-Scale Turbulence Model*'. Elsevier, Coastal Engineering 51 53-80, 2004

- Study of breaking waves, with a 2D multi scale turbulence model based on the VOF method, but without interaction with structures.
- Improvements compared to the RANS- approach are most clear under spilling breakers. Air entrainment is not accounted (neither in the other models) and still needs attention.

- Interesting for the modelling of the external water motions.

Scaling problems

Ettema R., Arndt, R., Roberts, P., Wahl, T., *'Hydraulic Modelling – Concepts and Practice'*. American Society of Civil Engineers, 2000

- 1.6.1: “Similitude and scaling: Geometric, kinematic and dynamic similarity should be maintained between model and prototype.” In practical situations this is however not possible. Therefore, a dimensional analysis can be made to identify the processes and parameters of primary importance.
- A dimensional analysis is a useful tool to formulate the problem and ensure that similitude conditions are taken into account properly.
- “Scale-series” can be very useful: applying a model at different scales, extrapolating the results to the prototype scale. The results should be handled with caution.
- Conservation-of-momentum-equation for flow: after being made dimensionless, four important parameters are found: Euler number, Reynolds number, Froude number and Weber number. In general, Fr is the dominant similitude parameter for free surface flow. Re is always important, but Fr and Re cannot be preserved simultaneously. Eu is usually preserved when Fr or Re is. Surface tension becomes important when We is smaller than 100, which occurs in drops, bubbles, capillary flow or very shallow flow (p.41).
- For oscillation flow, the Strouhal number, St, can be important, but it is usually not the prescribing criterion.
- Table of common dimensionless groups on p. 44
- Π -theorem: a dimensionally homogeneous linear equation is reducible to a functional relationship among a set of dimensionless parameters. (p. 45)
 - List all n relevant physical quantities, expressed in terms of the fundamental dimensions
 - Note the number of fundamental dimensions, m
 - Select m physical quantities as repeating variables, such that:
 - None is dimensionless
 - No two have the same dimensions
 - Together they do not form a Π parameter
 - They include all fundamental dimensions involved
 - Express the terms as the product of the terms selected in step 3
 - Solve the unknown exponents
- Waves and flow in coastal situations: p.239
- Planar bed in the breaking zone: p. 249
- P. 248: when sand is used in a model, the particle Reynolds number will be highly distorted, as will the mobility number and the geometry.
- Basic scaling ratio for bedload and suspended sediment transport under waves: $(u_*)_r = Y_r^{1/2}$, in which Y is the waterdepth. (p.250)
- Dean number for beach erosion/ accretion: $\frac{H_0}{wT}$ expresses the importance of the fall velocity and breaking waves that lift the particles. Fowler and Hughes (1991) recommend similitude of this Dean number for sediment movement in the breaking zone. (p.252)

- Simultaneous modelling of bedload and suspended sediment transport is complicated by differences in the fluid motion process.

Hughes S.A., 'Physical models and laboratory techniques in coastal engineering'. World Scientific, 1993

- Explains the dimensional analysis and gives examples specified to coastal engineering. The four main steps are:
 - Identify the important independent variables of the process
 - Decide which variable is to be the dependent variable
 - Determine how many independent dimensionless products can be formed from the variables
 - Reduce the system variable to the proper number of independent dimensionless variables.
- Put the variables in the three main categories Geometry, Material Properties and External Effects. Some, like time, do not fit one of them, but can be very important.
- Rule of thumb for the Buckingham Pi theorem (also called Pi-theorem or Π -theorem): In a dimensionally homogeneous equation involving n variables, the number of dimensionless products that can be formed from n variable is $n - r$, where r is the number of fundamental dimensions encompassed by the variables. In a dimensionally homogeneous equation, the dimension of the left-hand side variable equals the dimension of any of the terms on the right-hand side that stands by itself. E.g.: $x_1 = f(x_2, x_3, x_4, \dots, x_n)$. According to the Pi-theorem, such equation can be rearranged into a new equation expressed in terms of dimensionless products (Pi-terms) as: $\Pi_1 = \Psi(\Pi_2, \Pi_3, \dots, \Pi_{n-r})$.
- Similitude criteria are imposed by physical relationships between parameters, also called scale laws.
- Similarity conditions are chosen by the experimenter to make the model reproduce satisfactory results.
- Methods to establish model similitude:
 - Calibration, a lengthy trial and error method, sometimes still used for very complicated processes, like movable-bed models.
 - Differential Equations, if they are known and shown to be accurate, they can be made dimensionless and used for similitude.
 - Dimensional Analysis, a method to come up with dimensionless products from the process variables, the dimensionless terms to be preserved in the scaling process. Physical insight in the process is required for making the right choices.
 - Scale Series, several models constructed at different scales. Useful for complicated processes, but the extrapolation of results to prototype scale must be done with great care, as scale effects might still be introduced.
- A distinction is made between geometric similarity, kinematic similarity and dynamic similarity (p.54).
- Froude criterion, p.64, Reynolds criterion p.65, etc.
- The Reynolds number for porous flow in a breakwater: the length scale should be the average void dimension. The Reynolds number for this case should be above 30.000 in order to be able to neglect the viscous effects, p.70. For higher Re numbers, the viscous force does not depend on it.

- Models that maintain geometric similitude are called undistorted models, p.76.
- Conditions for short-wave model similarity, p.91:
 - o The Froude number must be preserved
 - o The Strouhal number must be preserved
 - o The Reynolds number must be preserved
 - o The Euler number must be preserved
- The first two indicate that Froude scaling must be applied, with the period scaled the same as the Froude time scale. The third is usually not fulfilled, while the fourth is automatically met.
- Wave transmission through rubble mound structures is reduced in small scale models because the frictional losses on the small scale are greater. Usually the size of model stones is increased to counter this effect, p.101.
- Surface tension rule of thumb: effects important for periods $< 0,35$ s and water depth < 2 cm. p.107.
- Wave breaking: difference in air entrainment between model and prototype have no significant dynamic influence, as the total energy budget remains in similitude by the momentum theory, p. 116.
- Salt vs fresh water: 3 % density difference, but up to 15 % difference in breakwater stability if no corrections are made. P. 117.
- P. 170: definition rubble mound structures.
- P.173: needed knowledge before designing a model.
- From p. 175: Dimensional analysis of rubble mound structures. Main findings:
 - o Rubble mound structure models must be geometrically undistorted in length scale.
 - o Flow hydrodynamics is a rubble-mound structure model must conform to the Froude criterion.
 - o Rubble-mound structure models must have turbulent flow conditions throughout the primary armour layer.
 - o The surface of structure units is to be made as smooth as possible.
 - o The ratio of density of stone and water is to be preserved.
- Hudson, et al. (1979) recommended that the stability number is to be preserved, p.180. This is aimed at armour stability mainly.
- P.185: Graph with viscous scale effect as a function of Re, interesting, shows that for a H of 0,10 m and a D_{50} of 0,033 m, $Re = 2,5 \times 10^4$, which gives some scale effect, but not very great, about 10%.
- For core material, viscous effects are more important, and core material can therefore be made too large in the model to compensate the viscous effects. This can be done with a distortion factor K, p.186.
- Tests of Van der Meer (1988) with irregular waves and Dai and Kamel (1969) show that H_s for irregular waves corresponds reasonably well to H of regular waves for the determination of minimum Re numbers.
- Minimum Re ranges from 6×10^3 to $4,5 \times 10^5$, but values in the order of 3×10^4 to 4×10^4 seem safe as they were found in more experiments.
- Air entrainment: the water bubbles are relatively larger in the model than in the prototype. The scale effect is not understood well enough to quantify, but indications are given. Larger bubbles lead to too much energy dissipation in the model, reducing the wave run-up.
 - o Most air entrainment occurs above SWL
 - o Air entrained during run-up, bubbles rise due to buoyancy
 - o Aeration increases with T for constant H

- Bubbles penetrate deeper for increasing H
- Plunging breakers give highest aeration
- Aeration and penetration increase with increase slope steepness
- Aeration is more severe in highly permeable structures
- 1:50 is a very common length scale; Hudson recommends 1:5 to 1:70 as feasible, p.192.
- From p.199: model operation, types of testing.
- P.246: dimensional analysis for coastal sediment transport.
- Perfect similitude is impossible for many sediment transport situations, however, if the different parameters are adjusted in the right way, the results can be good. P.252.
- For bed-load transport, the grain size Re number and the densimetric Froude number come into play. P.248.
- Different models that satisfy part of the requirements of eqn. 6.4, for bedload transport, p.256.
 - The Best Model works well for bedload transport, but the problem is that sediment scaled down with the length scale factor often leads to particle sizes in the range of clay, and the Reynolds number is not preserved, so viscous forces can give scale effects.
 - The Lightweight Model needs lighter materials in the model, which gives other complicated effects.
 - The densimetric Froude Model is similar to the Lightweight Model, but with more freedom of choice because the Re number is not preserved.
 - The Sand Model only preserves the relative density, therefore introducing scale effects by distorted Fr and Re numbers. Scale series are recommended for the investigation of scale effects.
- For suspended sediment transport, fall speed is more important, one approach is to preserve the Dean Number, or fall speed parameter, $\frac{H}{wT}$. This parameter gives some indication of the importance of suspended load relative to bedload transport, as it can be seen as the ratio of a sediment fall time (H/w) and the wave period.
- Noda got good results for wave flume tests for equilibrium beach erosion profiles when the fall speed parameter was preserved, and much poorer results when it was not preserved. He used $\frac{\pi w}{gT}$ as fall speed parameter. Interesting because of the similarity with beach erosion profiles.
- P.296: explanation and scale factors for the fall speed parameter scaling conditions, and calculation of the fall speed. The fall speed parameter is preserved if $n_H = n_w n_T$, so e.g. with $n_w = n_T$ and $n_H = n_T^2$, which is in accordance with $n_{Fr} = 1$ for the scaling of waves.
- Criteria by Dean for geom. undistorted suspended transport models:
 - The model must be geometrically undistorted
 - Hydrodynamics should be scaled according to the Froude criterion
 - Similarity of the fall speed parameter should be maintained
 - The model must be large enough to preclude significant viscous, surface tension, and cohesive sediment effects so that the character of wave breaking is properly simulated
 - Sand is preferred as the model material

- The above criteria satisfy the Froude hydrodynamic criterion, the ratio of wave steepness H/L_0 , the ratio of fall speed parameter and the ratio of relative density. The drawback is that the Shields parameter is not preserved.
- P.312: tests by Hughes and Fowler indicate that comparison between regular and irregular waves gives best correspondence for $H_s = H_{regular}$.

Tirindelli M. & Lamberti A. 'Wave Action on Rubble Mound Breakwaters: the Problem of Scale Effects'. DELOS EVK3-CT-2000-00041

- $Fr = \frac{U}{\sqrt{gL}}$ Froude scaling: maintaining the same Froude number, $n_{Fr} = 1$. Often used when waves are the dominant force. $n_t = n_u = n_l^{1/2} = n_p^{1/2}$. Froude scaling, however, neglects the effects of viscosity and surface tension. For breaking waves, these effects can be very important, especially when $L < 0,5m$, or $T < 0,5s$.
- $Re = \frac{UL}{\nu}$ Reynolds scaling: $n_{Re} = 1$. $n_t = n_l^2$; $n_u = n_l^{-1}$; $n_p = n_l^{-2}$. Focuses on viscosity.
- $We = \frac{\rho U^2 l}{\sigma}$ Weber scaling: is important for surface tension and air entrainment. The latter might play a role in this research, as it causes a scale effect on breaking waves.
- Cauchy number scaling is related to the Mach number, and is important when compressibility is the dominant factor.
- Both intrinsic water properties of water and external factors like interaction, give scaling problems.
 - o Entrained air alters the density and compressibility of the mixture, and has a "cushioning" effect on jet impacts. Air in fresh water behaves differently than in sea water, causing different void ratios, and can influence test results. Even when sea water is used, field observations have shown higher aeration in full scale waves than in test waves.
 - o Air compression during wave impact results in a highly non-linear process, that is very difficult to model. All methods mentioned give problems.
 - o The damage of armour layers gives less scaling problems, as long as Re is high enough.
 - o Run-up and overtopping are underestimated in Froude-scaling, except for high Re numbers or for high overtopping discharges.
- Porous flow: when core material gets smaller, turbulence disappears and laminar flow becomes dominant, where in the full scale model, turbulence might give significant differences. (see also Burcharth et al. (1999))
- Transport of sediment (movable bed or in this case movable core material) gives extra scaling problems: the sediment parameters have to be scaled as well.
 - o Grains remain in suspension when $v_* > w_s$. The bed shear stress depends on various mechanisms. Suspended and bed transport cannot be scaled simultaneously in a quantitatively accurate way.
 - o For bed load the Best Model works quite well in the turbulent regime, Re is not preserved.
 - o For suspended load the dimensionless fall speed parameter is important. Shields is not preserved, but is less relevant than turbulence. The scaling of sediment particles is a problem.

- The inability to scale down the grain size correctly gives the most pronounced scale effects with mobile beds.
- P.5: properties of sea water with comparisons to fresh water. For 10^0 water:
 - Density = 1027 kg/m^3 , ratio = 1,0272
 - Viscosity = 1.356×10^{-6} , ratio = 1,037
 - Together the ratio = $1,0272 \times 1,037 = 1,0652$, or 6,5% error.
- Waves with $L < 0,5 \text{ m}$ or $T < 0,5 \text{ s}$: surface tension and viscosity effects give scale effects.
- Bullock et al. (2001) found 10% higher impact pressures in the model than in the prototype for Froude scale factor 1:25 and $H_s = 0,25 \text{ m}$.
- Scale effects for wave-structure interactions with Re_c as critical Reynolds number with $U = \sqrt{gH_s}$. The Froude criterion is applied for the scaling.
 - Dai and Kamel (1969) found no scale effects on armour damage for $Re_c > 3 \times 10^4$ with $D_{n50} = 20\text{-}300 \text{ mm}$ and regular waves.
 - Thompson and Shuttler (1975) found no clear dependency of the erosion of Re with $D_{n50} = 20\text{-}40 \text{ mm}$ with irregular waves.
 - Van der Meer (1988) and others found no significant scale effects on armour stability for $Re_c = 1 \times 10^4 - 4 \times 10^4$ with irregular waves.
 - Jensen and Klinting (1983) argued from theoretical considerations that $Re_c > 0,7 \times 10^4$.
 - Sharp and Khader (1984) proposed $Re_c = 4 \times 10^5$, but Kajima and Sakakiyama (1994) suggested $Re_c = 3 \times 10^4$ for regular waves.
- Wave run-up can be underestimated in the model. Re_c values are suggested to be the same as for wave impact.
- Van der Meer and Veldman (1991) found no significant scale effects for berm breakwater erosion patterns between a 1:7 and a 1:35 scale model. Wave overtopping and reflection were similar, only wave transmission was 10 – 50% higher in the larger model for the largest waves.
- Sediment transport scale effects are already mentioned for Hughes (1993).

Burcharth H.F., Liu Z. & Troch P. 'Scaling of Core Material in Rubble Mound Breakwater Model Test'. Coastal and Port Structures, South Africa, April, 1999

- Froude scaling gives too low Reynolds numbers (too high viscous forces), especially in the finer materials like the core.
- $I_p = I_m$, keeping the hydraulic gradient the same in modal and prototype, is a better way. I can be calculated with the extended Forchheimer equation, in which the last term can be disregarded for the porous flow is a breakwater core.
- Now the model grain structure is scaled with $I_p = I_m$ and Forchheimer, and the flow velocities with Froude scaling.
- The problem is that I and U are varying both in space and time, so a characteristic value for I has to be chosen, based on knowledge about the wave-induced pore pressure distribution in the prototype core.
 - The amplitude seems to decrease exponentially inside the core.
 - Pressures increase almost linearly with H (for constant T).
 - The horizontal pressure-amplitude-gradients are much higher than the vertical ones.
- A formula for the estimation of the pore velocities in the core is presented, using the exponential decay function, assuming harmonic oscillation of the pore pressure in a fixed point, neglecting the internal water set-up and using the Forchheimer equation to get from I to U/n . $P_{0,max}$, the reference pressure being the

pressure amplitude at $x = 0$ where the wave enters the core, has to be known beforehand.

- Suggested scaling procedure: the core grain size is such that the Froude scaling law holds for a characteristic pore velocity, which can be chosen as the average velocity of 6 characteristic points (see fig.8), averaged over one wave period. (example for the Zeebrugge breakwater is given)

Martín F., Martínez C., Lomónaco P. & Vidal C. 'A new Procedure for the Scaling of Core Material in Rubble Mound Breakwater Model Tests'. International Conference on Coastal Engineering, Cardiff, 2002

- Presents a method of defining a characteristic pore velocity in the core of rubble mound breakwaters under wave attack.
- Direct Froude scaling leads to problems if $Re < 10.000$.
- VOF calculations are used as input, RMS averaging of the instantaneous velocities is preferred above Burcharth's averaging over T.
- A four-point spatial average of the RMS value of the pore velocities is presented to replace the six-point averaging of Burcharth.
- This paper gives a further elaboration on the scaling method presented by Burcharth et al. (1999), making it more applicable in practice.
- The problem of scaling down sand remains, as the core material in these papers is much larger than sand.

Oumeraci H. 'Role of Large-Scale Model Testing in Coastal Engineering -Selected Examples Studies performed in GWK Hannover'. Towards a Balanced Methodology in European Hydraulic research, Budapest, May 2003

- Discusses the importance of large-scale model testing to overcome scaling problems.
- Physical modelling is important, especially in complex, highly non-linear situations.
- Scaling problems for various applications are discussed and examples of large-scale test set-ups are presented.
- Promising developments are in the field of combining small-scale and large-scale tests, adding numerical modelling and field measurements to validate and calibrate the tests.
- Interesting, validation of small-scale tests with large-scale tests was one idea to carry out, but is not feasible within the Msc. thesis.

Lara J.L. 'A Numerical Wave Flume to Study the Functionality and Stability of Coastal Structures'. PIANC Magazine AIPCN, no 121, October 2005

- Discussions on present state models:
 - Potential-theory models cannot describe the breaking of waves; the rotational and turbulent processes during and after breaking gives problems.
 - Smooth Particle Hydrodynamic (SPH) models calculate the kinematics of each particle and its interaction with its neighbours. This works very well, but SPH models need too many calculations for large domains and porous flow cannot be solved.
 - Navier-Stokes equation (NSE) based modelling is coming up, but still in a developing phase for the field of coastal engineering. The

technical developments in computers make these models become feasible.

- NSE models still take no turbulence generation-dissipation into account. Models that take this better into account are available now, like RANS-based models. They work better, but need large computational power. The COBRAS model is the best example at this stage.
- The COBRAS model is presented and discussed; validation gives good results and practical applications are presented.
- It would be interesting to try to model the sandy-core breakwater with the open filter, but this would rather be a thesis topic in itself than a supplement to my thesis. Further, the transport itself remains a problem to model.

Troch P., De Rouck J. & Burcharth H.F. *'Experimental Study and Numerical Modelling of Wave induced Pore Pressure Attenuation inside a Rubble Mound Breakwater'*. International Conference on Coastal Engineering, Cardiff, 2002

- Practical application of the method presented by Burcharth et al. (1999) for the Zeebrugge breakwater.
- Numerical simulation of the same situation with VOFbreak².
- Comparison shows good results, pore pressure attenuation is governed by an exponential damping model.

Troch P., de Somer M., de Rouck J., van Damme L., Vermeir D., Martens J.P. & van Hove C. *'Full Scale Measurements of Wave Attenuation inside a rubble Mound Breakwater'*. International Conference on Coastal Engineering, Orlando, Florida, 1996

- Data from full scale measurements are obtained and can be used for physical and numerical model validation.
- Wave run-up levels of up to 50% higher than in laboratory tests were found, indicating scale effects.
- The exponential decay of wave-induced pore pressure inside the breakwater is found here.

Helgason E., Burcharth H.F. & Grúne F. *'Pore Pressure Measurements inside Rubble Mound Breakwaters'*. International Conference on Coastal Engineering, Lisbon, 2004

- Comparison of small-scale and large-scale tests. In this case no large scale effects have been observed in the pore pressures.

Oumeraci H. & Partenscky H.W. *'Wave-Induced Pore Pressure in Rubble Mound Breakwaters'*. Coastal Engineering, Ch 100, 1990

- Pore pressure study starting from wave energy.
- Use of wave gauges inside the filter layer
- Wave damping by filter layer studied. The amount of dissipation in armour and filter layer is strongly dependent on ξ .

Other articles

den Adel H. *'Transportmodel voor filters dl 1 Samenvatting'*. 1992

den Adel H. *'Transportmodel voor filters dl 2 loodrechte stroming'*. 1992

den Adel H. *'Transportmodel voor filters dl 3 parallelle stroming'*. 1992

de Groot M.B., Yamazaki H., van Gent M.R.A. & Kheyruri Z. *'Pore Pressure in Rubble Mound Breakwaters'*. Coastal Engineering 124, 1994

Halter W., *'The behaviour of erosion filters under the influence of wave loads'*, MSc thesis, Delft University of Technology, 1999

Jansens R., *'Turbulent velocity fluctuations in filterlayer due to wave action'*, MSc thesis, Delft University of Technology, 2000

de Rouck J. & van Damme L. *'Overall Slope Stability Analysis of Rubble Mound Breakwaters'*. International Conference on Coastal Engineering, Orlando Florida, 1996

Indrarantna B. & Radampola S. *'Analysis of Critical Hydraulic Gradient for Particle Movement in Filtration'*. Journal of Geotechnical and Geo environmental Engineering, April 2002

Indraratna B. & Vafal F. *'Analytical Model for Particle Migration within Base Soil-Filter System'*. Journal of Geotechnical and Geo environmental Engineering, February, 1997

Locke M., Indraratna B. & Adikari G. *'Time-Dependent Particle Transportation through Granular Filters'*. Journal of Geotechnical and Geoenvironmental Engineering, June 2001

Os P., *'Hydraulic loading on a geometrically open filter structure'*, MSc thesis, Delft University of Technology, 1998

Watanabe A, *'A Sheet-Flow Transport Rate Formula for Asymmetric, Forward-Leaning Waves And Currents'*, International Conference on Coastal Engineering, Lisbon, 2004

de Vries M. *'Waterloopkundig onderzoek college handleiding b 80'*. Delft, 2004

van der Hoeven M.A. *'behavior of a falling apron'*. Msc thesis TuDelft, 2002

de Jong W., Verhagen H.J. & Olthof J. *'Experimental Research on the Stability of Armour and Secondary Layer in a Single Layered Tetrapod Breakwater'*. International Conference on Coastal Engineering, Lisbon, 2004

- This article is focussed on the interface between armour and filter, rather than between filter and (sandy) core material.

Hagerty D.J. & Parola A.C. '*Seepage Effects in some Riprap Revetments*'. Journal of Hydraulic Engineering, July, 2001

- Does not seem interesting for now, maybe for assessing failure types at a later stage.

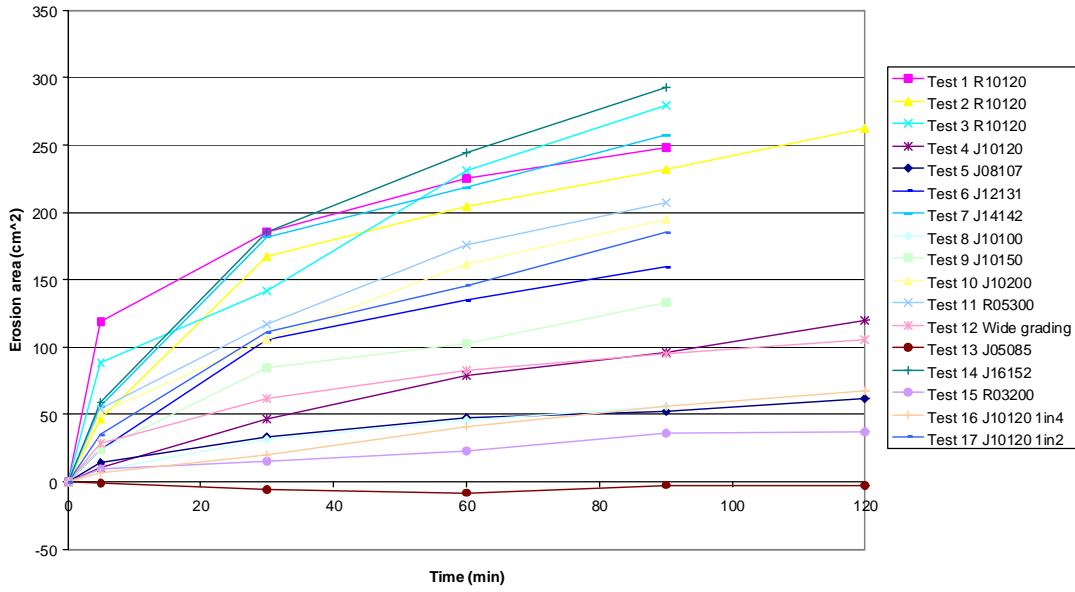
Lone M.A., Hussain B. & Asawa G.L. '*Filter Design Criteria for Graded Cohesionless Bases*'. Journal of Geotechnical and Geoenvironmental Engineering ASCE, February, 2005

- Research into closed filter behaviour, taking into account gradation of both filter and core material. Improvement of the Terzaghi- and comparable rules.

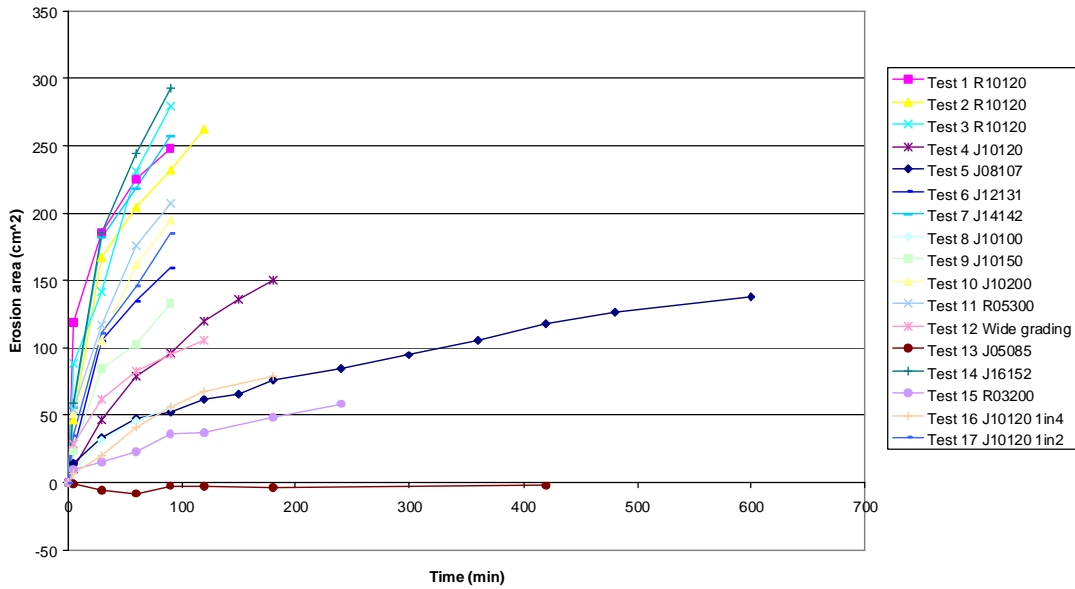
Appendix III Erosion growth curves

Only one figure with the erosion growth curves has been shown in the report, with all the tests for up to 120 minutes. Some tests have lasted longer and for easy comparison tests are excluded from figures to get groups of interesting tests. The figures are shown for completion.

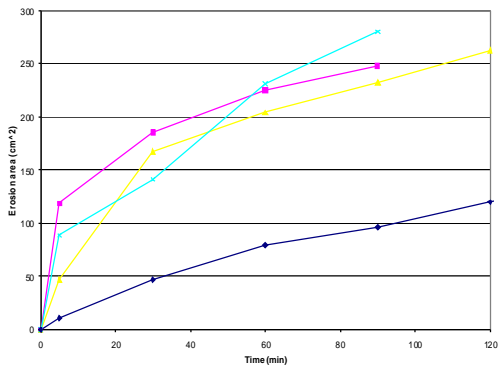
Erosion area growth comparison



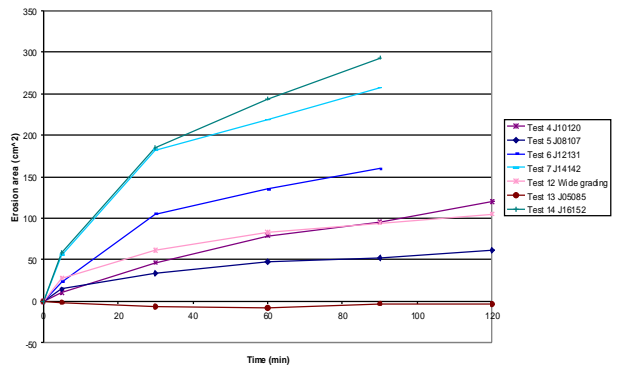
Erosion area growth comparison of tests with a long duration



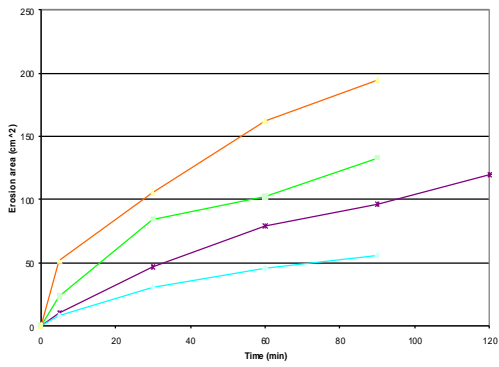
Erosion area growth comparison of the reference tests



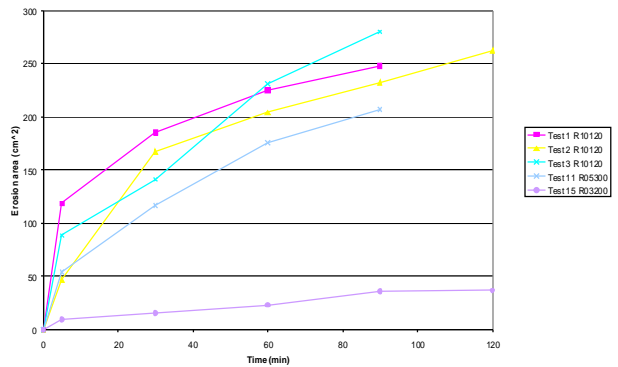
Erosion area growth comparison of the tests with varying H



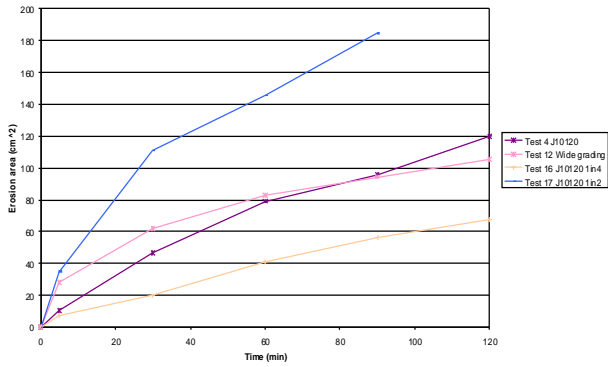
Erosion area growth comparison of the tests with varying T



Erosion area growth comparison of the tests with regular waves



Erosion area growth comparison tests with $H_s = 10$ cm and $T_p = 1.2$ s slope variation and wide grading



Appendix IV Work plan and time schedule

The thesis work will be divided into a number of steps that should be taken in order to reach the objective. The time planning serves as an indication and as a guideline to measure the progress during the thesis study.

Work plan

Literature study, 4 weeks

A literature study is a logical start of the thesis and is necessary to get acquainted with the subject and the theory, and knowledge already present. Chapter 6 gives an overview of the studied materials with short summaries of the information interesting for this study.

Problem analysis, 4 weeks

The theory has to be analysed for what is known and what is lacking for the specific problem. When the lacking knowledge is known, the objective can be formulated and the possibilities for research explored. Choices have to be made at the end of the analysis, see chapter 3 for this.

Test preparation, 8 weeks

Before tests can be performed, the set up of the different tests has to be determined. The tests will probably be performed in a wave flume of the Fluid Mechanics Laboratory of the faculty of Civil Engineering and Geosciences. This wave flume is about 40 m. long, 0,80 m. wide and 1,00 m. deep. A wave generator at one end can generate regular and irregular waves. These preparations do not necessarily take eight weeks, but because the facility is only available from January, this period takes such a long time. During this time, all the preparations that can be done prior to the testing will be done, to assure that as soon as the flume is available, the testing can start. Besides this, focus will be on the final report, as considerable parts of this can be written already.

Testing, 7 weeks

The most time consuming part of the test is the preparation, the construction of the right sand slope and the proper filter placement. The test itself will take about a few hours, while the rest of the day and the next day are expected to be needed to prepare the next test. This way, possibly one test every two days can be performed, once the set up and way of working are familiar. The duration of the testing depends on the number of tests to be performed, the time needed per test and the availability of the facility.

Analysis, 4 to 8 weeks

When all tests are performed, the results can be analysed. For this purpose, the data from visual and measured observations have to be put in a practical form. Computer programs are available to create coordinates from a photograph of a profile. Other ways of processing will depend on the form the data from the tests have.

The deformation of the structure, the development of erosion and accretion in time and space, dependent on the loading parameters and layout, are what has to be examined.

Reporting, 7 weeks

The findings have to be reported in a clear and solid way. The results are presented in a thesis report and finally a presentation.

Time schedule

In order to keep a good view on the progress of the thesis work, a time schedule is made and will be updated during the study. The schedule presented here is only a first estimation of the time needed per part of the study and will be updated when new information is available.

Month	September				October				November				December				Januari				February				March				April				May			
Weeknumber	36	37	38	39	40	41	42	43	44	45	46	47	48	49	50	51	52	1	2	3	4	5	6	7	8	9	10	11	12	13	14	15	16	17	18	19
Activity																																				
Literature study	█																																			
Problem analysis					█																															
Workplan									█																											
Test preparation													█																							
Testing																	█																			
Analysis																					█															
Reporting																									█											
Presenting																													█							

Figure 8-3 Time schedule

This schedule shows four weeks for the problem analysis and choices for the tests, eight weeks for the preparations, seven weeks to do the actual tests, four weeks to analyse the data and three more weeks to process the findings and put all the information and followed procedures into a final report.

Seven weeks of testing and the rough estimate of one test every two days, results in the performance of about 14 tests. The suggested choices ask for 12 to 15 tests, which should be possible to perform within the planned time. Eventually 17 tests have been performed in about 7 week.

Acknowledgements

This thesis project was the final part of my master of Hydraulic Engineering. Many have supported me with the completion of this report which documents my work. To execute a project of such size by myself and to manage all the aspects of it was a very interesting experience from which I have learned a lot.

I would like to thank the members of my committee for the help and good advice on the subject, theory, test results, analysis and the contents of the report. I would also like to thank the Fluid Mechanics Laboratory for facilitating the physical model tests and Van Oord bv for initiating and supporting this research.

During the project I could work in the graduate students' room. I thank my fellow graduate students for their good company and Geeske and Erik for their support.

*Wouter Ockeloen
May 2007*